# NAVAL POSTGRADUATE SCHOOL
# MONTEREY, CALIFORNIA




# THESIS

**FLUXES ACROSS THE WEST COAST RESOLVED BY PICKET FENCE OBSERVATIONS DURING STORMFEST**

by

Steven J. Bolduc

September, 1994

Co Advisors: Paul A. Hirschberg and
Russell L. Elsberry

# REPORT DOCUMENTATION PAGE

Form Approved OMB No. 0704-0188



| 1. AGENCY USE ONLY *(Leave blank)* | 2. REPORT DATE | 3. REPORT TYPE AND DATES COVERED |
|---|---|---|
| | September 1994 | Master's Thesis |

4. TITLE AND SUBTITLE FLUXES ACROSS THE WEST COAST RESOLVED BY PICKET FENCE OBSERVATIONS DURING STORMFEST (U)

5. FUNDING NUMBERS

6. AUTHOR(S) Steven J. Bolduc

7. PERFORMING ORGANIZATION NAME(S) AND ADDRESS(ES)
Naval Postgraduate School
Monterey CA 93943-5000

8. PERFORMING ORGANIZATION REPORT NUMBER

9. SPONSORING/MONITORING AGENCY NAME(S) AND ADDRESS(ES)
National Science Foundation, Arilington, VA

10. SPONSORING/MONITORING AGENCY REPORT NUMBER

11. SUPPLEMENTARY NOTES The views expressed in this thesis are those of the author and do not reflect the official policy or position of the Department of Defense or the U.S. Government.

12a. DISTRIBUTION/AVAILABILITY STATEMENT
Approved for public release; distribution is unlimited.

12b. DISTRIBUTION CODE

13. ABSTRACT *(maximum 200 words)*

Meteorological features that force mesoscale weather systems that develop in the central U.S. often form far upstream over the data-sparse Pacific Ocean. It is hypothesized that the temporal and spatial resolution of the current rawinsonde network along the west coast may not be sufficient to detect and measure flow features moving inland. During the STORMFEST experiment in February-March 1992, a "Picket Fence" of seven rawinsonde stations were interspersed among the seven regular rawinsonde sites from Port Hardy, British Columbia to San Diego, CA. All sites obtained observations every 3 h rather than the normal 12 h. The objective was to examine the feasibility of utilizing extra observations in time and space to improve upstream boundary conditions for forecasts of mesoscale weather events in the central U.S. Fluxes of mass, heat, momentum, moisture, kinetic energy, and potential energy across the west coast resolved with various spatial and temporal combinations of Picket Fence data were compared with the 12-h regular site sondes as the standard. In the best case in which a wave system crossed the middle of the Picket Fence, significantly different fluxes were calculated with the full spatial and 3-h Picket Fence observations. For other systems that crossed near the ends of the axis, only small changes were detected by the additional observations.

14. SUBJECT TERMS Picket Fence, STORMFEST, mesoscale analysis and forecasting.

15. NUMBER OF PAGES 162

16. PRICE CODE

| 17. SECURITY CLASSIFICATION OF REPORT | 18. SECURITY CLASSIFICATION OF THIS PAGE | 19. SECURITY CLASSIFICATION OF ABSTRACT | 20. LIMITATION OF ABSTRACT |
|---|---|---|---|
| Unclassified | Unclassified | Unclassified | UL |

NSN 7540-01-280-5500

Standard Form 298 (Rev. 2-89)
Prescribed by ANSI Std. 239-18 298-102

Approved for public release; distribution is unlimited.

FLUXES ACROSS THE WEST COAST RESOLVED BY PICKET FENCE OBSERVATIONS DURING STORMFEST

by

Steven J. Bolduc, Lieutenant Commander, United States Navy
B.S., Elmhurst College, 1980
M.A., Western Illinois University, 1982

Submitted in partial fulfillment
of the requirements for the degree of

**MASTER OF SCIENCE IN METEOROLOGY AND PHYSICAL OCEANOGRAPHY**

from the

**NAVAL POSTGRADUATE SCHOOL**
**September 1994**

Author: 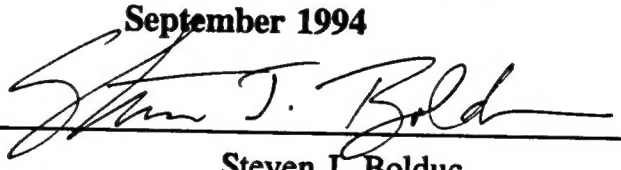

Steven J. Bolduc

Approved by: 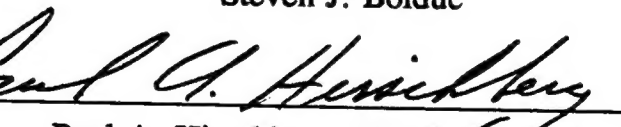

Paul A. Hirschberg, Co Thesis Advisor

Russell L. Elsberry, Co Thesis Advisor

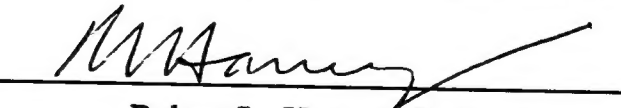

Robert L. Haney, Chairman
Department of Meteorology

## ABSTRACT

Meteorological features that force mesoscale weather systems that develop in the central U.S. often form far upstream over the data-sparse Pacific Ocean. It is hypothesized that the temporal and spatial resolution of the current rawinsonde network along the west coast may not be sufficient to detect and measure flow features moving inland. During the STORMFEST experiment in February-March 1992, a "Picket Fence" of seven rawinsonde stations were interspersed among the seven regular rawinsonde sites from Port Hardy, British Columbia to San Diego, CA. All sites obtained observations every 3 h rather than the normal 12 h. The objective was to examine the feasibility of utilizing extra observations in time and space to improve upstream boundary conditions for forecasts of mesoscale weather events in the central U.S. Fluxes of mass, heat, momentum, moisture, kinetic energy, and potential energy across the west coast resolved with various spatial and temporal combinations of Picket Fence data were compared with the 12-h regular site sondes as the standard. In the best case in which a wave system crossed the middle of the Picket Fence, significantly different fluxes were calculated with the full spatial and 3-h Picket Fence observations. For other systems that crossed near the ends of the axis, only small changes were detected by the additional observations.

## TABLE OF CONTENTS

## LIST OF TABLES

## LIST OF FIGURES

**ACKNOWLEDGMENTS**

I would like to extend my most sincere thanks to my Co-Advisors, Professors Russell Elsberry and Paul Hirschberg, for providing their experience, assistance and patience during my thesis research. Additionally, Mr. Richard Lind was instrumental in the preparation and generation of the data sets used in this study. Without his helpful advice and guidance in computer programming I could not have completed this study.

Finally, I would like to recognize and thank my wife, Terry, and my children Matt, Alyssa and Philip, for putting up with the hours away from them to complete this thesis.

## I. INTRODUCTION

The flow features that force some of the mesoscale weather systems that develop in the Central U.S. often form far upstream. Rapidly moving jet streaks, etc., that can trigger inland mesoscale developments may propagate from the Pacific Ocean. In such cases, present satellite-based and other observational platforms over the Pacific Ocean may not provide the required vertical and horizontal resolution necessary to specify accurately the environmental features that will influence the mesoscale developments over the central U.S. Furthermore, the temporal and spatial resolution of the operational rawinsonde network may not be sufficient to capture important details of these flows as they move inland. This problem was addressed during the STORM-Fronts Experiment Systems Test (STORMFEST) by deploying a "Picket Fence" of extra rawinsonde stations along the west coast. In conjunction with other attempts to utilize aircraft to resolve the conditions over the data-sparse Pacific Ocean, the Picket Fence approach was to intercept and observe accurately features as they crossed the coast and approached the STORMFEST domain.

The Picket Fence experiment was intended to demonstrate the feasibility of utilizing a high resolution quasi-linear array of extra observation stations to improve the upstream

boundary conditions for forecasts of mesoscale weather events in the Central U.S., using the 12-h National Weather Service (NWS) rawinsonde network as the standard. Specifically, operational NWS stations were supplemented during the Picket Fence experiment by research rawinsonde stations along the west coast of the United States to record primary upper-air data from three-hourly soundings during significant weather periods that occurred during four Intensive Operating Periods (IOPs) from February-March 1992.

The purpose of this study is to examine whether the increased temporal and spatial data resolution provided by the Picket Fence stations improves calculations of boundary fluxes across the west coast. A consequence of more accurate boundary fluxes may be improved prediction of mesoscale features downstream. In particular, this study documents the fluxes of mass, heat, momentum, moisture, and kinetic energy with and without Picket Fence data during IOP-3. This IOP occurred from 0000 UTC 20 February to 0000 UTC 21 February 1992, and featured a disturbance that crossed the center of the Picket Fence. The other three IOPs were not as conducive to objective evaluation of the Picket Fence concept because they involved circulations that crossed the west coast along the extreme southern portion of the Picket Fence.

## II. BACKGROUND

STORMFEST was designed to provide research background and operational experience for the STORM I field experiment (STORM, 1991) that had been planned for 1994 in the central United States (see STORMFEST Operations Plan, 1992). The three main objectives of STORMFEST were: (i) to investigate the mesoscale structure of fronts and other mesoscale phenomena associated with winter storms that occur in the central United States; (ii) to test and evaluate the utility of the various observing network and systems; and (iii) to investigate mesoscale weather prediction capabilities and limitations in active frontal regions with the goal of improving forecast performance.

To accomplish the objectives of STORMFEST, an array of operational and research observational instrumentation was set up in a limited region within the central U.S. (Cunning and Williams 1993). Upper-air data collected during the experiment included three- to six-hourly soundings provided by the approximately 20 NWS sites within the STORMFEST region and from the Wind Profiler Demonstration Network established in the central U.S. (Fig. 1). These soundings were augmented by Cross-chain LORAN Atmospheric Sounding Systems (CLASS) and CLASS-type sounders. The CLASS units were positioned within the STORMFEST domain to fill gaps in the coverage of the operational sounding network and array of profilers.

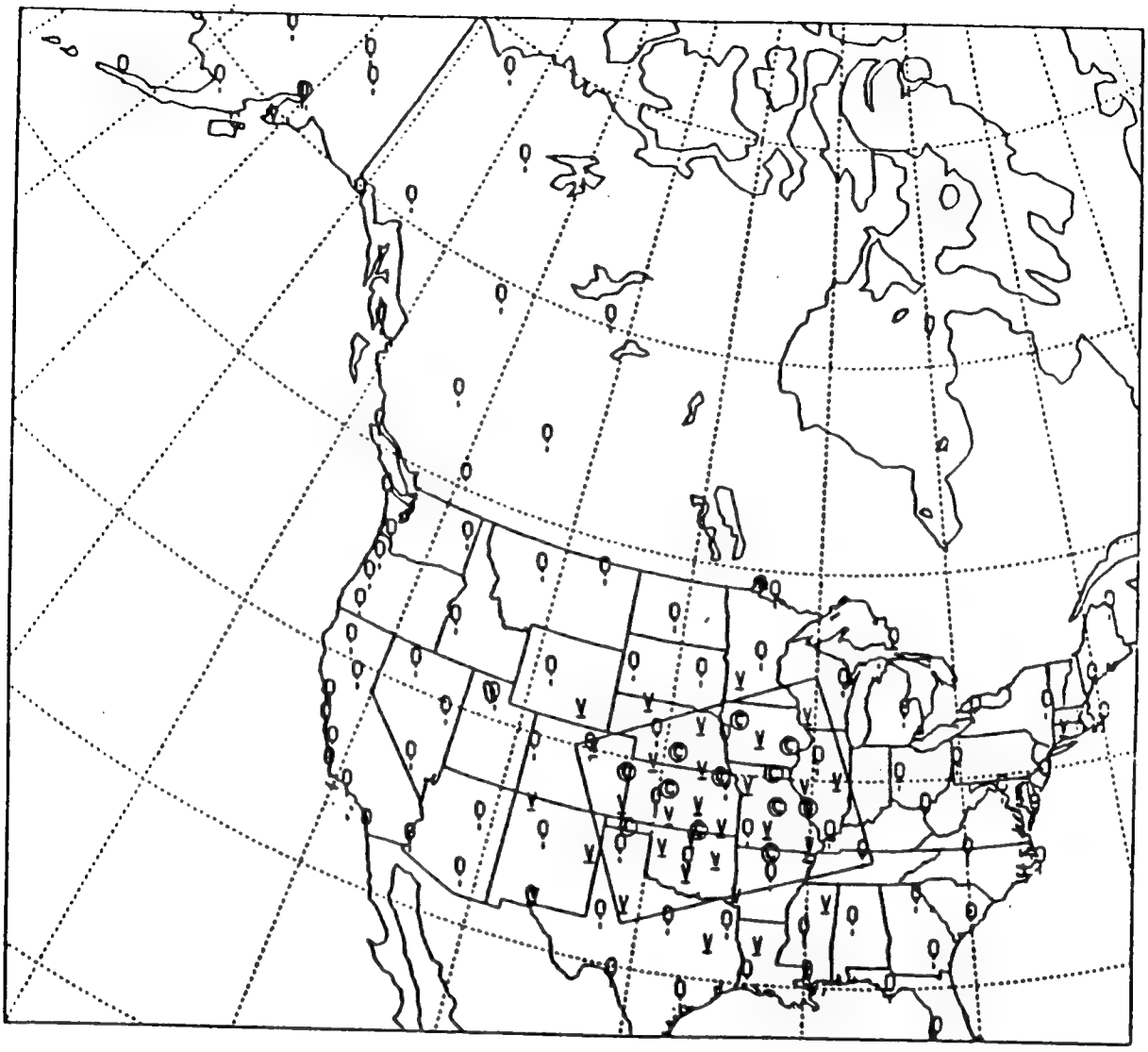

Fig. 1 Upper air stations (balloon symbol for rawinsondes; C for CLASS sites; and V for radar wind profilers) within the STORMFEST domain (box over Midwest), and in the West Coast Picket Fence from Pt. Hardy, British Columbia on the north to San Diego, CA on the south. The NWS Western Region stations between the STORMFEST domain and the west coast and selected Canadian sites also participated (STORMFEST Operations Plan 1992).

Therefore, the STORMFEST upper-air observations had an average horizontal spatial resolution of 150 to 200 km.

The West Coast Picket Fence provided additional observations during STORMFEST to potentially improve data resolution and boundary conditions as weather systems moved across the coast. The scientific justification for the West Coast Picket Fence concept is that a certain type of forced mesoscale phenomena is triggered by the interaction of the environmental flow (e.g., jet streaks, short waves, potential vorticity anomalies, etc.) with topography, diurnal heating patterns, etc. Given accurate representations of the forcing mechanisms and environmental flow, the timing and location of the onset of these mesoscale phenomena may be better predicted. Even though massive vertical redistribution of energy and momentum may occur when the mesoscale circulation is triggered, prediction of the downstream advection and propagation (relative to steering flow) of the mesoscale system will ultimately be limited by the accuracy of the environmental flow. These forced mesoscale phenomena require an improved understanding of the forcing mechanisms, observations of the environmental flow in the domain, and observations of the upstream systems that enter the domain. It is the latter aspect that is addressed by the Picket Fence experiment.

The mesoscale prediction problem is greatly increased when the upstream environmental features originate over a data-

sparse region (e.g., the Pacific Ocean). Present satellite-based remote sensors do not have the vertical and horizontal resolution necessary to identify accurately the environmental conditions associated with jet streaks, short waves, etc. Even if improved surface specifications of pressure, temperature, and humidity were available from a network of drifting buoys to anchor the satellite profiling techniques, the energetics of rapidly moving jet streaks and short waves would be difficult to resolve accurately by present satellites. Although wind reports from commercial aircraft provide occasional observations in jet streaks, the coverage over the Pacific tends to be confined to the great circle flight tracks between the U.S. and Asia, which leaves large data gaps. Other possible solutions to eliminate the Pacific Ocean data gap, such as special aircraft reconnaissance, may not be advantageous due primarily to cost limitations. Therefore, it is desirable to explore other options for providing upstream boundary conditions.

Precedence for using the Picket Fence approach is provided by the experience with nested grid models of atmospheric phenomena. In the nested grid technique, the boundary conditions for the high resolution inner grid are provided by the time tendencies predicted on a coarser resolution grid that surrounds the inner domain. Studies (Anthes 1983; Ross 1986) have shown that one of the limitations to the accuracy of the solutions on the inner grid is the accuracy of the

boundary conditions provided on the edge of the grid. After the time it takes for the coarse grid information provided at the upstream boundary to fill the inner domain, the solution tends to be no more accurate than if the nested grid had not been used. Therefore, a fundamental limitation to the predictability of the inner domain solution will be the accuracy and resolution of the initial data and upstream boundary conditions (Anthes 1986).

Previous studies (Anthes 1983; Ross 1986; Anthes 1986) on boundary fluxes and other large-scale motions indicate that predictability varies with: 1) numerical aspects (e.g. grid size and the boundary conditions for the mathematical equations); 2) physical aspects (e.g. parameterization); and 3) data analysis and initialization. The Picket Fence concept focuses on increasing predictability through improved boundary conditions and higher resolution of initial data, since both are solvable with existing technology by simply adding more recording stations (Anthes 1983).

From the very onset of atmospheric prediction, researchers realized the importance of an accurate data base. Bjerknes (1919) hypothesized that the state of the atmosphere could be determined completely if initial conditions were known with sufficient accuracy. Although predictability depends on the nature of initial errors, significant improvements can be realized by the implementation of an improved data network that will produce more accurate boundary conditions and

initial environmental representation (Anthes 1986). Most likely, the necessary resolution of the data network is scale dependent. The success of the current generation of limited-area numerical models in simulating some meso-alpha (Orlanski 1975) scale flows suggests that a satisfactory representation of the initial atmosphere for these flows may be derived from the operational rawinsonde network (Sanders 1987; Sanders and Auciello 1989).

However, the horizontal resolution of the operational network may not be sufficient to resolve smaller-scale features (Ross 1986). For example, Thomson (1986) shows that phenomena detectable with current observational networks have scales of 500 km and 12 h, which are too large to resolve important mesoscale features. Other studies (e.g., Smith 1980) have investigated boundary flux energetics using data from augmented rawinsonde networks and have calculated fluxes across vertical cross sections directly from the soundings. These studies illustrate the complex effects of potential and kinetic energy fluxes and the resultant transformations in extratropical cyclones.

During special field experiments, the temporal resolution sites has been enhanced to 6- or 3-h intervals (Smith 1980; Fuelberg and Scoggins 1978). This strategy of temporally increased soundings at the existing rawinsonde sites has been favored over spatial improvements, primarily due to the high

cost of establishing new observing stations to improve the spatial resolution.

The West Coast Picket Fence was designed to provide both higher spatial and temporal resolution observations needed to resolve subsynoptic atmospheric features as they exit the data-sparse Pacific Ocean area. In this study, the additional Picket Fence soundings are used to illuminate deficiencies in the boundary fluxes calculated from the operational network at 12 h resolution. Specifically, the goal of the Picket Fence is to better identify mesoscale phenomena, through both improved spatial and temporal resolution, for the ultimate purpose of improving predictability of mesoscale weather systems downstream.

## III. DATA

To demonstrate the feasibility of improving the accuracy of the upstream boundary conditions via the West Coast Picket Fence, seven new rawinsonde stations were established between the five operational NWS rawinsonde stations and the U.S. Air Force site at Vandenberg AFB, CA and the Canadian Atmospheric Environmental Service (AES) site at Pt. Hardy. See Table 1 and Fig. 2 for the specific station locations. In addition, rawinsondes were launched every 3-h at all sites rather than the regular 12-h intervals to improve the temporal resolution of the data during the four IOPs. The following sections describe how the data were collected and used in this study.

### A. OBSERVATIONS

Two types of rawinsonde receivers were used at the seven special Picket Fence sites. Special stations OLM, CGO, RDD, ILA, and PRB (see Table 1 for locations) used a Department of Navy version of the Vaisala Marwin MW-12 system, which is called the AN/UMQ-12 Mini-Rawindsonde System (MRS). The MRS uses Omega and Sigma navigational aids to track the position of the radiosonde during ascent in which 200-300 gm balloons were used. The rawindsonde receiver at NPS was a Vaisala Digicora MW-11 system. The Digicora system is capable of using either LORAN or Omega and Sigma navigational aids.

Both the MRS and Digicora system used Vaisala RS80-15 radiosondes, which are pre-calibrated and have a perforated

TABLE 1 WEST COAST PICKET FENCE LOCATIONS THAT INCLUDE NWS, CANADIAN, U.S. AIR FORCE AND SPECIAL SITES.

| Location | | Elevation (m) | Latitude/ Longitude | Call sign |
|---|---|---|---|---|
| 1. Port Hardy | Canadian | 17 | 50 43'<br>127 29' | YZT |
| 2. Quillayute WA | NWS (contract) | 56 | 47 57'<br>124 33' | UIL |
| 3. Olympia WA | Special (Note 1) | 59 | 47 02'<br>122 52' | OLM |
| 4. Salem OR | NWS | 61 | 44 55'<br>123 03' | SLE |
| 5. Cottage Grove, OR | Special (Note 2) | 195 | 43 48'<br>123 04' | CGO |
| 6. Medford OR | NWS | 397 | 42 19'<br>122 52' | MFR |
| 7. Redding CA | Special (Note 3) | 177 | 40 36'<br>122 25' | RDD |
| 8. Williams CA | Special (Note 4) | 25 | 39 09'<br>122 05' | ILA |
| 9. Oakland CA | NWS (contract) | 6 | 37 48'<br>122 16' | OAK |

TABLE 1 (CONTINUED).

| Location | | Elevation (m) | Latitude/ Longitude | Call sign |
|---|---|---|---|---|
| 10. Monterey CA | Special (Note 3) | 30 | 36 36' 121 53' | NPS |
| 11. Paso Robles CA | Special (Note 3) | 249 | 35 38' 120 44' | PRB |
| 12.Vandenberg CA | U.S. Air Force | 100 | 34 33' 120 37' | VBG |
| 13. Point Mugu CA | Special (Note 5) | 2 | 34 07' 119 07' | NTD |
| 14. San Diego CA | NWS (contract) | 134 | 32 34' 117 10' | NKX |

Notes: (see also the Acknowledgments)

1. Launches by University of Washington and Submarine Group 9
2. Launches by Oregon State University
3. Launches by Naval Postgraduate School and Mobile Environmental Team personnel
4. Launches by Naval Postgraduate School and University of California at Davis
5. Launches by Pacific Missile Test Center

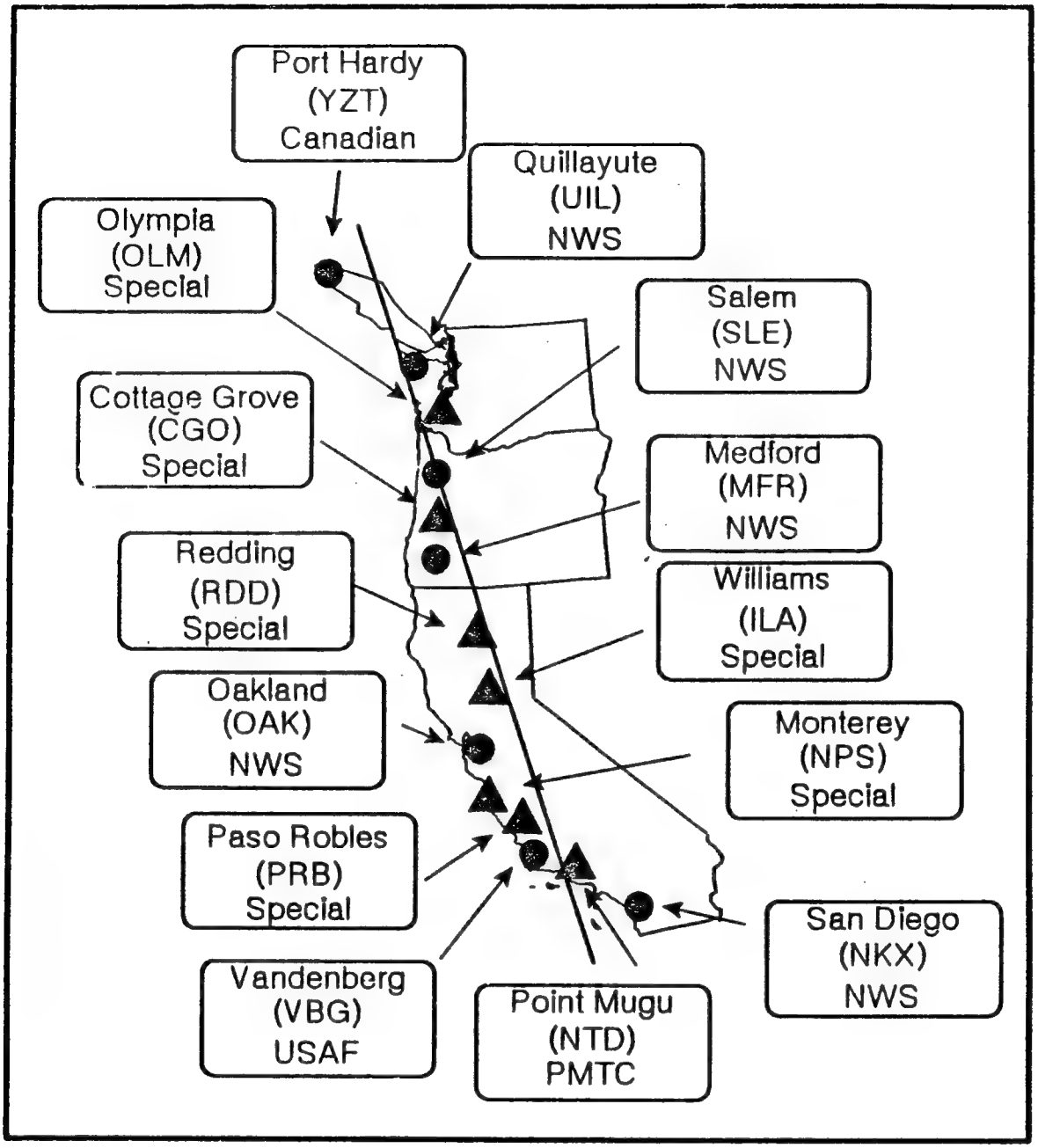


Fig. 2 Locations of the west coast Picket Fence (NWS, filled circles and special, filled triangles). Line of best fit (Picket Fence axis) through the sites is denoted by solid line.

paper tape to enter the calibration coefficients. Winds from these two systems are generated by each receiver system according to the following steps:

(1) Phase detection from navigation aids;

(2) Phase filtering/quality control;

(3) Phase derivative computation; and

(4) Calculation of different frequency phase derivatives from one station to produce a single phase derivative corresponding to each particular transmitter;

(5) Wind vector computation;

(6) Consistency checking; and

(7) Wind quality control.

A buffer of the most recent four minutes for Omega (two minutes for LORAN) of quality-controlled wind values is continuously updated during the sonde ascent. For the first two (Omega) or one (LORAN) minutes of the ascent, winds are extracted at 5-second (Omega) or 10-second (LORAN) intervals using cubic spline interpolations of the eastward (U) and northward (V) components. Although the surface wind observation is utilized in the spline fits, the strong center weighting of the spline fits may lead to discontinuities in the lowest 100 m, especially if there is strong shear occurring at low altitudes. The older samples in the buffer are overwritten as newer data are collected, and winds are calculated from the reinterpolated spline fits. The resulting

winds for the Omega (LORAN) system are equivalent to 2-min (1-min) radar-tracked rawindsonde winds.

The Pacific Missile Test Center at Pt. Mugu, CA (NTD) used a radar tracking system to follow the radiosonde during ascent. Winds were computed from the 6-sec elevation and azimuth angles. Data from the regular NWS and AES stations were received and prepared by the STORMFEST Project Office at the National Center for Atmospheric Research (NCAR). The Vandenberg (VBG) sounding data were taken at the regular U.S. Air Force rawindsonde station and were post-processed at NPS from printouts of data at 200-foot increments. The seven Picket Fence special sites collected and processed rawindsonde data with 5 s or 10 s resolution for the duration of each launch. The Vaisala MW-11 and MW-12 systems automatically compute significant and mandatory-level reports for each launch.

Temperatures from the RS80-15 rawinsondes are derived from a silvered bead thermistor. Relative humidity (RH) is obtained from the Vaisala HUMICAP sensor, which uses a capacitor that is sensitive to RH changes. A silvered hood covers the sensing portion of the HUMICAP to reduce solar heating and deposition of moisture on the sensing surface.

## B. POST-PROCESSING OF RAWINSONDES

Vertical plots of the rawindsonde measured variables were generated to subjectively check for any problems in the soundings. Surface observations from each of the soundings

were tabulated and checked for launch-to-launch consistency. Anomalous observations and corrective procedures are described in Lind *et al.* (1992).

C. DATA FORMATS

The Picket Fence rawindsonde data base was converted into the First GARP Global Experiment (FGGE) format and passed through an objective quality-control procedure (Baker 1991) that checked each sounding for hydrostatic consistency and vertical wind shear. Levels that were flagged as having erroneous geopotential heights were recomputed, and those winds that were flagged as suspect were changed to missing values. Layers that were slightly super-adiabatic were not corrected (for more details see Lind *et al.* 1992).

A second data base was created by interpolating the observations to 10 mb intervals. An algorithm was developed to search in the rawinsonde record for the nearest levels with data above and below each 10 mb interpolation level. These adjacent levels had to be within 50 mb of the desired 10 mb interpolation level, or that level was recorded as missing. If this interval criterion was satisfied both above and below the level, a linear pressure interpolation was performed.

D. STATION SUMMARIES

A list of launch times, maximum altitude of soundings, and special notes related to every launch, during each IOP, can be found in Lind *et al.* (1992). In addition, Lind *et al.* (1992) provides time plots of rawinsondes during each IOP.

## IV. METHODOLOGY

The goal of this study is to demonstrate that flux quantities resolved by all Picket Fence stations at 3- and 6-h intervals are improved relative to those resolved by the 12-h NWS stations. The key question is: Do extra soundings add any new boundary flux information? In particular, is the improved spatial resolution necessary and does the time variability in the fluxes require 6-h or even 3-h soundings?

The first task in converting the raw 3-hourly rawinsonde data into fluxes of heat, momentum, moisture, potential energy, and kinetic energy was to define a uniform pressure-space cross sectional grid along the Picket Fence sites, hereafter referred to as the Picket Fence axis. The location of the axis was determined by calculating a best-fit line through the 14 Picket Fence stations with the method of least squares. Specifically, two linear regressions were performed of the latitude and longitude of each station; one latitude versus longitude and the other longitude versus latitude. The geographic center of the axis was defined where the two regression lines intersected and the slope of the axis was defined as the mean of the two regressions. The resulting axis line (Fig. 2) runs northwest to southeast from 50.68° N, 127.37° W to 32.80° N, 117.10° W at an angle of 22° off true north. Station locations east and north of the center of the axis in kilometers were then determined. From these distances, projections of each station location onto the axis

were made. Justification for projecting stations to a position normal to the axis line, versus a more complicated two-dimensional interpolation or a simple translation based on latitude, was that fluxes normal to the cross section were desired. In addition, the assumption was made that errors incurred by this procedure were smaller, given the relatively small normal translation distance of the stations to the Picket Fence axis (see Fig. 2) than other factors such as delayed or irregular launch times, balloon drift, and sensor errors.

Next, the earth relative u- and v-wind components at each station site were rotated to normal ($u_r$) and parallel ($v_r$) components relative to the Picket Fence axis. Fluxes of heat ($u_r\theta$), momentum ($u_r u_r$), moisture ($u_r q$), kinetic energy ($u_r V^2/2$), and potential energy ($u_r \phi$) normal to the Picket Fence axis were then computed at each level and time for each site utilizing the 10-mb raw rawinsonde data (see Chapter III). These raw fluxes were then interpolated to a 23 x 20 grid along the Picket Fence axis at each 3-h time during each IOP. The horizontal resolution of the grid is 100 km and the vertical resolution is 50 mb from 1050 mb to 100 mb. The interpolation was performed utilizing a routine called ZGRID (Young and Van Woert 1987). This scheme allows either Laplacian, spline, or a Laplacian-spline combination interpolation based on the overrelaxation of

$$[\nabla^2 X(z) + \nabla^2 Y(z)] - (CAY)[\nabla^4 X(z) + \nabla^4 Y(z)] = 0. \qquad (4.1)$$

In (4.1), *CAY* is a user-defined parameter that determines the degree to which the Laplacian and spline functions are used in the interpolation. Specifically, a *CAY* value of 0.0 (100000) results in pure Laplacian (spline) interpolations, while intermediate *CAY* values result in combinations of both. Figures 3 and 4 illustrate the effects of varying *CAY* between 0.0 and 100000. In general, the pure Laplacian interpolation tends to produce sharp maximums and minimums at data point locations in comparison to the pure spline, but does not extrapolate gradients past the edge of data as readily as the spline.

Another user-defined parameter in ZGRID is *NRANGE*. This integer defines the rectangular area ($A_d$) in which data can influence the interpolated value at a particular grid point. This area of influence is centered at the grid point and is given by

$$A_d = NRANGE\ (\Delta x)\ (\Delta y),$$

where $\Delta x$ and $\Delta y$ are the grid resolution in the x and y directions, respectively (Fig. 5).

After experimentation, a *CAY*=100000 (pure spline) and *NRANGE*=5 were found to produce the most realistic

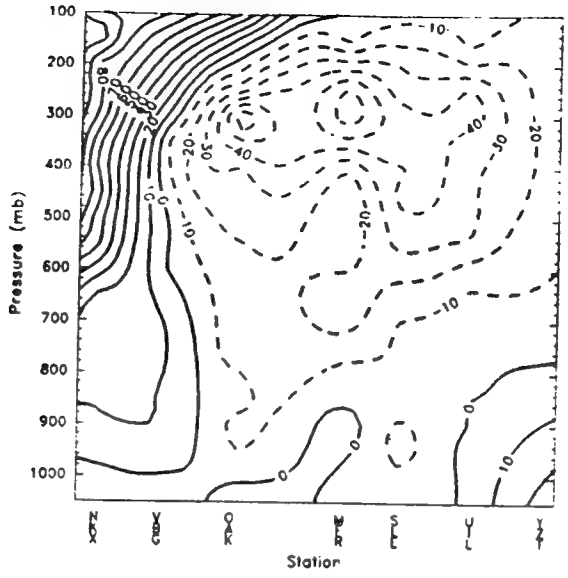


Fig. 3 Heat flux ($10^2$ m $^oK$ $s^{-1}$) at 1200 UTC 7 March 1992 normal to the Picket Fence interpolated to pressure-space cross section from only the regular NWS rawinsondes at 50 mb intervals using a spline with CAY= 100000 in eq. (4.1). Positive (solid and negative (dashed) contours indicate fluxes from the west or the east respectively.

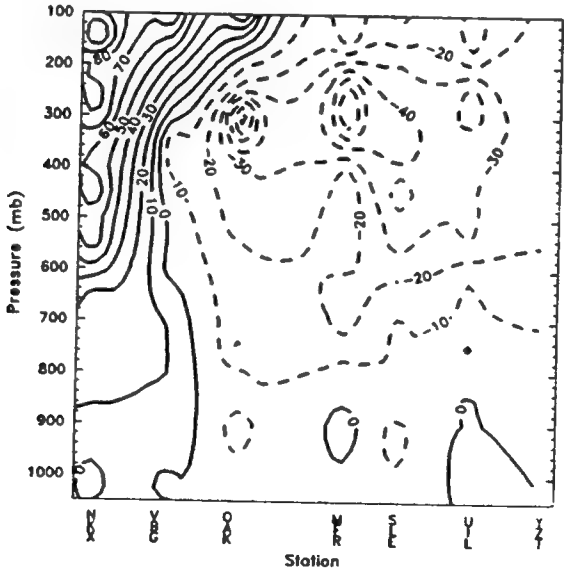


Fig. 4 As in Fig. 3, except for a Laplacian interpolation with CAY=0.0 in eq. (4.1).

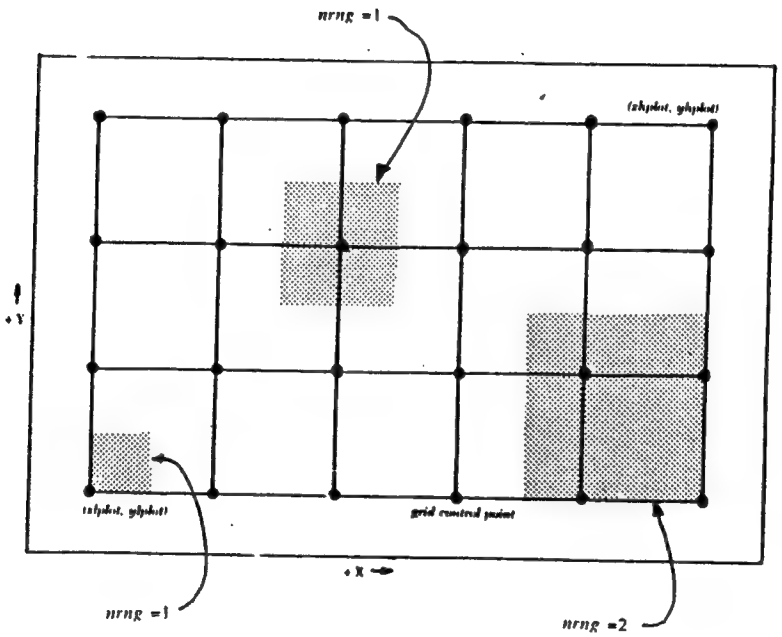


Fig. 5 Examples of the areas relative to grid points that are searched for observations for *NRANGE*=1 and 2 in the ZGRID interpolation program (Young and Van Woert 1987).

interpolations of the station-flux quantities to the Picket Fence grid. Regions with missing data were only replaced by interpolated values if enough data surrounding the location were available. Erroneous data "flagged" in the initial FGGE data quality control process were assigned to be undefined ($1xe^{35}$), and were ignored by the ZGRID algorithm.

With this procedure, sets of spatial cross sections along the Picket Fence axis were produced as a function of time for 3-h NWS-only soundings and 3-h NWS plus special site soundings. Recall that the NWS sites are taken to include the Air Force Base at Vandenberg, CA and the Canadian AES site at Pt. Hardy, British Columbia as well. In Chapter VI, the vertical cross sections will be used to examine implications of Picket Fence network in terms of spatial and temporal flux analysis improvements that result from the additional stations and 3-h sonde launches.

## V. SYNOPTIC DISCUSSION

The four Picket Fence IOPs were initiated when a disturbance was expected to cross the Picket Fence domain and subsequently contribute to mesoscale development over the STORMFEST region. As shown in Table 2 below, each IOP was followed by a STORMFEST IOP.

TABLE 2. PICKET FENCE IOP BEGINNING AND TERMINATION TIMES:

| Picket Fence IOP | Beginning Time | Ending Time | Associated STORMFEST IOP |
|---|---|---|---|
| 1 | 06 UTC 13 Feb | 18 UTC 13 Feb | 6 |
| 2 | 18 UTC 14 Feb | 18 UTC 16 Feb | 7,8 |
| 3 | 00 UTC 20 Feb | 00 UTC 21 Feb | 9,10 |
| 4 | 12 UTC 05 Mar | 12 UTC 07 Mar | 17 |

The NWS and special sites along the Picket Fence required 24-h notice before the start of an IOP. This constraint, along with the scientific criteria that disturbances cross the Picket Fence domain and later become associated with mesoscale development over the Central U.S., required the Picket Fence alerts to be initiated based on 84-h to 120-h numerical guidance from the global forecast models. This led to challenging forecasts during the experiment, and hampered not only start times, but also coordination between Picket Fence and STORMFEST IOP events (for more details see Lind *et al.* 1992). Overviews of each IOP are provided in the individual summaries below.

A. IOP 1

The feature of interest during IOP 1 was a rapidly propagating short wave that detached from a persistent closed-low system southwest of the Queen Charlotte Islands, and became mobile in the southern branch of the Polar jet stream (Fig. 6a). The 500 mb vorticity maximum associated with this wave crossed the California coast near Vandenberg around 1500 UTC 13 February 1992 (Fig. 6b), with an associated 56 m $s^{-1}$ jet streak at 260 mb over southern California and northern Baja, Mexico.

B. IOP 2

The main feature during IOP 2 was a short-wave trough rotating around a slowly eastward moving closed low system (Fig. 7a). This trough system was the second of two that rotated around a closed-low over the Queen Charlotte Islands. The first was the subject of IOP 1. The second wave had more thermodynamic support, which enabled it to dig slightly farther south than the first wave. The 500 mb vorticity maximum associated with the short wave crossed the West Coast near the Mexico-California border around 0300 UTC 16 February. The vorticity center associated with the upper low crossed the central Oregon coast around 1800 UTC 16 February (Fig. 7b). The IOP was extended six hours to 1800 UTC 16 February for the special Picket Fence sites north of Monterey, CA to observe this upper-low passage (See Lind *et al.* 1992).

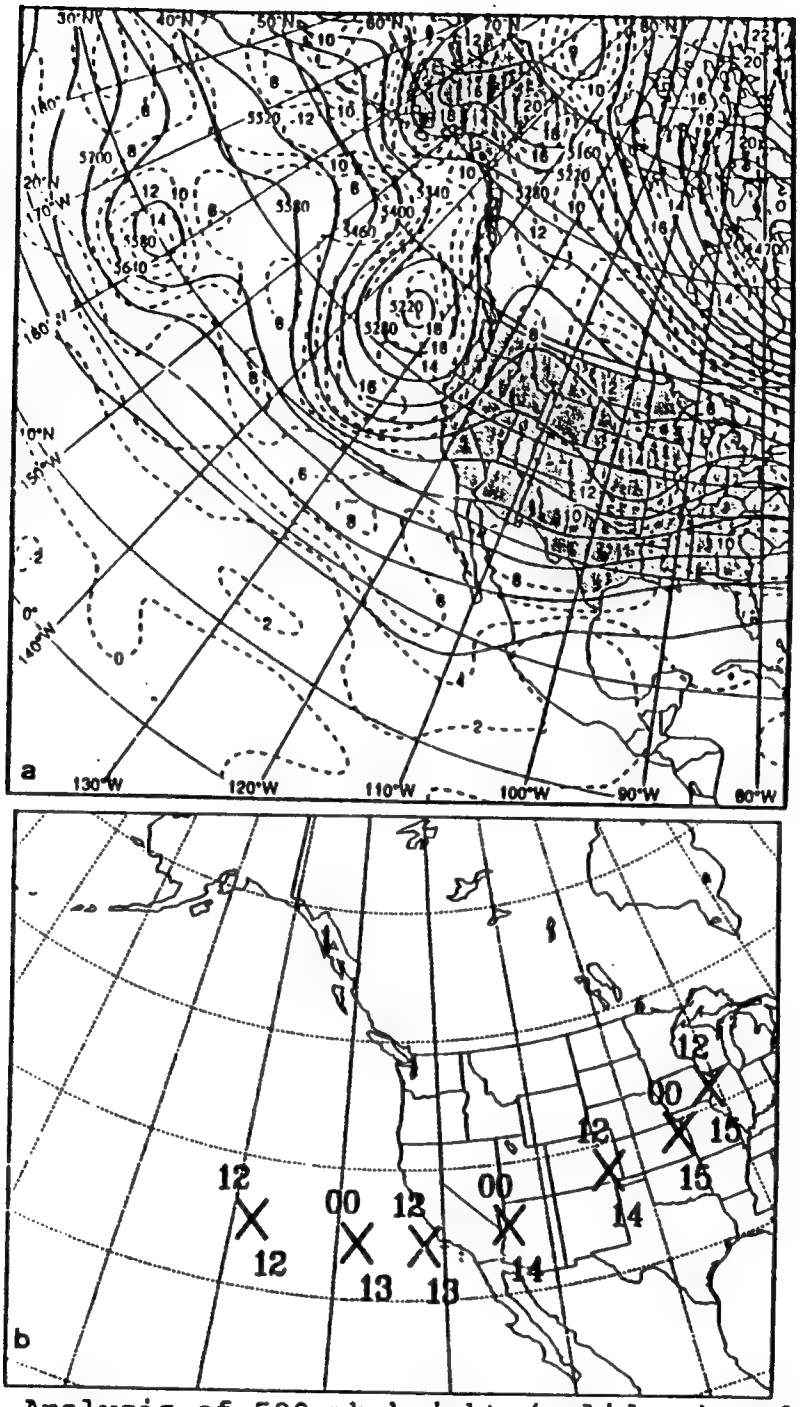


Fig. 6 a). Analysis of 500 mb height (solid, m) and absolute vorticity (dashed, 10 $^{-5}$ s$^{-1}$) for 0000 UTC 13 February 1992 based on the National Meteorological Center Aviation model analysis. b). Track of the 500 mb vorticity maxima observed during IOP-1 in 12-h increments from 1200 UTC 12 February through 1200 UTC 15 February 1992. Numbers to the upper left and lower right of each X denotes UTC hour and date, respectively.

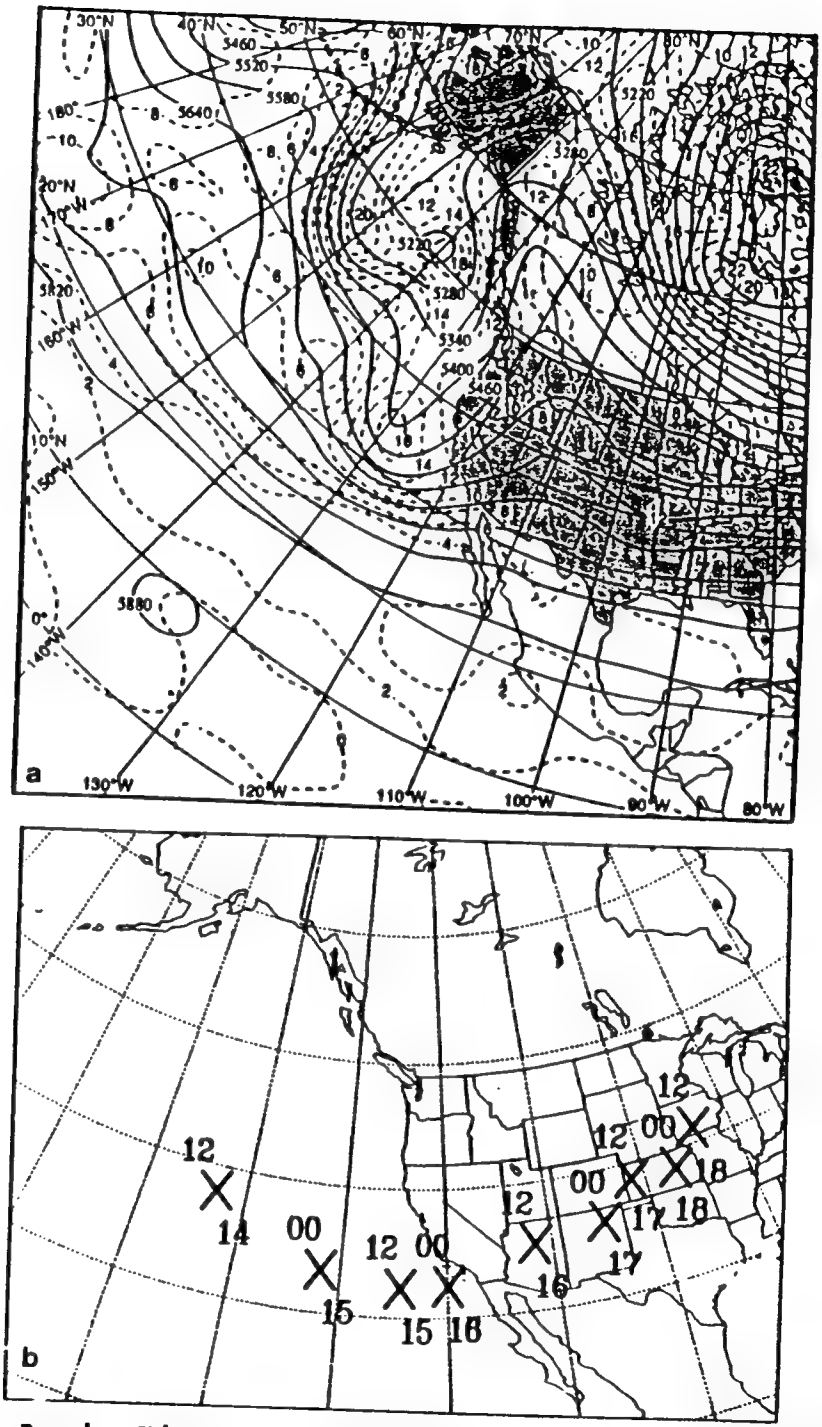


Fig. 7. a). As in Fig. 6 a., except for 0000 UTC 15 February 1992. b). As in Fig. 6 b., except during IOP-2 from 1200 UTC 14 February through 1200 UTC 18 February 1992.

C. IOP 3

The main feature of interest during IOP 3 was a subtropical disturbance that moved into the southern branch of the jet stream north of Hawaii, and migrated quickly eastward (Fig. 8a). This disturbance crossed the full extent of the Picket Fence observing network, as the associated 500 mb vorticity maximum crossed the central Oregon coast around 1200 UTC 20 February (Fig. 8b). This storm system was interesting for a number of reasons. The NMC analyses of the disturbance over the eastern Pacific indicated that it was fairly weak with little baroclinic support in the lower troposphere. However, satellite imagery indicated a more defined feature, which prompted the initiation of the IOP. This relatively warm, subtropical disturbance was associated with substantial rainfall over northern California, Oregon, and Washington. Unlike typical baroclinic systems, maximum wind speeds were observed between 600 mb and 700 mb as the wave crossed the Picket Fence.

D. IOP 4

The main feature of interest during the final IOP was a slow moving long-wave trough with embedded short waves rotating through it (Fig. 9a). The most significant of these waves crossed the coast along the California-Mexico border around 1800 UTC 7 March just after the conclusion of the study period (Fig. 9b). Lee surface cyclogenesis subsequently occurred in northeast New Mexico around 1800 UTC 8 March.

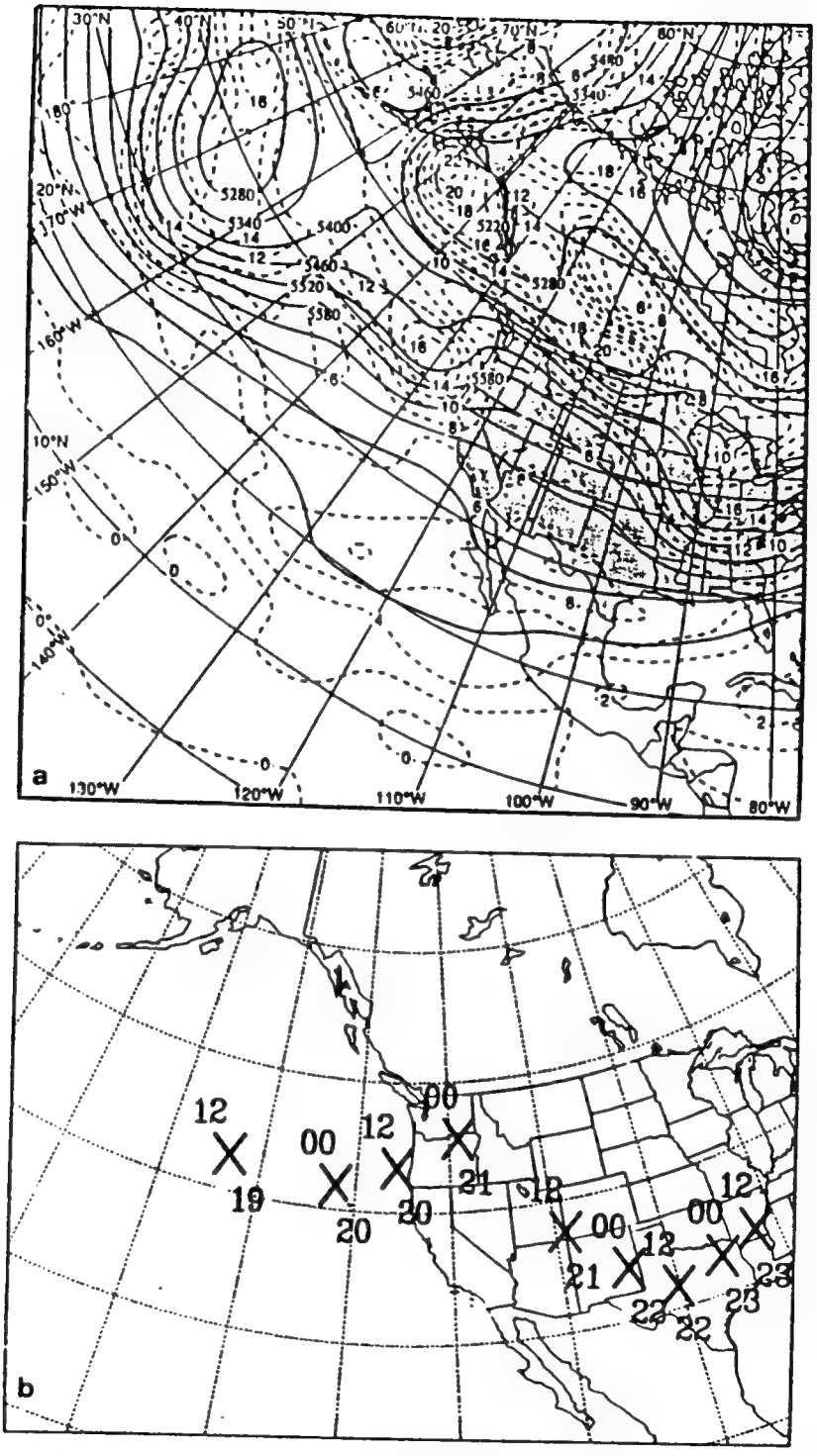


Fig. 8. a). As in Fig. 6 a., except for 0000 UTC 20 February 1992. b). As in Fig. 6 b., except during IOP-3 from 1200 UTC 19 February through 1200 UTC 23 February 1992.

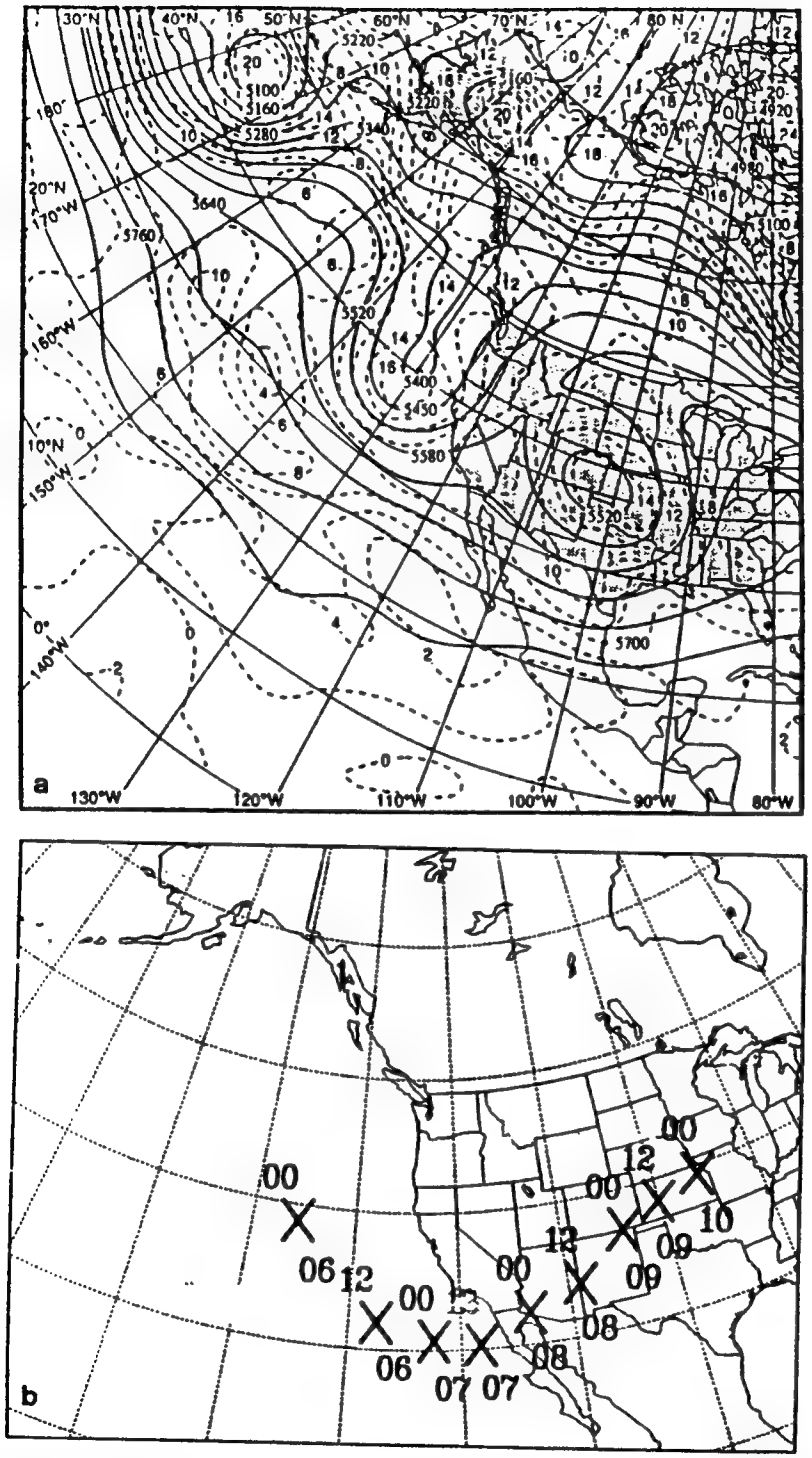


Fig. 9. a). As in Fig. 6 a., except for 0000 UTC 5 March 1992. b). As in Fig. 6 b., except during IOP-4 from 0000 UTC 06 March through 0000 UTC 10 March 1992.

The 500 mb trough axis was along 130° W on 1200 UTC 5 March. Numerical guidance and satellite 6.7 μm water vapor channel imagery suggested that a series of embedded short-wave disturbances would rotate around this trough and progress inland as the trough slowly moved eastward and closed off over southern California. The primary short-wave vorticity center crossed the coast near the California-Mexico border around 1800 UTC 7 March. During the next 24 h, this primary vorticity maxima moved northeastward and was located over southern New Mexico at 1200 UTC 08 March (see Fig. 9b) as another short-wave impulse crossed the west coast.

From a forecasting perspective, this system provided an example of prediction problems for the central U.S. Accurately locating the embedded short-wave impulses moving through the slowly moving trough over the data-sparse Pacific, and predicting their eventual impact inland, was a challenge. Unfortunately, the absence of good guidance prevented optimal timing of the Picket Fence observation period, which ideally would have extended 12 more hours to 0000 UTC 8 March.

The synoptic evalution during IOPs 1, 2, and 4 illuminate the necessity for a longer Picket Fence, including sites in northwestern Mexico and southwestern Canada, to capture the full extent of features crossing the west coast of North America in the southern and northern branches of the jet stream. In particular, these three cases had disturbances that crossed the coast along the southern periphery of the

Picket Fence, which made the northern special sites irrelevant. As will be demonstrated below, this situation precluded much impact on the boundary flux calculations from the extra stations. For this reason, the primary focus will be on the calculations during IOP-3, which featured a disturbance crossing the middle of the Picket Fence domain.

## VI. RESULTS

In this chapter, spatial and temporal differences between flux quantities resolved by the NWS-only stations (NWS) and NWS-plus the addition of special stations (ALL) are examined to determine whether the extra soundings along the Picket Fence add any new boundary flux information. In particular, spatial differences are examined to determine the impact of the improved horizontal resolution provided by the additional stations by comparing NWS and ALL cross sections of various flux quantities across the Picket Fence axis for selected times during IOPs 3 and 4. Temporal differences are examined to determine the impact of the additional 3-hourly launches by comparing the evolution of the NWS and ALL mean cross-section values of flux quantities during IOPs 3 and 4 with and without the extra launches.

### A. SYSTEMS THAT CROSS THE INTERIOR OF THE PICKET FENCE

As discussed in the Synoptic Overview (Chapter V), IOP-3 was the only IOP that featured a system that crossed the interior of the Picket Fence observational network. It therefore represents the best opportunity to explore differences between the NWS and ALL flux quantities. In particular, spatial differences are examined at three times during the 24 h period of IOP-3. The first (0000 UTC 20 Feb), second (0600 UTC 20 Feb), and third (1800 UTC 20 Feb), are representative of conditions before, during, and after,

respectively, the passage of the upper-level vorticity center over the Central Oregon Picket Fence axis.

Cross sections of $U_r$, and fluxes of heat, momentum, potential energy, kinetic energy, and moisture (Fig. 10) before the vorticity center crossed the Picket Fence axis indicate small but distinct differences between the NWS and ALL analyses. In general, the ALL cross sections depict more structure in the interior of the analyses than the NWS cross sections, while the borders are almost identical since NWS sites anchor the ends of the Picket Fence.

Comparison of the ALL and NWS analyses of $U_r$ are representative of the flux comparisons because $U_r$ is utilized to calculate each of the fluxes. Specifically, the dual jet maxima near 200 mb over OAK and YZT are slightly better defined in the ALL versus the NWS cross section (cf, Fig. 10a and 10b) and appear more continuous. Heat fluxes based on ALL and NWS stations (Fig. 10c,d) have similar patterns to those in the $U_r$ cross sections, which suggests the mass flux variability is more important than the potential temperature variability. The maxima at 200 mb over OAK, MFR, and YZT are discernable in both the NWS and ALL cross sections, but the ALL soundings provide additional detail and have larger central values. For example, the >120 m $^{o}$K/sec region in the ALL cross section (Fig. 10c) does not appear in the NWS cross section. Similarly, the momentum (Fig. 10e,f), potential energy (Fig. 10g,h), and kinetic energy (Fig. 10i,j) cross

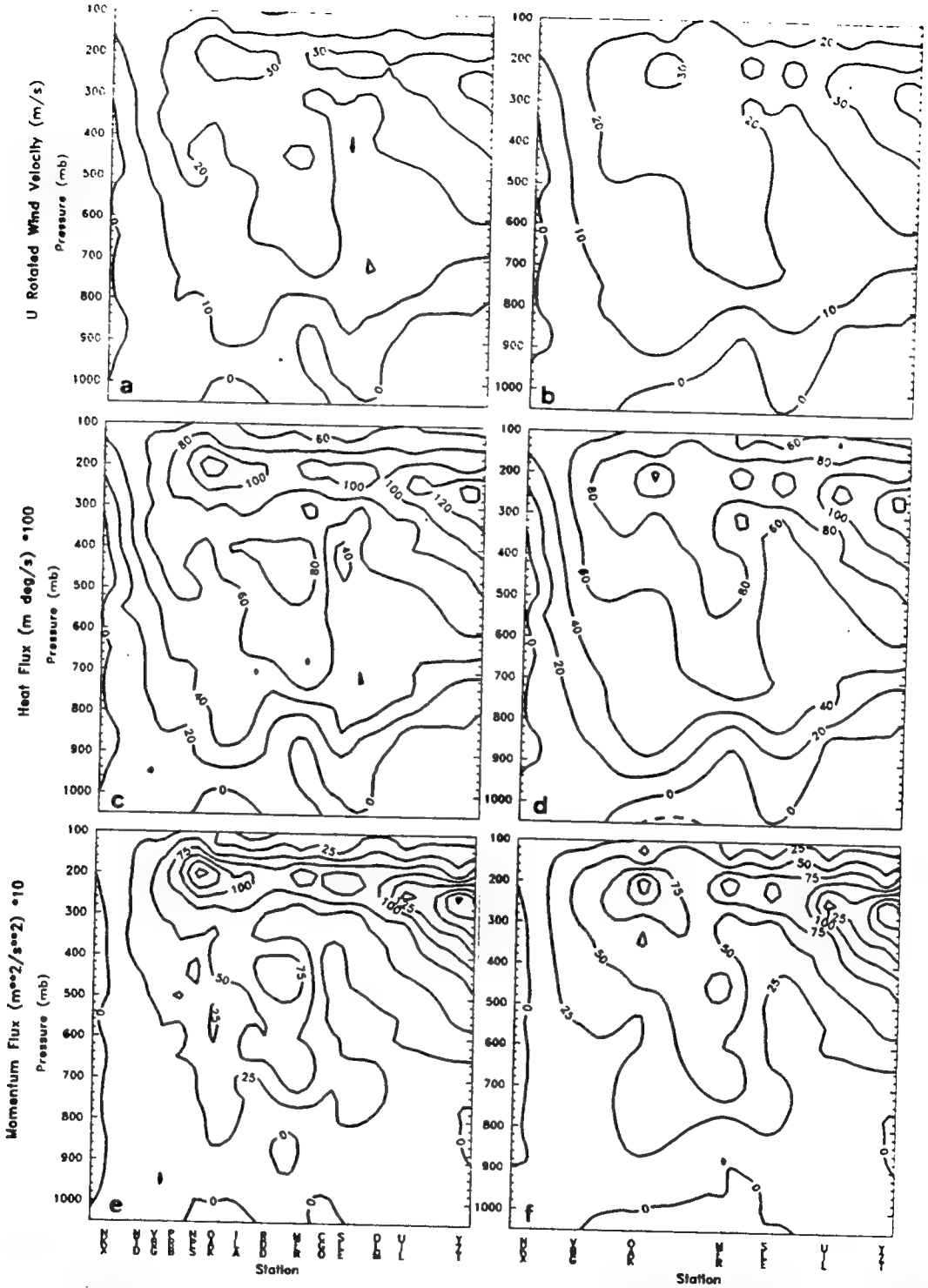


Fig. 10. 0000 UTC 20 Feb vertical cross sections of (a) ALL $U_r$, (b) NWS $U_r$, (c) ALL heat flux, (d) NWS heat flux, (e) ALL momentum flux, and (f) NWS momentum flux.

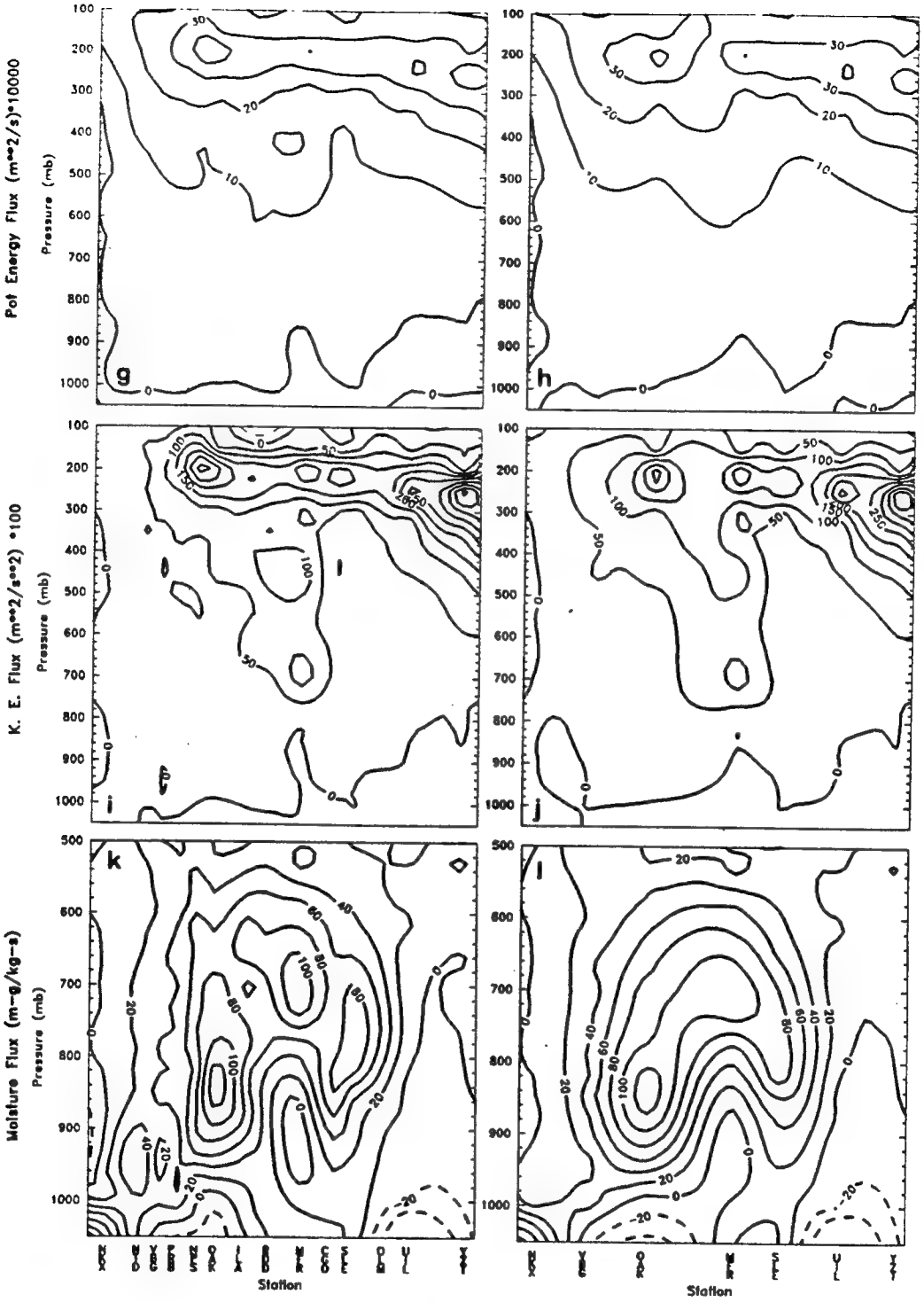


Fig. 10. (continued). 0000 UTC 20 Feb vertical cross sections of (g) ALL potential energy flux, (h) NWS potential energy flux, (i) ALL kinetic energy flux, (j) NWS kinetic energy flux, (k) ALL moisture flux, and (l) NWS moisture.

sections depict fluxes that are clearly related to the jet cores at 200 mb along the center of the Picket Fence axis for both the ALL and NWS stations. However, the ALL cross sections (Fig. 10 e,g, and i) better depict the locations and strengths of maximum fluxes in association with the 200 mb flow between OAK and YZT. The moisture flux (Fig. 10 k,l) is displayed only up to 500 mb since most of the moisture in the atmosphere is in the lower troposphere. The ALL cross section (Fig. 10 k) has three cores of >80 ms/kgs moisture flux between OAK and SLE, while only one such area between OAK and MFR is evident in the NWS cross section (Fig. 10 l). This extra detail in the ALL moisture flux may be important in forecasting precipitation and cloud cover for areas downstream.

Since the vorticity maximum associated with IOP-3 crossed the Picket Fence around 1200 UTC 20 Feb, the 0600 UTC cross sections (Fig. 11) represent the fluxes present as the system began to cross the Picket Fence. These cross sections also exhibit the most striking differences between the ALL and NWS soundings found in this study.

The $U_r$ wind component along the Picket Fence as resolved by the ALL cross section (Fig. 11 a) has a complex double jet structure near 250 mb with a >30 m/s center near PRB and a >40 m/s center near ILA. Although the corresponding NWS cross section (Fig. 11 b) has a similar pattern, it does not contain the structural detail and maximum wind speed (<30 m/s) that

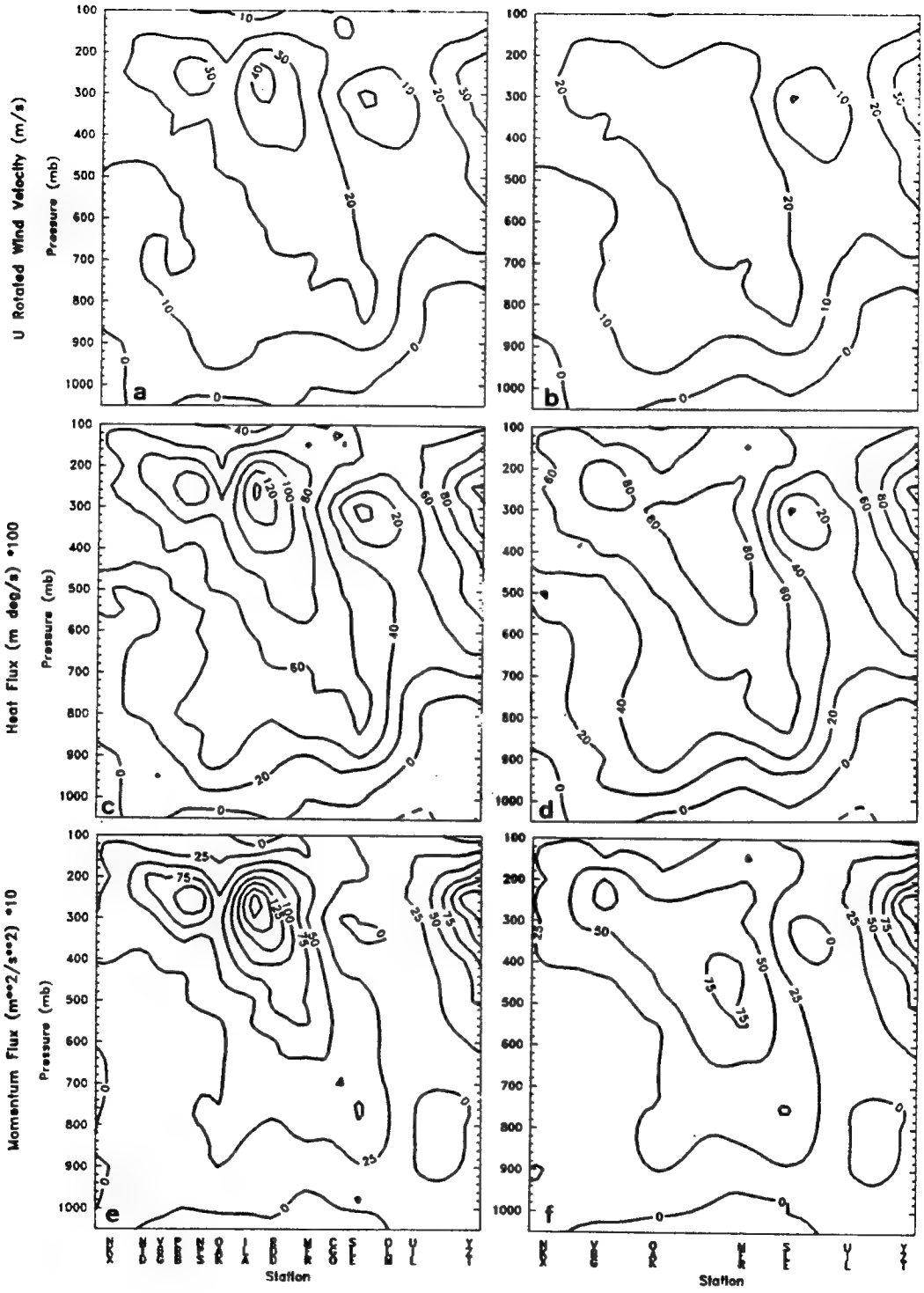


Fig. 11. As in Fig. 10 (a-f), except for 0600 UTC 20 Feb 1992.

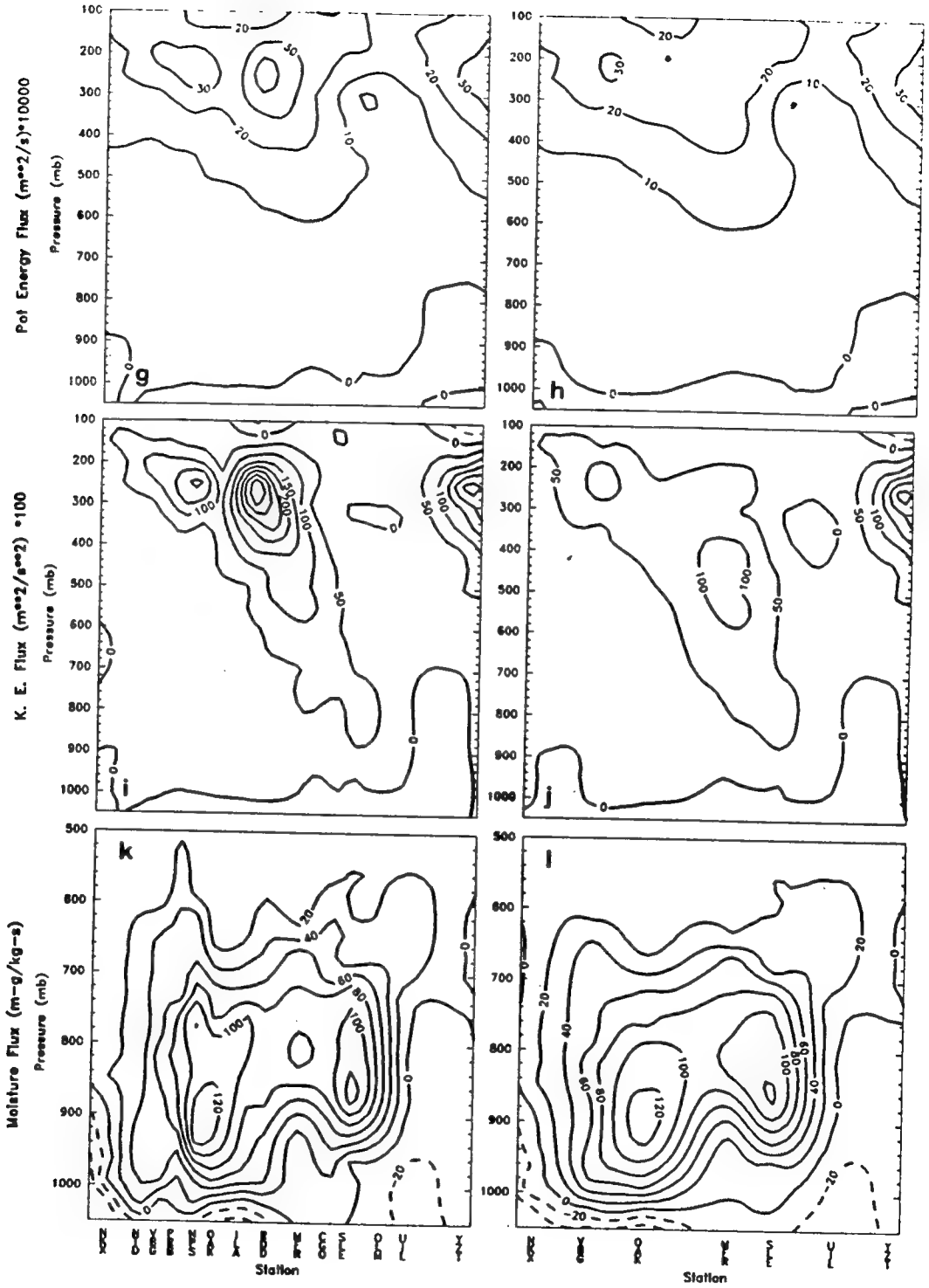


Fig. 11. (continued). As in Fig. 10 (g-l), except for 0600 UTC 20 Feb 1992.

the four special sites (PRB, NPS, ILA, and RDD) provide to the ALL analysis. Clearly, the definition of the double jetfeature over Northern California at this time is critically dependent on the soundings between VBG and MFR.

After considering the wind differences between the NWS and ALL analyses, it is not surprising to find considerable differences in the fluxes as well. The cross section of ALL heat flux (Fig. 11c) indicates a strong core (>140 m $^{o}$K $s^{-1}$) over ILA that is not evident in the corresponding NWS cross section (Fig. 11d). Similarly, the momentum (Fig. 11e), potential energy (Fig. 11g), and kinetic energy (Fig. 11i) ALL cross sections have maximum fluxes over ILA at the 300 mb level that are not present in the NWS cross sections (Figs. 11f, 11h, 11j).

Finally, both the ALL and NWS moisture flux (Fig. 11k,l) cross sections have maximum fluxes between 900 mb and 750 mb. Similar to the earlier time (0600 UTC), the ALL moisture flux analyses appear more detailed. However, since the differences in the ALL and NWS $U_r$ wind components are minimal below 500 mb (Fig. 11 a,b), the locations and strength of the moisture fluxes are similar as well with maxima over OAK and SLE.

The ALL and NWS cross sections at 1800 UTC 20 Feb (Fig. 12) are representative of the fluxes present after the system passed the Picket Fence axis. Cursory inspection of these cross sections suggest that the differences between the ALL and NWS are similar to the time before system passage (0000

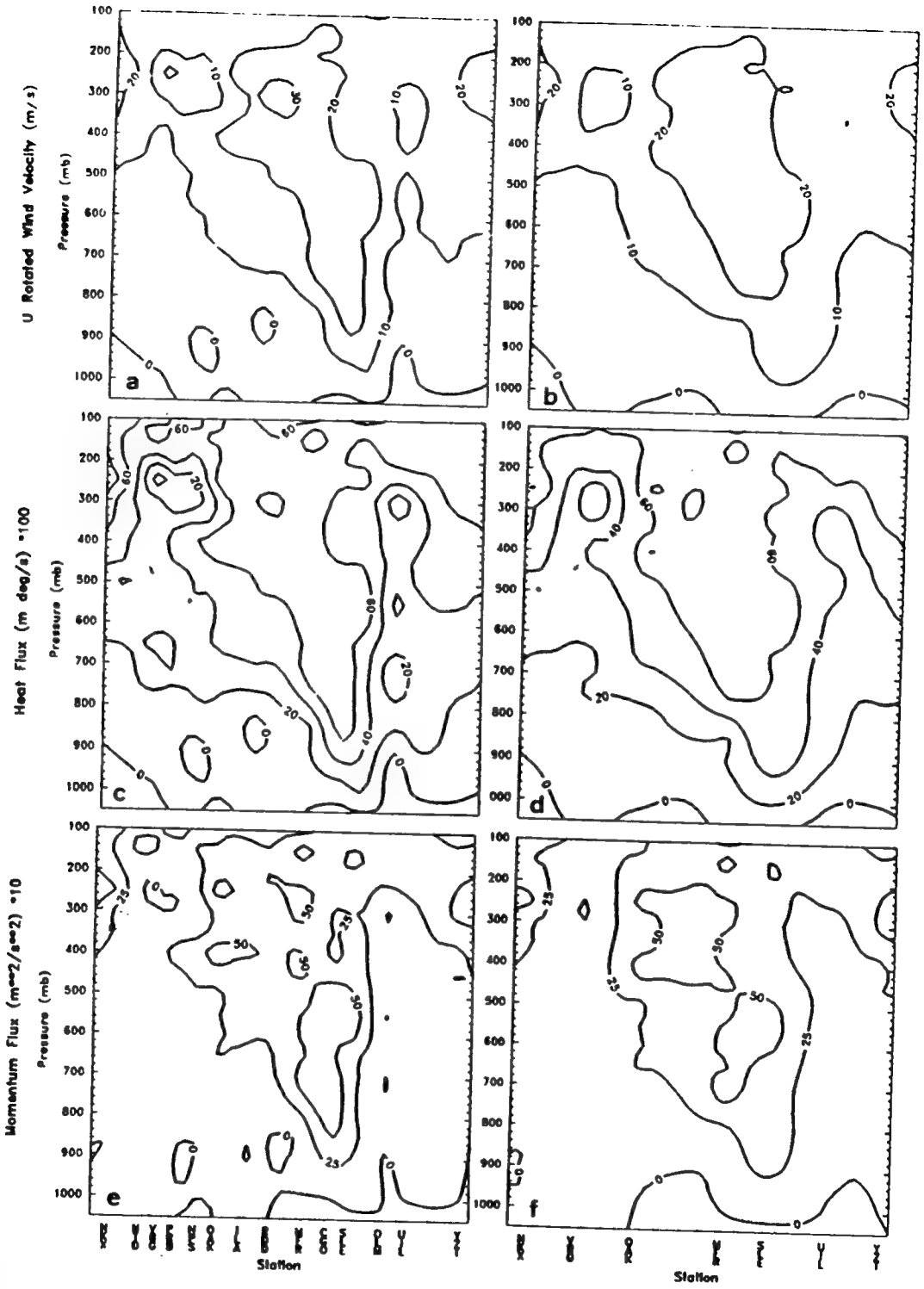


Fig. 12. As in Fig. 10 (a-f), except for 1800 UTC 20 FEB 1992.

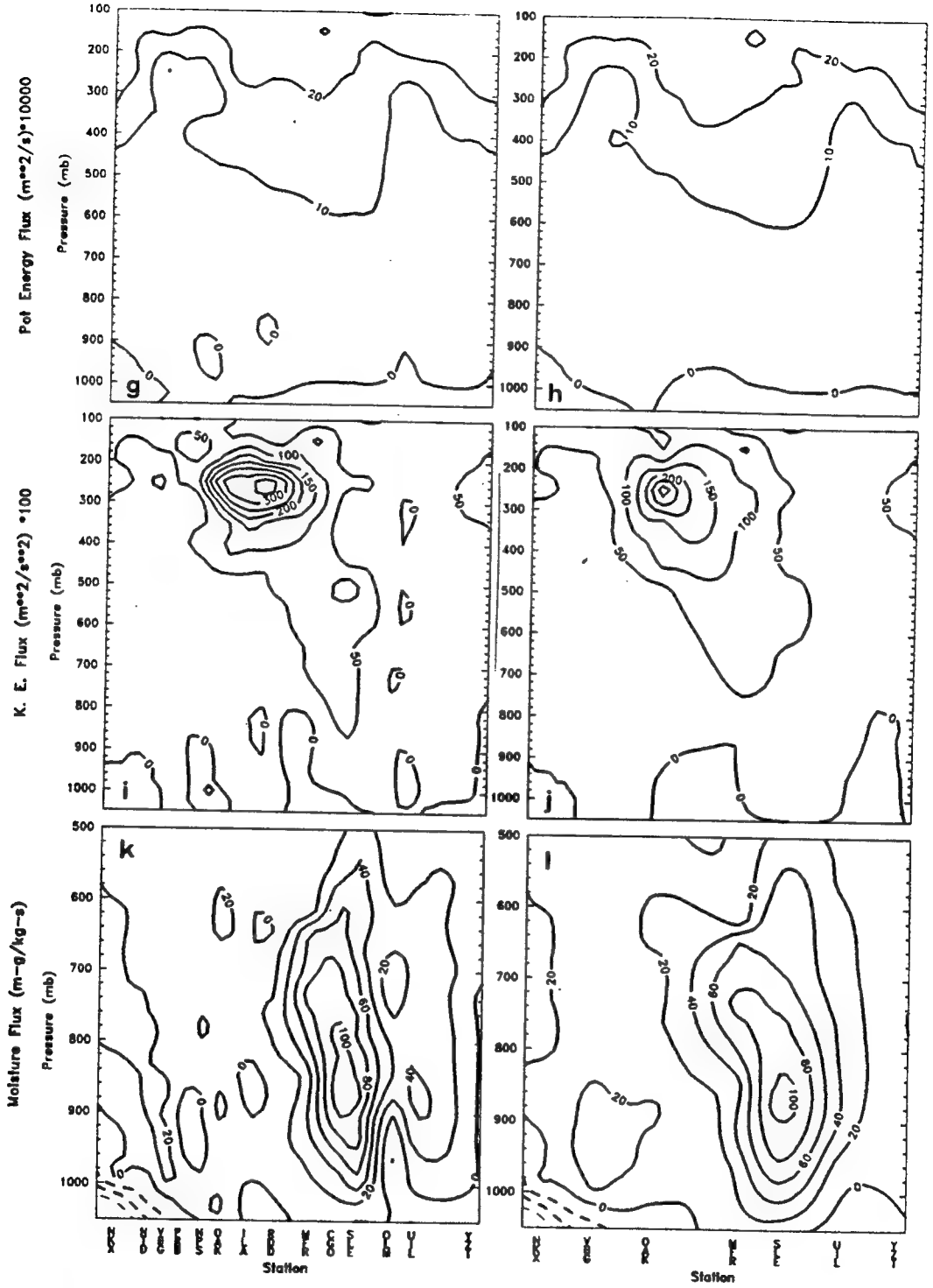


Fig. 12. (continued). As in Fig. 10 (g-l), except for 1800 UTC 20 FEB 1992.

UTC 20 Feb, Fig. 10) and not as striking as when the system passed over the coast (0000 UTC 20 Feb, Fig. 11). Specifically, the mass flux differences in the ALL (Fig. 12a) and NWS (Fig. 12b) cross sections are much smaller than at 0600 UTC 20 Feb (Fig. 11a,b). Although the $U_r$ component of the wind in the ALL cross section indicates jets over ILA and NTD, the maximum wind speeds are weaker (>30 m/s and >20 m/s, respectively) than at 0600 (>40 m/s and >30 m/s, respectively). The NWS cross section (Fig. 12b) has a similar pattern over these locales, but the maxima are less intense with the well-defined ALL jet core near 250 mb over ILA not even evident.

The cross sections of heat (Fig. 12c,d), momentum (Fig. 12e,f), potential energy (Fig. 12g,h), and kinetic energy (Fig. 12i,j) flux also show that the ALL analyses have higher flux values near 250 mb over the special sites between VBG and MFR. Without the data from the special sites in the central area of the Picket Fence, the NWS analyses do not have adequate horizontal resolution to resolve possibly important flux structures that the ALL soundings provide. Furthermore, the moisture flux in the ALL cross section (Fig. 12 k) has a distinct minimum over the OLM site, which makes the moisture core over SLE and CGO at 850 mb narrower and more confined than is indicated by the NWS cross section (Fig. 12 l). Without the adjacent special sites, the NWS cross section depicts a larger core over SLE.

In general, these spatial results suggest that the wind and flux patterns accompanying systems that cross the central west coast can be more fully defined with the increased horizontal resolution provided by the special Picket Fence sites. That new information is also obtained by increasing the frequency of data collection during these passages is illuminated by contrasting the 3-h evolution of the mean wind and fluxes across the Picket Fence with the 12-h NWS standard during IOP-3 (Fig. 13). The mean values of the $U_r$-wind component and the five quantities are computed by averaging over the 460 equally mass-weighted points contained in the 3-h ALL and NWS Picket Fence cross section grids. Clearly, both the 3-h ALL and NWS means have high frequency variations in the fluxes crossing the coast compared to the 12-h NWS standard (Fig. 13). For example, the rapid decrease in the quantities (except moisture flux) between 3 and 6 h and the increase between 6 and 9 h are not evident in the 12-h NWS trends. Likewise, the concavity of the 3 h flux trends between 9 and 24 h is not captured in the 12-h NWS standard. Therefore, the 12-h NWS soundings may not capture possibly significant subsynoptic-scale pulses of energy that cross the coast during a trough passage.

B. SYSTEMS THAT CROSS THE PERIPHERY OF THE PICKET FENCE

In contrast to IOP-3, IOPs 1, 2, and 4 were characterized by circulation features that crossed the west coast at or near the southern end of the Picket Fence. For this reason, they

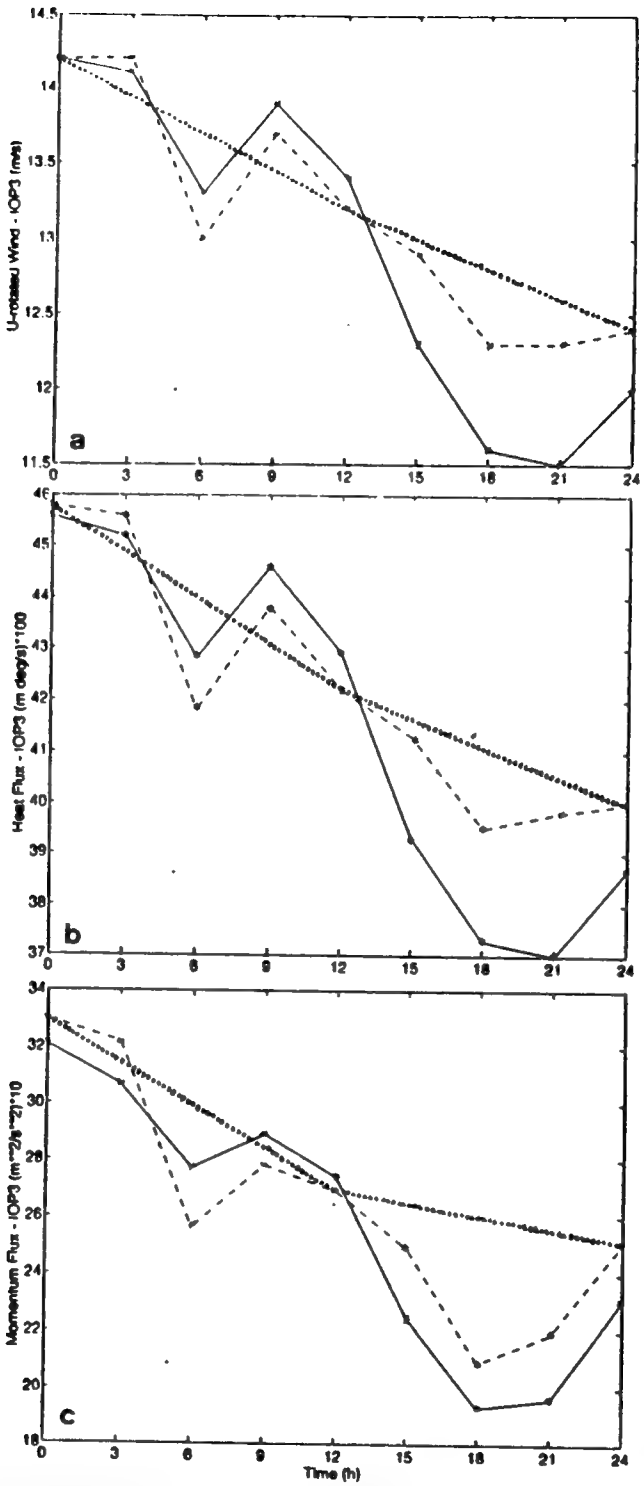


Fig. 13. Mean-cross-sectional value of (a) $U_r$, (b) heat flux, and (c) momentum flux as a function of time during IOP-3. Asterisks denote data points. The solid and dashed lines denote 3-hourly evolution for ALL and NWS sites, respectively. The dotted lines denote 12-hourly evolution for NWS sites.

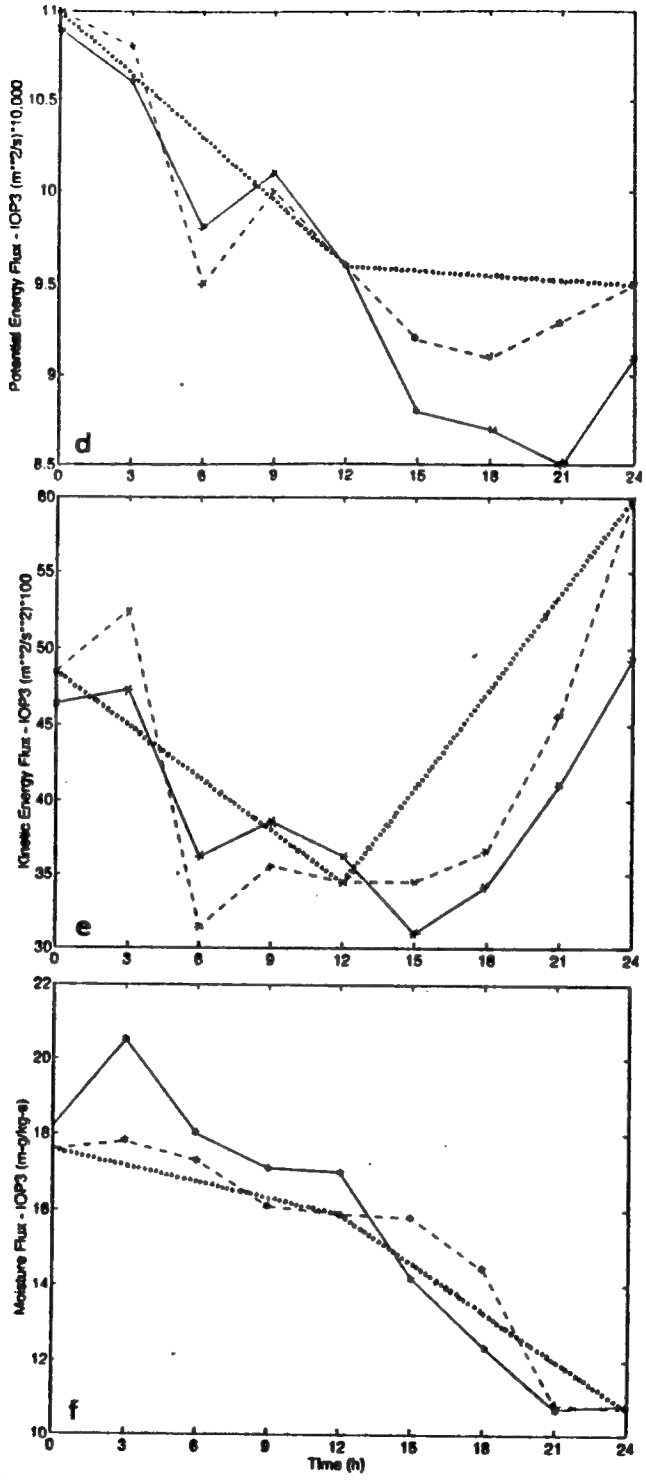


Fig. 13 (continued). As in Fig. 13 (a-c) except (d) potential energy flux, (e) kinetic energy flux, and (f) moisture flux.

represent an opportunity to investigate the utility of the Picket Fence concept when systems pass along the edge of the special observing network. In particular, spatial and temporal differences between the fluxes during IOP-4 will be examined.

As discussed in Chapter V, IOP-4 was the longest Picket Fence IOP. The upper-level wave system that crossed the coast during this time was later associated with significant weather in the STORMFEST area. Indeed, this was the first real winter-type event during STORMFEST and proved to be the highlight of the experiment. As shown in Fig. 9, IOP-4 featured a slow moving upper-level trough and jet system that dipped over the Baja Peninsula south of the Picket Fence. Unfortunately, the main 500-mb vorticity maximum crossed the Picket Fence near the California-Mexico border, after the IOP had been completed, at 1800 UTC March.

Spatial differences between the ALL and NWS wind and flux quantities at 1200 UTC 5 March are representative of other times during IOP-4 and will be the only one discussed here. The remainder of the cross sections are provided in the Appendix to document fully the results. In contrast to the IOP-3 comparisons, the 1200 UTC 5 March cross sections (Fig. 14) show little difference between the NWS and ALL flux analyses. Most significantly, the 200 mb jet maximum south of NKX is similarly identified in both the ALL (Fig. 14a) and NWS (Fig. 14b) cross sections. This similarity is due to the

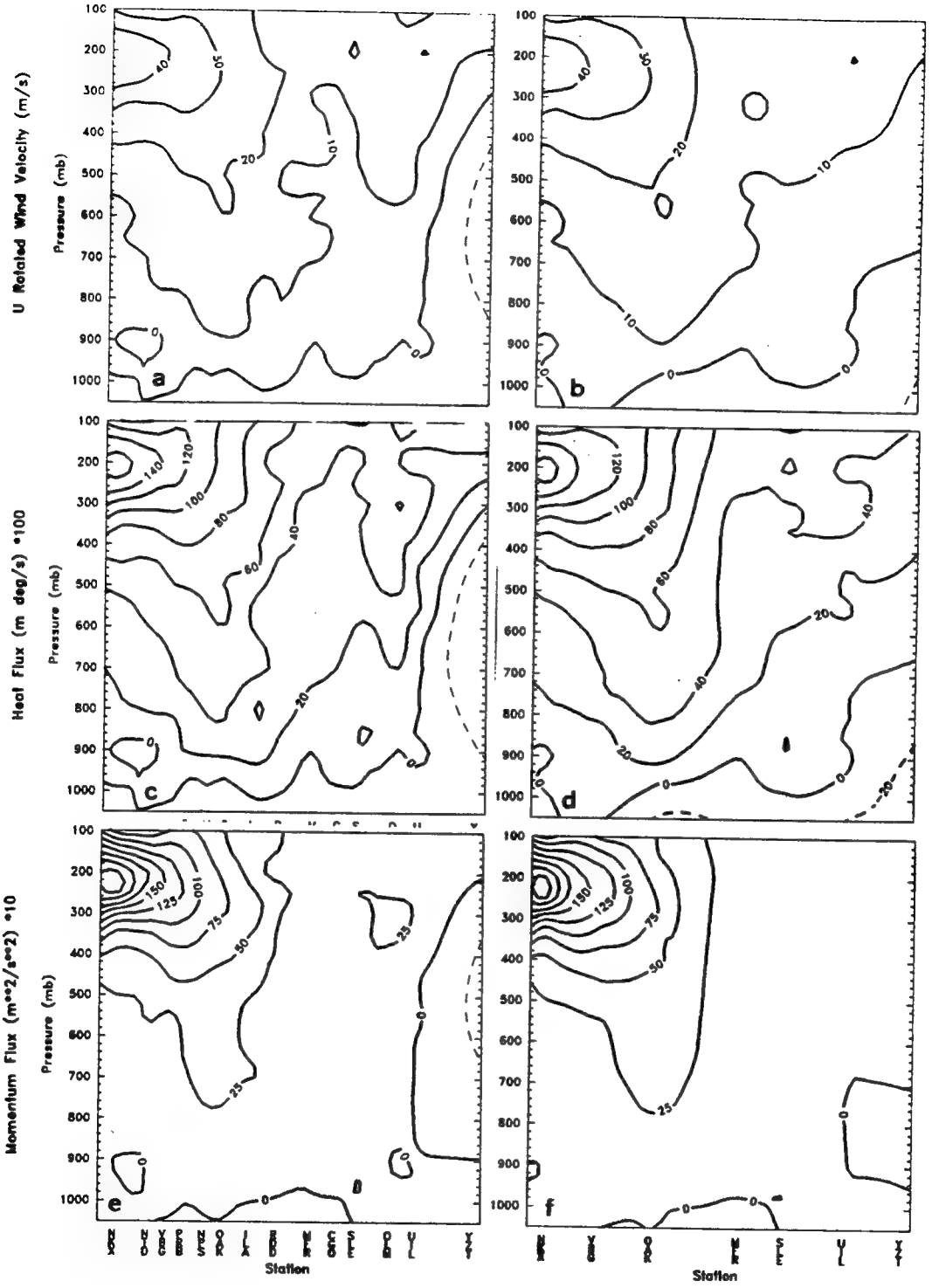


Fig. 14. As in Fig. 10 (a-f), except for 1200 UTC 5 Mar 1992.

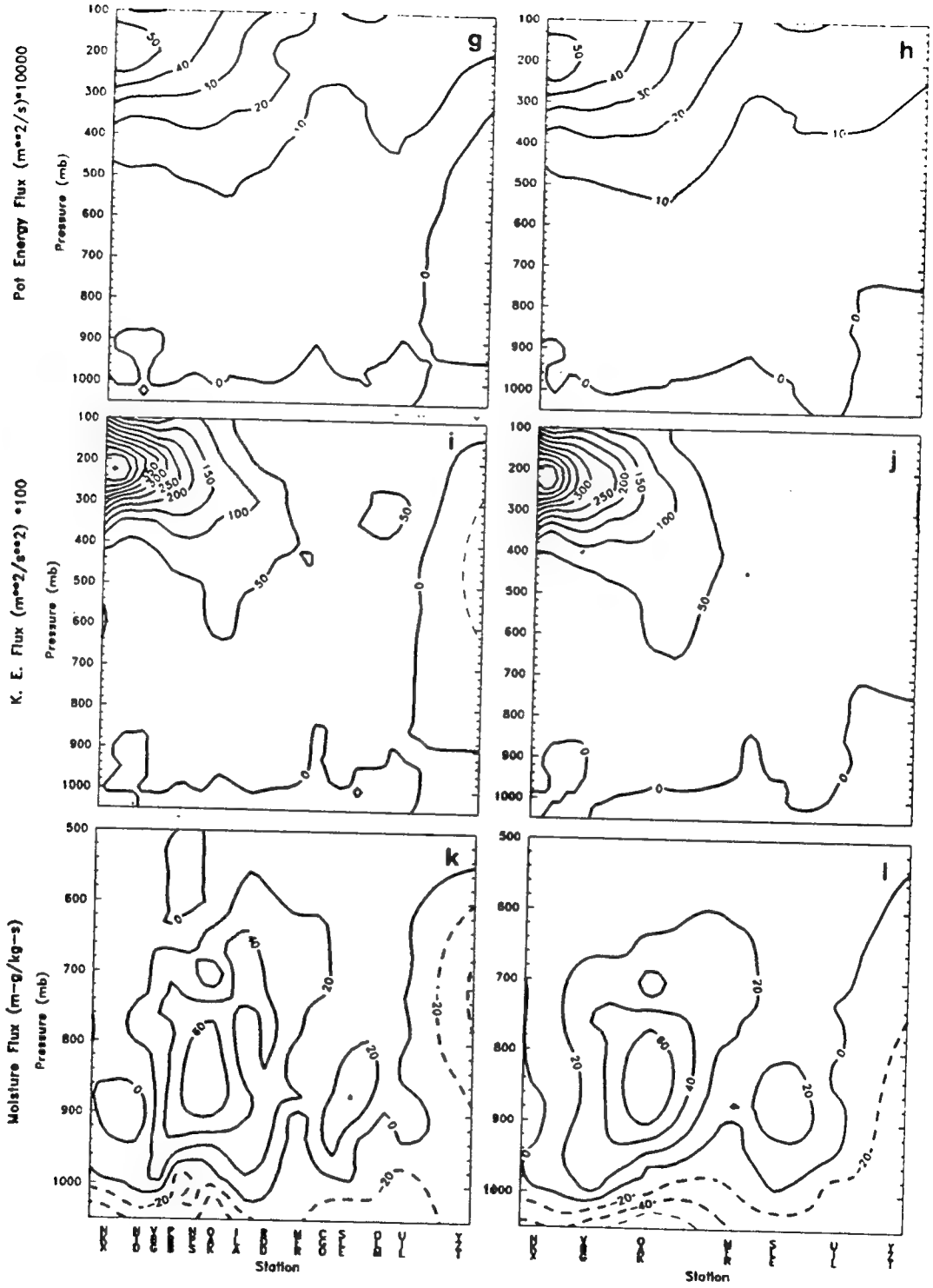


Fig. 14. (continued). As in Fig. 10 (g-l), except for 1200 UTC 5 Mar 1992.

strong influence of the NWS station (NKX) at the southern border of the Picket Fence, which in this case is closest to the circulation feature. Since, in addition, two of the three southern most stations are also NWS, it is not surprising that the NWS and ALL cross sections display only small structural differences in the westerly jet at the southern ends of the sections. Interestingly, the remaining portions of the cross sections also have little wind differences. The largest disparity between the ALL and NWS data are in the region above the special stations in the middle of the cross sections (between VBG and SLE). Although no significant mesoscale or synoptic feature is apparently present, the special sites in this region (Fig. 14a) do add structure not evident in the NWS cross section (Fig. 14b).

Not surprisingly, the flux patterns are similar to the $U_r$ patterns. Therefore, the ALL and NWS heat (Fig. 14c,d), momentum (Fig. 14e,f), potential energy (Fig. 14g,h), and kinetic energy (Fig. 14i,j) fluxes have similar values over NKX, with maxima centered around 150 mb in conjunction with the subtropical jet. Likewise, the remaining portions of the cross sections have little significant flux differences between the ALL and NWS. Since these results are representative of other times during IOP-4, and during IOPs 1 and 2 (see Appendix), they suggest that the additional special stations do not provide as much useful information during

peripheral trough passage as they do during more central passage over the Picket Fence.

The temporal variations in the fluxes during IOP-4, as indicated by the evolution of the mean cross section values (Fig. 15), have little high frequency behavior, especially in comparison to the IOP-3 results (Fig. 13). In particular, the 3-hourly mean $U_r$ wind component (Fig. 15a), heat (Fig. 15b), and potential energy (Fig. 15d) fluxes indicate only slight differences between the ALL and NWS and have linear trends that the 12-hourly NWS can resolve. Although the mean momentum (Fig. 15c), kinetic energy (Fig. 15e), and moisture (Fig. 15f) fluxes do display slightly more temporal variations than the other fluxes, the 3-h values do not obviously add much information beyond what the 12-h NWS observations provide.

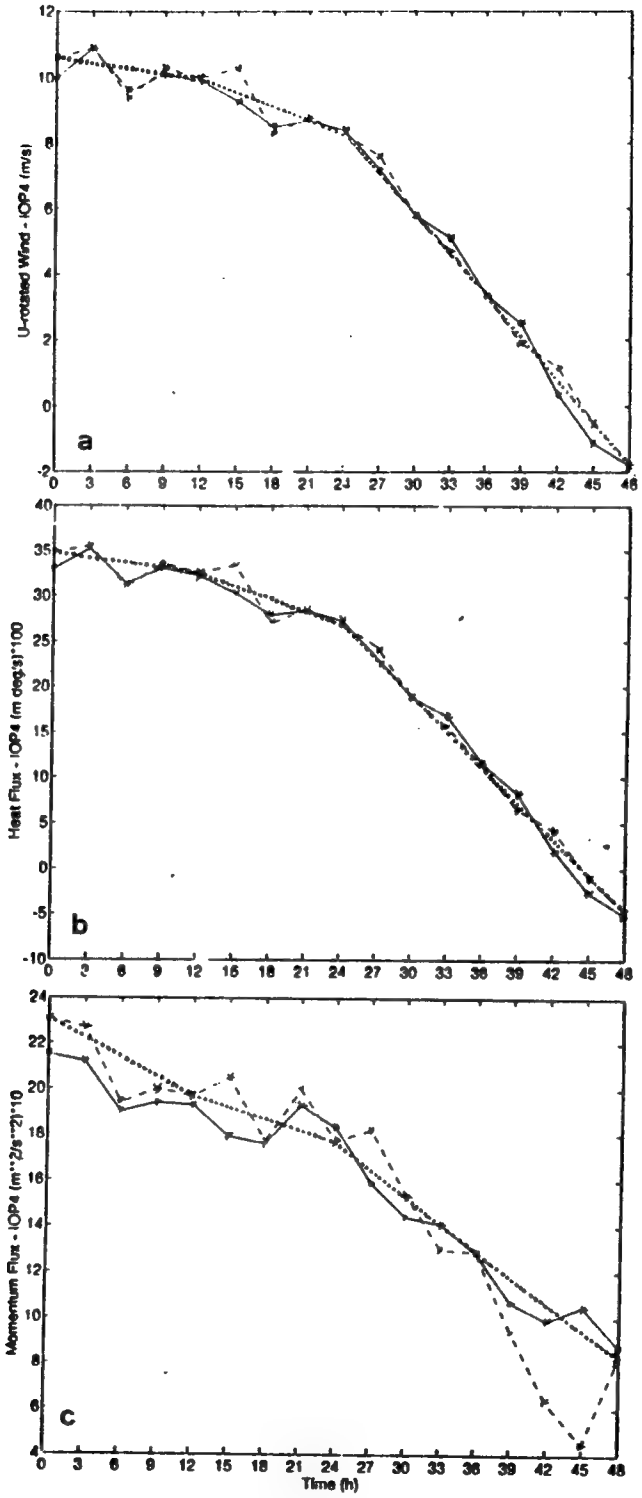


Fig. 15. As in Fig. 13 (a-c), except for IOP-4.

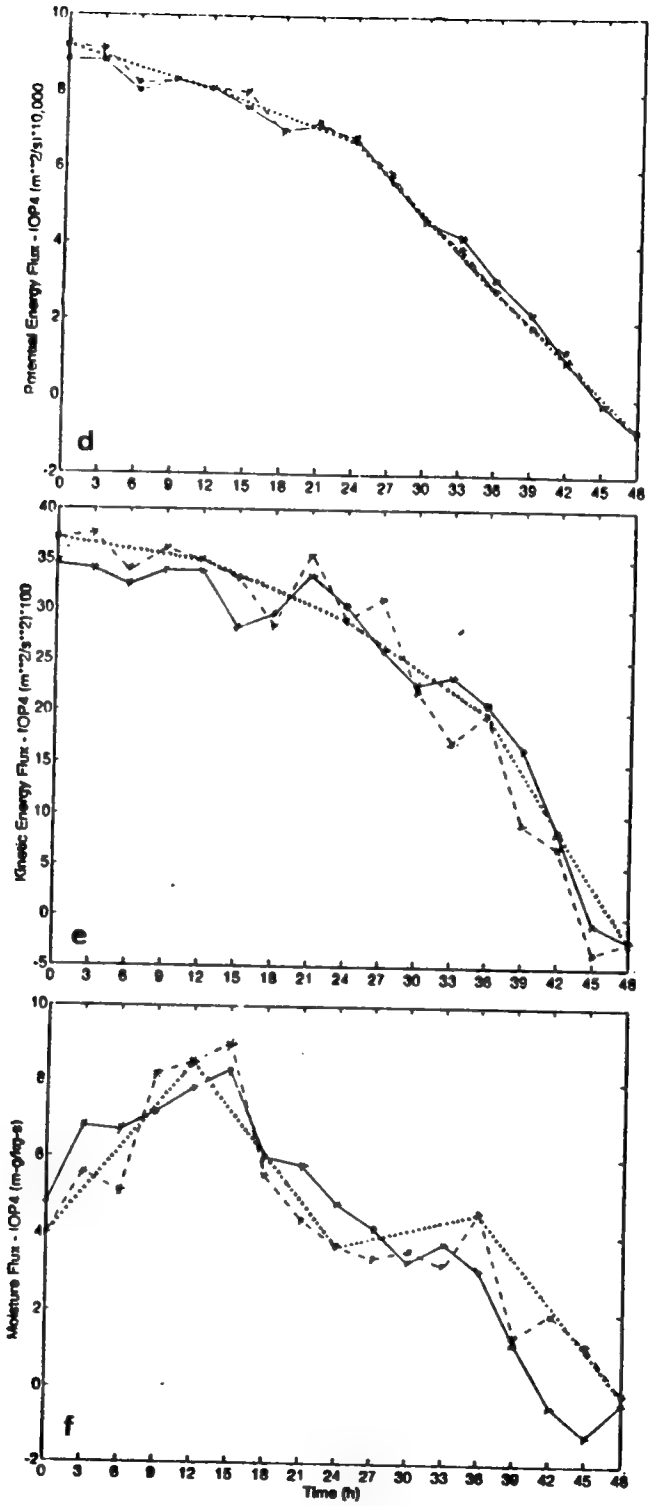


Fig. 15. (continued). As in Fig. 13 (a-c), except for IOP-4.

## VII. CONCLUSIONS AND RECOMMENDATIONS

The scientific hypothesis behind the Picket Fence experiment is that a high resolution, quasi-linear array of extra observations along the west coast can improve the upstream boundary conditions for forecasts of mesoscale weather events in the Central U.S. This study demonstrated that new flux information is indeed obtained when extra spatial and temporal observations are taken, at least when the main synoptic feature crosses the middle of the observation network. In particular, the IOP-3 results suggest that the increased spatial resolution, primarily between Vandenberg, CA and Salem, OR, allow the magnitude and location of the main circulation features to be better defined, especially when the system is just passing over the coast. In addition, the increased temporal resolution provided by the 3-h soundings result in the identification of high frequency variations in the fluxes accompanying the passage of the system that are not picked up by the 12-h NWS only analysis. It should be noted that these data are only flux calculations, and not a full four-dimensional data assimilation, which may make better use of the 3-h or 6-h soundings.

Conversely, the IOP-4 results suggest that when the main circulation center crosses the coast near the periphery of the observational network, little difference is detected between the ALL and NWS analysis. In such cases, NWS-only soundings appear to be adequate in analyzing the atmospheric conditions

and boundary fluxes across the west coast of the U.S., simply because there are no significant features for the special stations to detect. An obvious conclusion from this is that a larger Picket Fence, that included more stations south of San Diego (NKX), and north of Port Hardy (YZT), is needed to capture subtropical jet events over the Baja Peninsula and trough passages over western Canada. A longer Picket Fence probably would have shown differences between ALL and NWS fluxes during IOP-4 comparable to those obtained in IOP-3. Another conclusion is that when conditions are relatively quiescent, no additional observations beyond the 12-h NWS sites are necessary to define the boundary fluxes.

This study did not attempt to demonstrate that the extra observations had a downstream forecast impact. Clearly, the quantitative influence of the added resolution on analysis and forecasting downstream needs to be studied. Nevertheless, the boundary flux results presented here suggest that downstream errors may be incurred by not adequately defining features crossing the west coast that have smaller scales than are compatible with the current NWS observational network. In the future, analyses and forecasts with a modern four-dimensional data assimilation and modeling system should be used to compare the impact of the special data against the current 12-h sounding network to see if the poorly resolved boundary fluxes are significant.

It is also recommended that future analysis and forecast studies include potential vorticity flux calculations across the west coast Picket Fence. Potential vorticity could not be estimated from the Picket Fence data since only one-dimensional horizontal gradients along the Picket Fence could be estimated. The along-stream gradients require a two-dimensional analysis. Such potential vorticity fluxes may assist in tracing the features downstream and contribute to understanding the role of upper-level circulations in triggering mesoscale weather over the midwest U.S.

Finally, the ultimate application of the Picket Fence concept would be to have a permanent set of ground-based profiling instruments around the U.S. coast and borders that would continuously observe the winds, temperatures, humidities, etc. Given an appropriate horizontal spacing between stations, a permanent Picket Fence system could continually monitor the boundary fluxes of energy, mass, momentum, humidity, etc., and provide instantaneous information about the boundary flow. This Picket Fence approach to specifying upstream conditions may be more accurate and cost effective than other approaches in producing improved mesoscale weather prediction.

## REFERENCES


Anthes, R. A., 1983: Regional models of the atmosphere in middle latitudes. *Mon. Wea. Rev.*, **111**, 1306-1335.

Anthes, R.A., 1986: The general question of predictability. Chap. 27, Mesoscale Meteorology and Forecasting. P.S. Ray, Ed., Amer. Meteor. Soc., Boston, MA, 636-658.

Baker, N.L., 1991: Quality control of meteorological observations for the Fleet Numerical Oceanography Center Operational Atmospheric Database. Technical Note 124, Navy Oceanographic and Atmospheric Research Laboratory, Monterey, CA 93943-5000, 53 pp.

Bjerknes, V., 1919: Wettervorhersage. *Meteor. Z.*, **36**, 68.

Cunning, J. B., and S.F. Williams, 1993: STORMFEST Operations Summary and Data Inventory. Available from U.S. Weather Research Program Office, NOAA, 325 Broadway, Boulder, CO 80303.

Fuelberg, H.E., and J.R. Scoggins, 1978: Kinetic energy budgets during the life cycle of intense convective activity. *Mon. Wea. Rev.*, **106**, 637-653.

Lind, R.J., P.A. Hirschberg, D.W. Titley, and R.L. Elsberry, 1992: West Coast Picket Fence Feasibility Study During STORMFEST Field Program Summary. Tech. Rep., NPS-MR-92-003, Naval Postgraduate School, Monterey, CA. 140pp.

Orlanski, I., 1975: A rational subdivision of scales for atmospheric processes. *Bull. Amer. Meteor. Soc.*, **56**, 527-530.

Ross, B. B., 1986: An overview of numerical weather prediction. Chap. 30, Mesoscale Meteorology and Forecasting. P.S. Ray, Ed., Amer. Meteor. Soc., Boston, MA, 720-751.

Sanders, F., 1987: Skill of NMC operational models in prediction of explosive cyclogenesis. *Wea. and Forecasting*, **2**, 322-336.

Sanders, F.; and E.P. Auciello, 1989: Skill in prediction of explosive cyclogenesis over the western North Atlantic Ocean, 1987/88: A forecast checklist and NMC dynamical models. *Wea. and Forecasting*, **4**, 157-172.

Smith, P.J., 1980: The energetics of extratropical cyclones. *Rev. Geophy.*, **18(2)**, 378-386.

STORM, 1991: Winter/Spring Multiscale Experiment Design. Available from STORM Project Office, NCAR, P.O. Box 3000, Boulder, CO 80307.

STORMFEST Operations Plan, 1992: Available from STORM Project Office, NCAR, P.O. Box 3000, Boulder, CO 80307.

Thomson, D.W., 1986: Systems for measurements at the surface. Chap. 5, Mesoscale Meteorology and Forecasting. P.S.Ray, Ed., Amer. Meteor. Soc., Boston, MA, 71-84.

Young, T.L.; and M.L. Van Woert, 1987: Plot88 Software Library Reference Manual, ZGRID Subroutine. Plotworks, Inc., La Jolla, CA, 274pp.

## APPENDIX

Cross sections as in Fig. 10 for IOPs 1 and 2, and for launch times of IOP 3 and 4 not discussed in text, are enclosed. Cross section mean fluxes with time as in in Figs. 13 and 15 are also provided for IOPs 1 and 2.

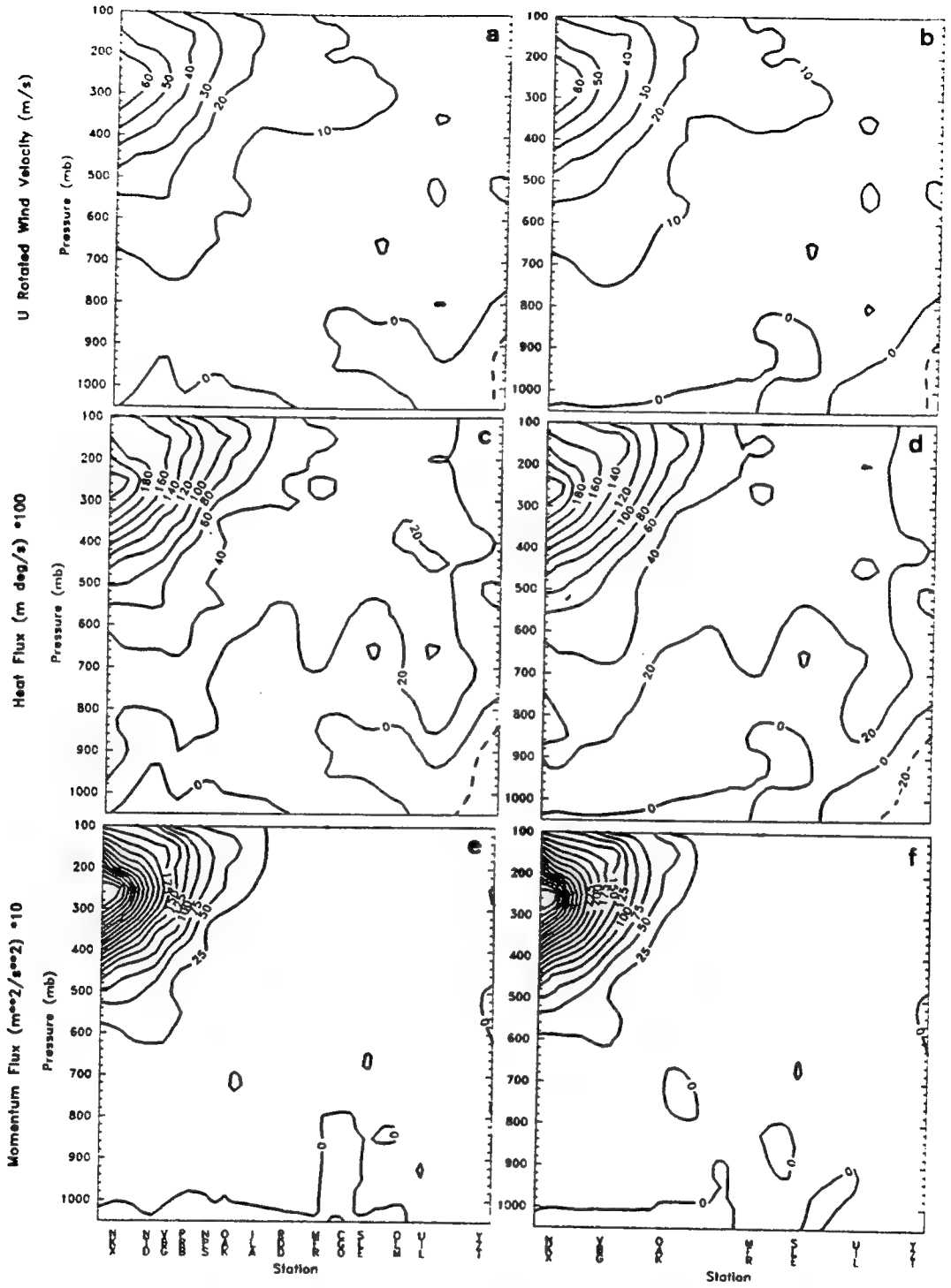


0600 UTC 13 Feb vertical cross sections for (a) ALL $U_r$ flux, (b) NWS $U_r$ flux, (c) ALL heat flux, (d) NWS heat flux, (e) ALL momentum flux, and (f) NWS momentum flux.

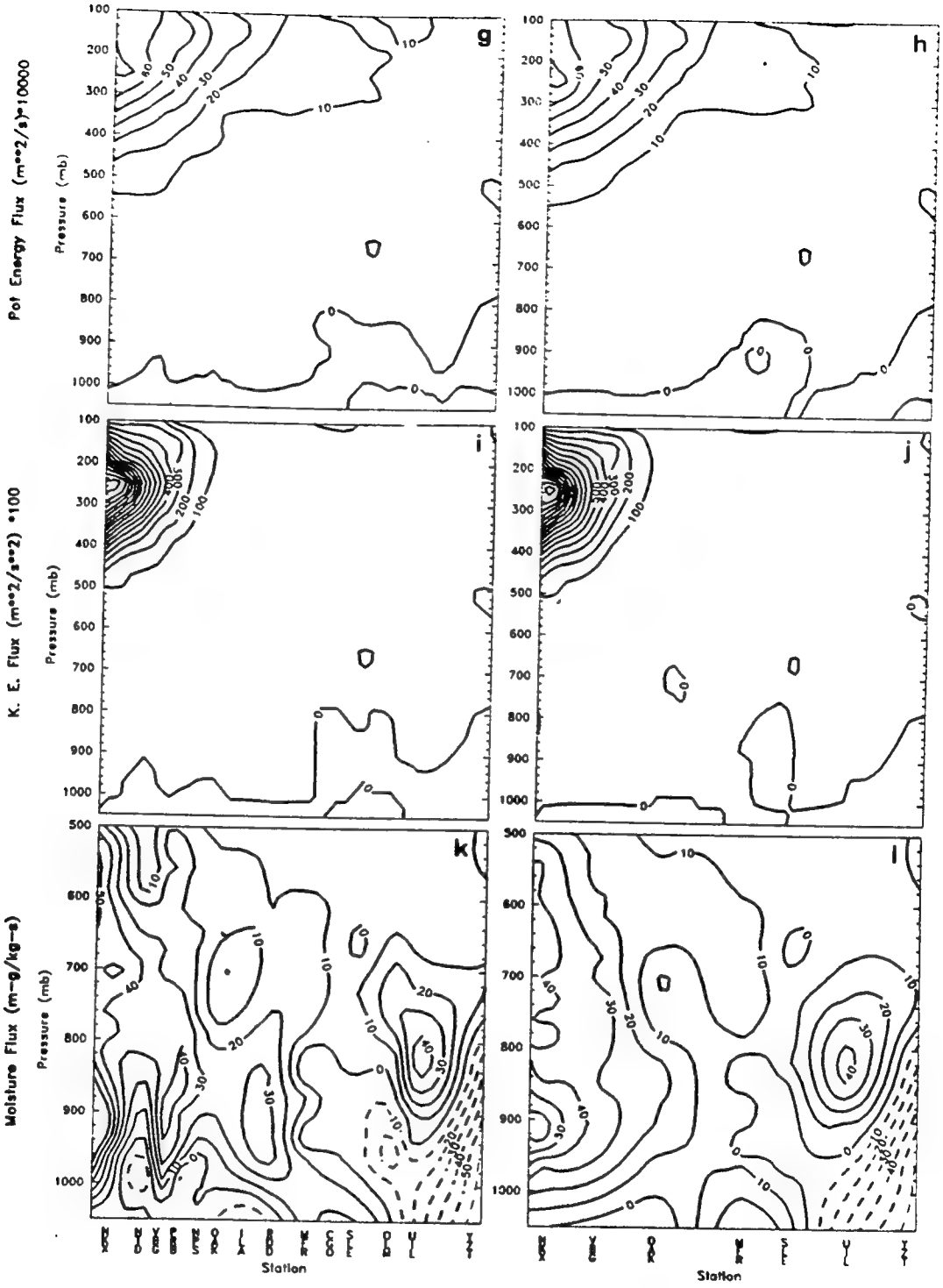


0600 UTC 13 Feb vertical cross sections for (g) ALL potential energy flux, (h) NWS potential energy flux, (i) ALL kinetic energy flux, (j) NWS kinetic energy flux, (k) ALL moisture flux, and (l) NWS moisture.

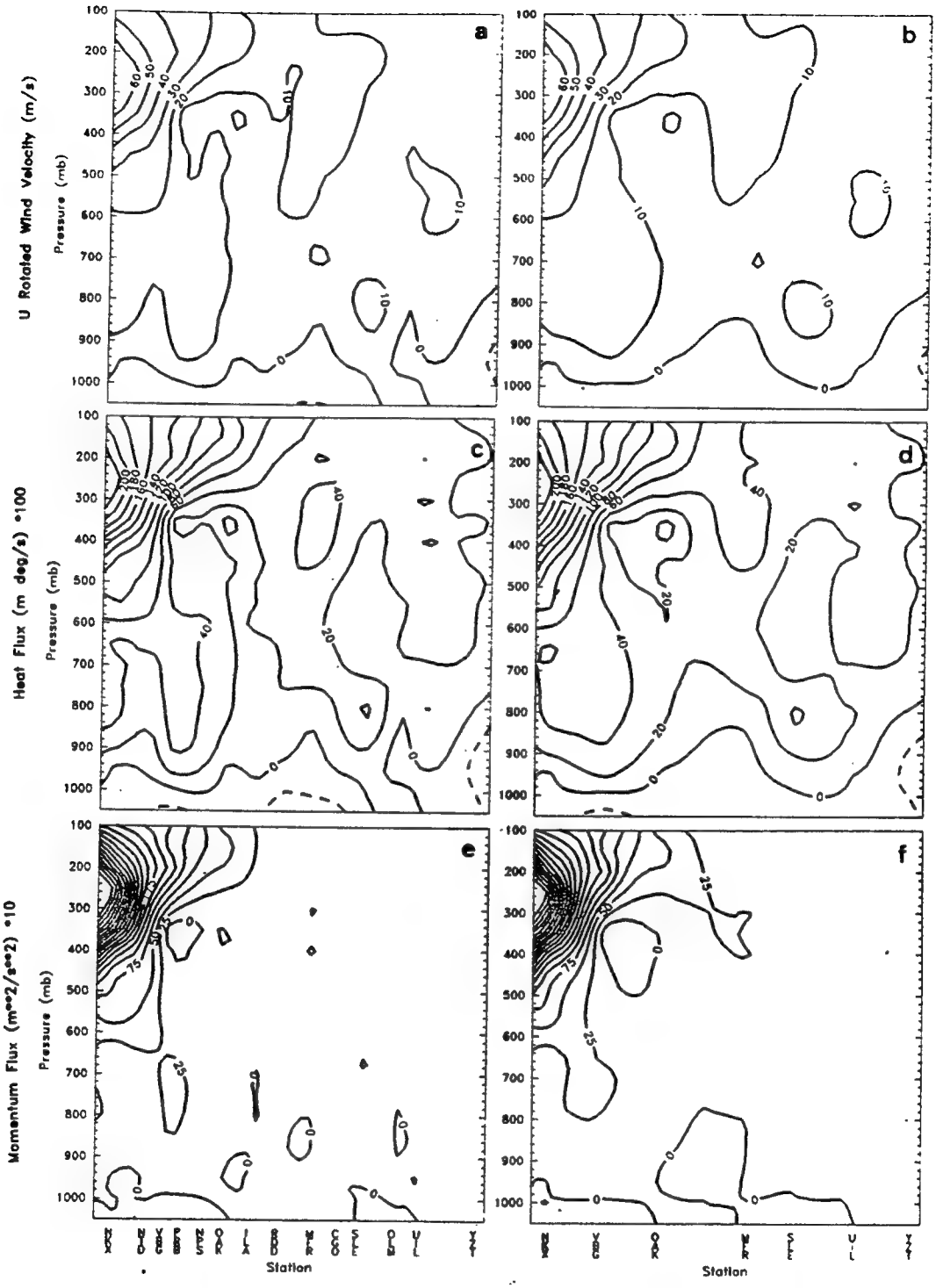


0900 UTC 13 Feb vertical cross sections for (a) ALL $U_r$ flux, (b) NWS $U_r$ flux, (c) ALL heat flux, (d) NWS heat flux, (e) ALL momentum flux, and (f) NWS momentum flux.

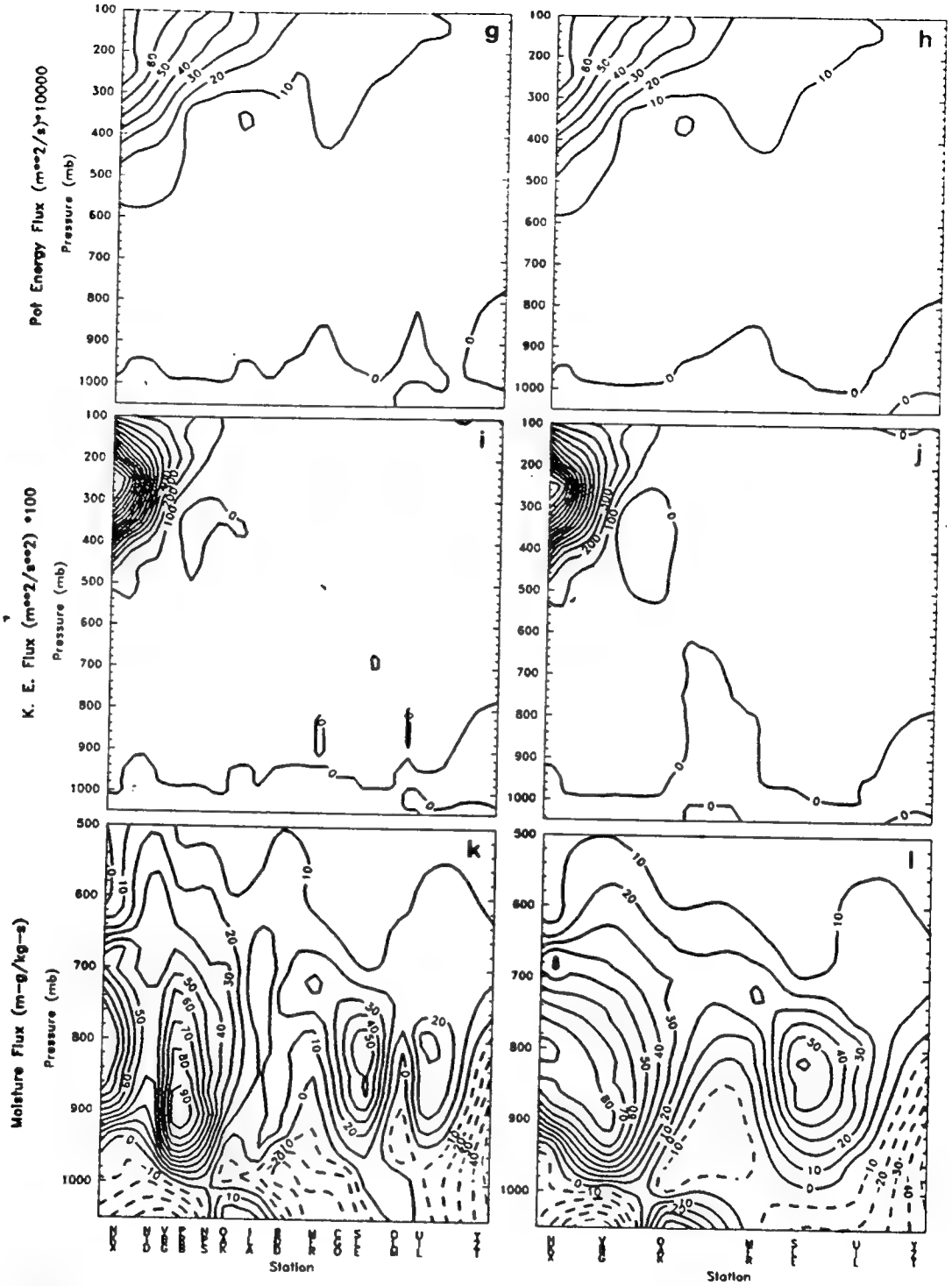


0900 UTC 13 Feb vertical cross sections for (g) ALL potential energy flux, (h) NWS potential energy flux, (i) ALL kinetic energy flux, (j) NWS kinetic energy flux, (k) ALL moisture flux, and (l) NWS moisture.

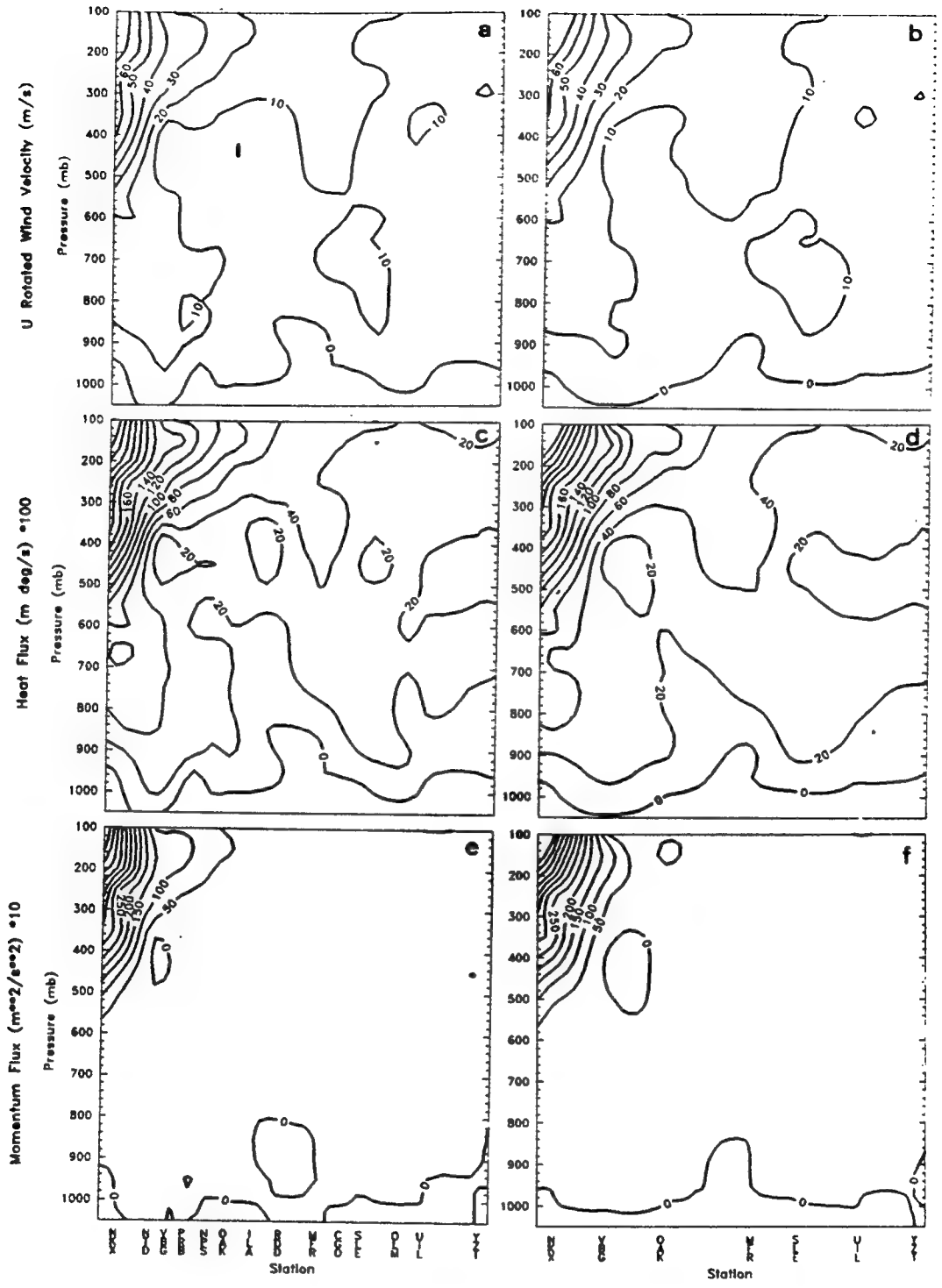


1200 UTC 13 Feb vertical cross sections for (a) ALL $U_r$ flux, (b) NWS $U_r$ flux, (c) ALL heat flux, (d) NWS heat flux, (e) ALL momentum flux, and (f) NWS momentum flux.

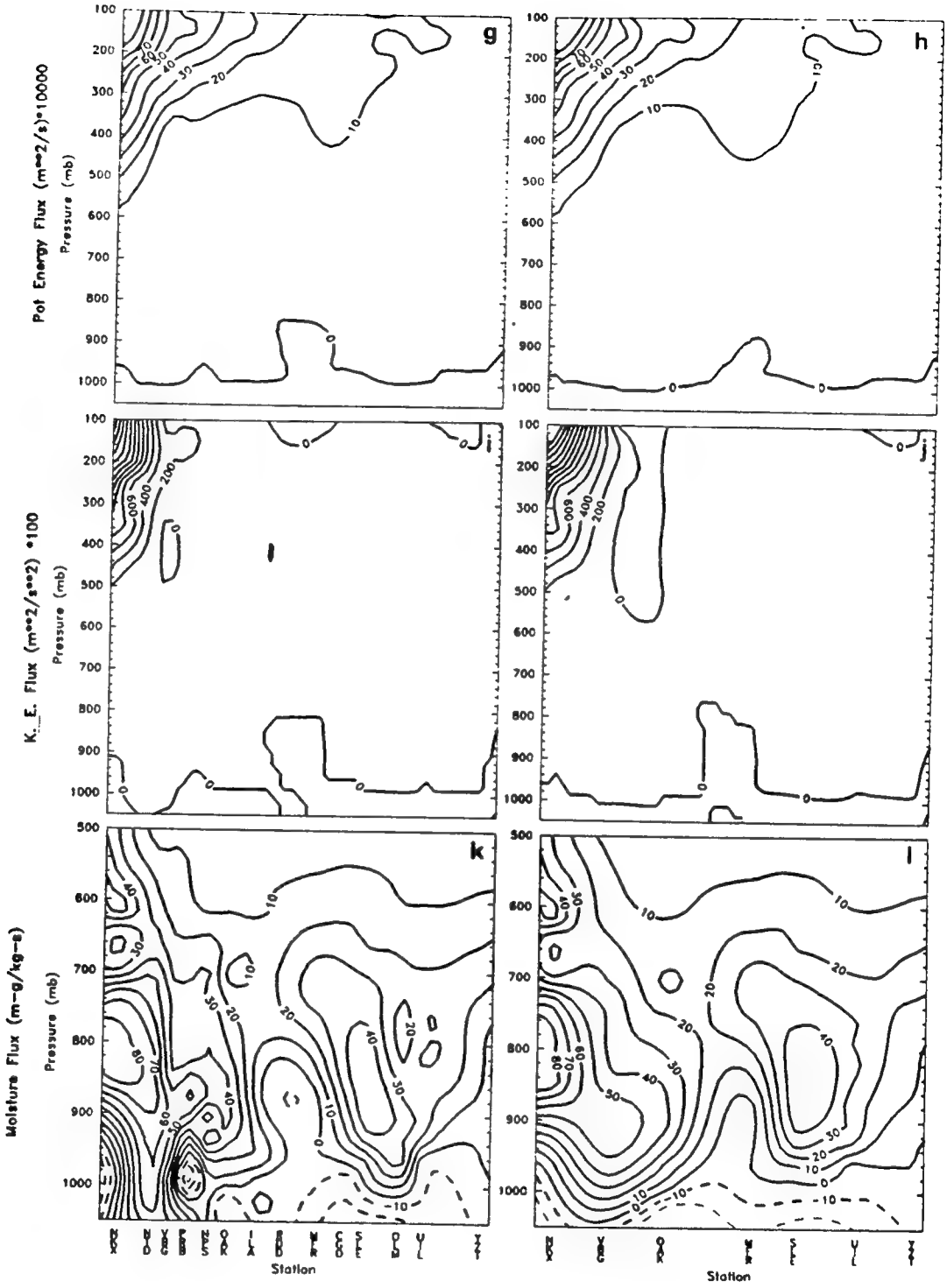


1200 UTC 13 Feb vertical cross sections for (g) ALL potential energy flux, (h) NWS potential energy flux, (i) ALL kinetic energy flux, (j) NWS kinetic energy flux, (k) ALL moisture flux, and (l) NWS moisture.

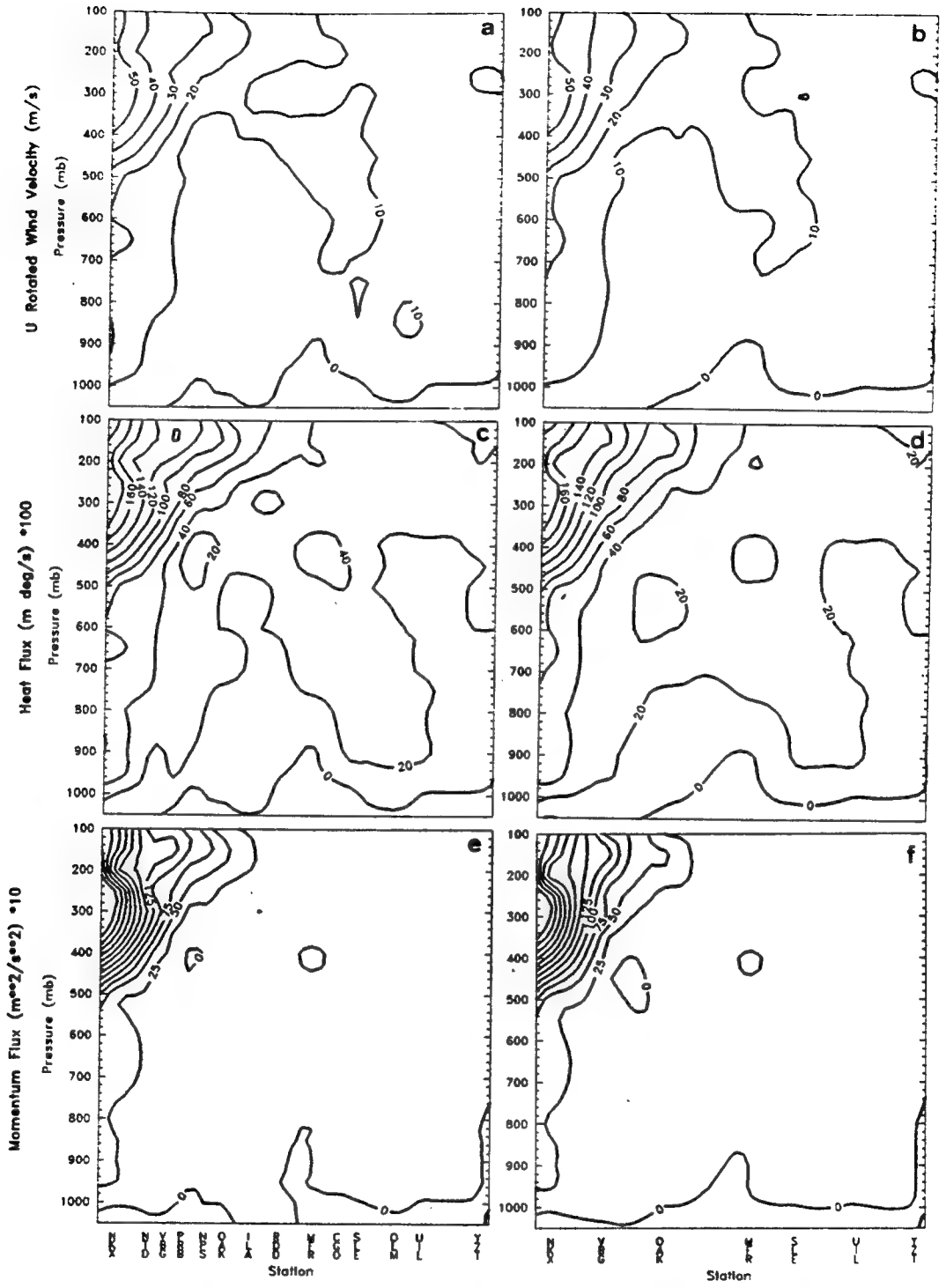


1500 UTC 13 Feb vertical cross sections for (a) ALL $U_r$ flux, (b) NWS $U_r$ flux, (c) ALL heat flux, (d) NWS heat flux, (e) ALL momentum flux, and (f) NWS momentum flux.

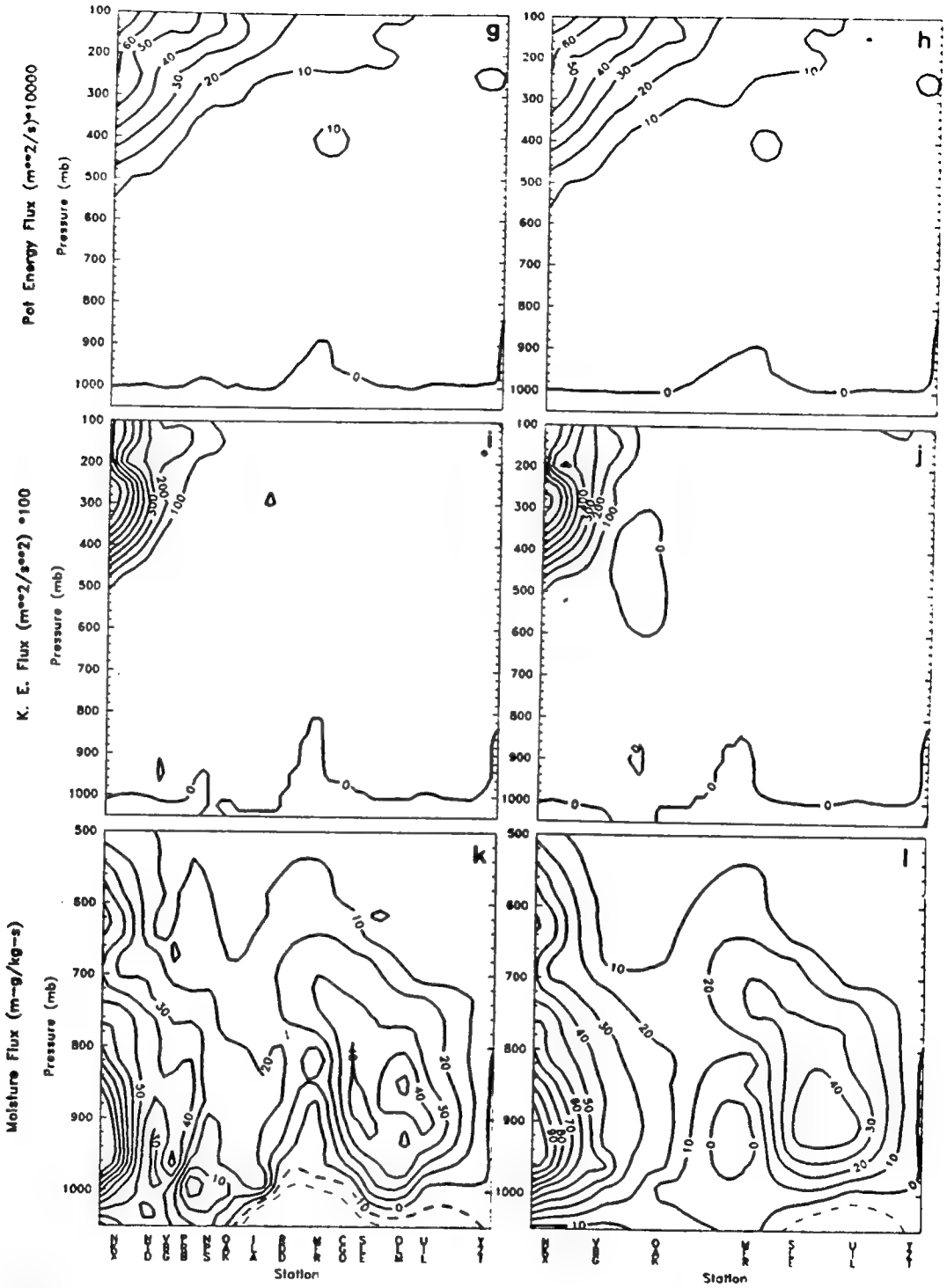


1500 UTC 13 Feb vertical cross sections for (g) ALL potential energy flux, (h) NWS potential energy flux, (i) ALL kinetic energy flux, (j) NWS kinetic energy flux, (k) ALL moisture flux, and (l) NWS moisture.

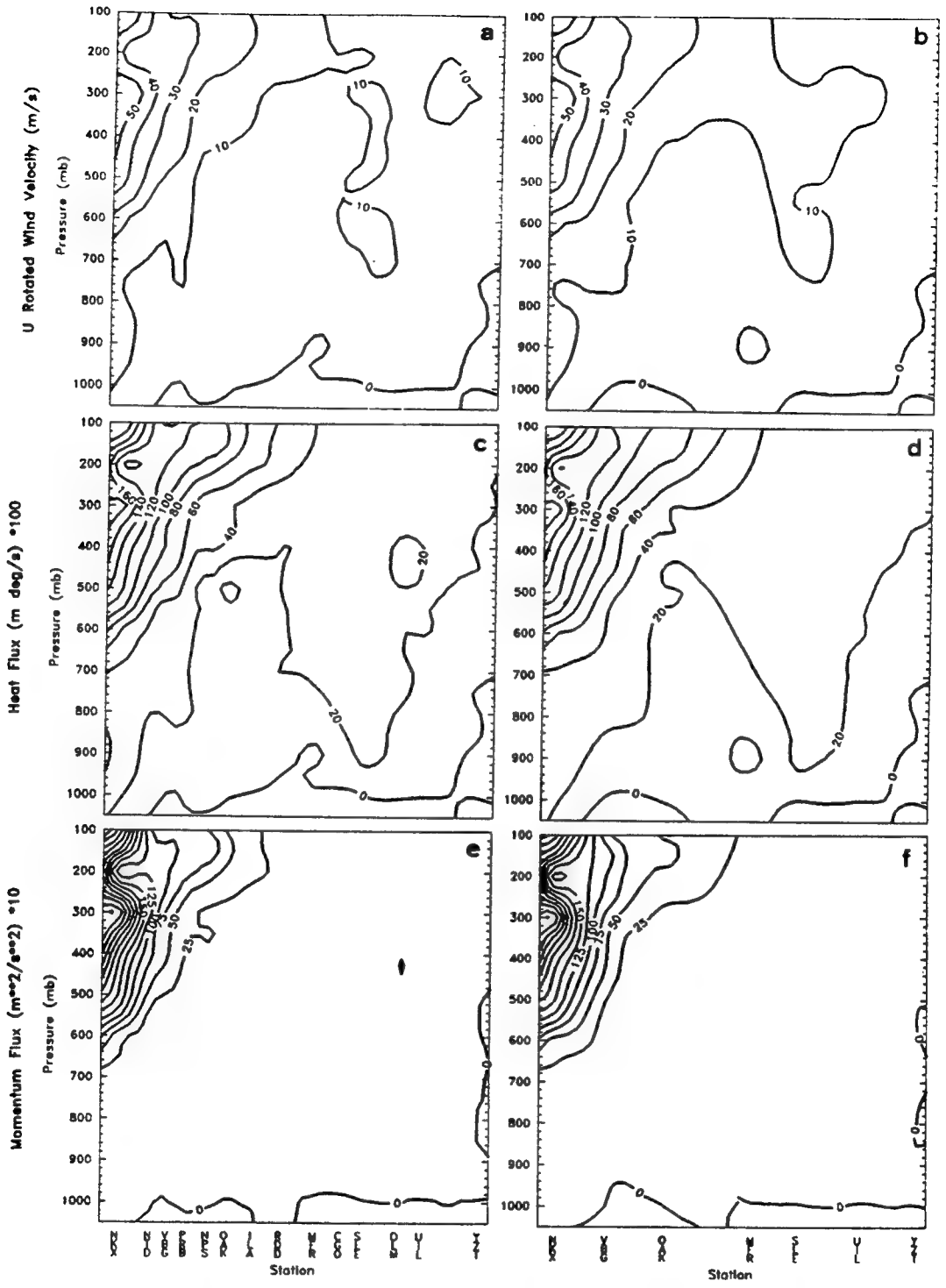


1800 UTC 13 Feb vertical cross sections for (a) ALL $U_r$ flux, (b) NWS $U_r$ flux, (c) ALL heat flux, (d) NWS heat flux, (e) ALL momentum flux, and (f) NWS momentum flux.

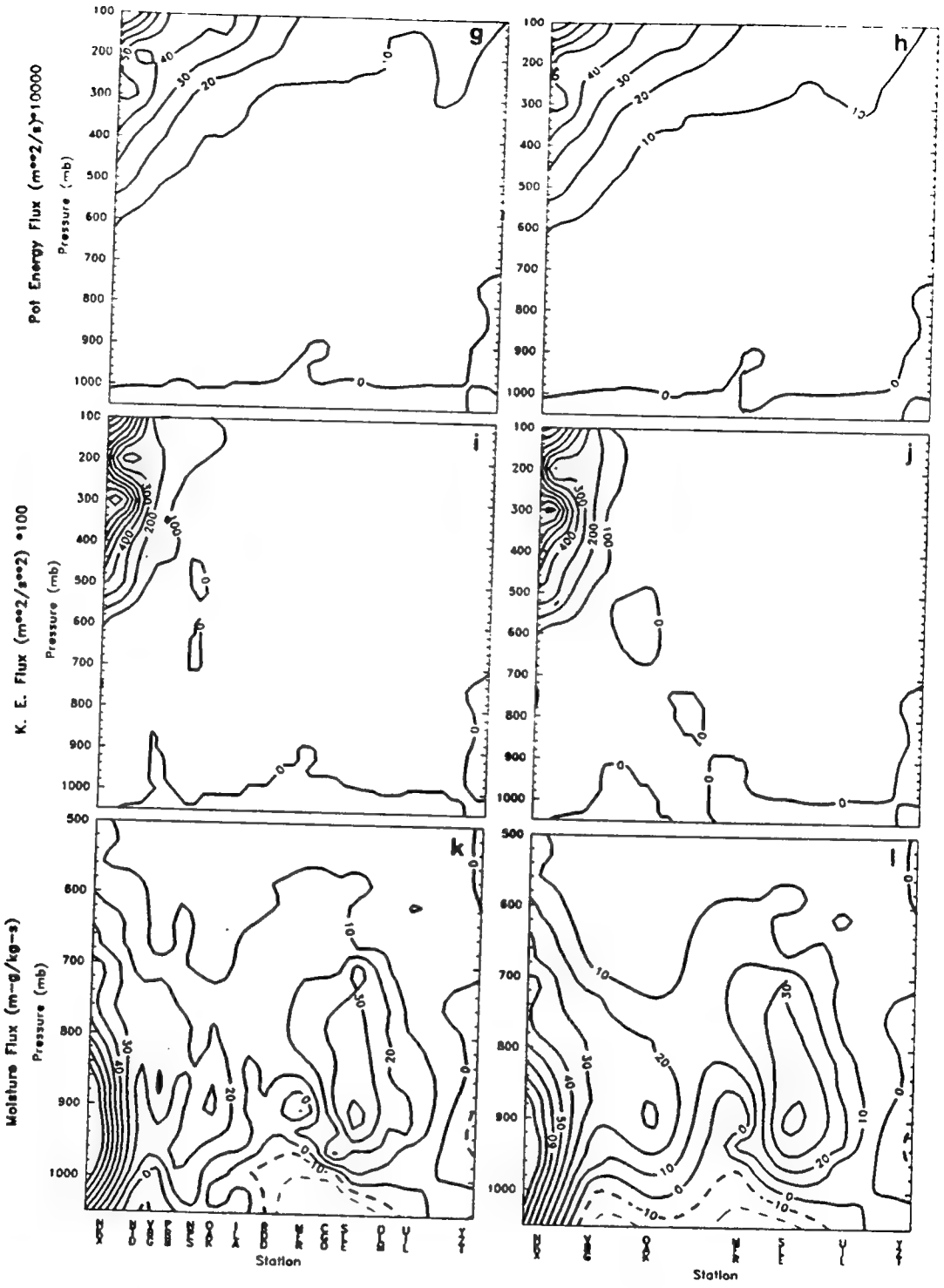


1800 UTC 13 Feb vertical cross sections for (g) ALL potential energy flux, (h) NWS potential energy flux, (i) ALL kinetic energy flux, (j) NWS kinetic energy flux, (k) ALL moisture flux, and (l) NWS moisture.

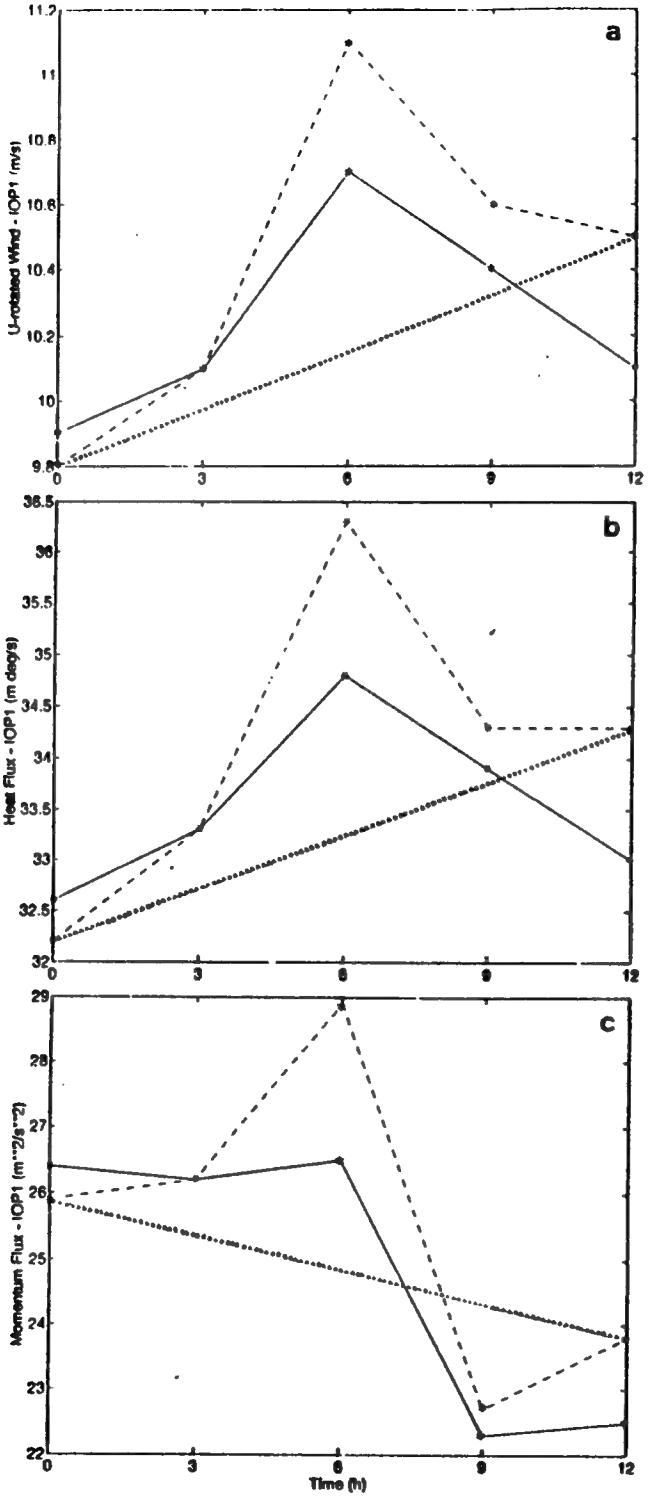


Fig. 15. (a-c) As in Fig. 13 (a-c), except for IOP-1.

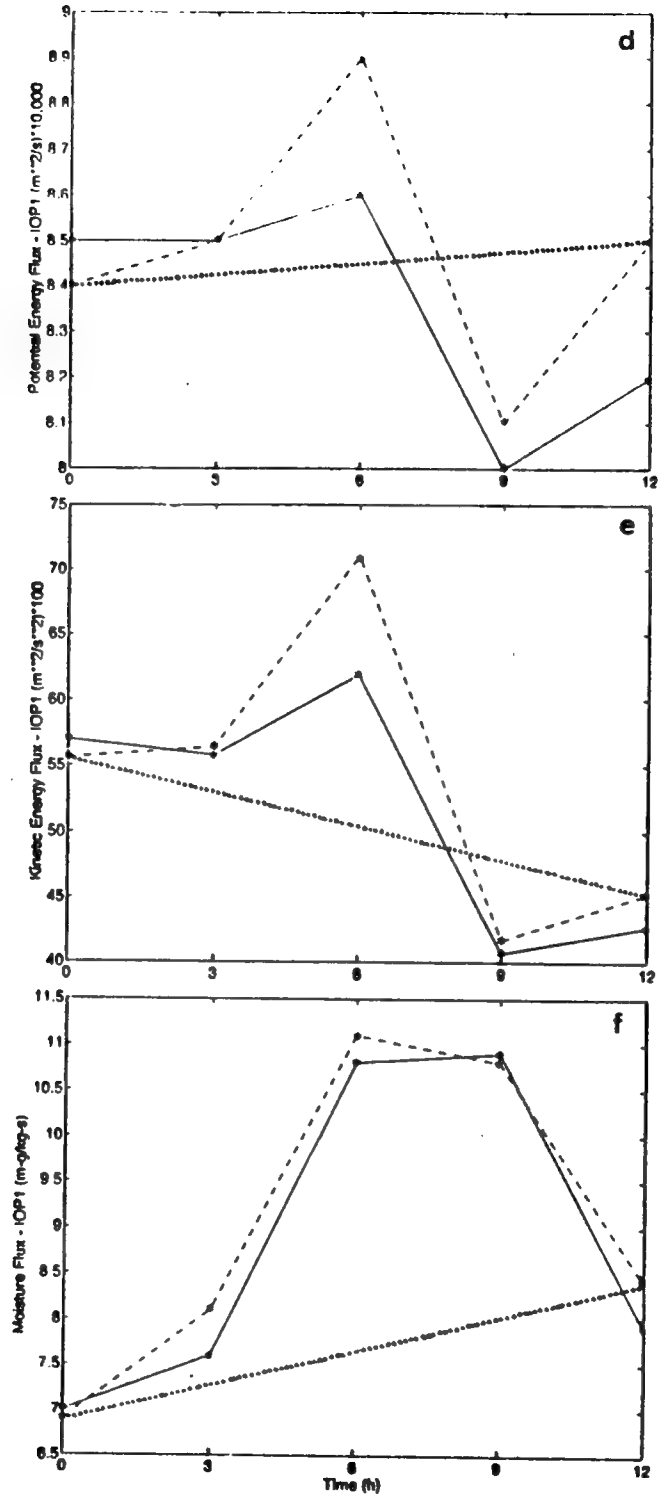


Fig. 15. (d-f) As in Fig. 13 (a-c), except for IOP-1.

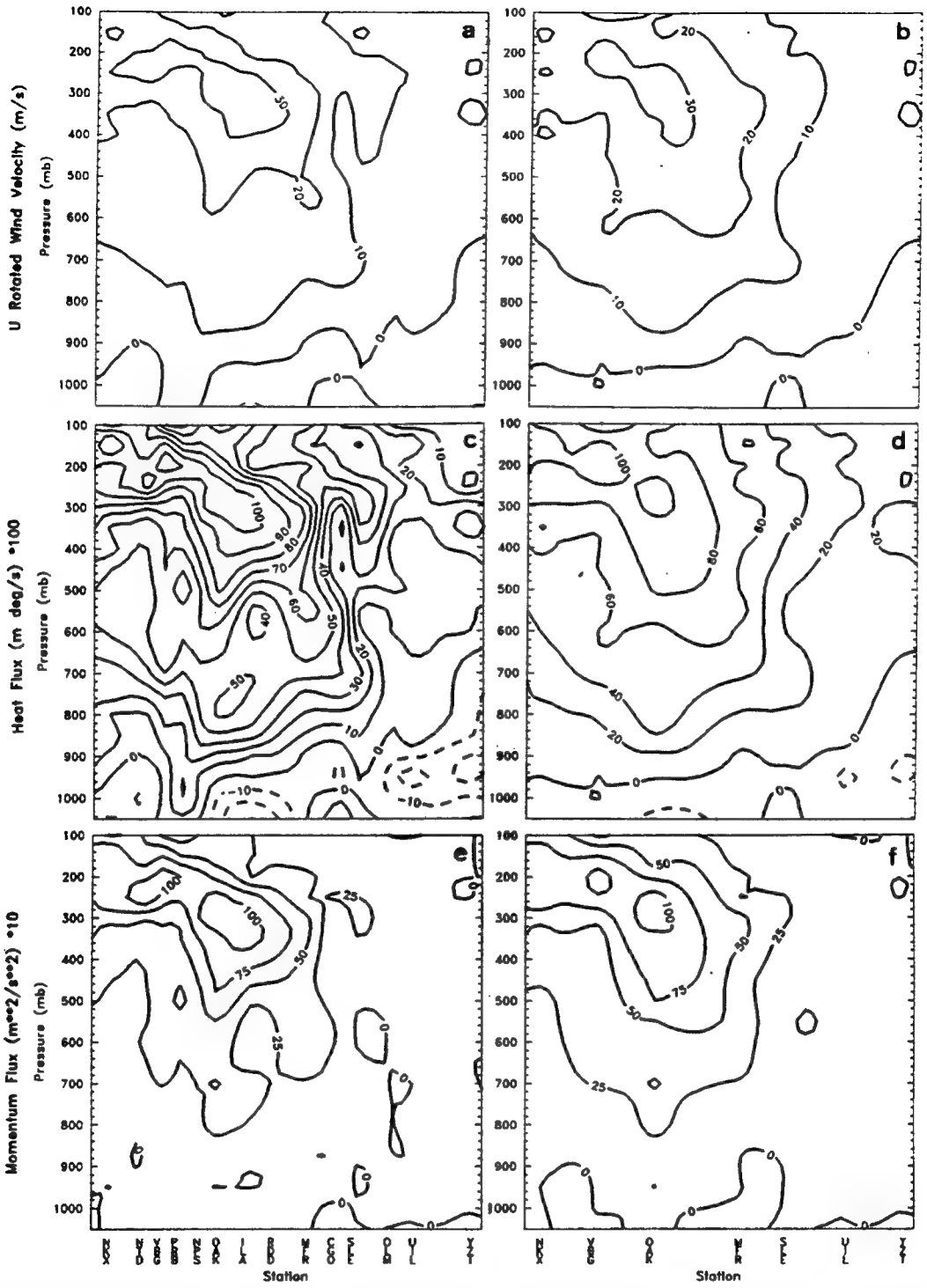


1800 UTC 14 Feb vertical cross sections for (a) ALL $U_r$ flux, (b) NWS $U_r$ flux, (c) ALL heat flux, (d) NWS heat flux, (e) ALL momentum flux, and (f) NWS momentum flux.

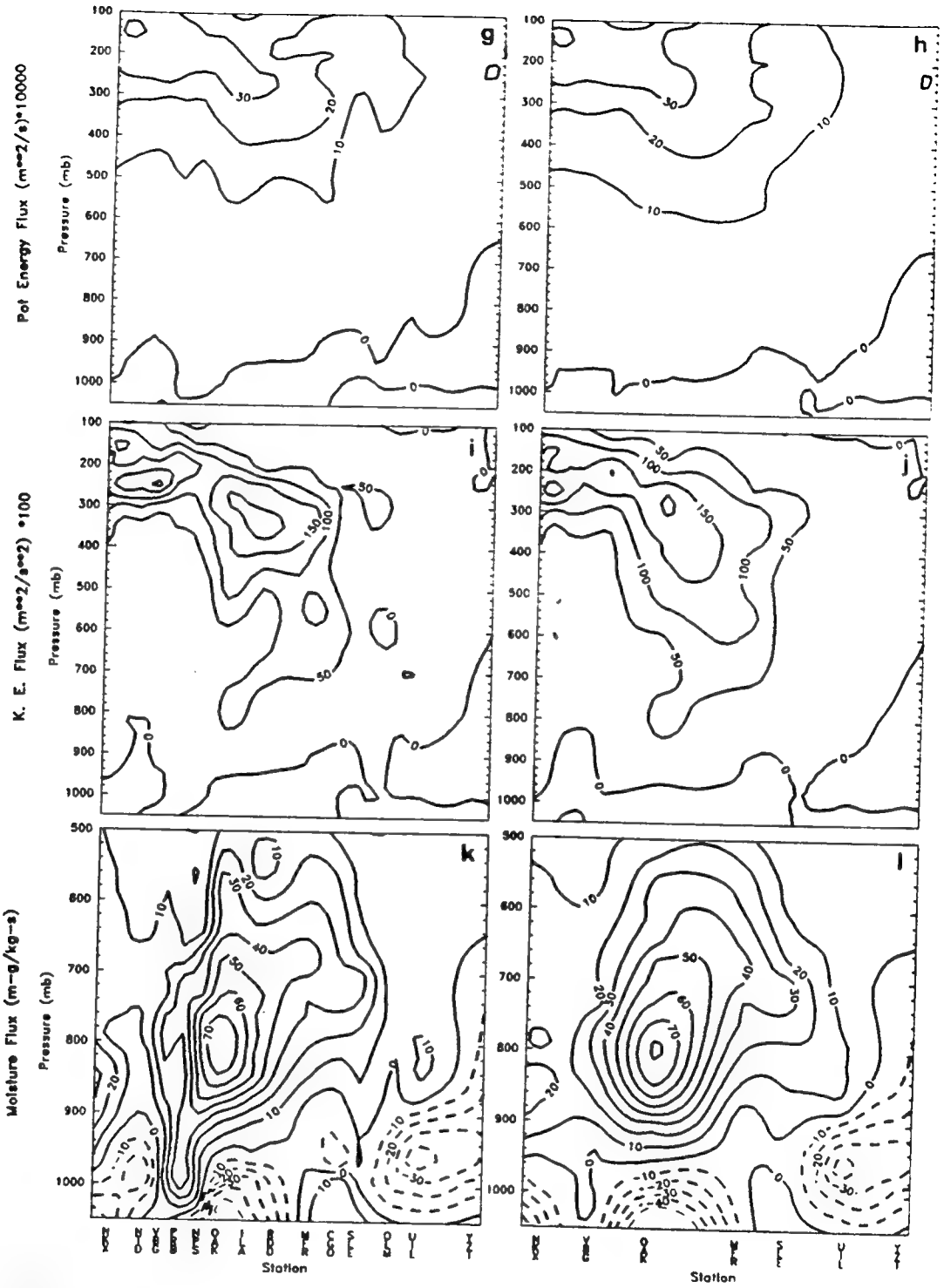


1800 UTC 14 Feb vertical cross sections for (g) ALL potential energy flux, (h) NWS potential energy flux, (i) ALL kinetic energy flux, (j) NWS kinetic energy flux, (k) ALL moisture flux, and (l) NWS moisture.

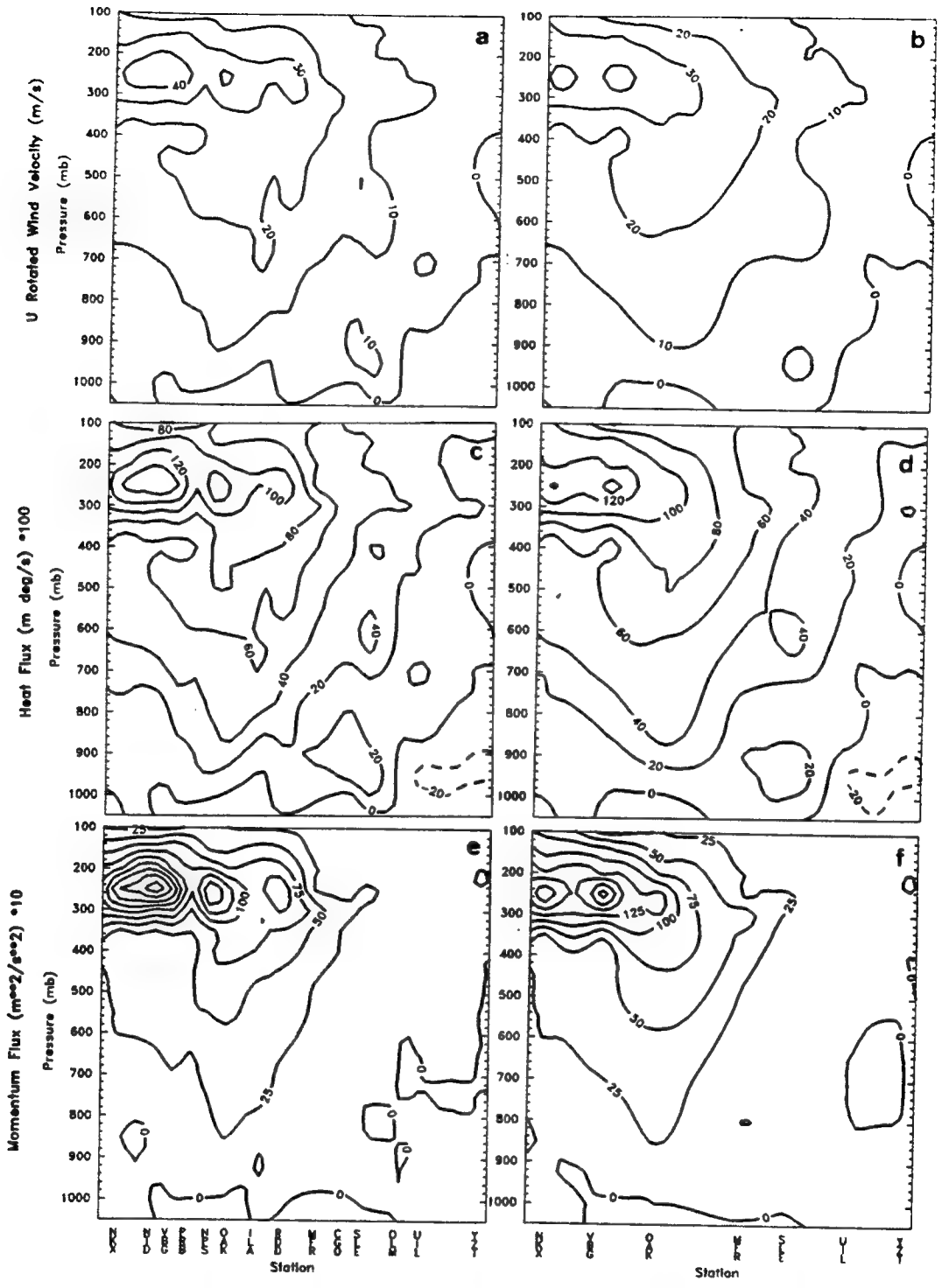


2100 UTC 14 Feb vertical cross sections for (a) ALL $U_r$ flux, (b) NWS $U_r$ flux, (c) ALL heat flux, (d) NWS heat flux, (e) ALL momentum flux, and (f) NWS momentum flux.

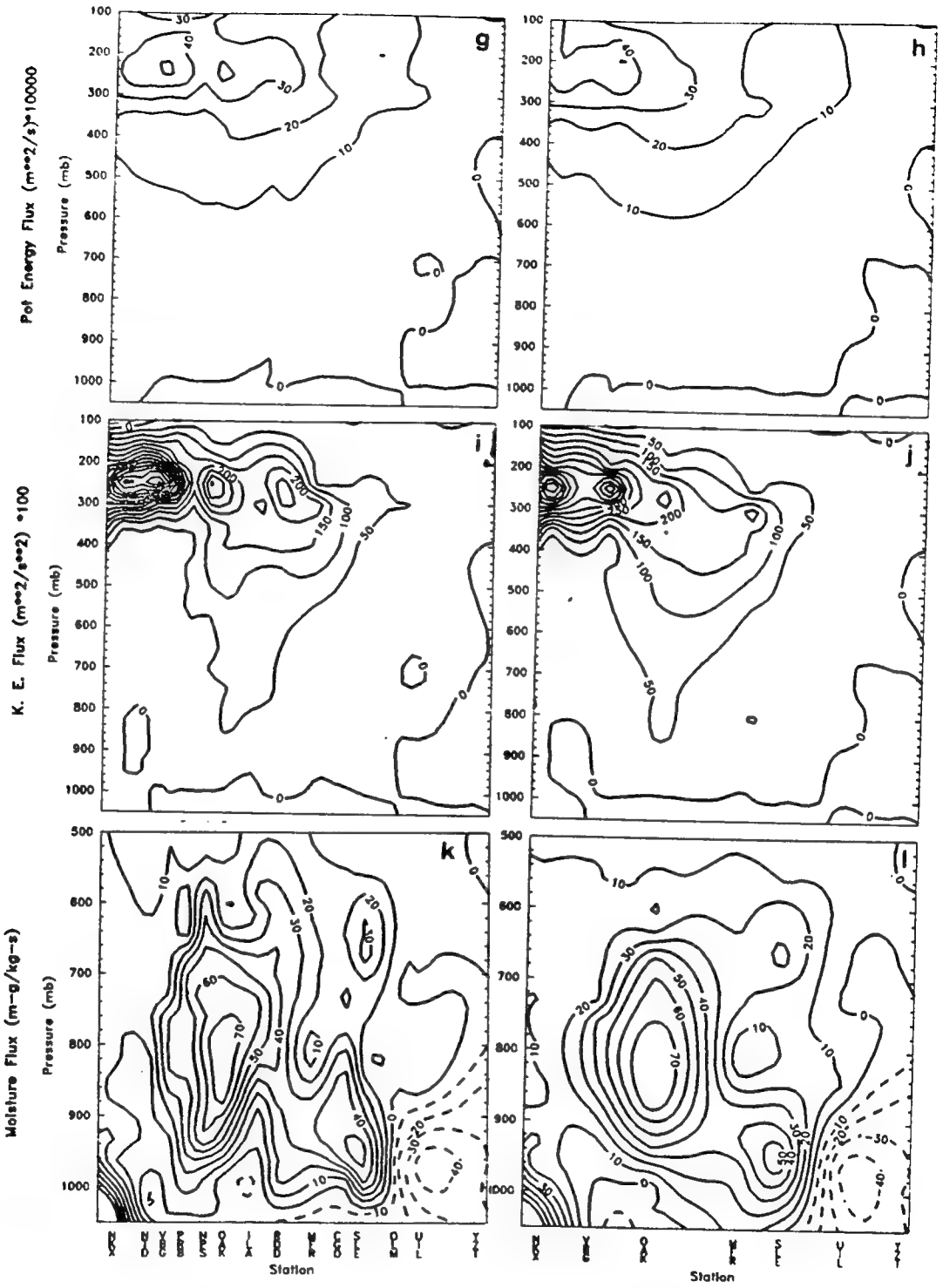


2100 UTC 14 Feb vertical cross sections for (g) ALL potential energy flux, (h) NWS potential energy flux, (i) ALL kinetic energy flux, (j) NWS kinetic energy flux, (k) ALL moisture flux, and (l) NWS moisture.

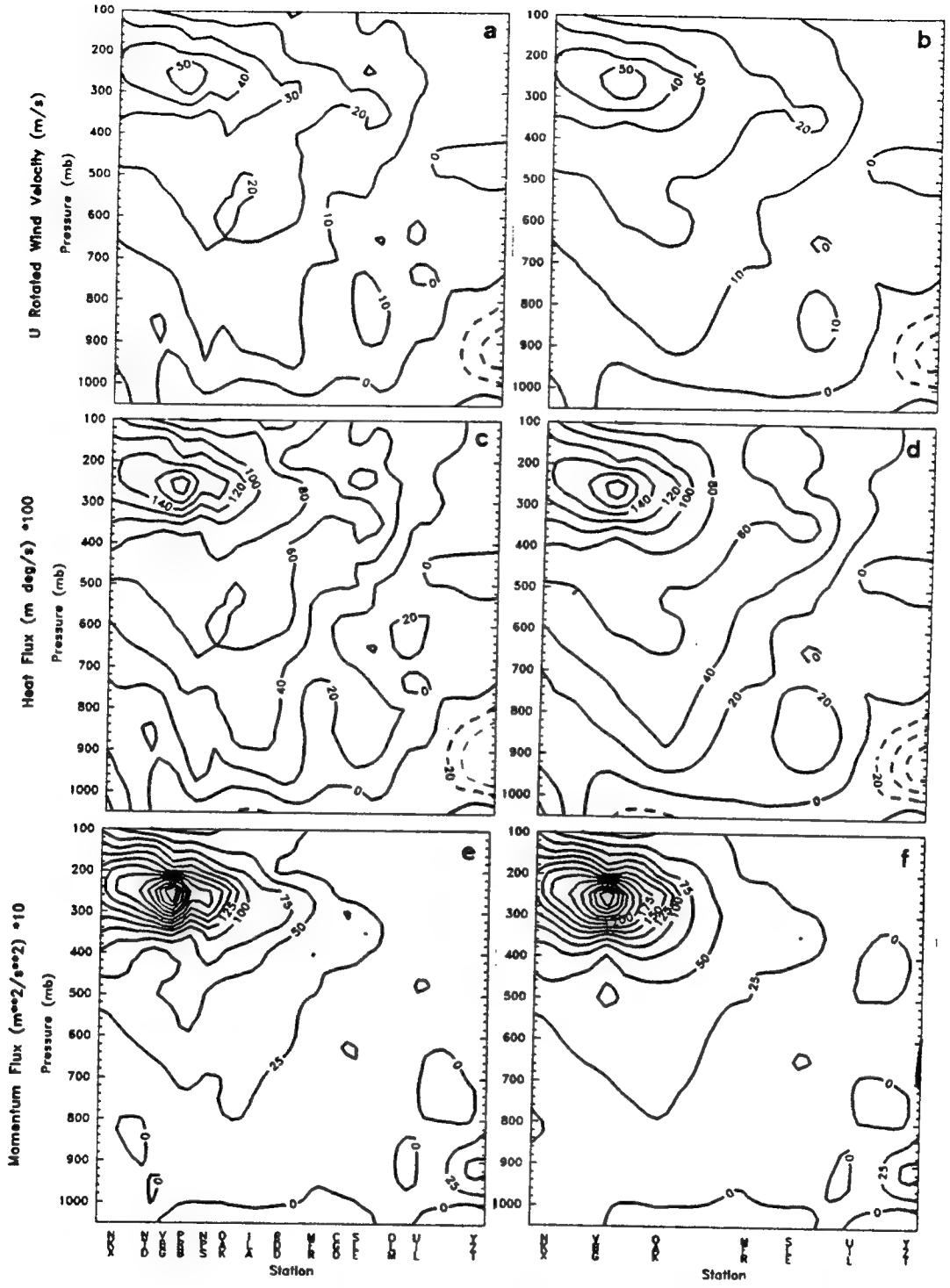


0000 UTC 15 Feb vertical cross sections for (a) ALL $U_r$ flux, (b) NWS $U_r$ flux, (c) ALL heat flux, (d) NWS heat flux, (e) ALL momentum flux, and (f) NWS momentum flux.

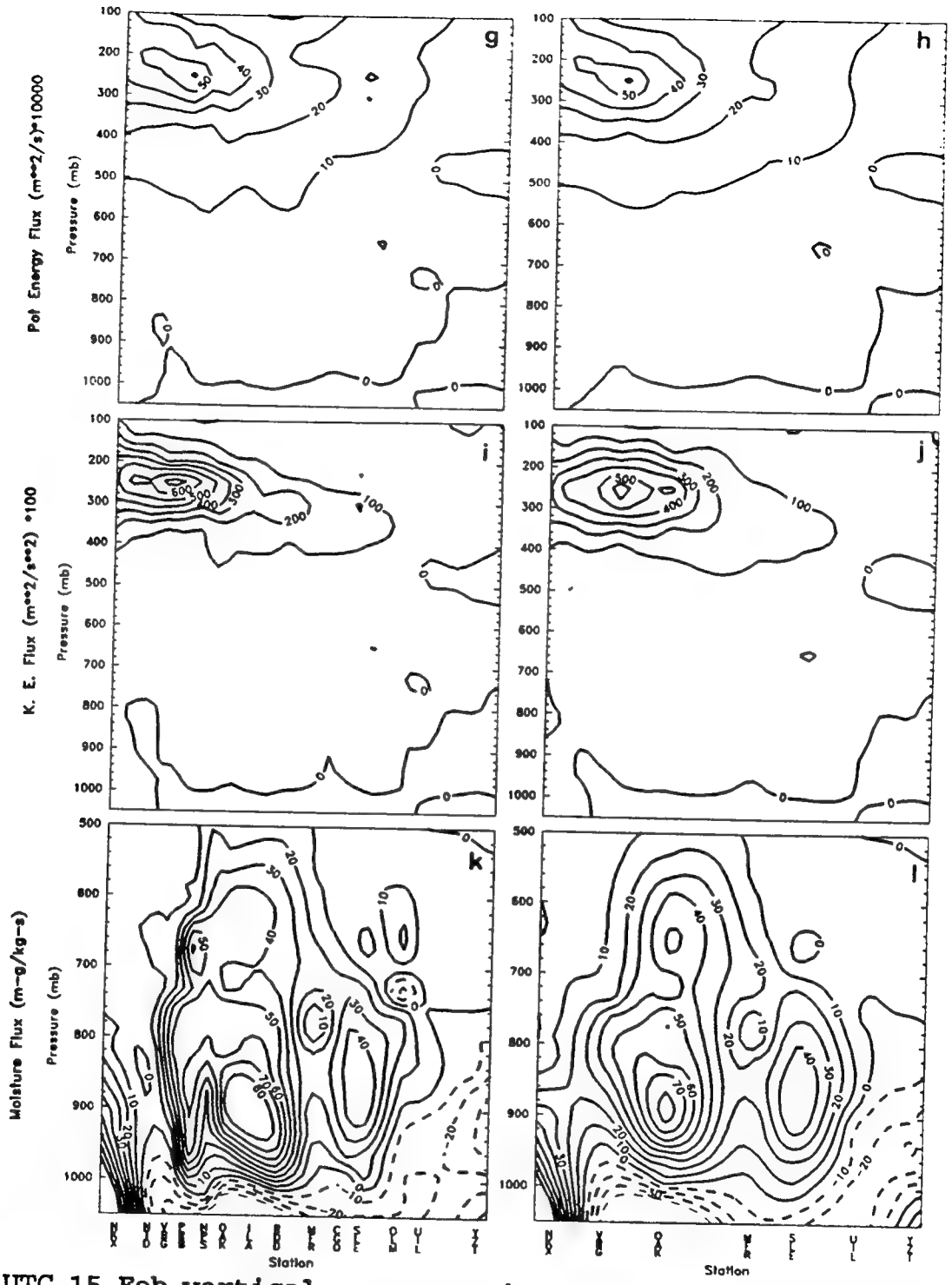


0000 UTC 15 Feb vertical cross sections for (g) ALL potential energy flux, (h) NWS potential energy flux, (i) ALL kinetic energy flux, (j) NWS kinetic energy flux, (k) ALL moisture flux, and (l) NWS moisture.

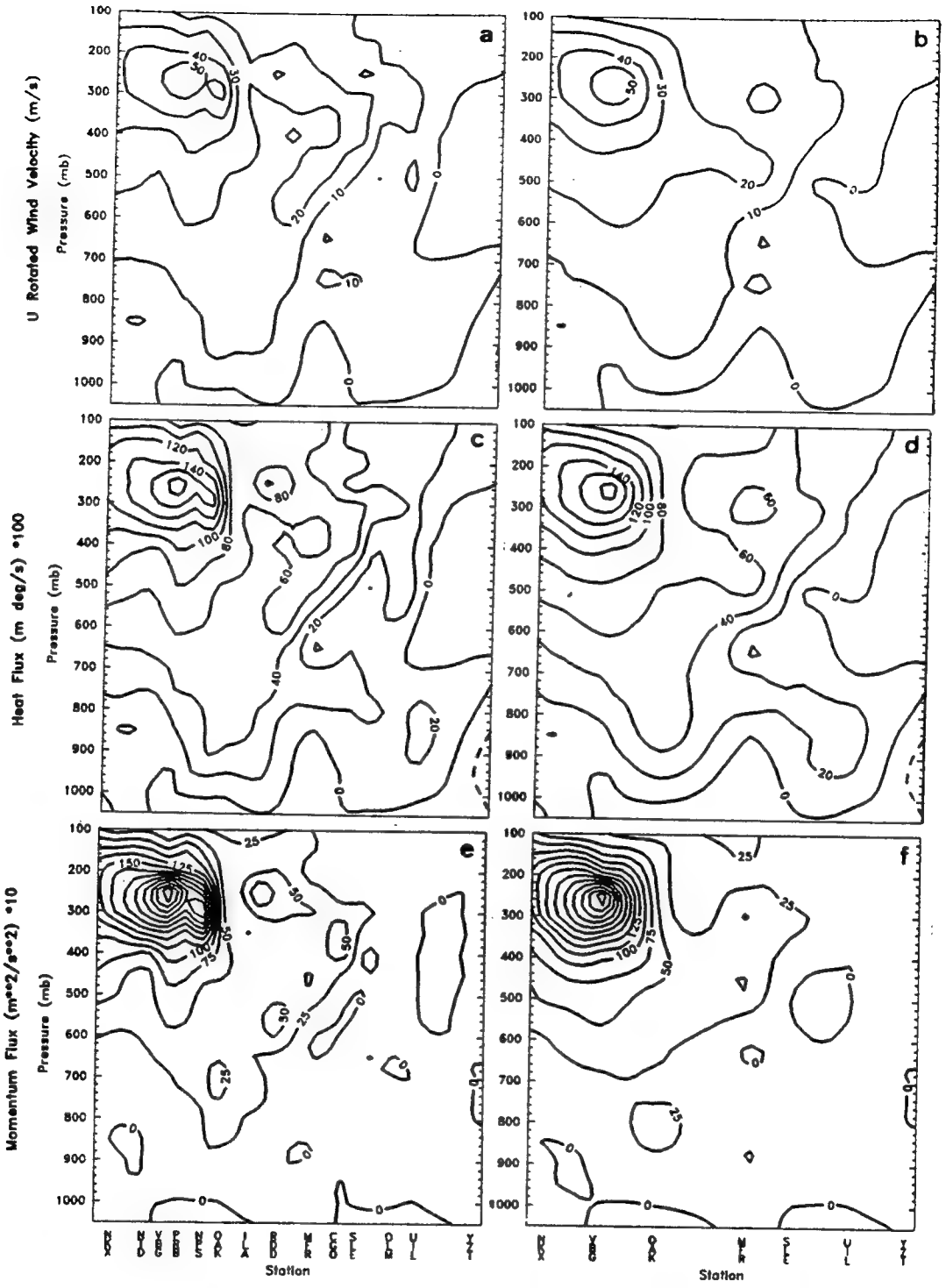


0300 UTC 15 Feb vertical cross sections for (a) ALL $U_r$ flux, (b) NWS $U_r$ flux, (c) ALL heat flux, (d) NWS heat flux, (e) ALL momentum flux, and (f) NWS momentum flux.

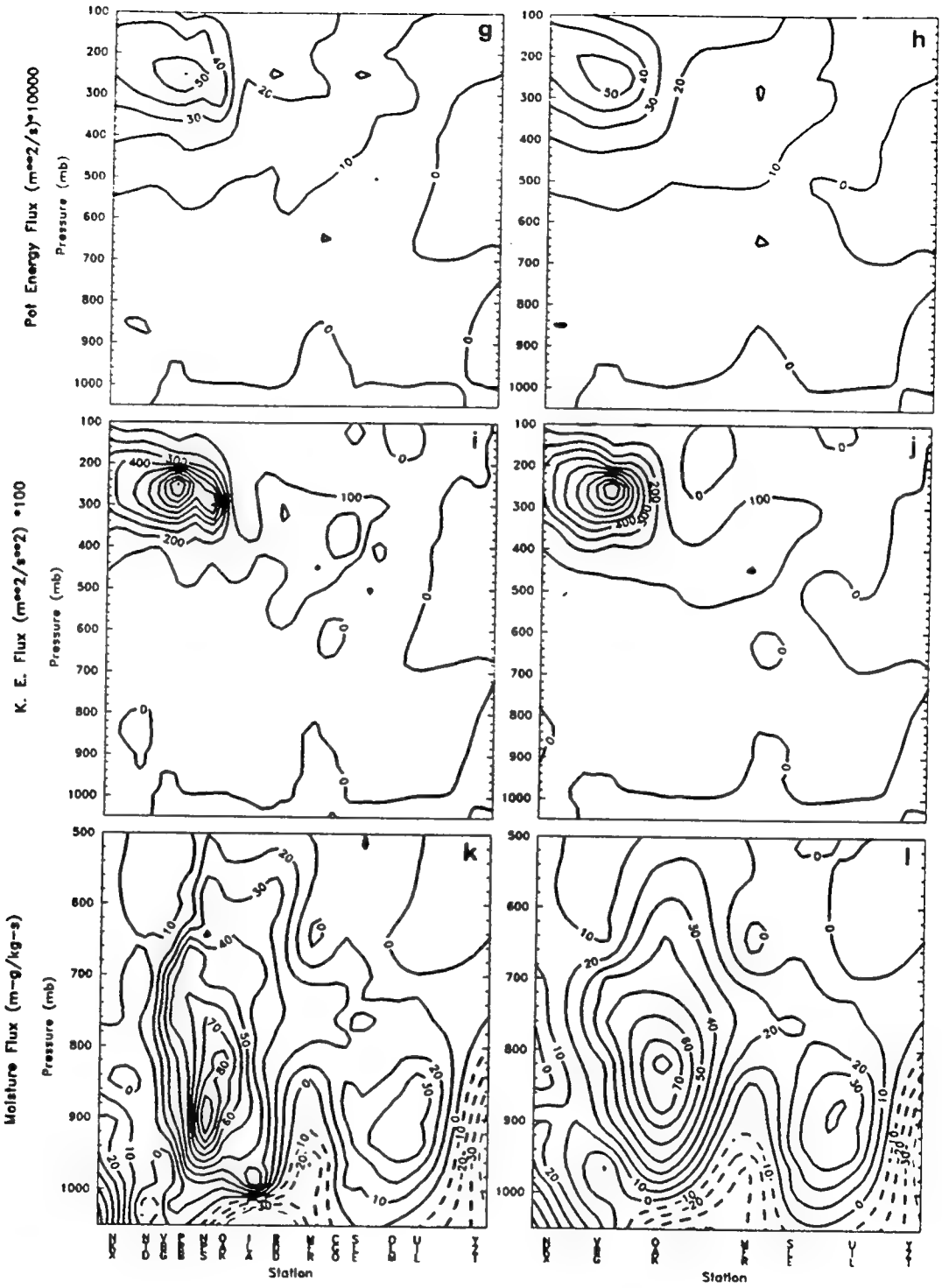


0300 UTC 15 Feb vertical cross sections for (g) ALL potential energy flux, (h) NWS potential energy flux, (i) ALL kinetic energy flux, (j) NWS kinetic energy flux, (k) ALL moisture flux, and (l) NWS moisture.

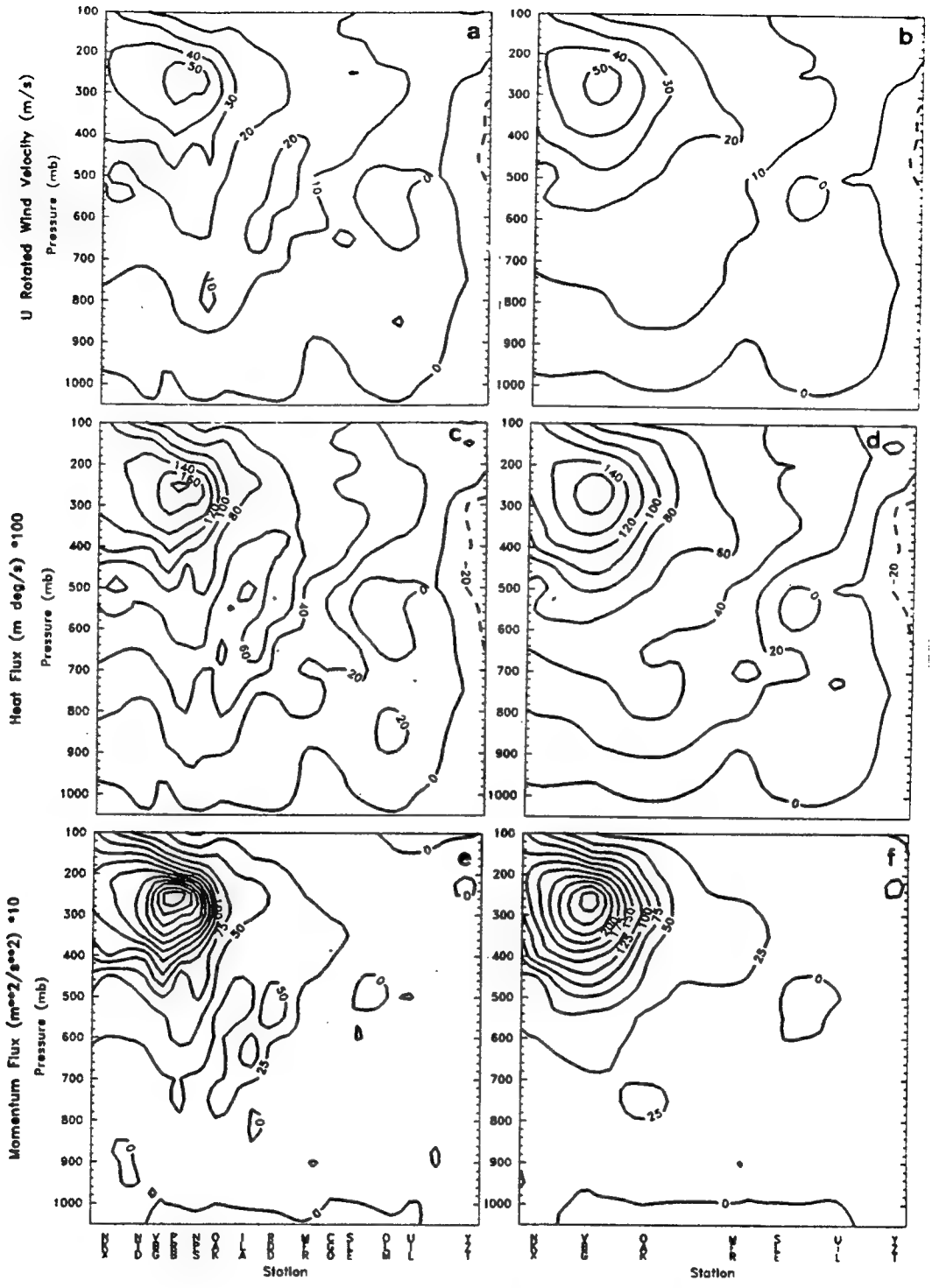


0600 UTC 15 Feb vertical cross sections for (a) ALL $U_r$ flux, (b) NWS $U_r$ flux, (c) ALL heat flux, (d) NWS heat flux, (e) ALL momentum flux, and (f) NWS momentum flux.

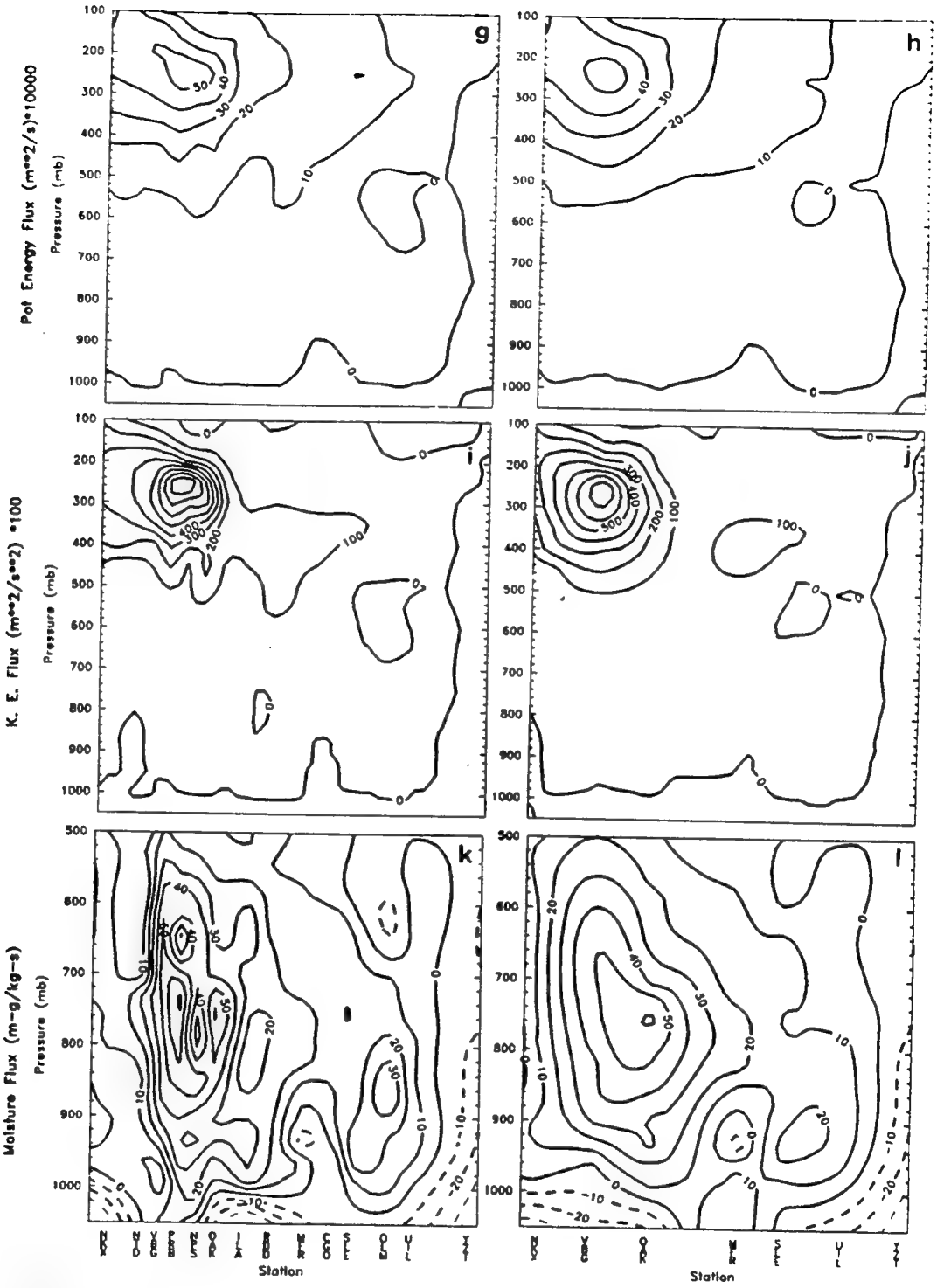


0600 UTC 15 Feb vertical cross sections for (g) ALL potential energy flux, (h) NWS potential energy flux, (i) ALL kinetic energy flux, (j) NWS kinetic energy flux, (k) ALL moisture flux, and (l) NWS moisture.

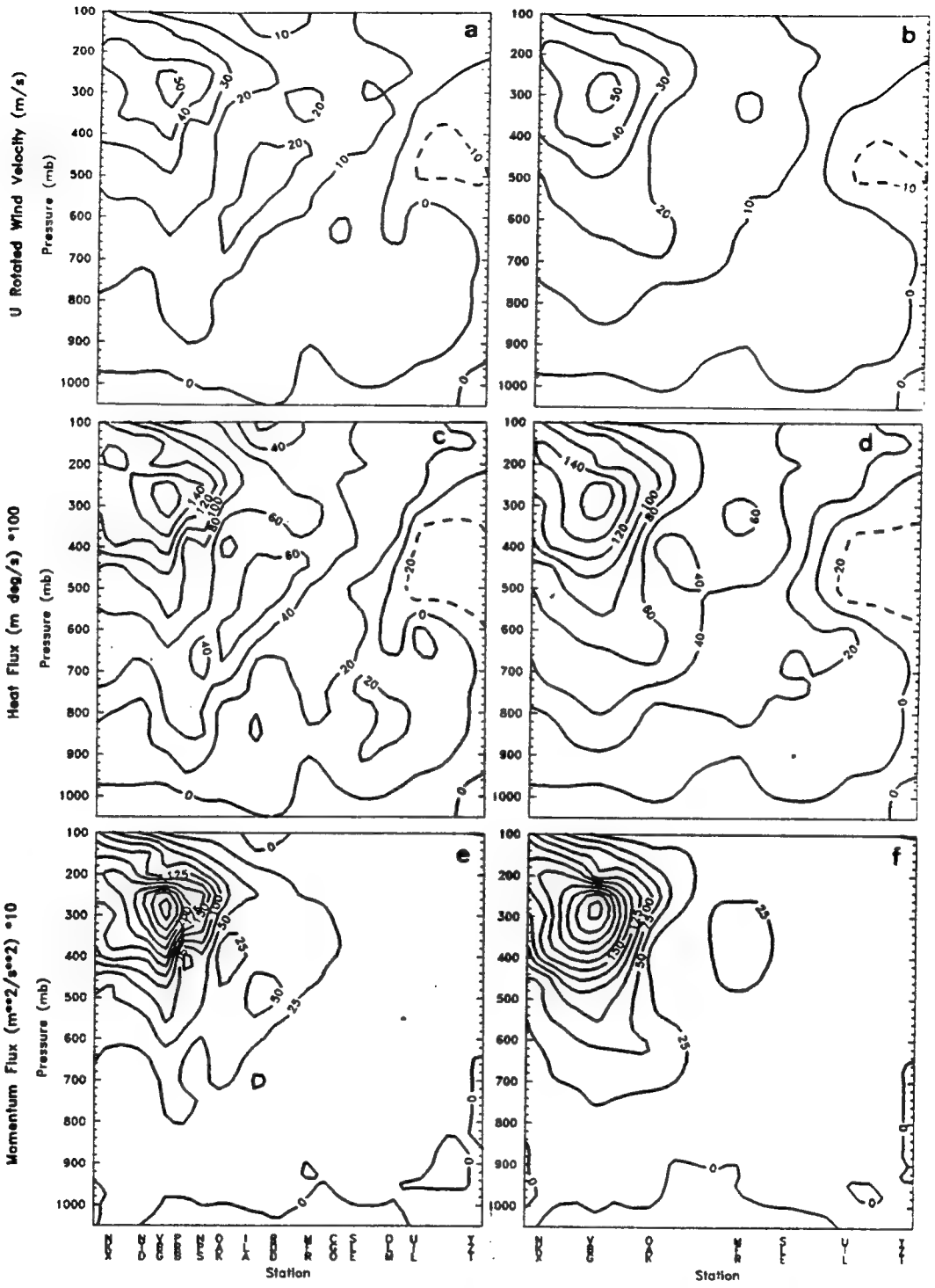


0900 UTC 15 Feb vertical cross sections for (a) ALL $U_r$ flux, (b) NWS $U_r$ flux, (c) ALL heat flux, (d) NWS heat flux, (e) ALL momentum flux, and (f) NWS momentum flux.

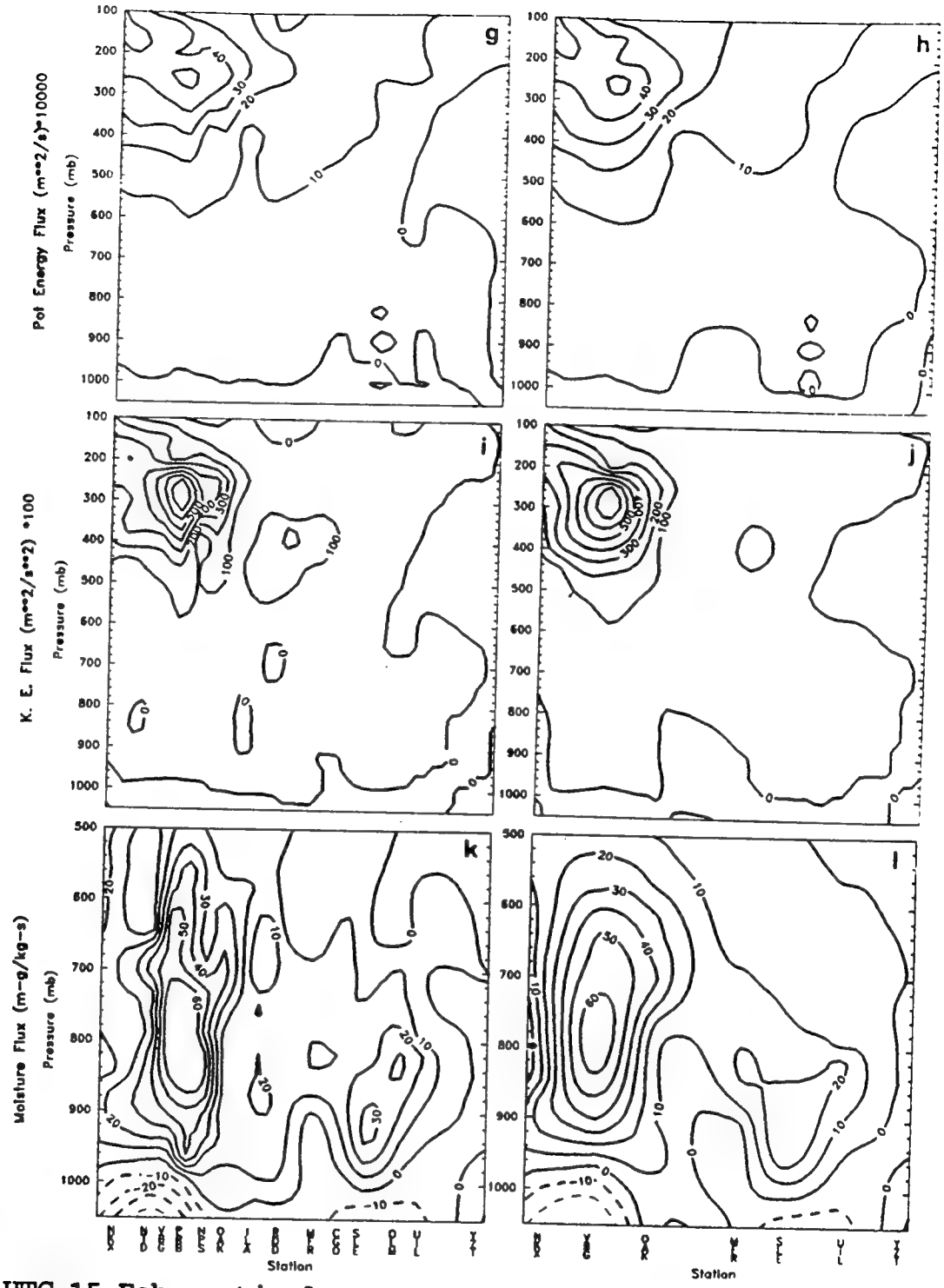


0900 UTC 15 Feb vertical cross sections for (g) ALL potential energy flux, (h) NWS potential energy flux, (i) ALL kinetic energy flux, (j) NWS kinetic energy flux, (k) ALL moisture flux, and (l) NWS moisture.

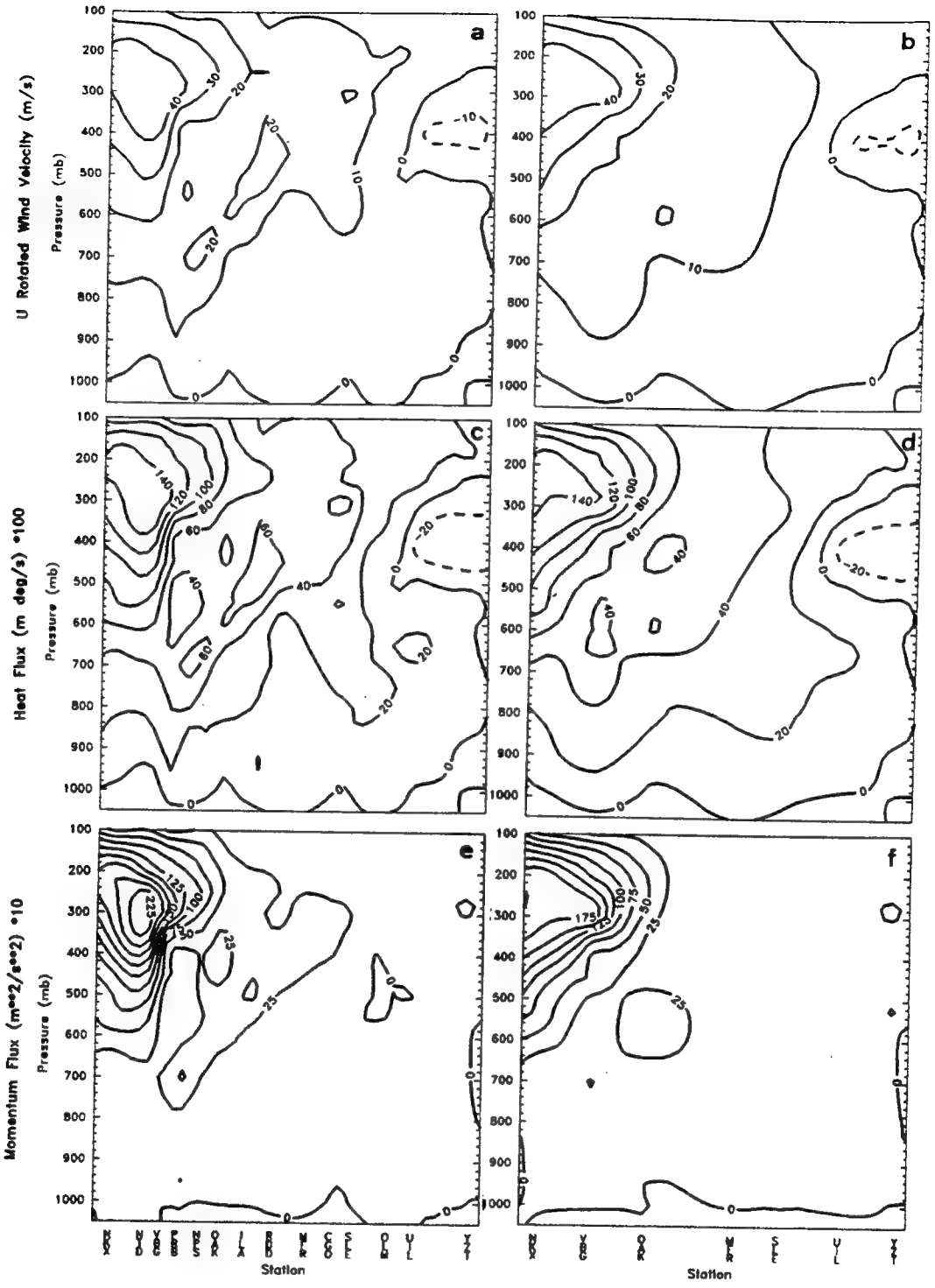


1200 UTC 15 Feb vertical cross sections for (a) ALL $U_r$ flux, (b) NWS $U_r$ flux, (c) ALL heat flux, (d) NWS heat flux, (e) ALL momentum flux, and (f) NWS momentum flux.

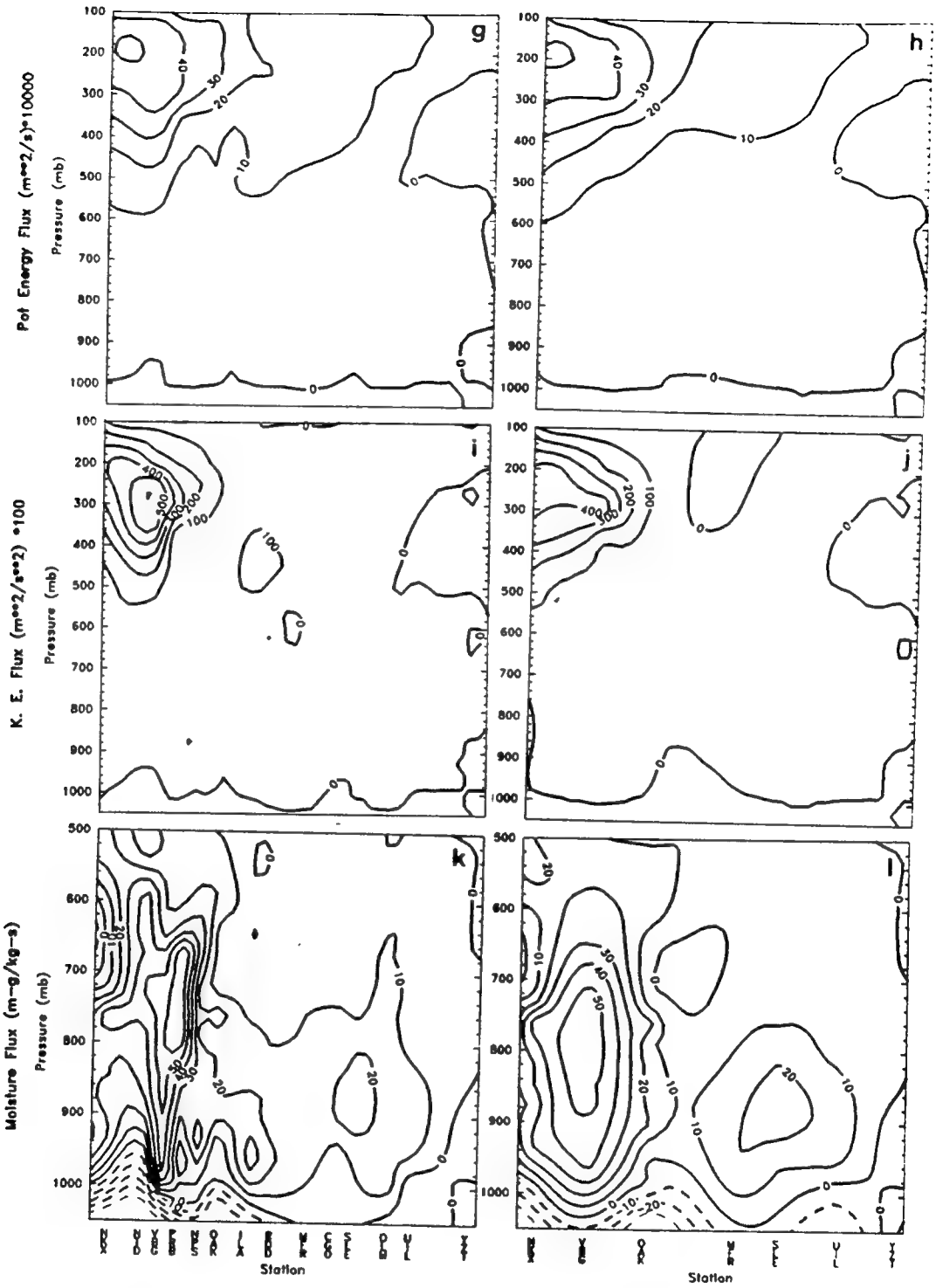


1200 UTC 15 Feb vertical cross sections for (g) ALL potential energy flux, (h) NWS potential energy flux, (i) ALL kinetic energy flux, (j) NWS kinetic energy flux, (k) ALL moisture flux, and (l) NWS moisture.

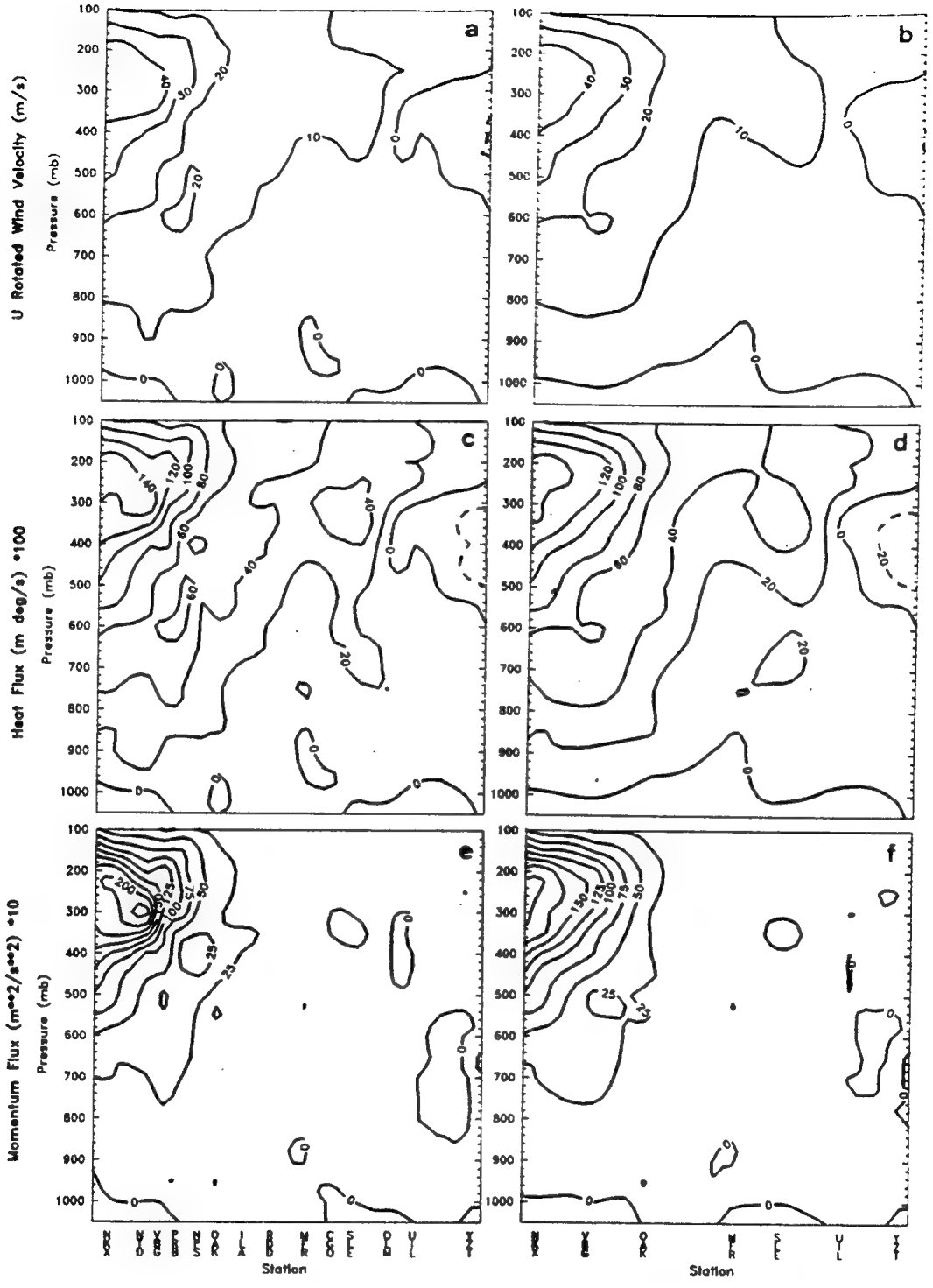


1500 UTC 15 Feb vertical cross sections for (a) ALL $U_r$ flux, (b) NWS $U_r$ flux, (c) ALL heat flux, (d) NWS heat flux, (e) ALL momentum flux, and (f) NWS momentum flux.

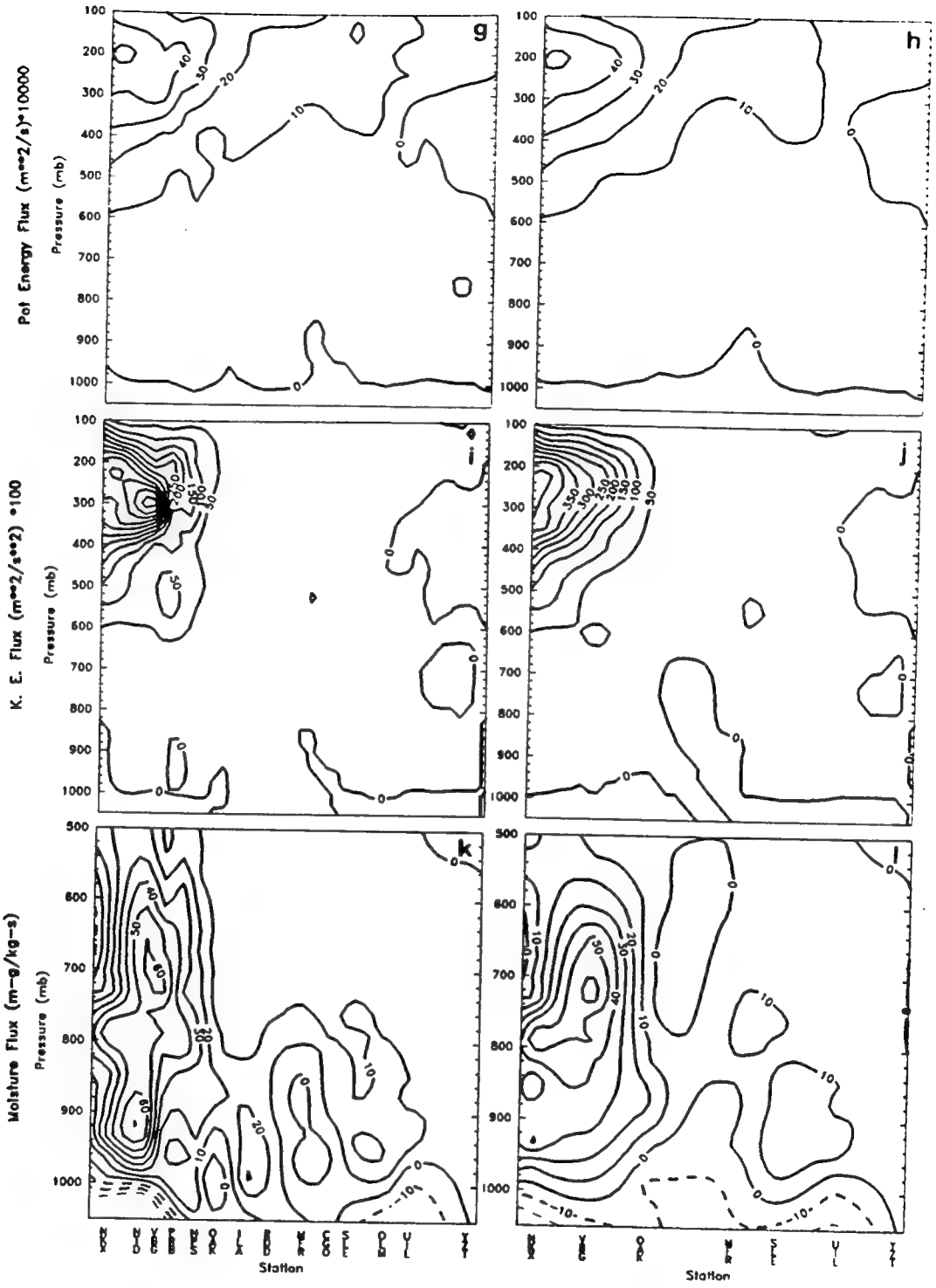


1500 UTC 15 Feb vertical cross sections for (g) ALL potential energy flux, (h) NWS potential energy flux, (i) ALL kinetic energy flux, (j) NWS kinetic energy flux, (k) ALL moisture flux, and (l) NWS moisture.

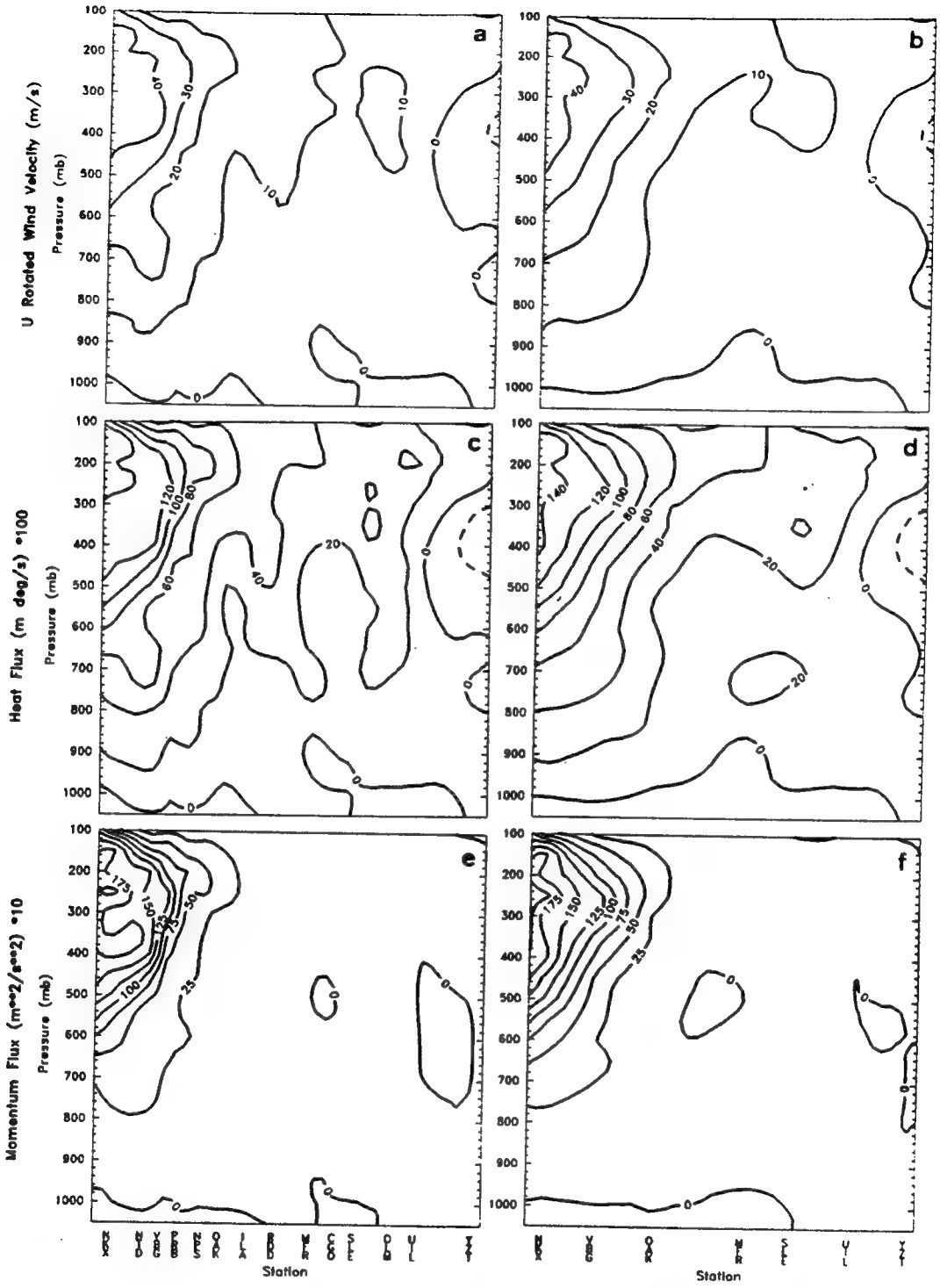


1800 UTC 15 Feb vertical cross sections for (a) ALL $U_r$ flux, (b) NWS $U_r$ flux, (c) ALL heat flux, (d) NWS heat flux, (e) ALL momentum flux, and (f) NWS momentum flux.

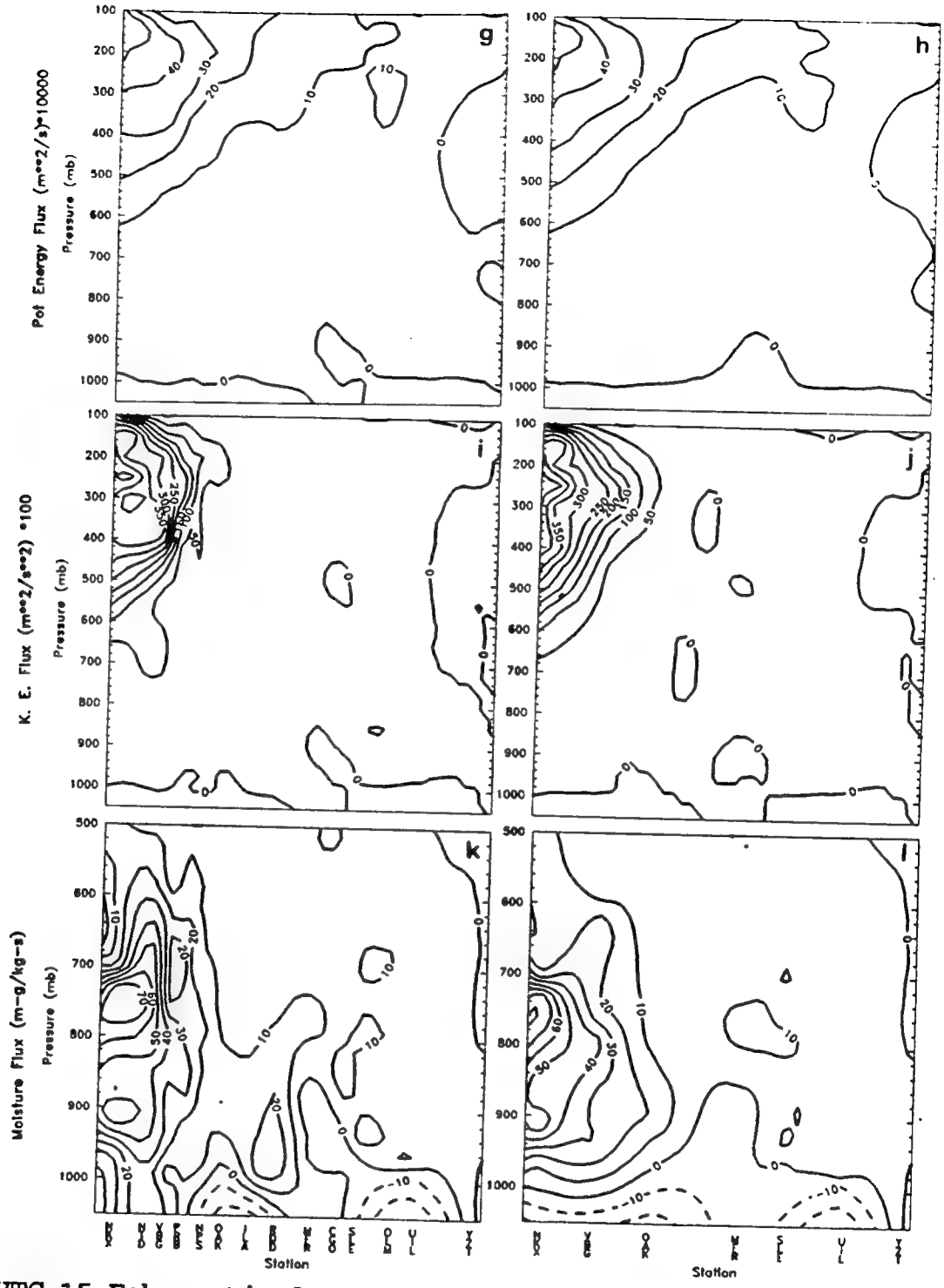


1800 UTC 15 Feb vertical cross sections for (g) ALL potential energy flux, (h) NWS potential energy flux, (i) ALL kinetic energy flux, (j) NWS kinetic energy flux, (k) ALL moisture flux, and (l) NWS moisture.

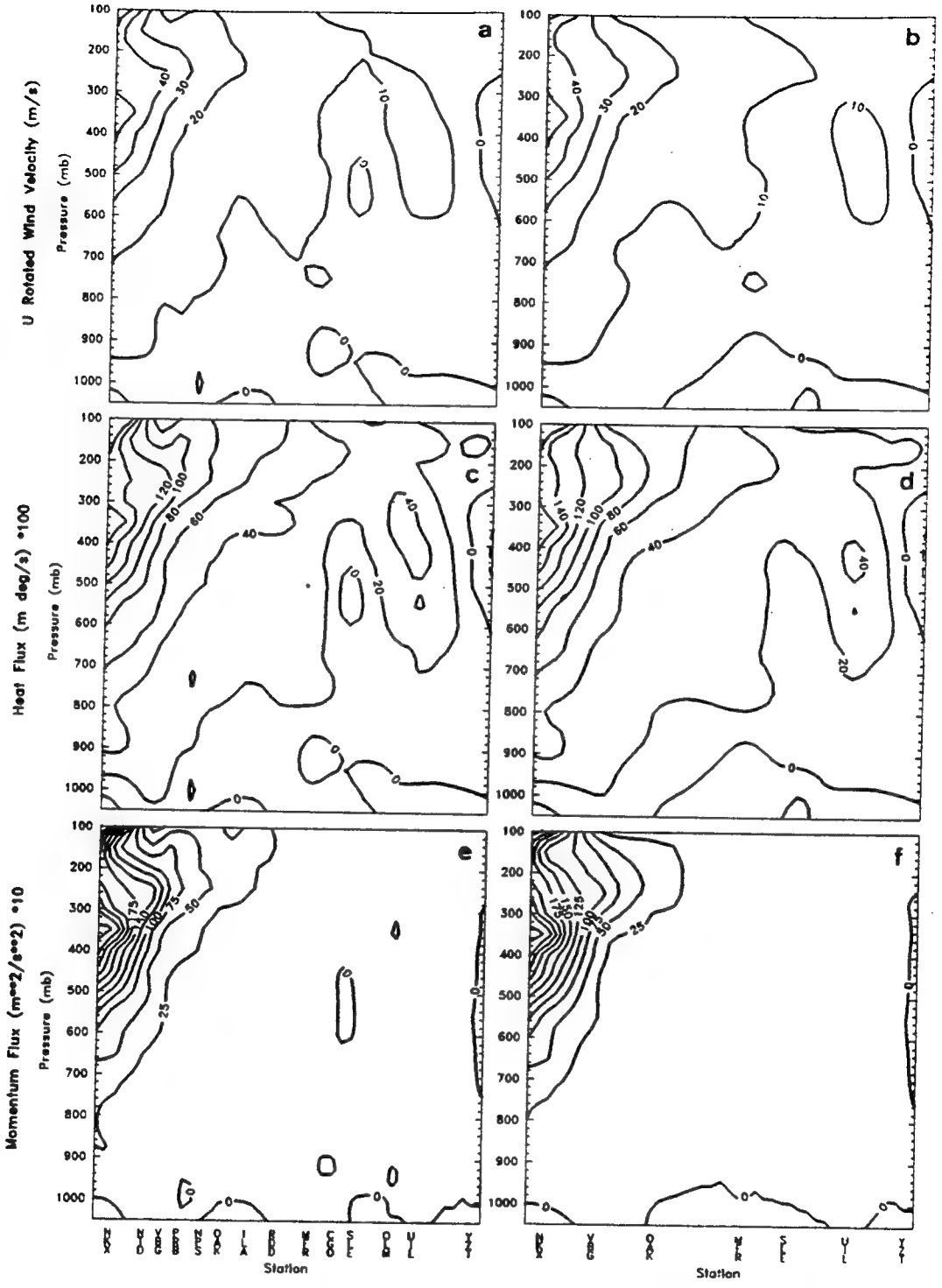


2100 UTC 15 Feb vertical cross sections for (a) ALL $U_r$ flux, (b) NWS $U_r$ flux, (c) ALL heat flux, (d) NWS heat flux, (e) ALL momentum flux, and (f) NWS momentum flux.

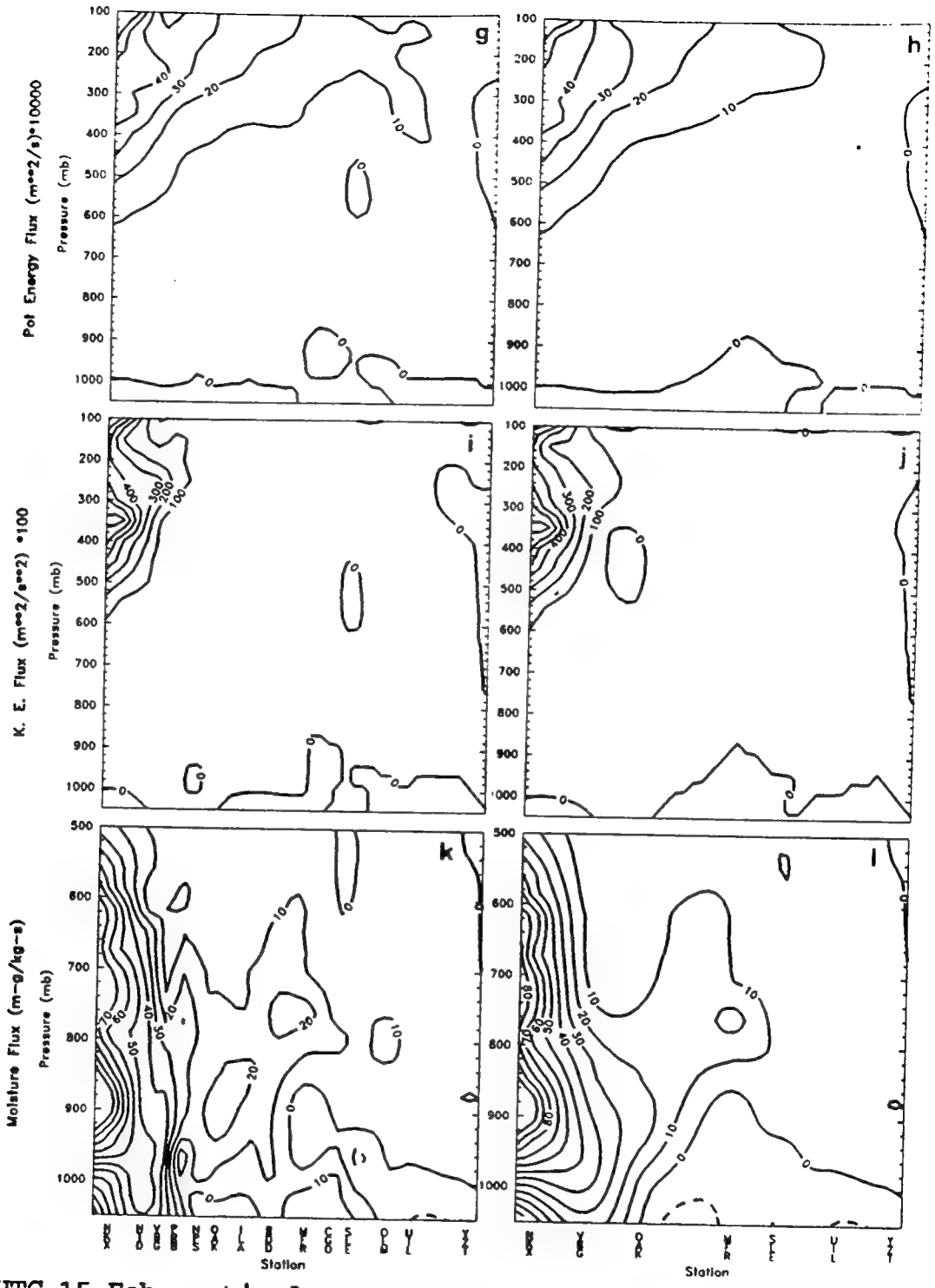


2100 UTC 15 Feb vertical cross sections for (g) ALL potential energy flux, (h) NWS potential energy flux, (i) ALL kinetic energy flux, (j) NWS kinetic energy flux, (k) ALL moisture flux, and (l) NWS moisture.

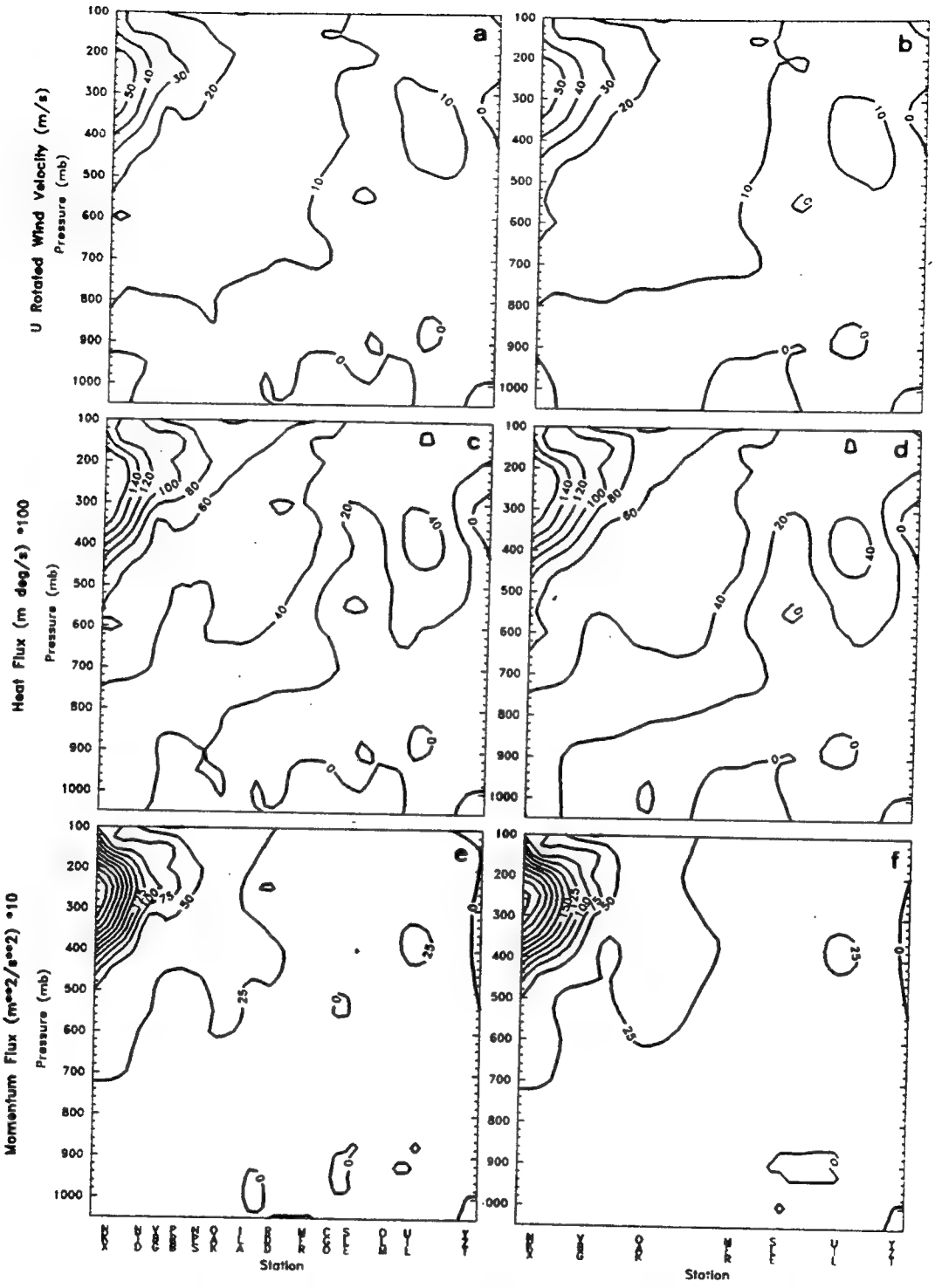


0000 UTC 16 Feb vertical cross sections for (a) ALL $U_r$ flux, (b) NWS $U_r$ flux, (c) ALL heat flux, (d) NWS heat flux, (e) ALL momentum flux, and (f) NWS momentum flux.

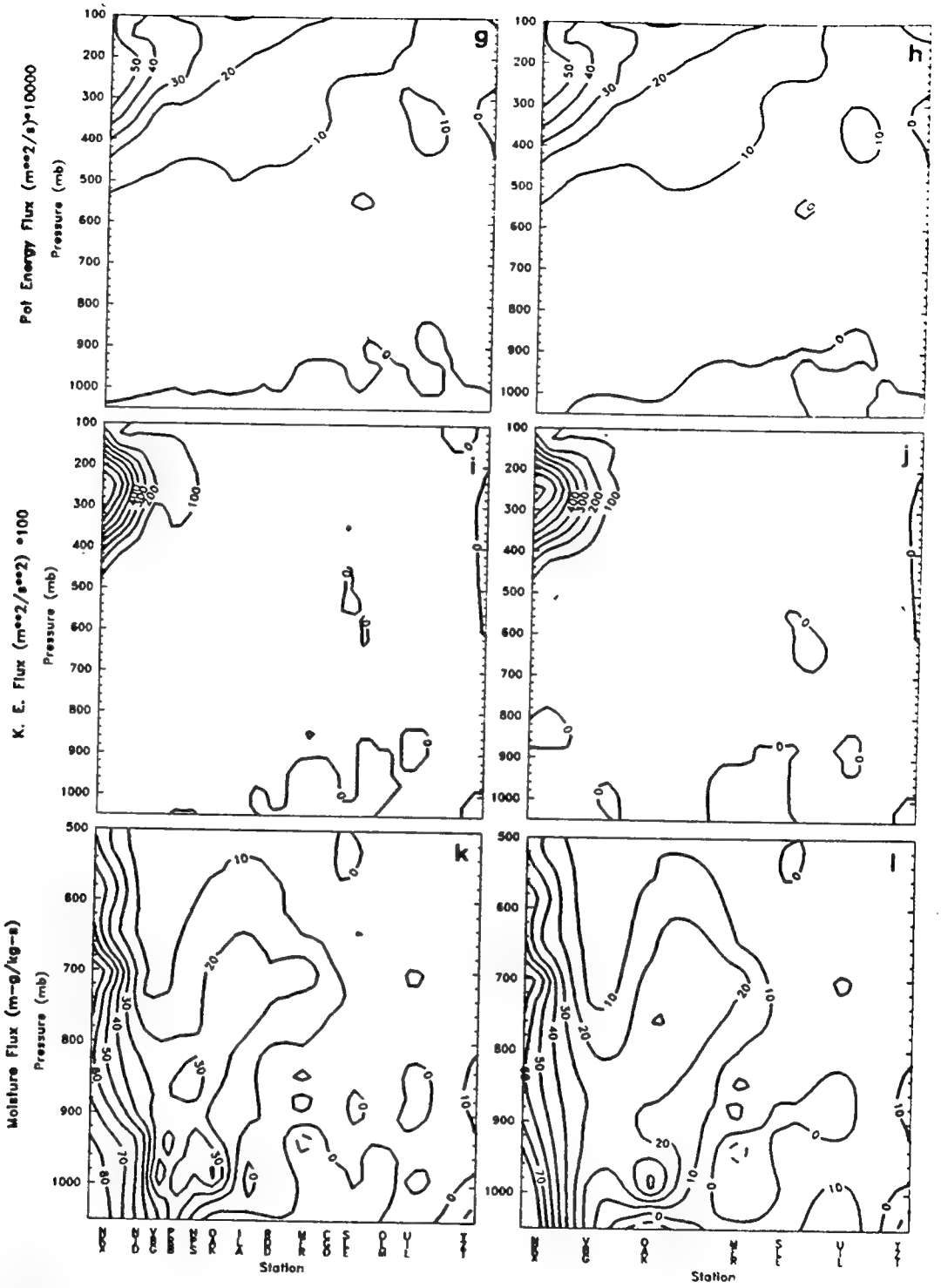


0000 UTC 16 Feb vertical cross sections for (g) ALL potential energy flux, (h) NWS potential energy flux, (i) ALL kinetic energy flux, (j) NWS kinetic energy flux, (k) ALL moisture flux, and (l) NWS moisture.

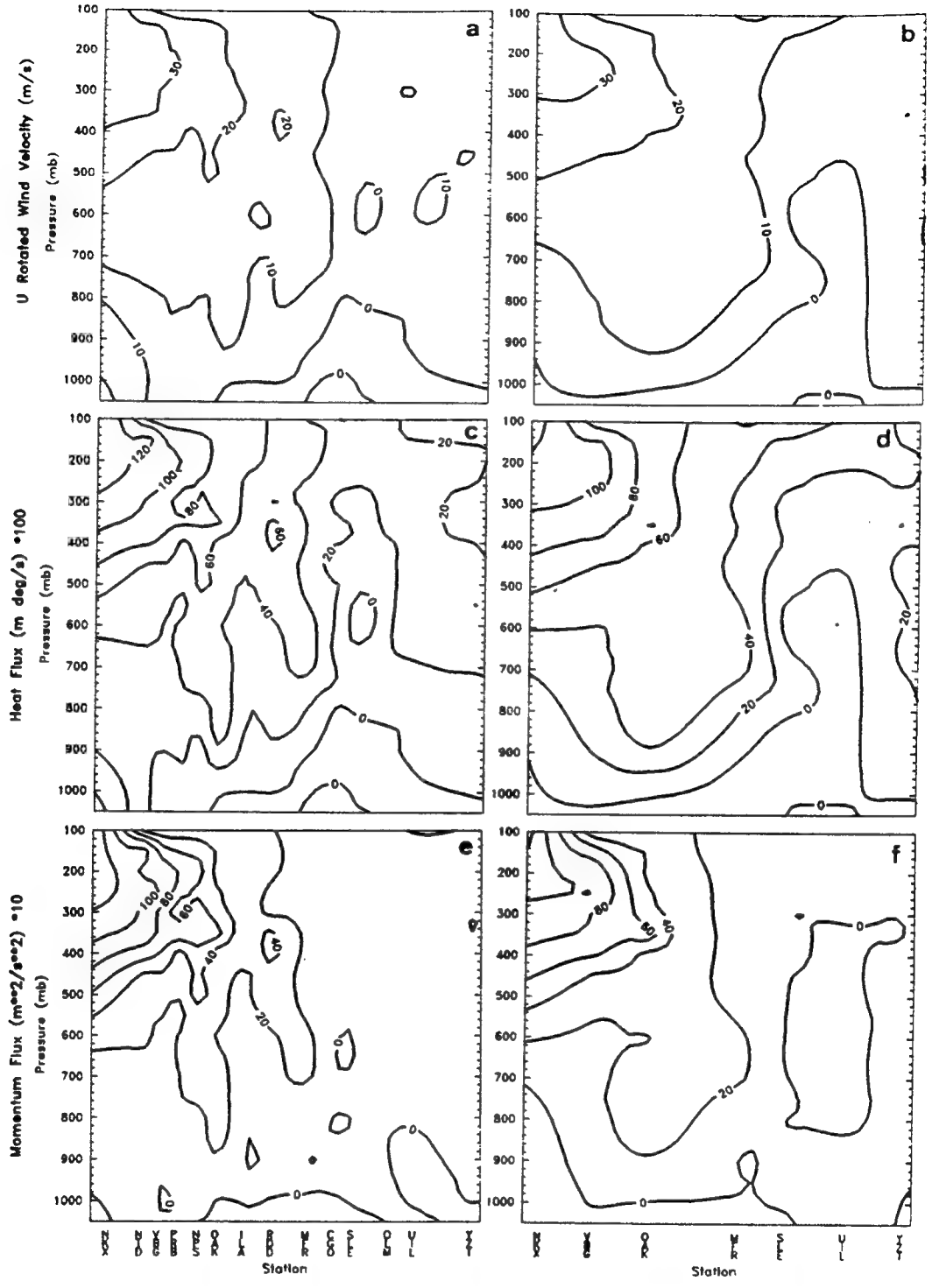


0300 UTC 16 Feb vertical cross sections for (a) ALL $U_r$ flux, (b) NWS $U_r$ flux, (c) ALL heat flux, (d) NWS heat flux, (e) ALL momentum flux, and (f) NWS momentum flux.

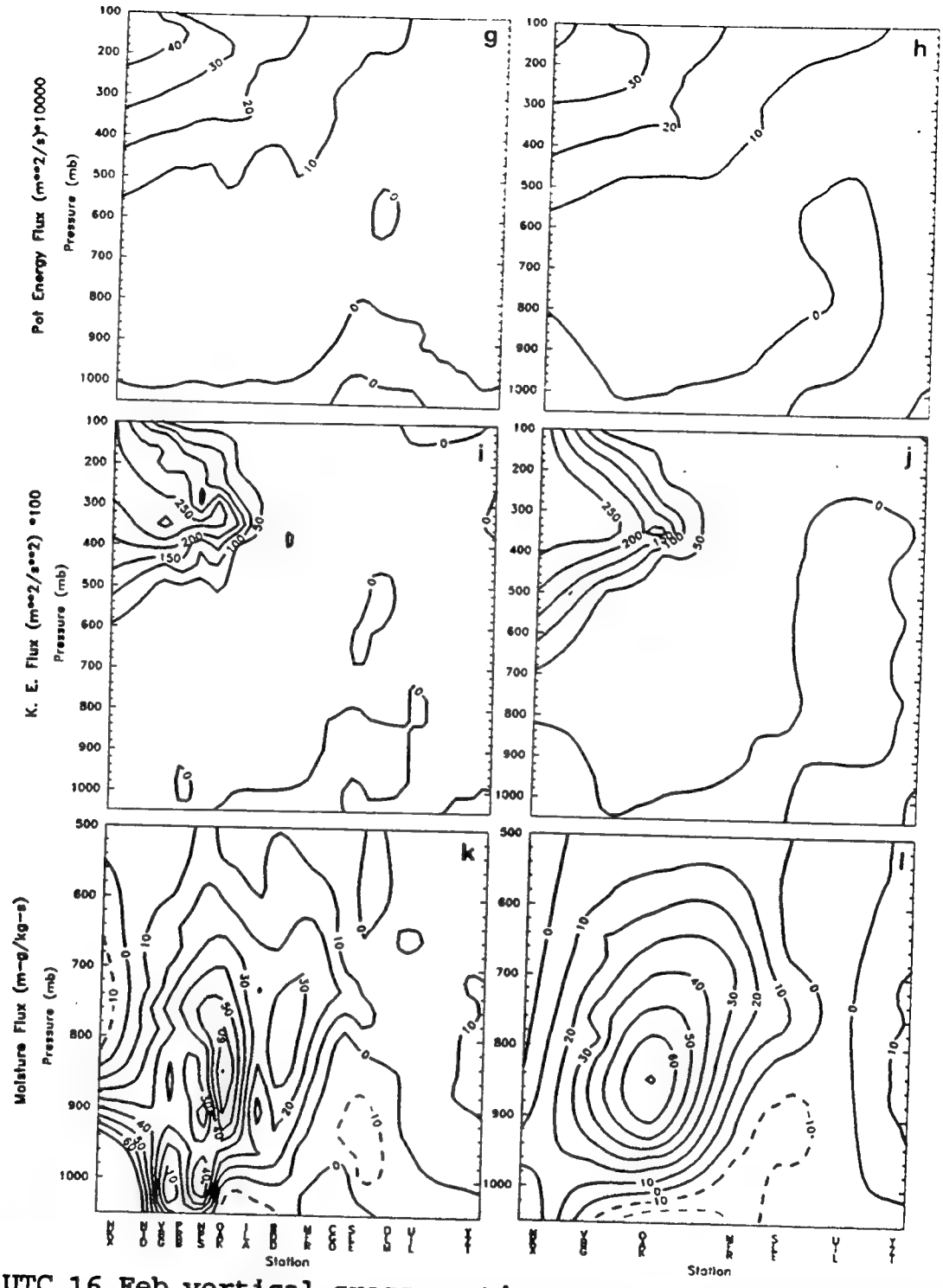


0300 UTC 16 Feb vertical cross sections for (g) ALL potential energy flux, (h) NWS potential energy flux, (i) ALL kinetic energy flux, (j) NWS kinetic energy flux, (k) ALL moisture flux, and (l) NWS moisture.

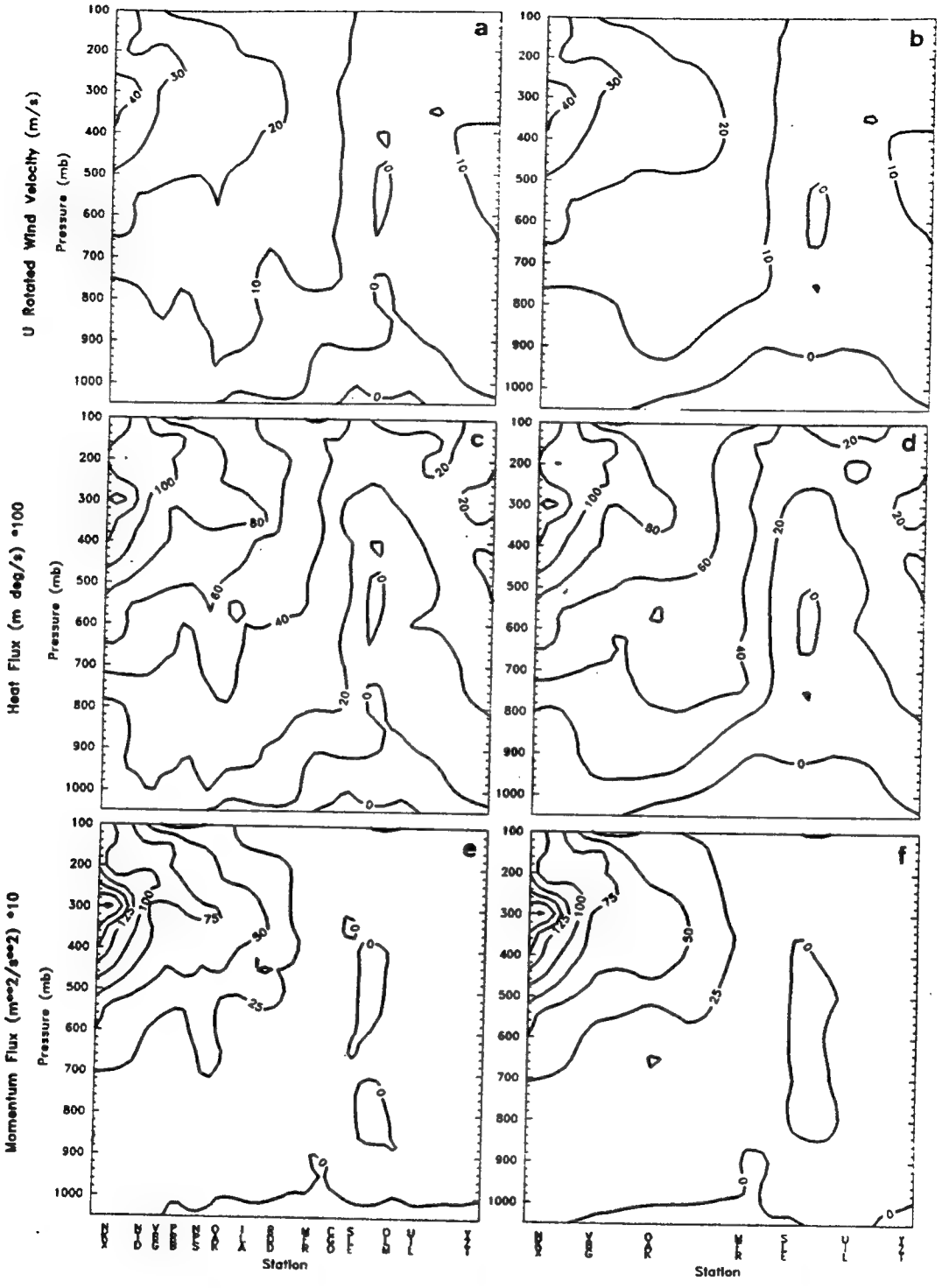


0600 UTC 16 Feb vertical cross sections for (a) ALL $U_r$ flux, (b) NWS $U_r$ flux, (c) ALL heat flux, (d) NWS heat flux, (e) ALL momentum flux, and (f) NWS momentum flux.

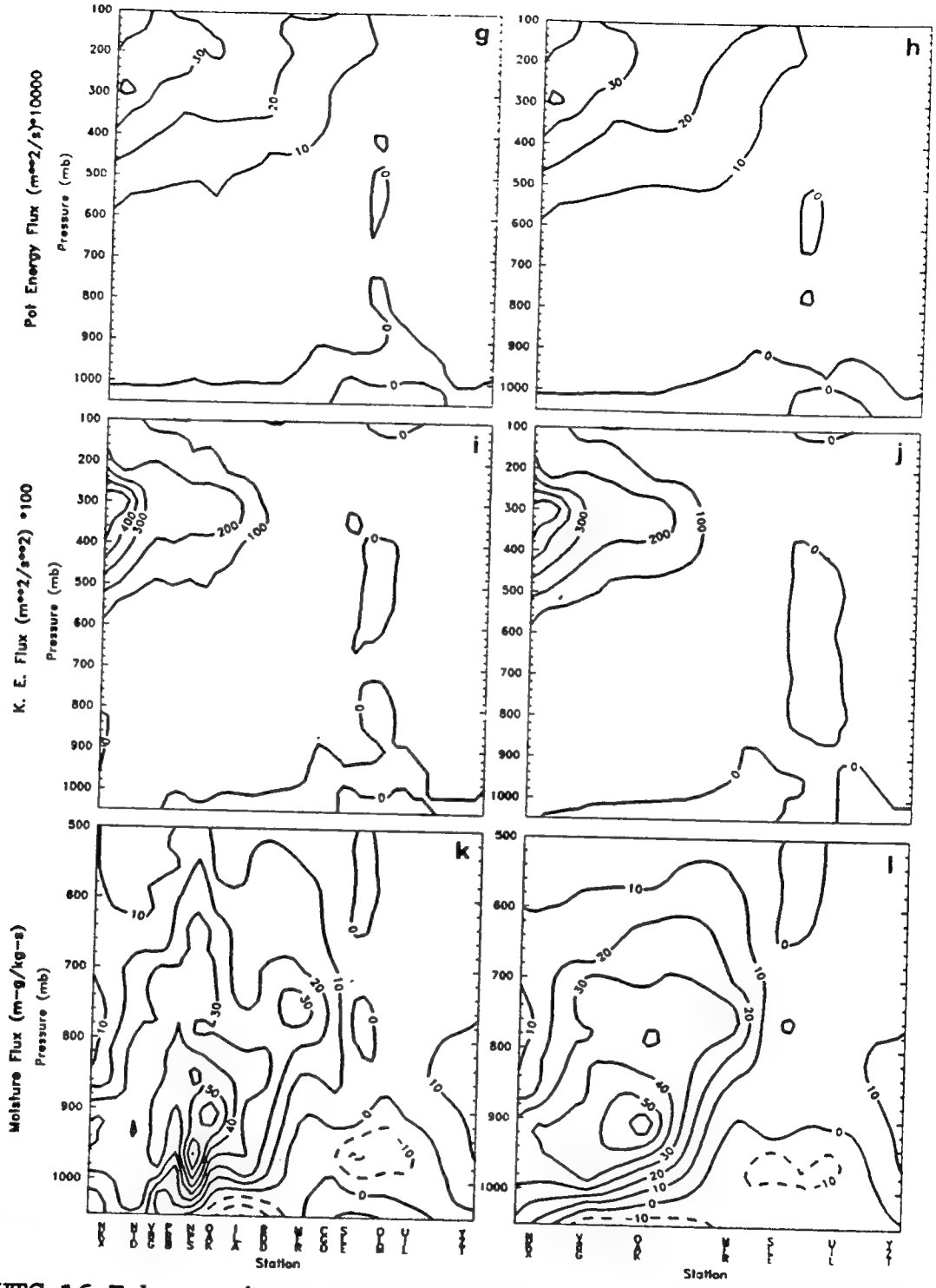


0600 UTC 16 Feb vertical cross sections for (g) ALL potential energy flux, (h) NWS potential energy flux, (i) ALL kinetic energy flux, (j) NWS kinetic energy flux, (k) ALL moisture flux, and (l) NWS moisture.

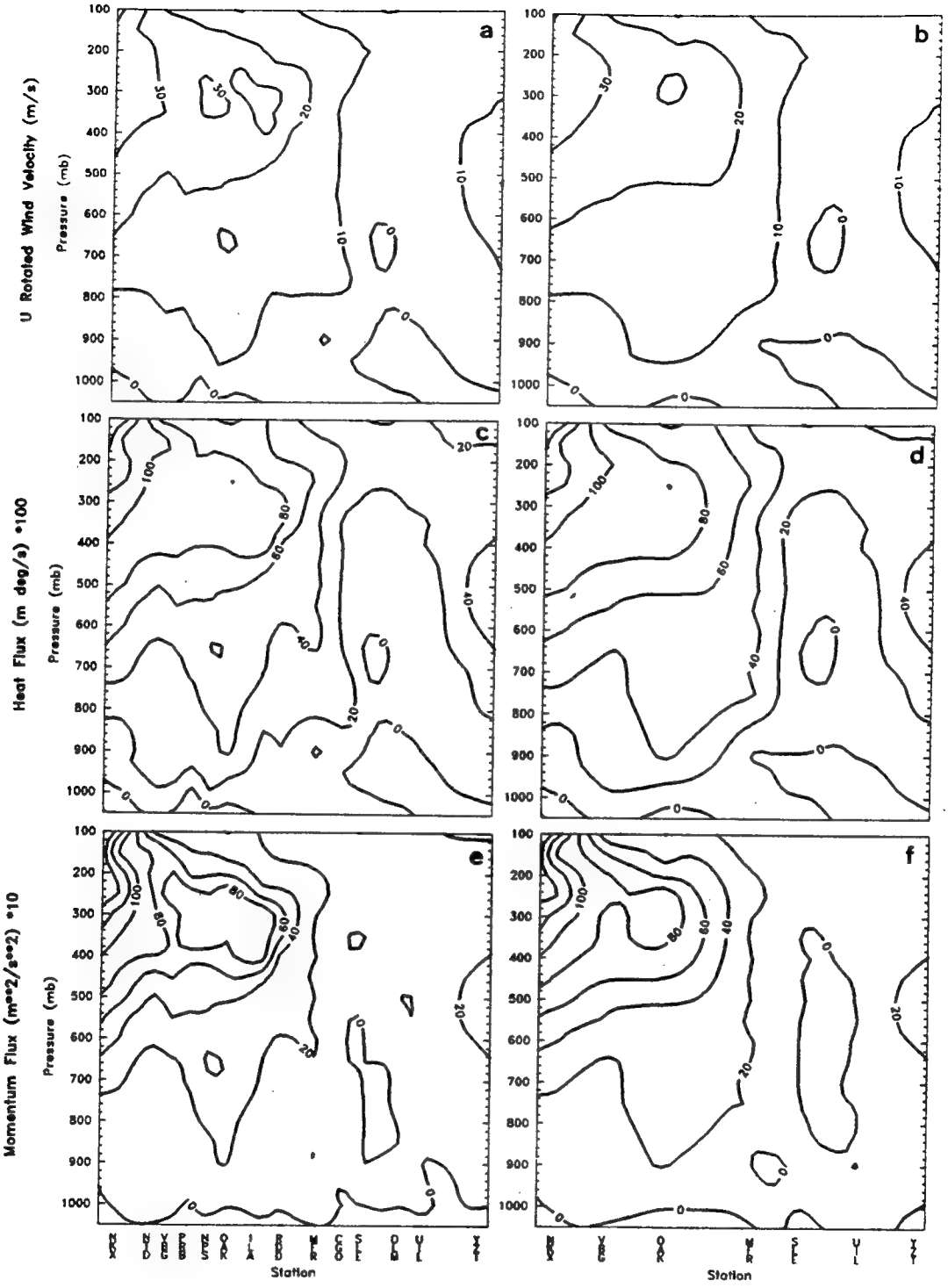


0900 UTC 16 Feb vertical cross sections for (a) ALL $U_r$ flux, (b) NWS $U_r$ flux, (c) ALL heat flux, (d) NWS heat flux, (e) ALL momentum flux, and (f) NWS momentum flux.

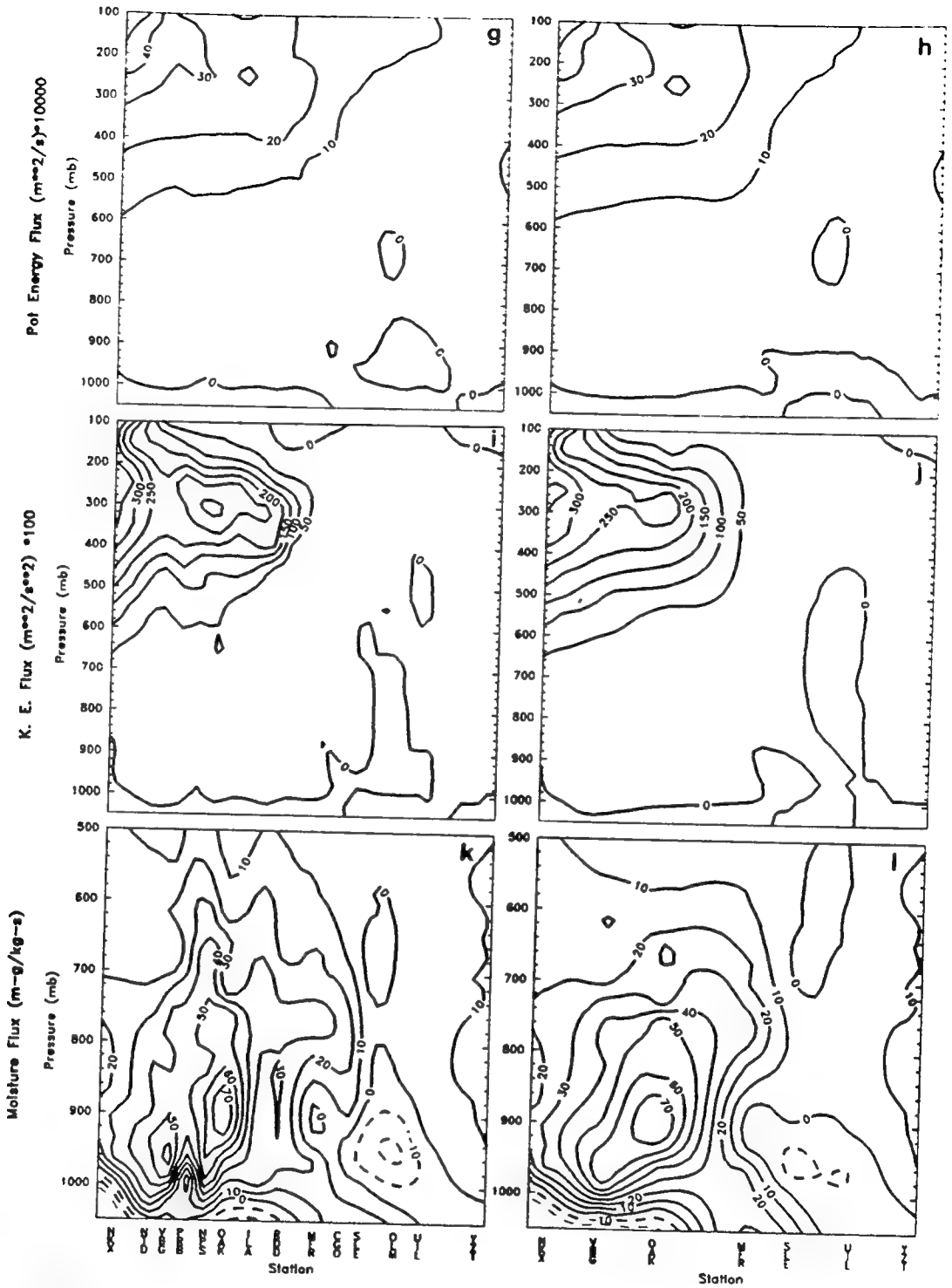


0900 UTC 16 Feb vertical cross sections for (g) ALL potential energy flux, (h) NWS potential energy flux, (i) ALL kinetic energy flux, (j) NWS kinetic energy flux, (k) ALL moisture flux, and (l) NWS moisture.

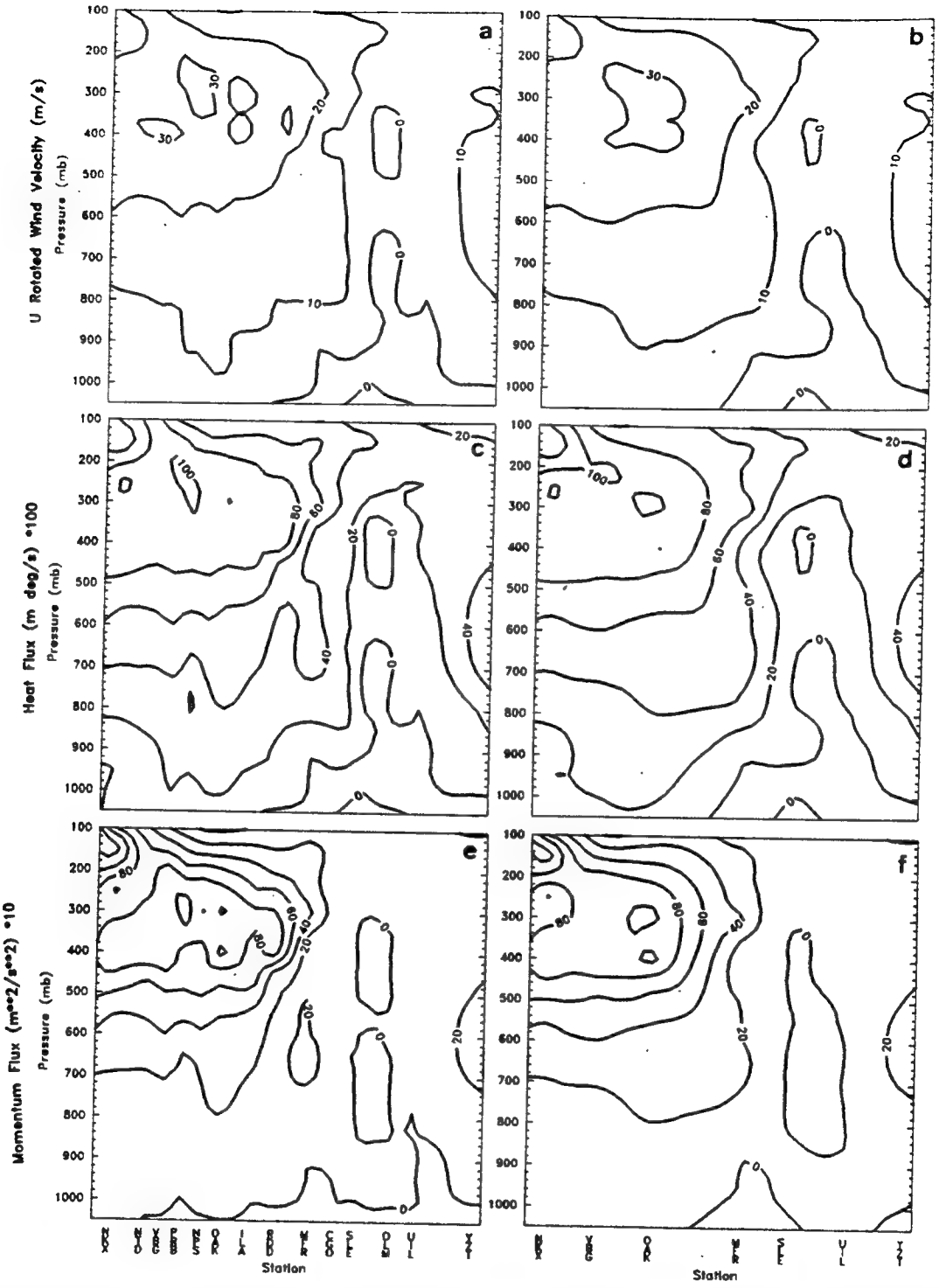


1200 UTC 16 Feb vertical cross sections for (a) ALL $U_r$ flux, (b) NWS $U_r$ flux, (c) ALL heat flux, (d) NWS heat flux, (e) ALL momentum flux, and (f) NWS momentum flux.

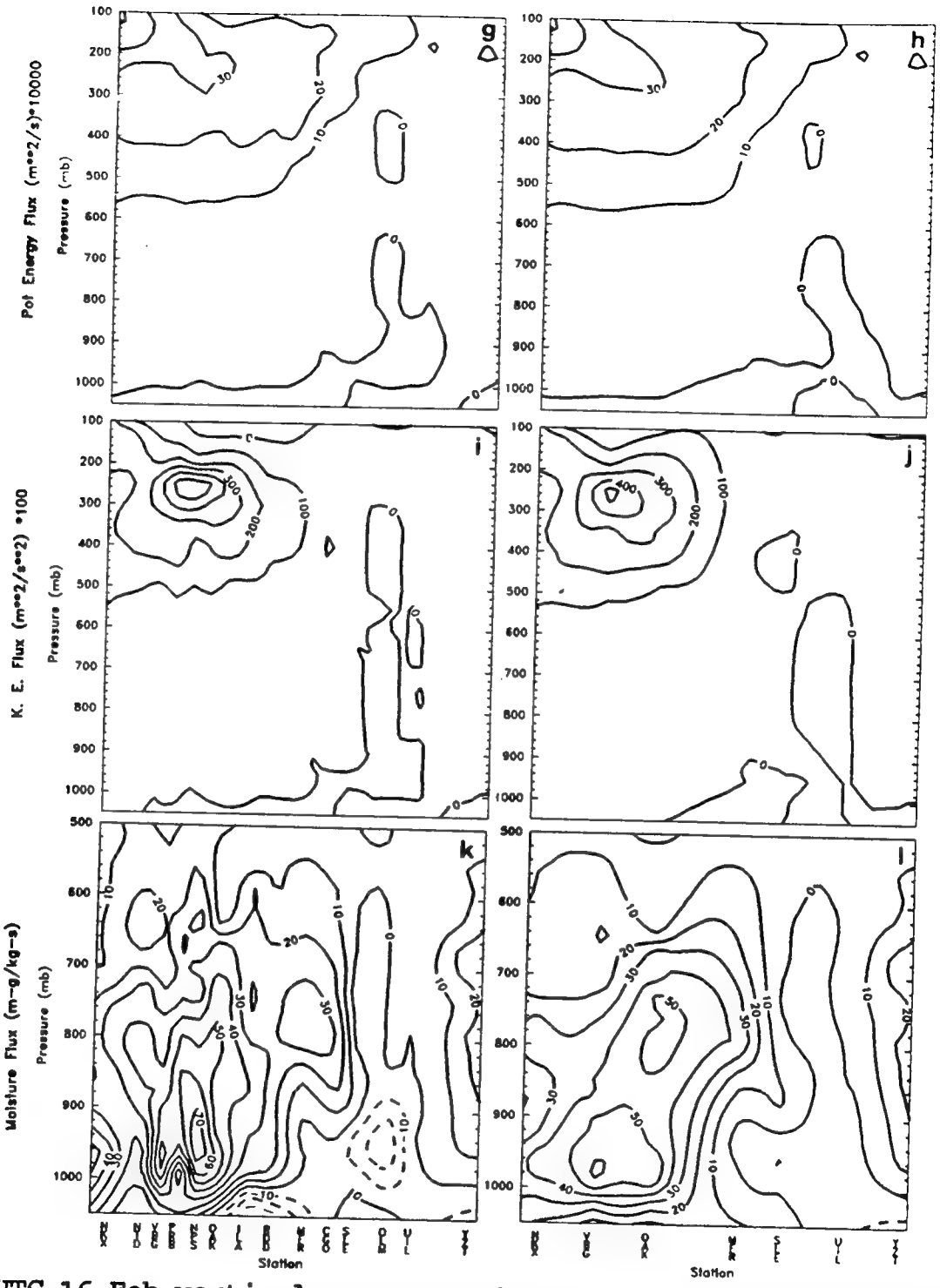


1200 UTC 16 Feb vertical cross sections for (g) ALL potential energy flux, (h) NWS potential energy flux, (i) ALL kinetic energy flux, (j) NWS kinetic energy flux, (k) ALL moisture flux, and (l) NWS moisture.

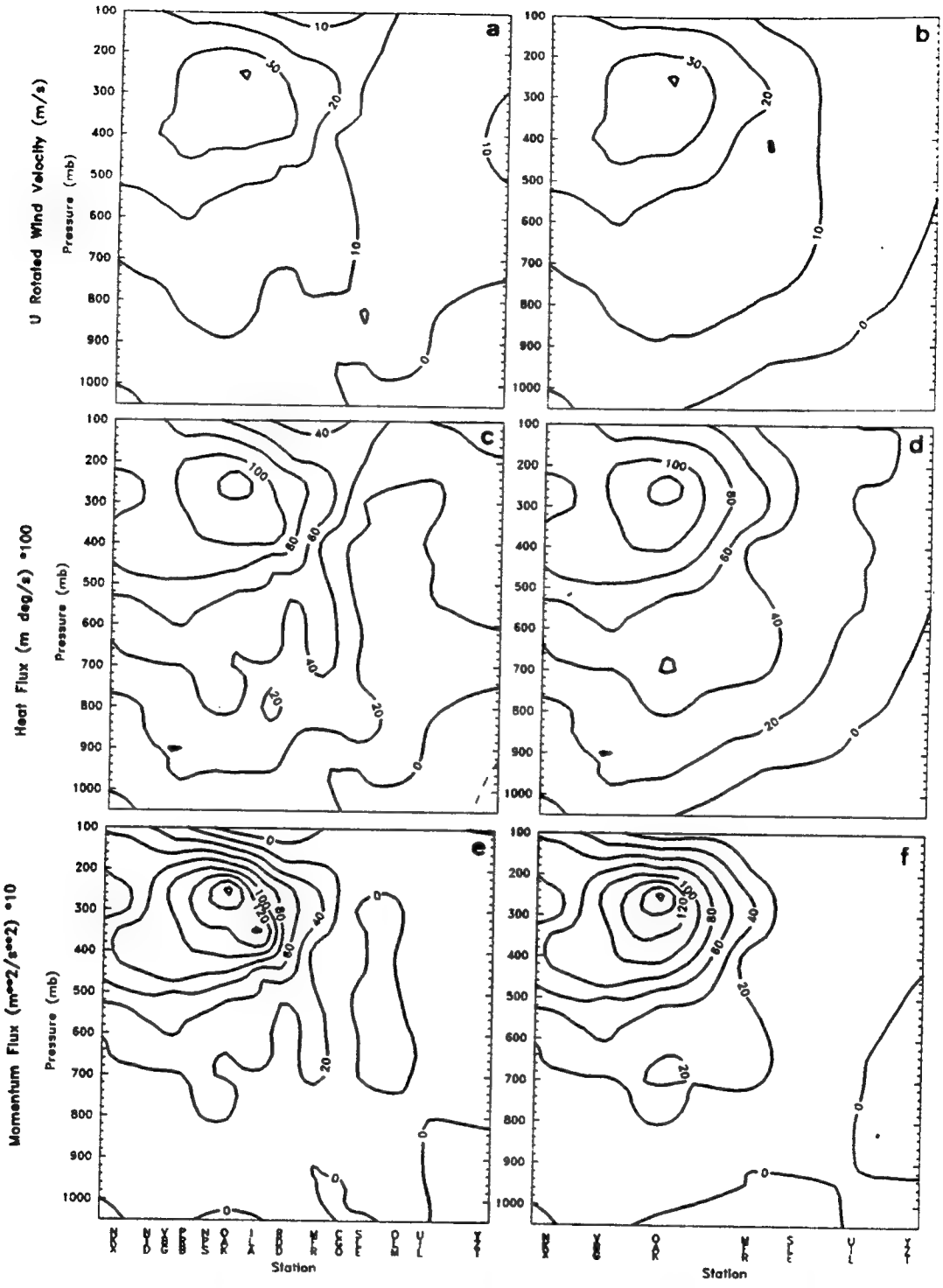


1500 UTC 16 Feb vertical cross sections for (a) ALL $U_r$ flux, (b) NWS $U_r$ flux, (c) ALL heat flux, (d) NWS heat flux, (e) ALL momentum flux, and (f) NWS momentum flux.

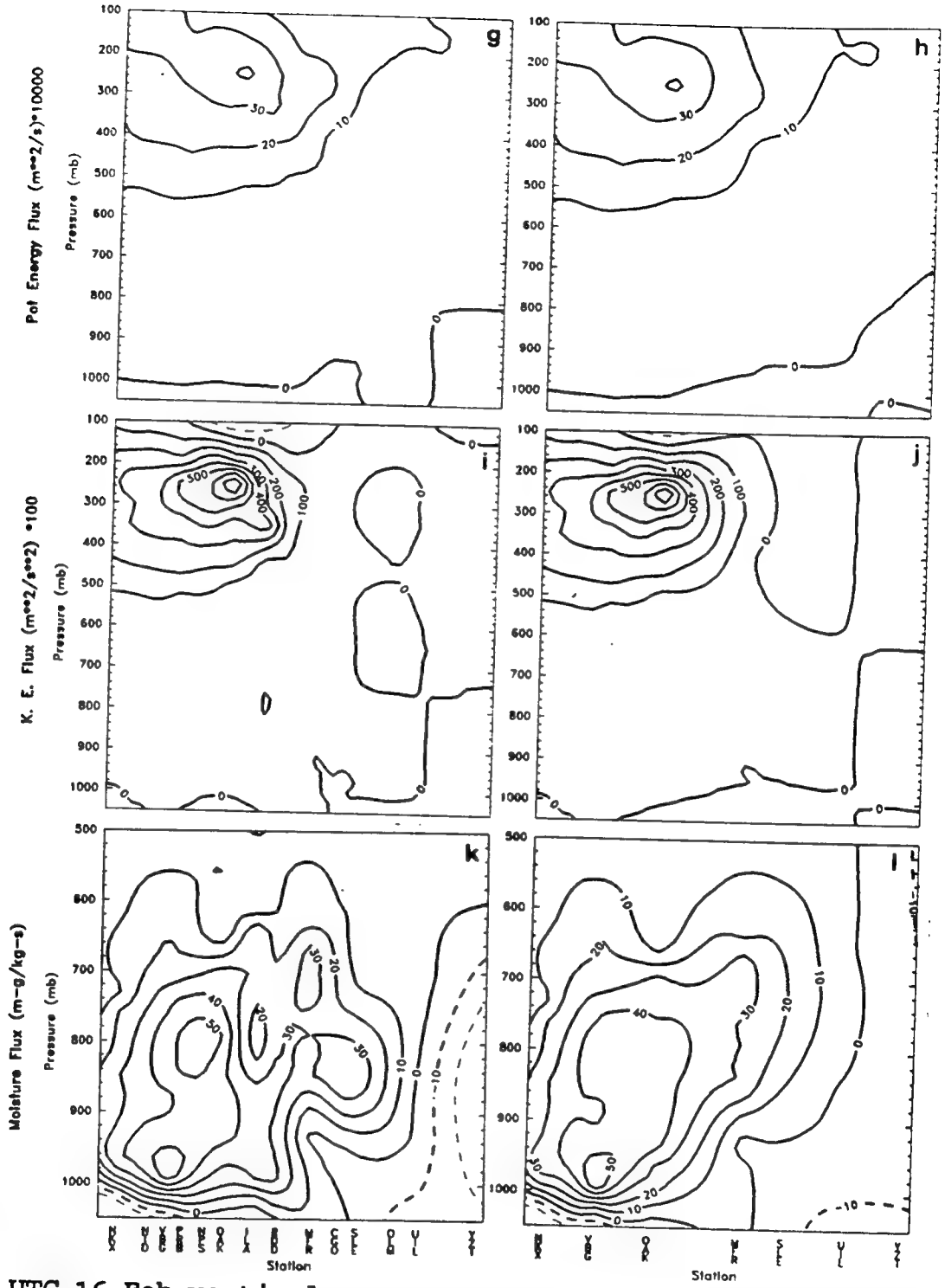


1500 UTC 16 Feb vertical cross sections for (g) ALL potential energy flux, (h) NWS potential energy flux, (i) ALL kinetic energy flux, (j) NWS kinetic energy flux, (k) ALL moisture flux, and (l) NWS moisture.

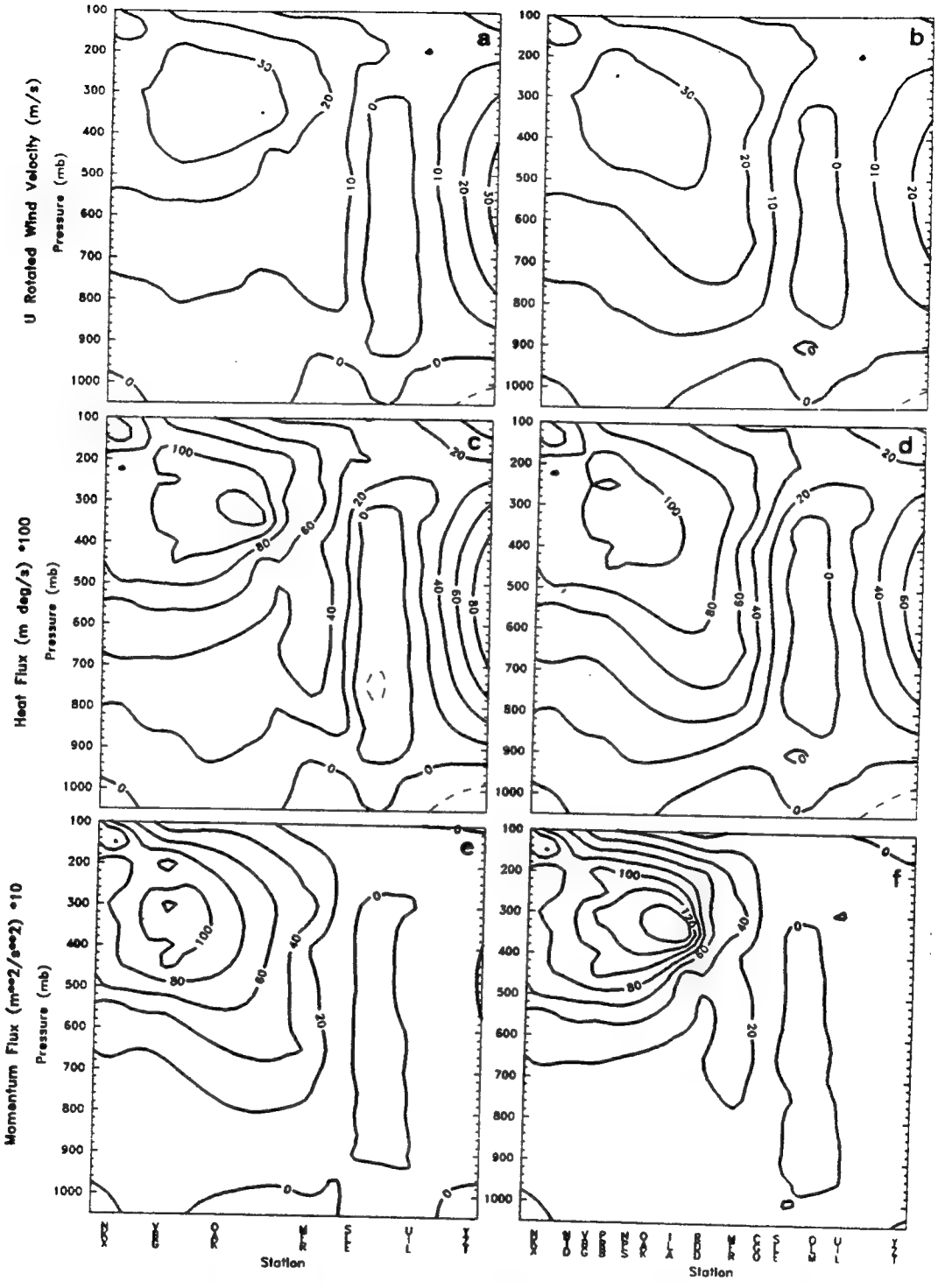


1800 UTC 16 Feb vertical cross sections for (a) ALL $U_r$ flux, (b) NWS $U_r$ flux, (c) ALL heat flux, (d) NWS heat flux, (e) ALL momentum flux, and (f) NWS momentum flux.

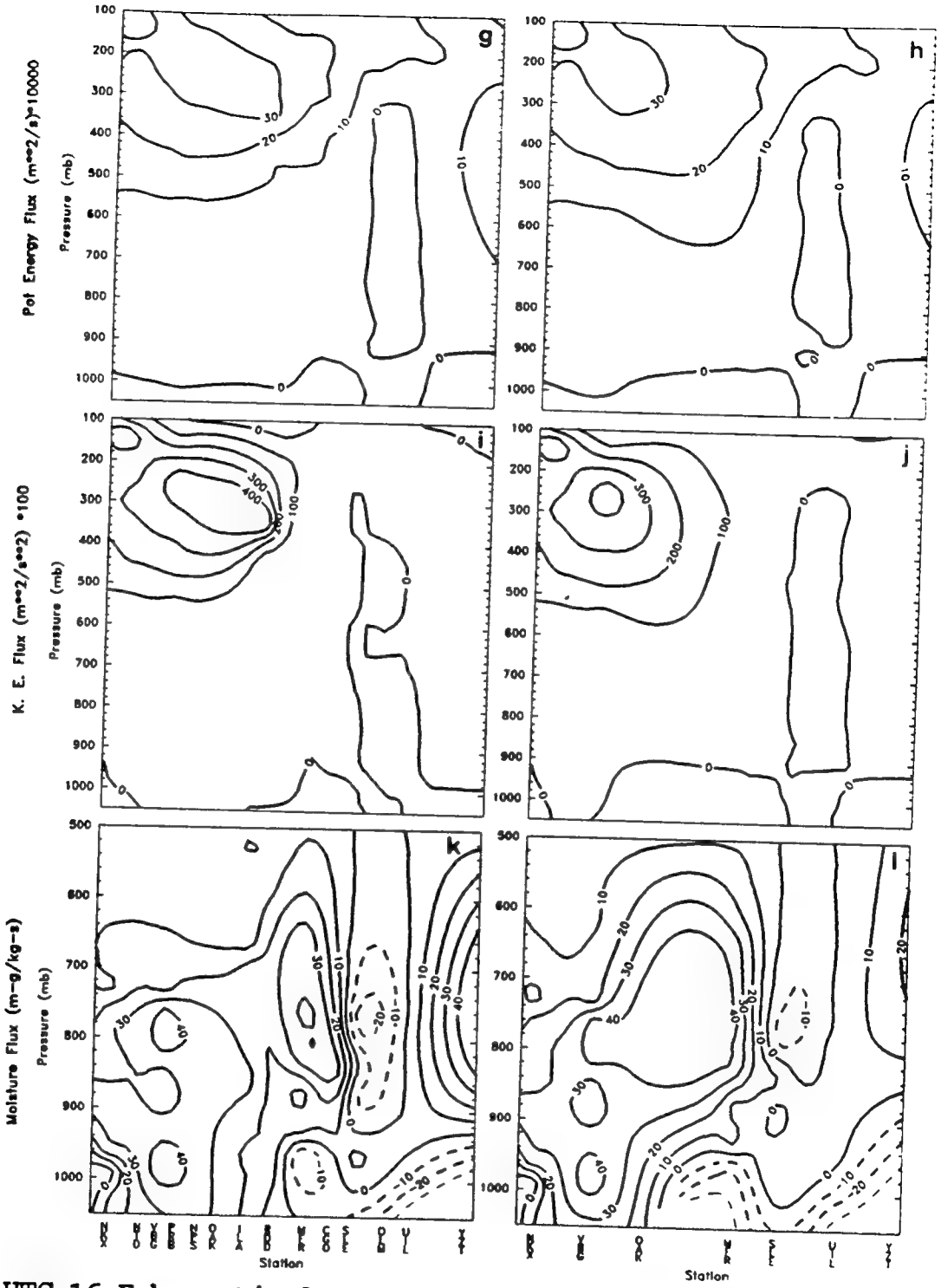


1800 UTC 16 Feb vertical cross sections for (g) ALL potential energy flux, (h) NWS potential energy flux, (i) ALL kinetic energy flux, (j) NWS kinetic energy flux, (k) ALL moisture flux, and (l) NWS moisture.

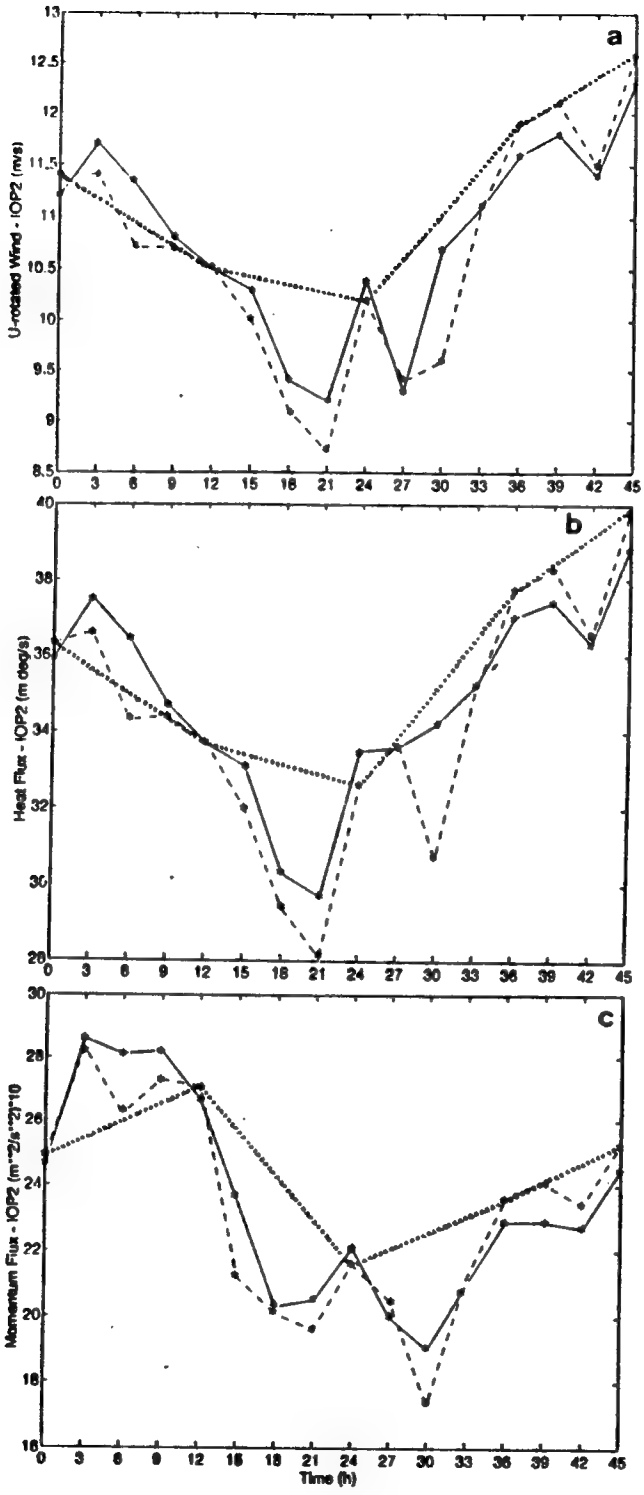


Fig. 15. (a-c) As in Fig. 13 (a-c), except for IOP-2.

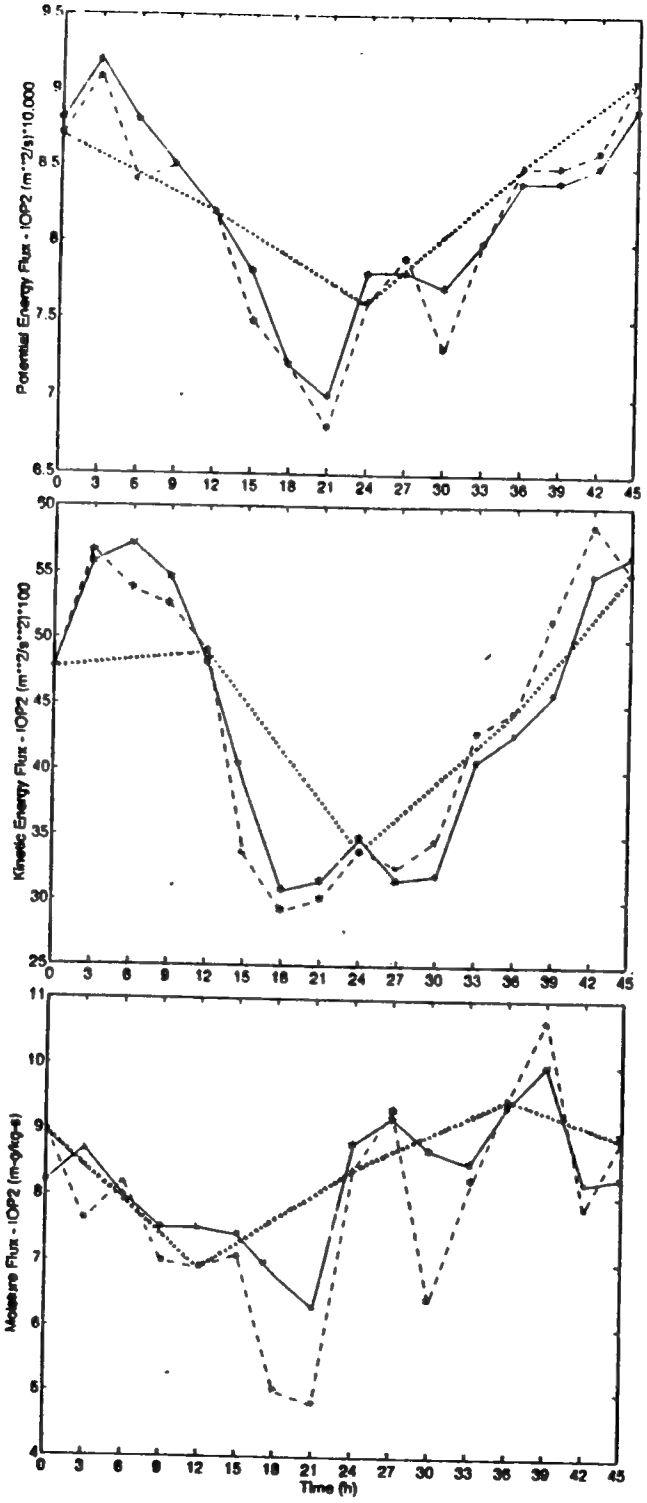


Fig. 15. (d-f) As in Fig. 13 (a-c), except for IOP-2.

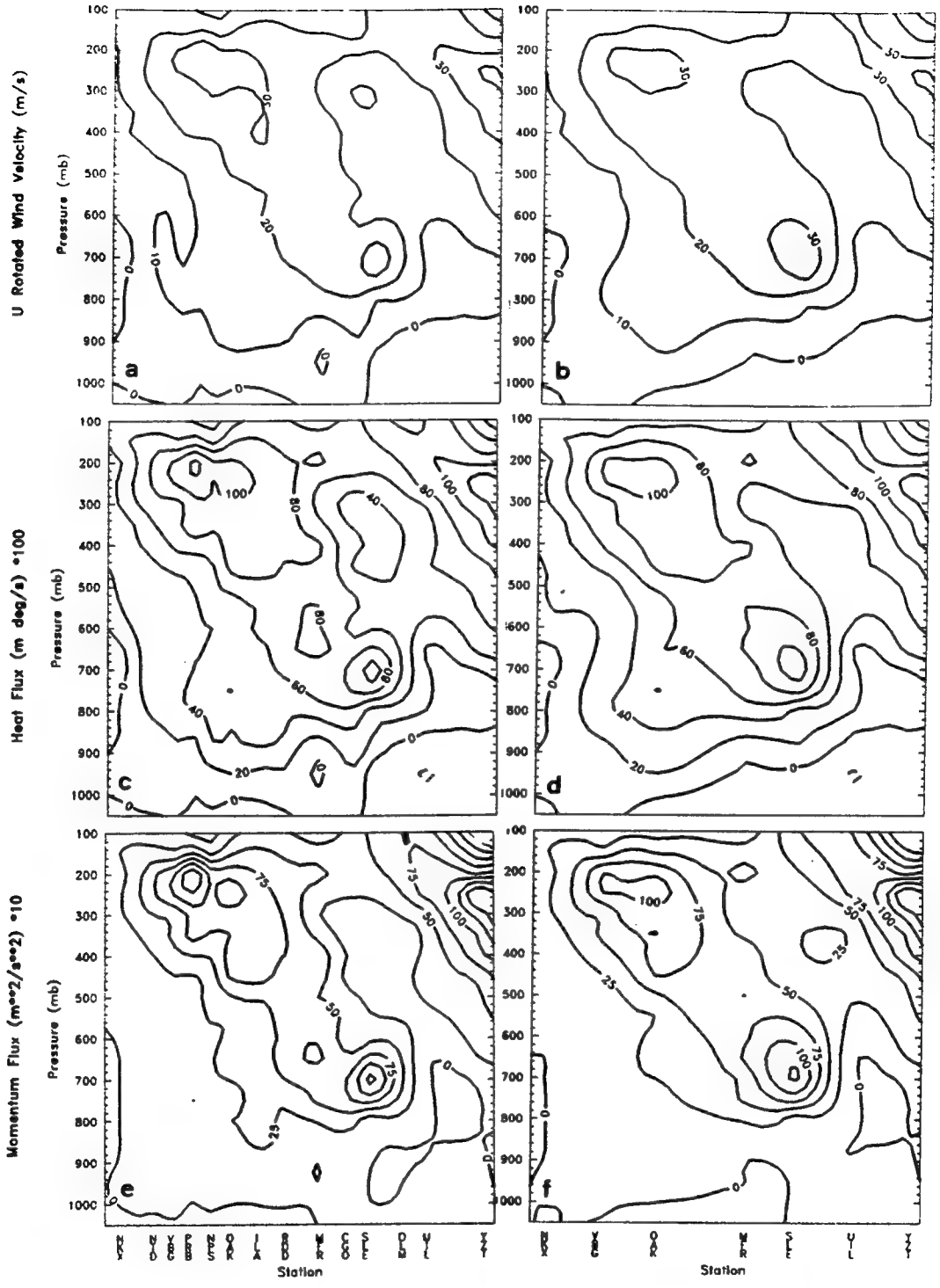


0300 UTC 20 Feb vertical cross sections for (a) ALL $U_r$ flux, (b) NWS $U_r$ flux, (c) ALL heat flux, (d) NWS heat flux, (e) ALL momentum flux, and (f) NWS momentum flux.

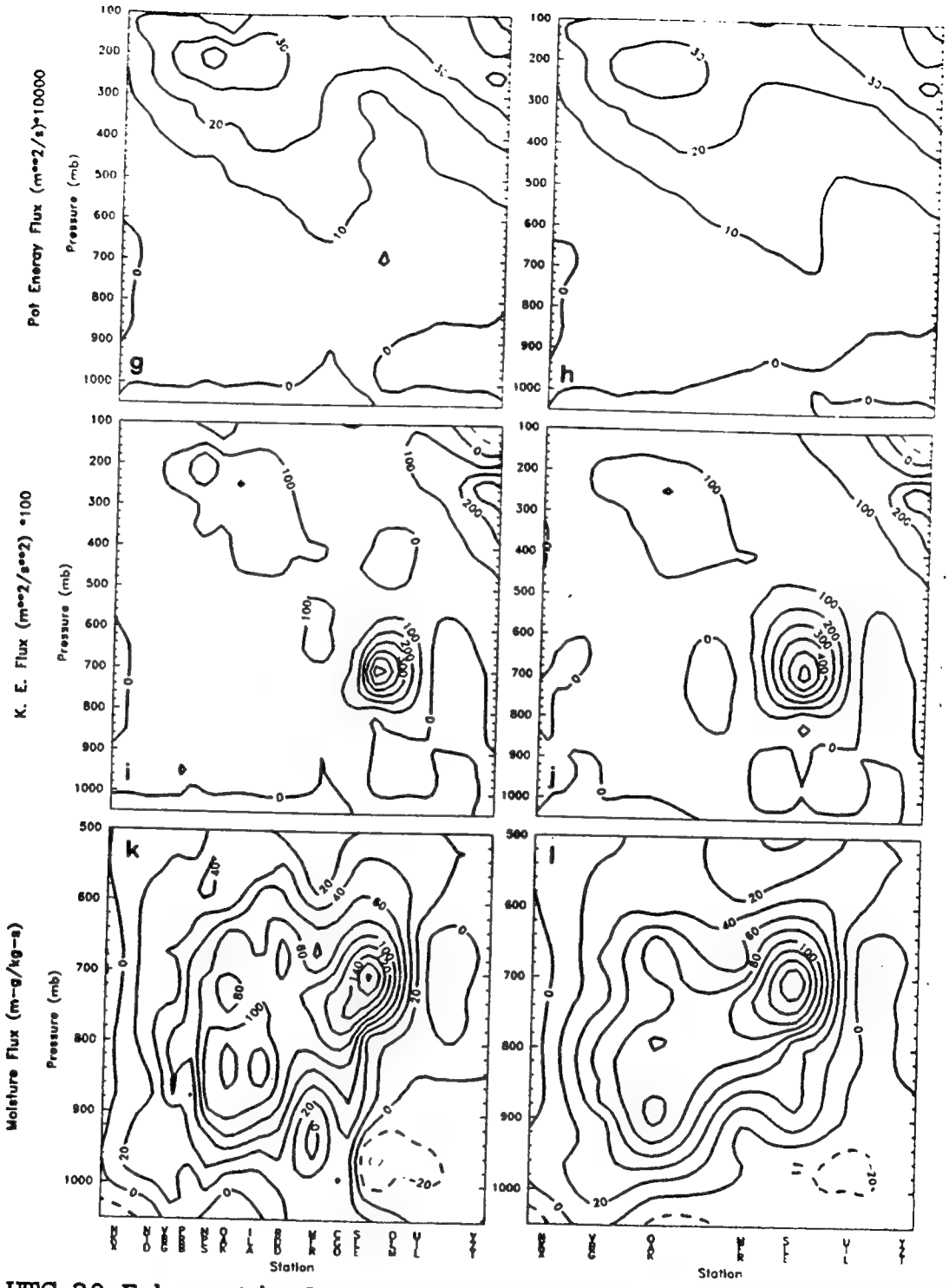


0300 UTC 20 Feb vertical cross sections for (g) ALL potential energy flux, (h) NWS potential energy flux, (i) ALL kinetic energy flux, (j) NWS kinetic energy flux, (k) ALL moisture flux, and (l) NWS moisture.

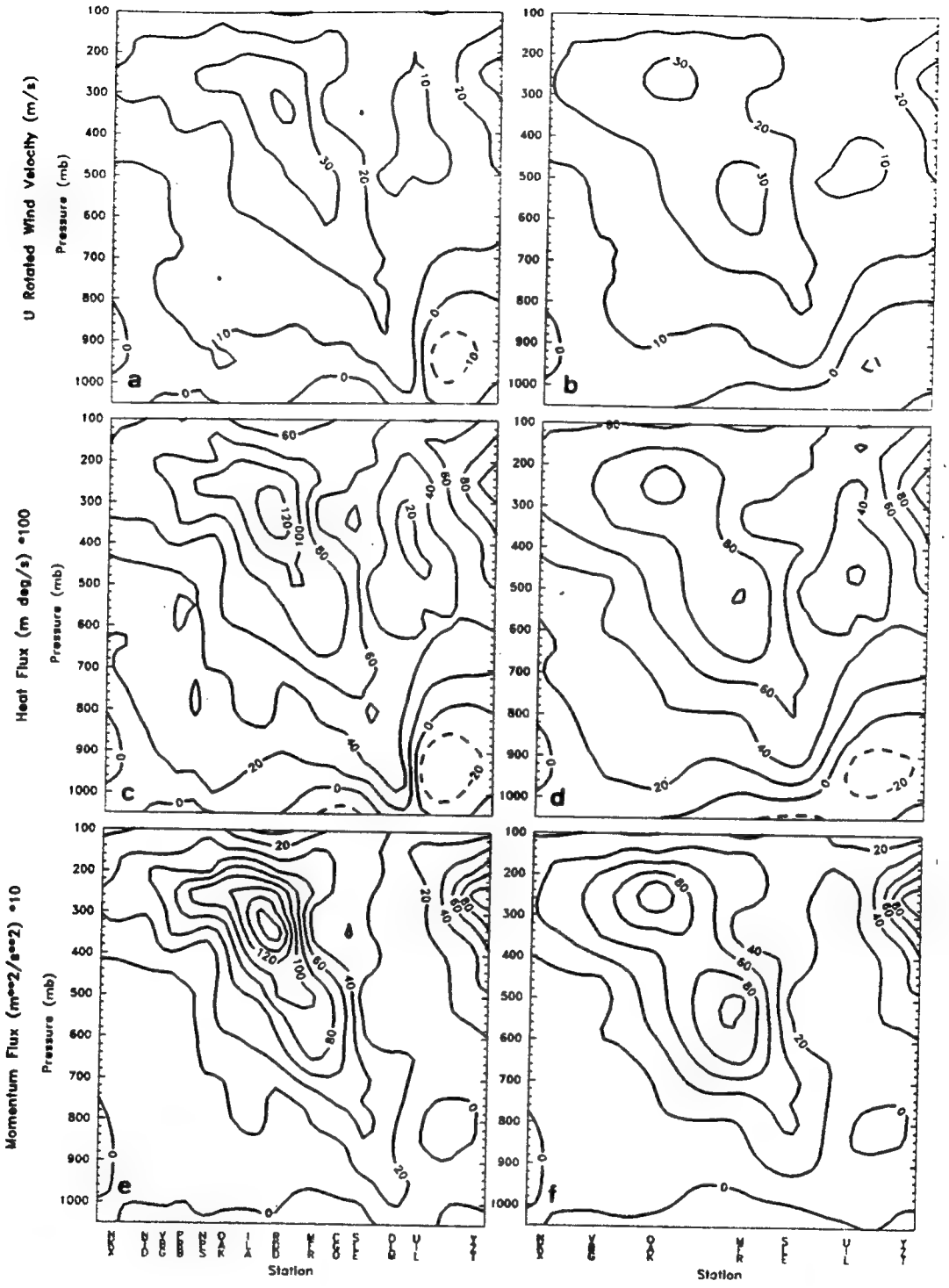


0900 UTC 20 Feb vertical cross sections for (a) ALL $U_r$ flux, (b) NWS $U_r$ flux, (c) ALL heat flux, (d) NWS heat flux, (e) ALL momentum flux, and (f) NWS momentum flux.

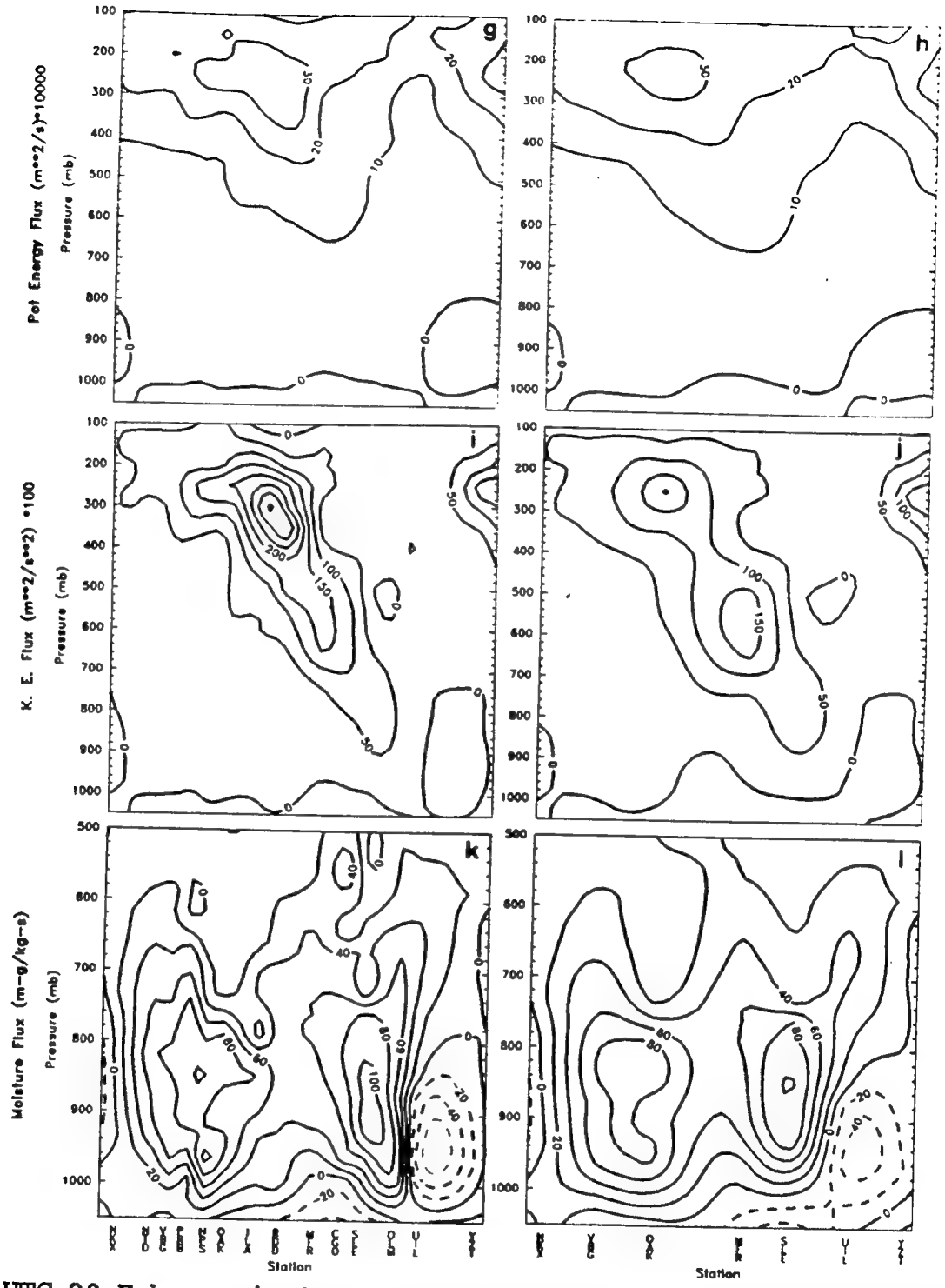


0900 UTC 20 Feb vertical cross sections for (g) ALL potential energy flux, (h) NWS potential energy flux, (i) ALL kinetic energy flux, (j) NWS kinetic energy flux, (k) ALL moisture flux, and (l) NWS moisture.

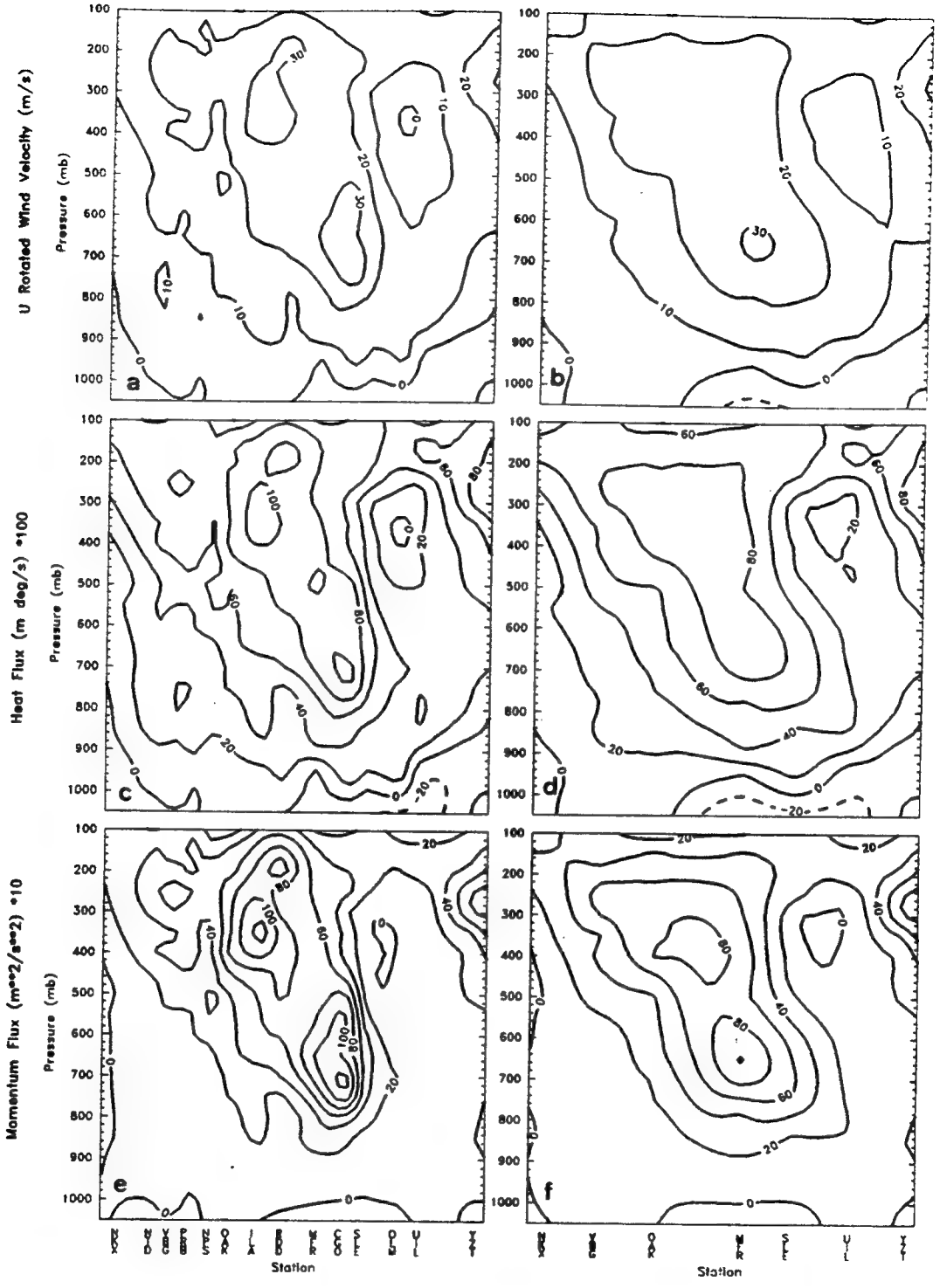


1200 UTC 20 Feb vertical cross sections for (a) ALL $U_r$ flux, (b) NWS $U_r$ flux, (c) ALL heat flux, (d) NWS heat flux, (e) ALL momentum flux, and (f) NWS momentum flux.

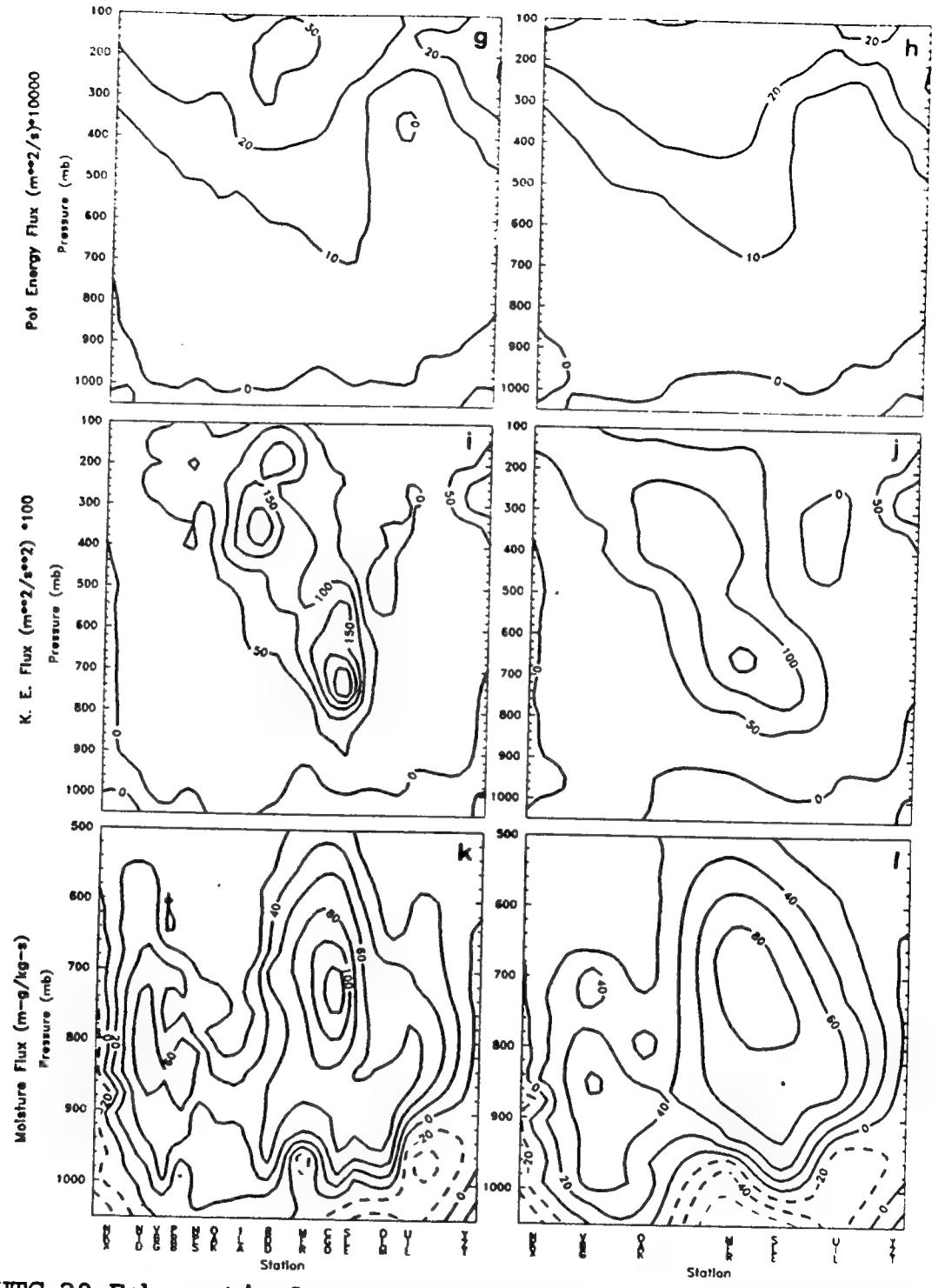


1200 UTC 20 Feb vertical cross sections for (g) ALL potential energy flux, (h) NWS potential energy flux, (i) ALL kinetic energy flux, (j) NWS kinetic energy flux, (k) ALL moisture flux, and (l) NWS moisture.

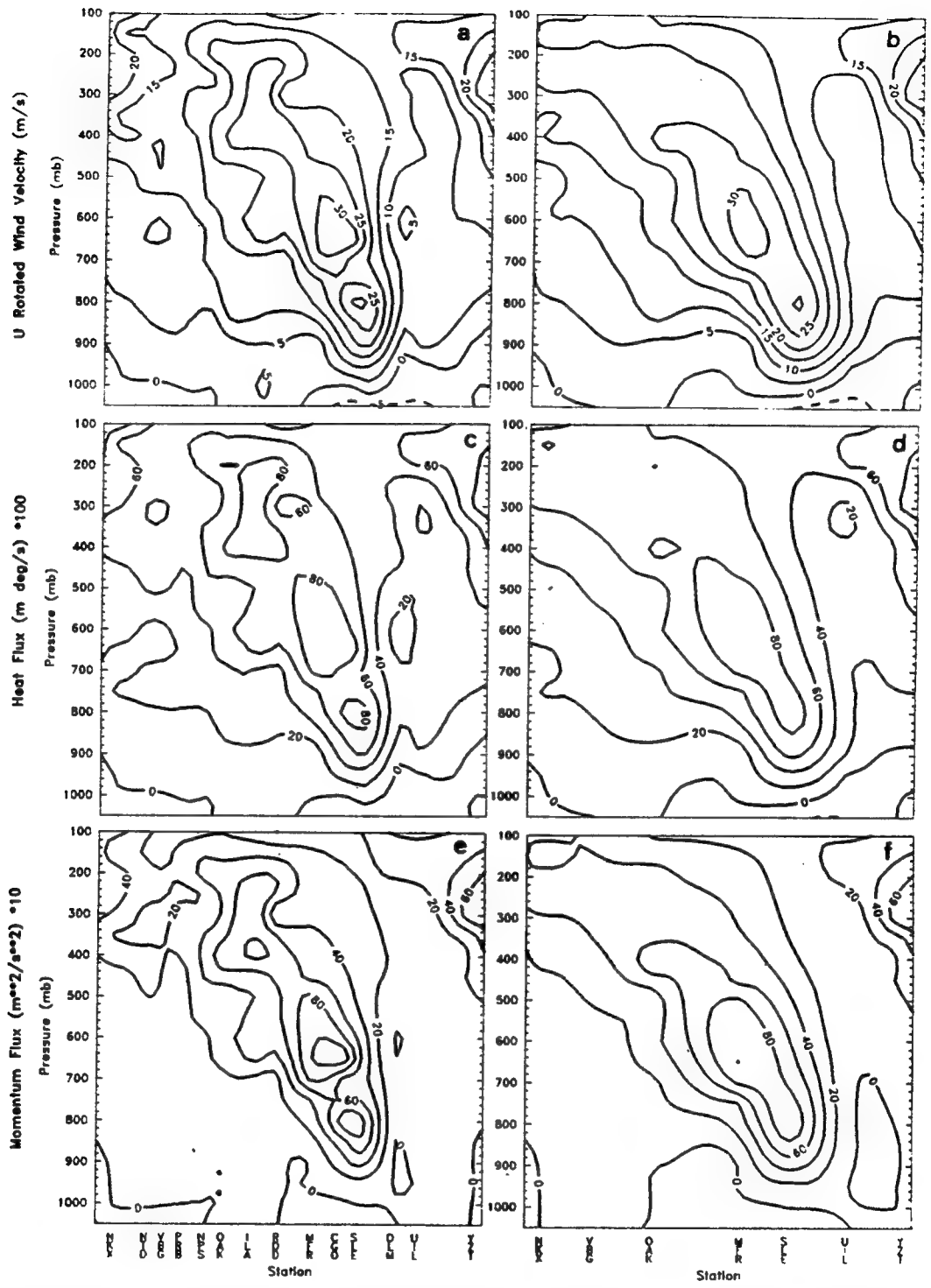


1500 UTC 20 Feb vertical cross sections for (a) ALL $U_r$ flux, (b) NWS $U_r$ flux, (c) ALL heat flux, (d) NWS heat flux, (e) ALL momentum flux, and (f) NWS momentum flux.

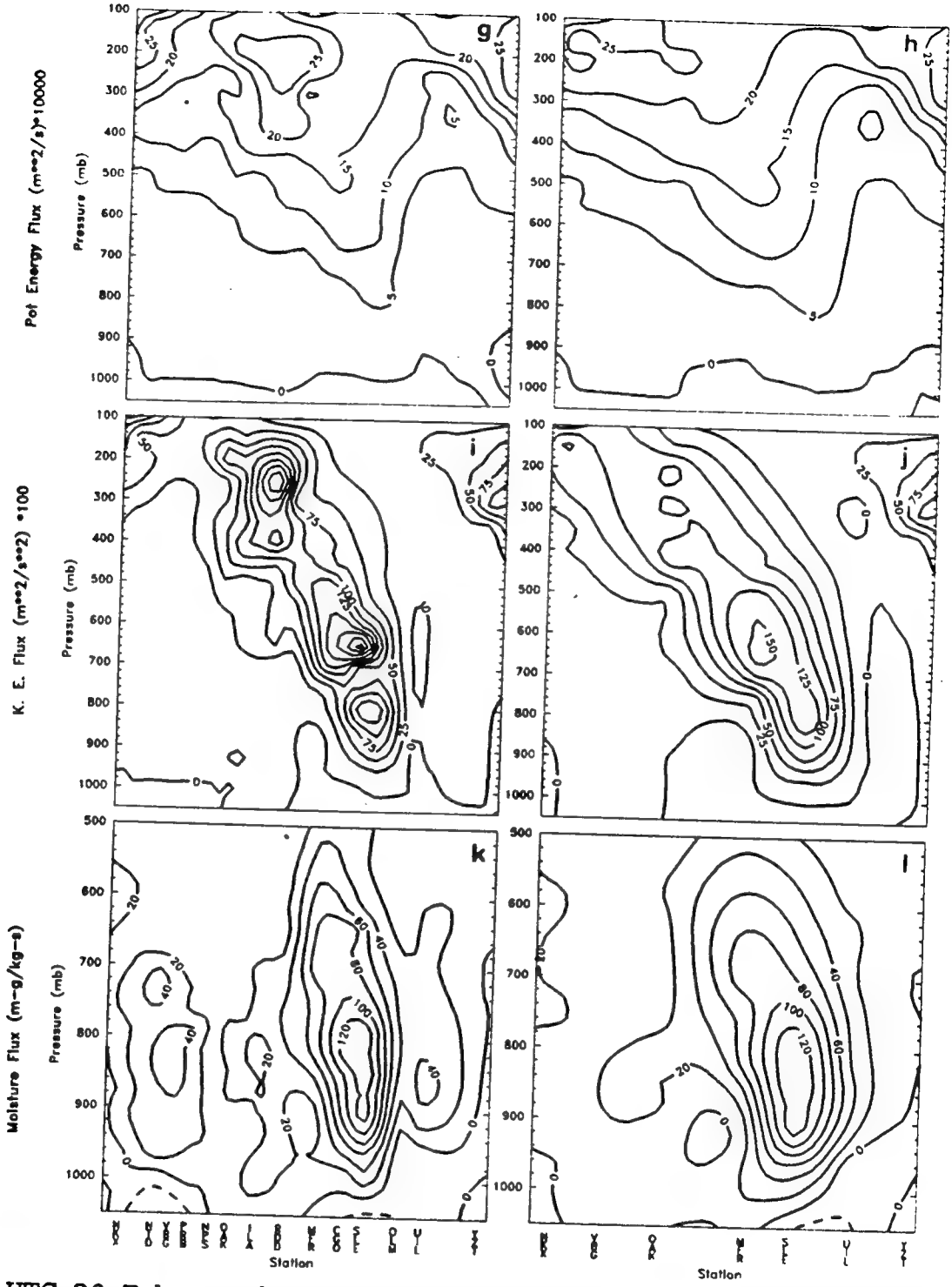


1500 UTC 20 Feb vertical cross sections for (g) ALL potential energy flux, (h) NWS potential energy flux, (i) ALL kinetic energy flux, (j) NWS kinetic energy flux, (k) ALL moisture flux, and (l) NWS moisture.

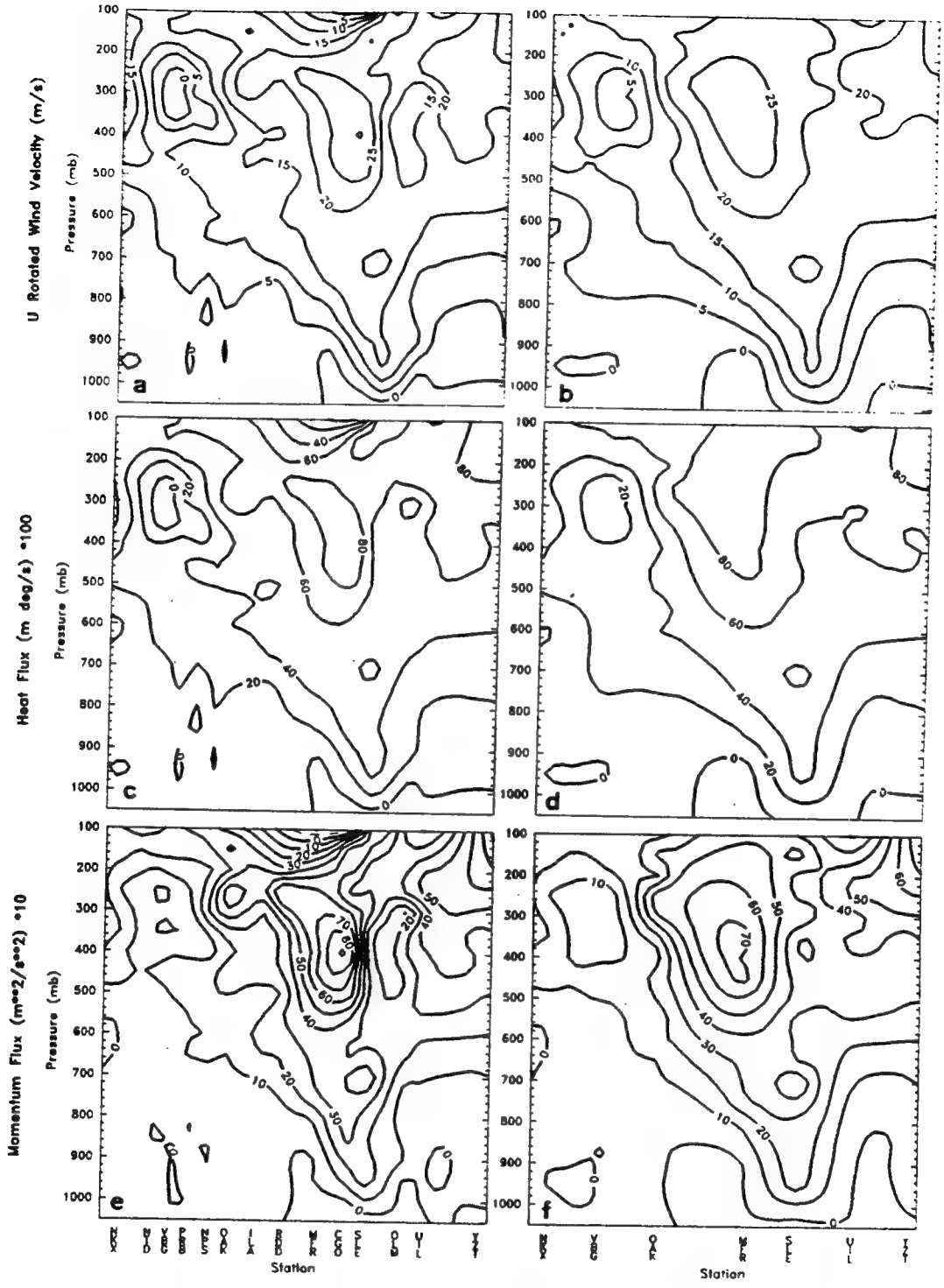


2100 UTC 20 Feb vertical cross sections for (a) ALL $U_r$ flux, (b) NWS $U_r$ flux, (c) ALL heat flux, (d) NWS heat flux, (e) ALL momentum flux, and (f) NWS momentum flux.

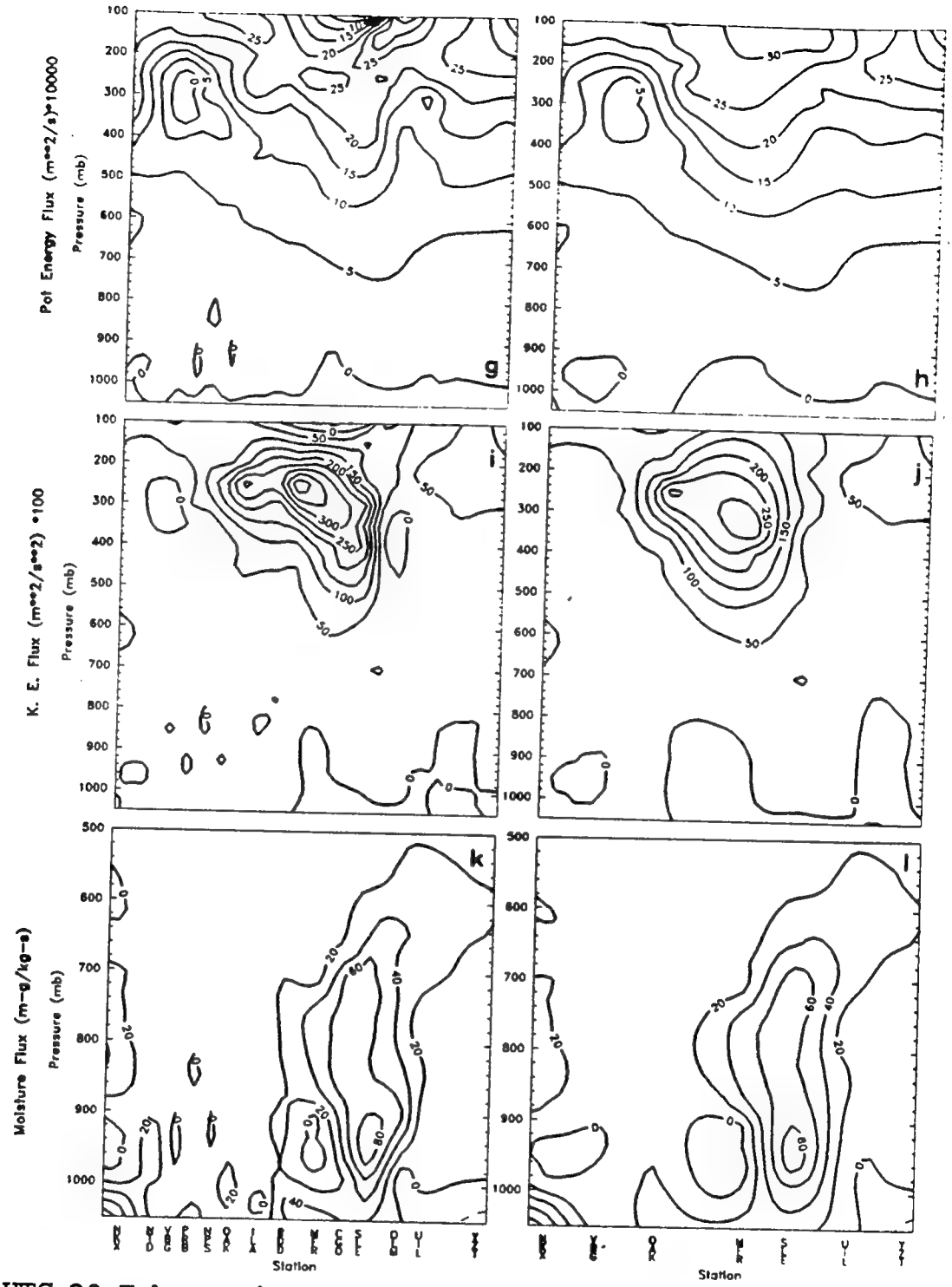


2100 UTC 20 Feb vertical cross sections for (g) ALL potential energy flux, (h) NWS potential energy flux, (i) ALL kinetic energy flux, (j) NWS kinetic energy flux, (k) ALL moisture flux, and (l) NWS moisture.

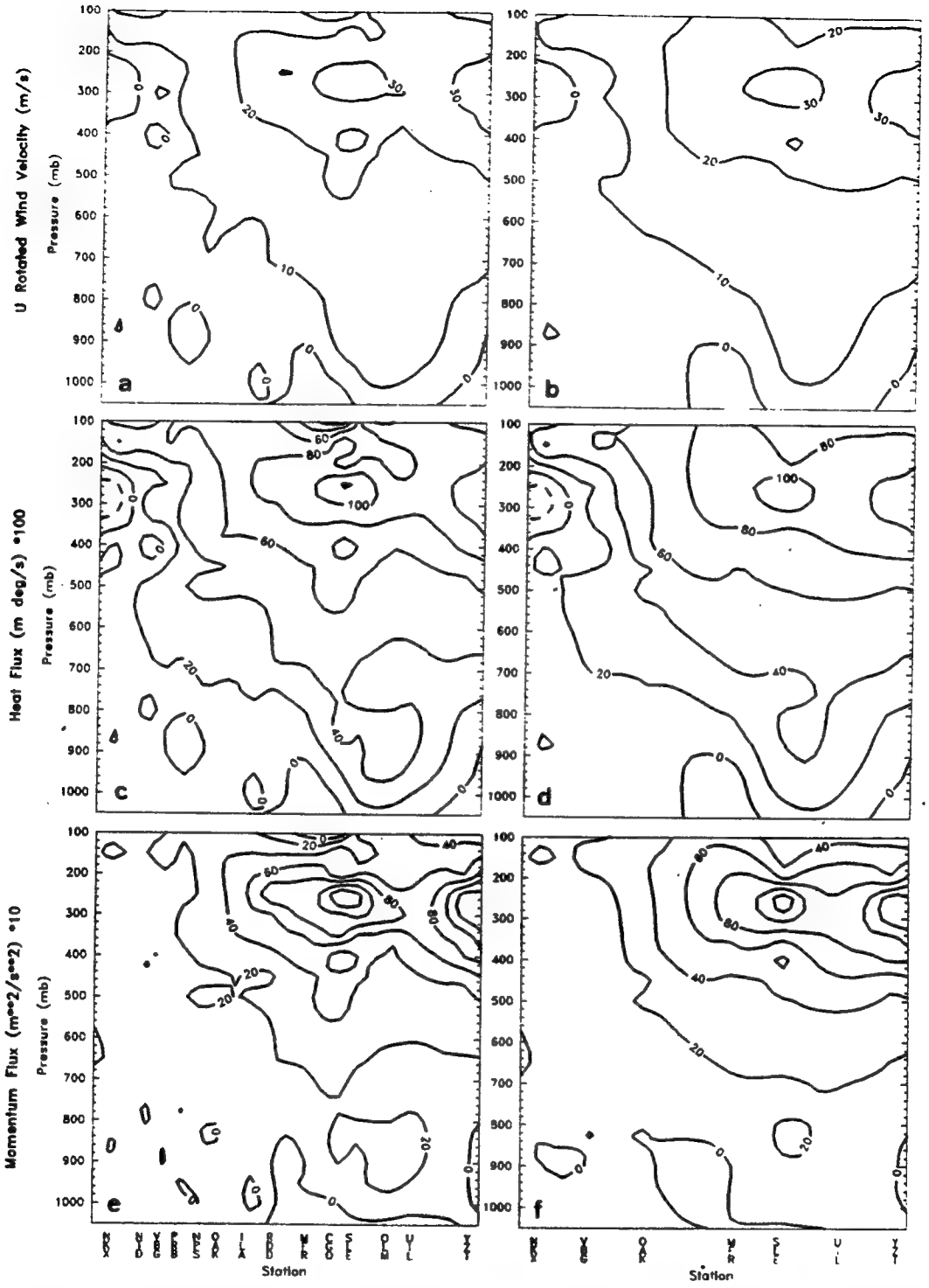


0000 UTC 21 Feb vertical cross sections for (a) ALL $U_r$ flux, (b) NWS $U_r$ flux, (c) ALL heat flux, (d) NWS heat flux, (e) ALL momentum flux, and (f) NWS momentum flux.

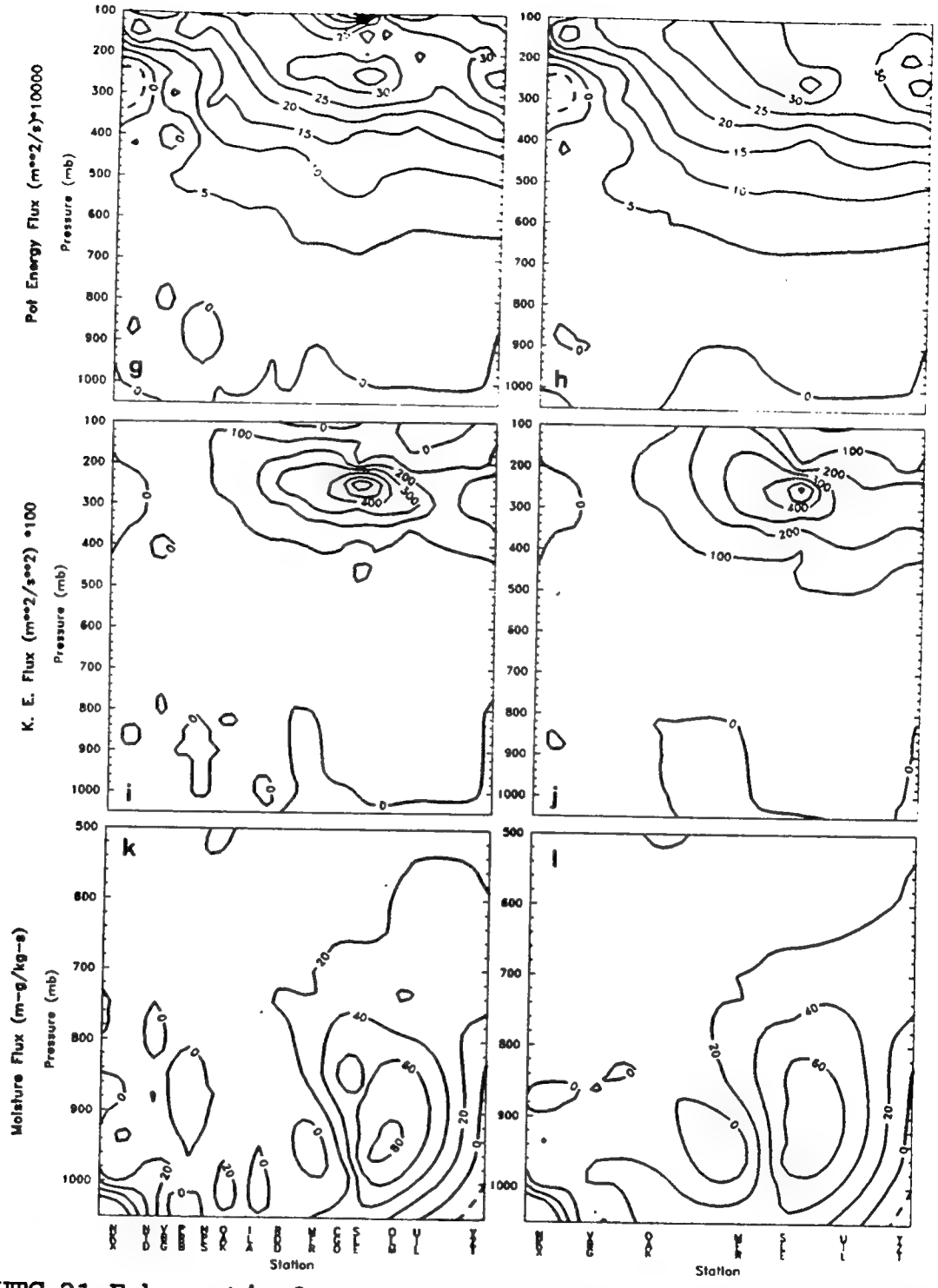


0000 UTC 21 Feb vertical cross sections for (g) ALL potential energy flux, (h) NWS potential energy flux, (i) ALL kinetic energy flux, (j) NWS kinetic energy flux, (k) ALL moisture flux, and (l) NWS moisture.

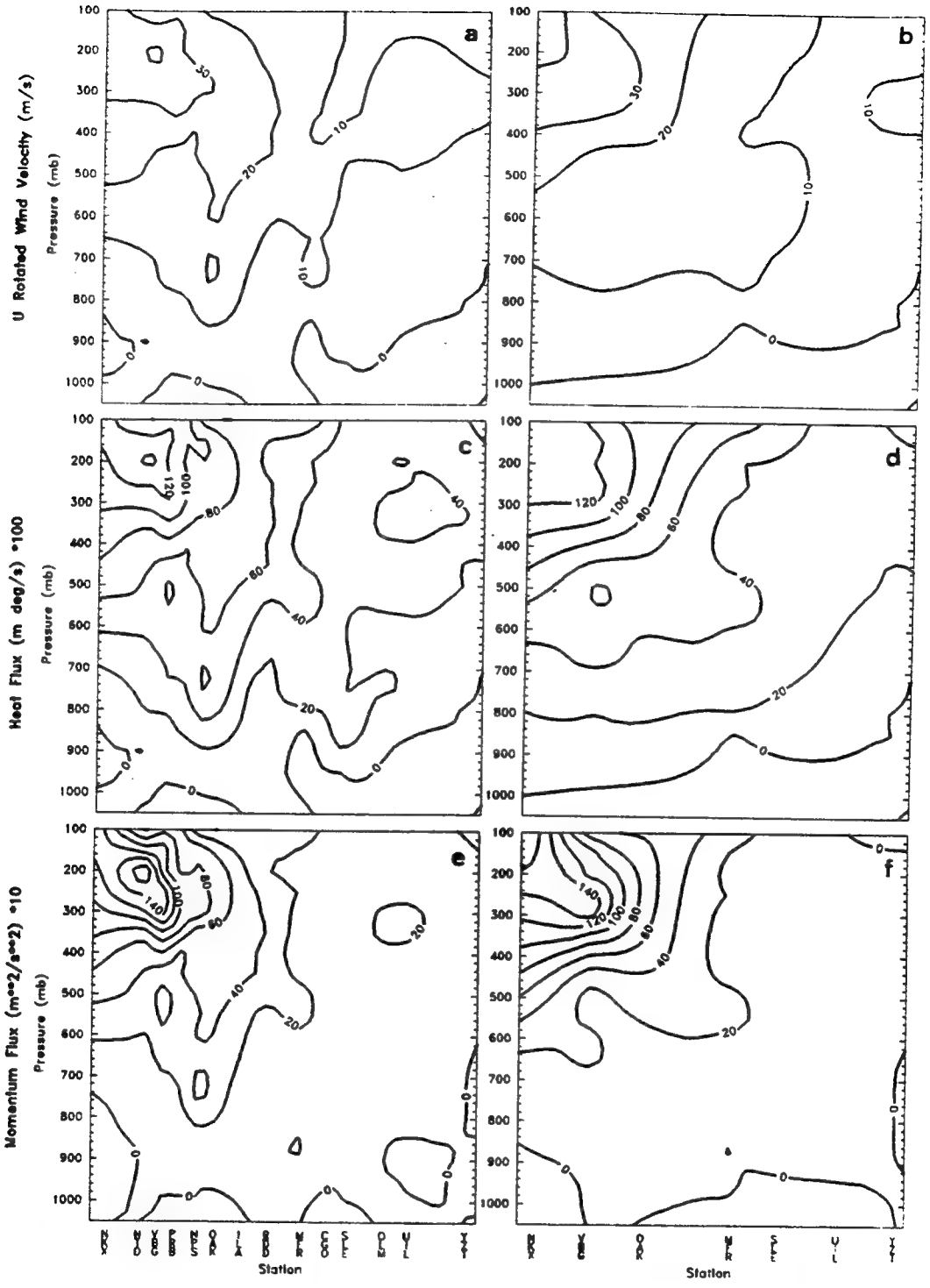


1500 UTC 5 Mar Vertical cross sections for (a) ALL $U_r$ flux, (b) NWS $U_r$ flux, (c) ALL heat flux, (d) NWS heat flux, (e) ALL momentum flux, and (f) NWS momentum flux.

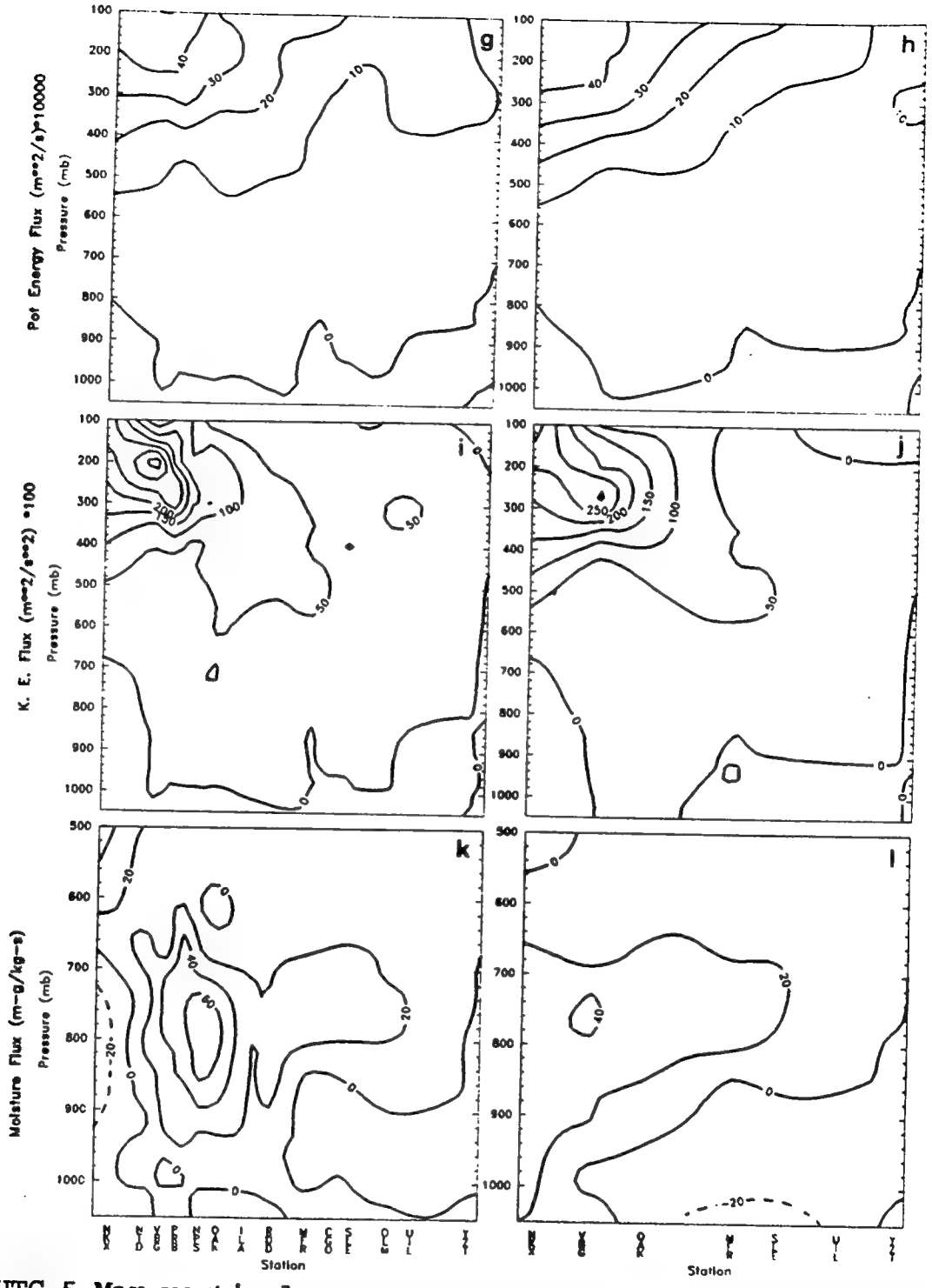


1500 UTC 5 Mar vertical cross sections for (g) ALL potential energy flux, (h) NWS potential energy flux, (i) ALL kinetic energy flux, (j) NWS kinetic energy flux, (k) ALL moisture flux, and (l) NWS moisture.

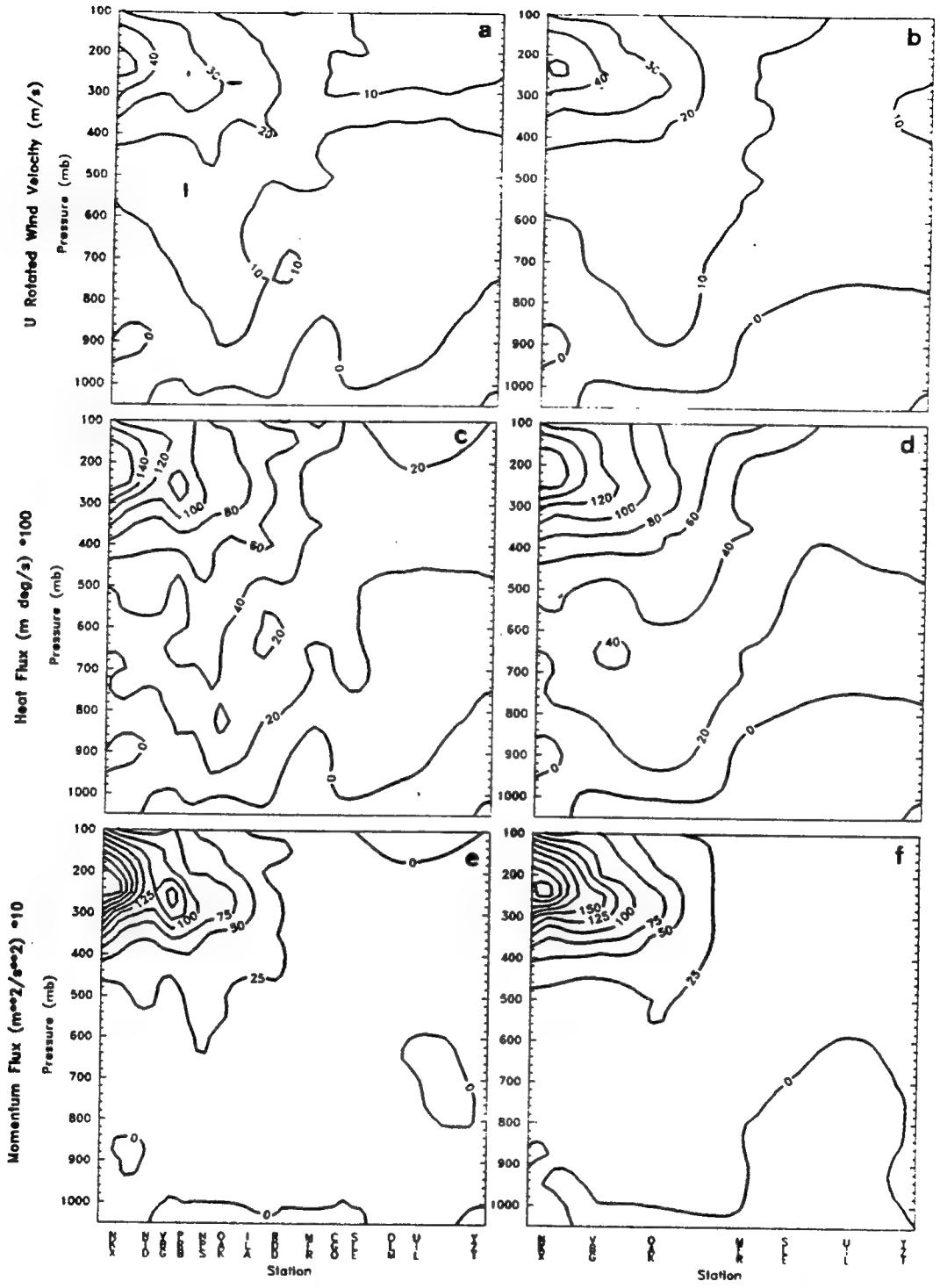


1800 UTC 5 Mar Vertical cross sections for (a) ALL $U_r$ flux, (b) NWS $U_r$ flux, (c) ALL heat flux, (d) NWS heat flux, (e) ALL momentum flux, and (f) NWS momentum flux.

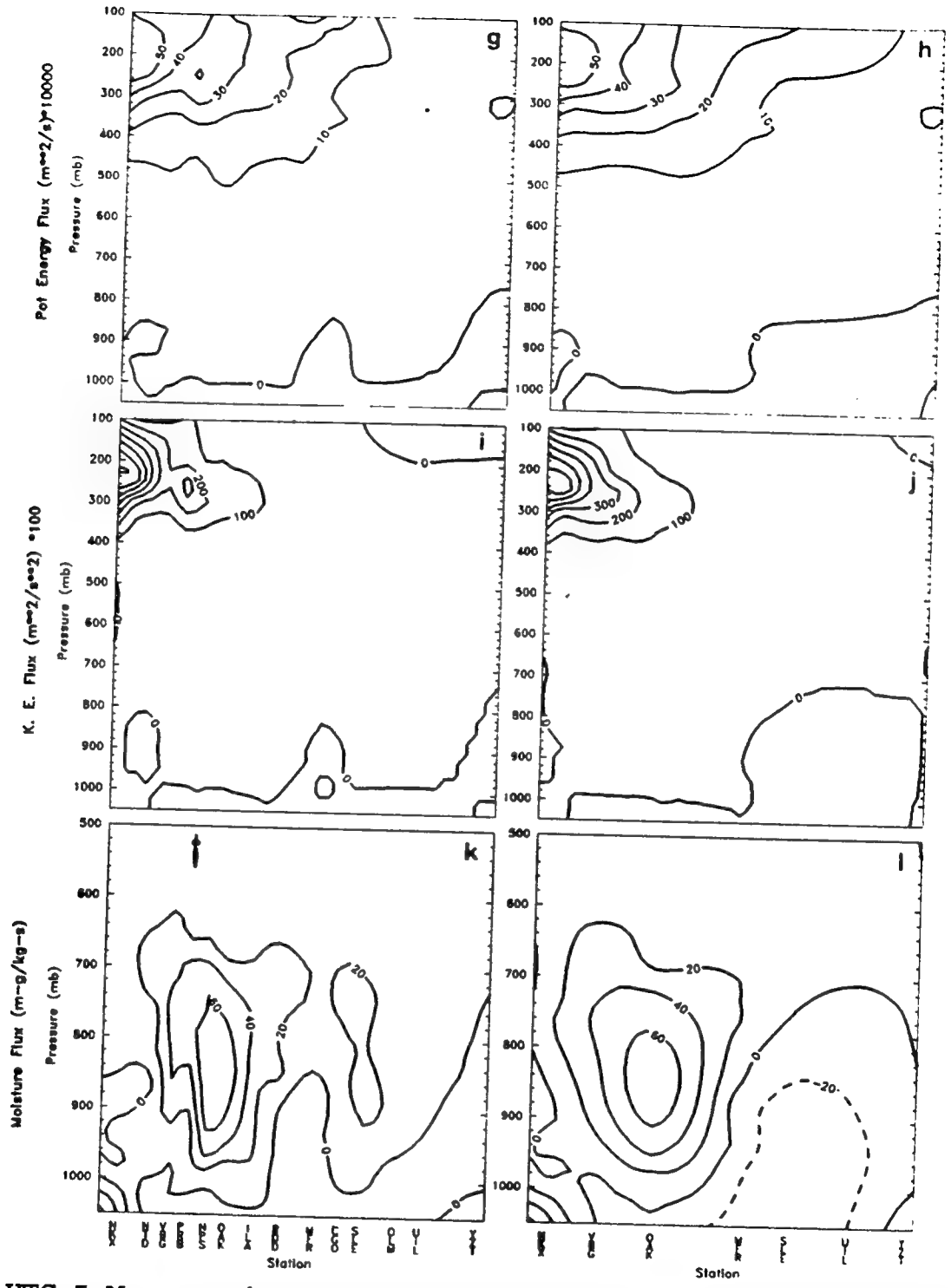


1800 UTC 5 Mar vertical cross sections for (g) ALL potential energy flux, (h) NWS potential energy flux, (i) ALL kinetic energy flux, (j) NWS kinetic energy flux, (k) ALL moisture flux, and (l) NWS moisture.

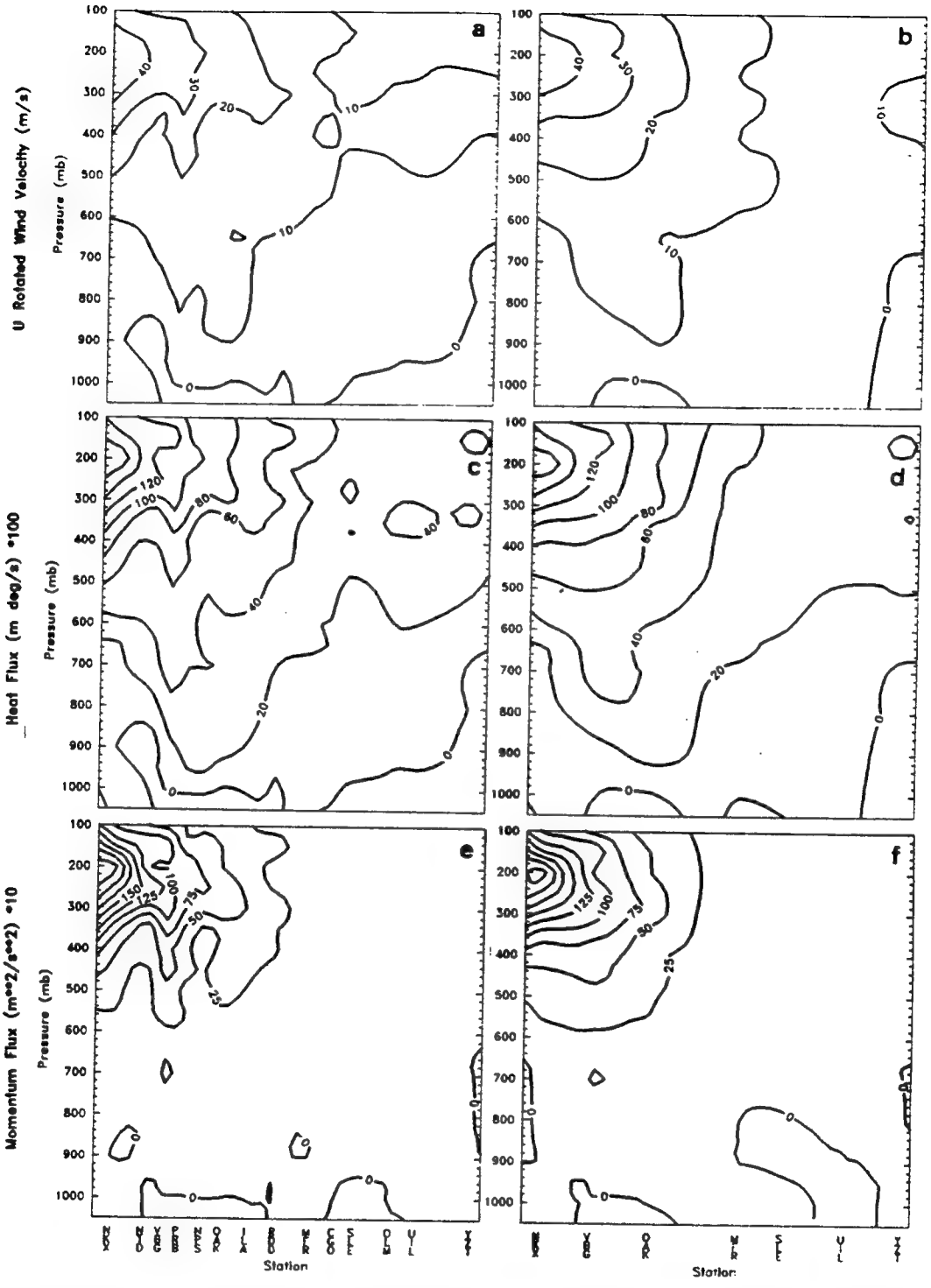


2100 UTC 5 Mar Vertical cross sections for (a) ALL $U_r$ flux, (b) NWS $U_r$ flux, (c) ALL heat flux, (d) NWS heat flux, (e) ALL momentum flux, and (f) NWS momentum flux.

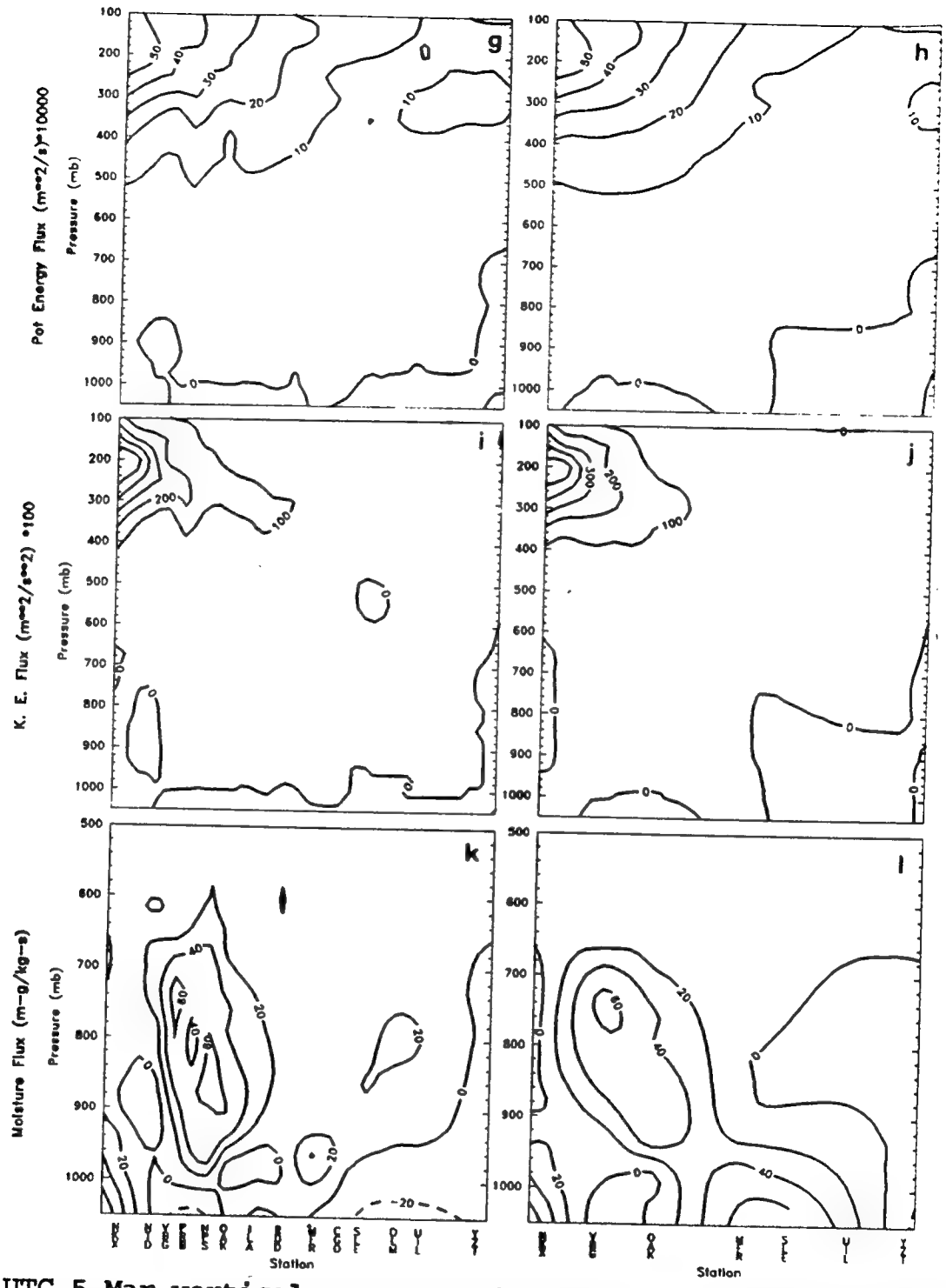


2100 UTC 5 Mar vertical cross sections for (g) ALL potential energy flux, (h) NWS potential energy flux, (i) ALL kinetic energy flux, (j) NWS kinetic energy flux, (k) ALL moisture flux, and (l) NWS moisture.

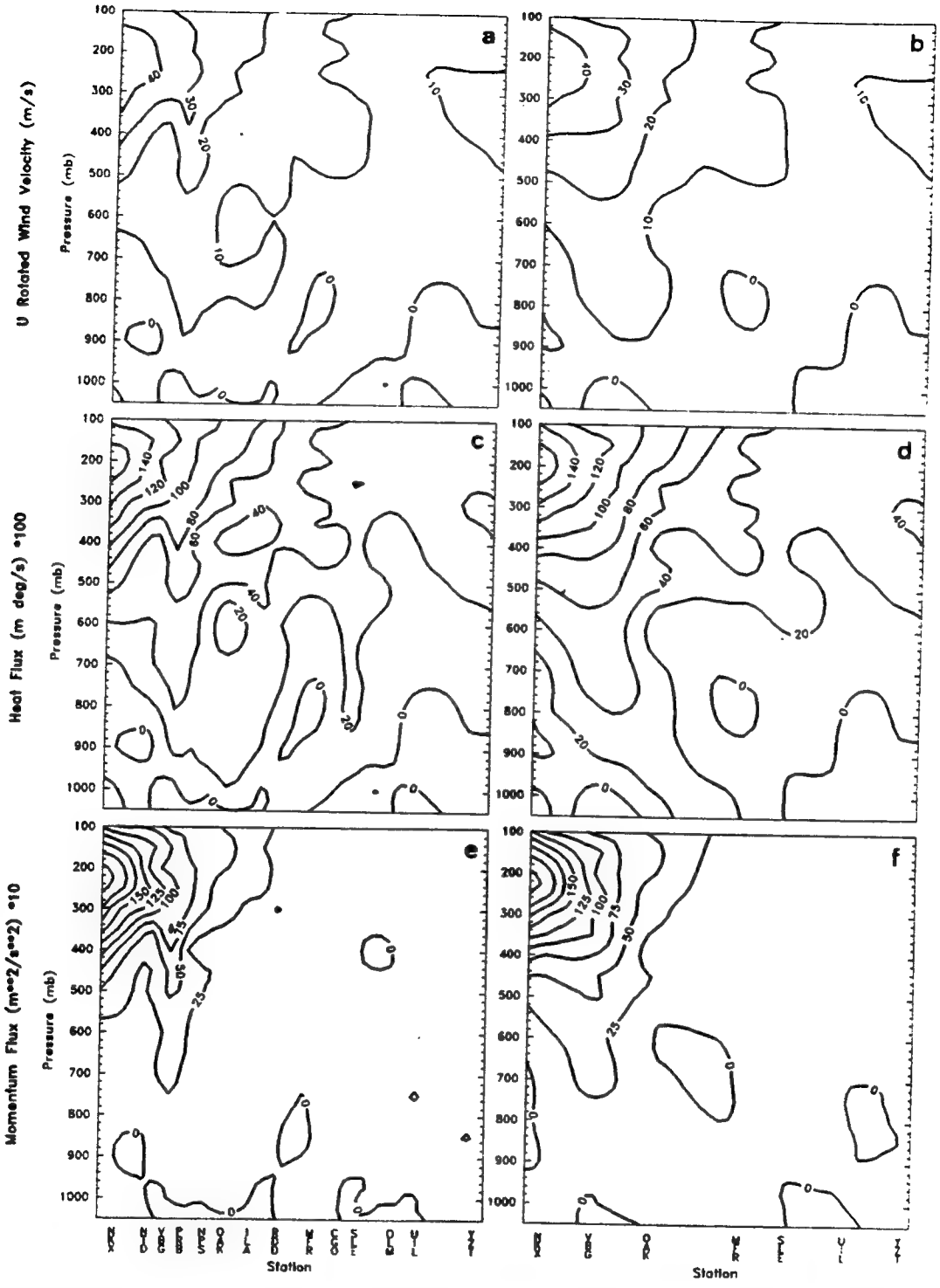


0000 UTC 6 Mar Vertical cross sections for (a) ALL $U_r$ flux, (b) NWS $U_r$ flux, (c) ALL heat flux, (d) NWS heat flux, (e) ALL momentum flux, and (f) NWS momentum flux.

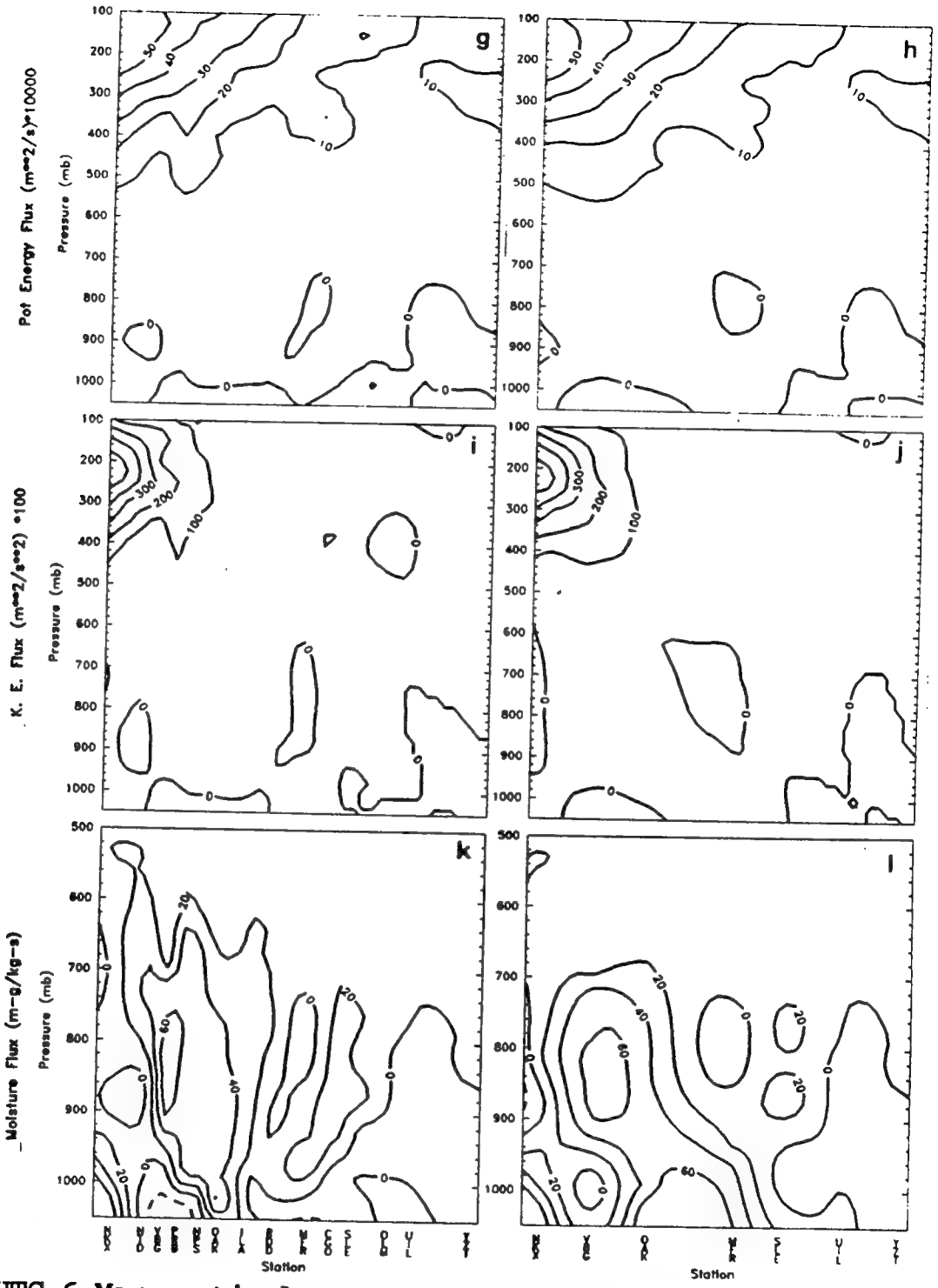


0000 UTC 6 Mar vertical cross sections for (g) ALL potential energy flux, (h) NWS potential energy flux, (i) ALL kinetic energy flux, (j) NWS kinetic energy flux, (k) ALL moisture flux, and (l) NWS moisture.

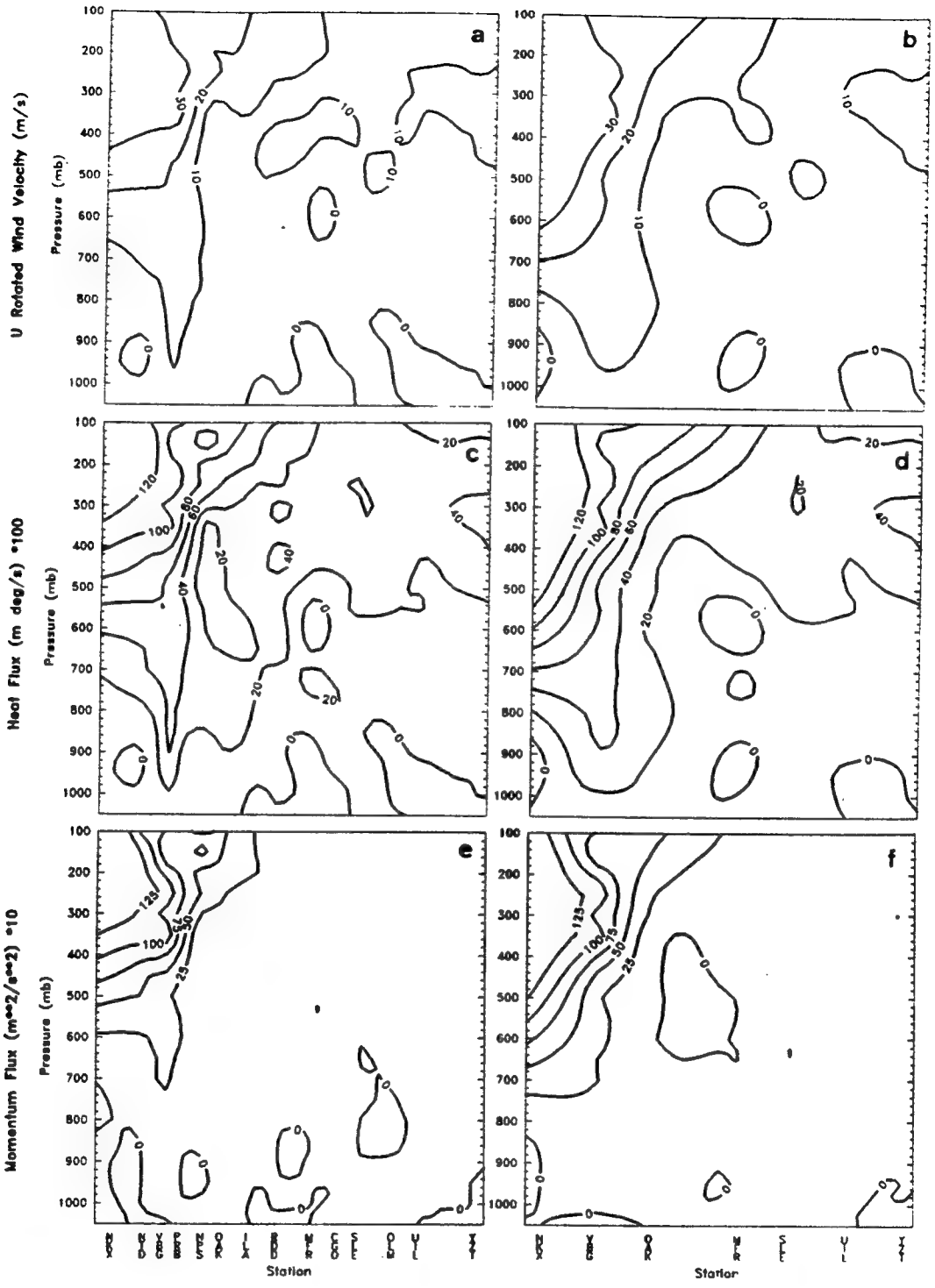


0300 UTC 6 Mar Vertical cross sections for (a) ALL $U_r$ flux, (b) NWS $U_r$ flux, (c) ALL heat flux, (d) NWS heat flux, (e) ALL momentum flux, and (f) NWS momentum flux.

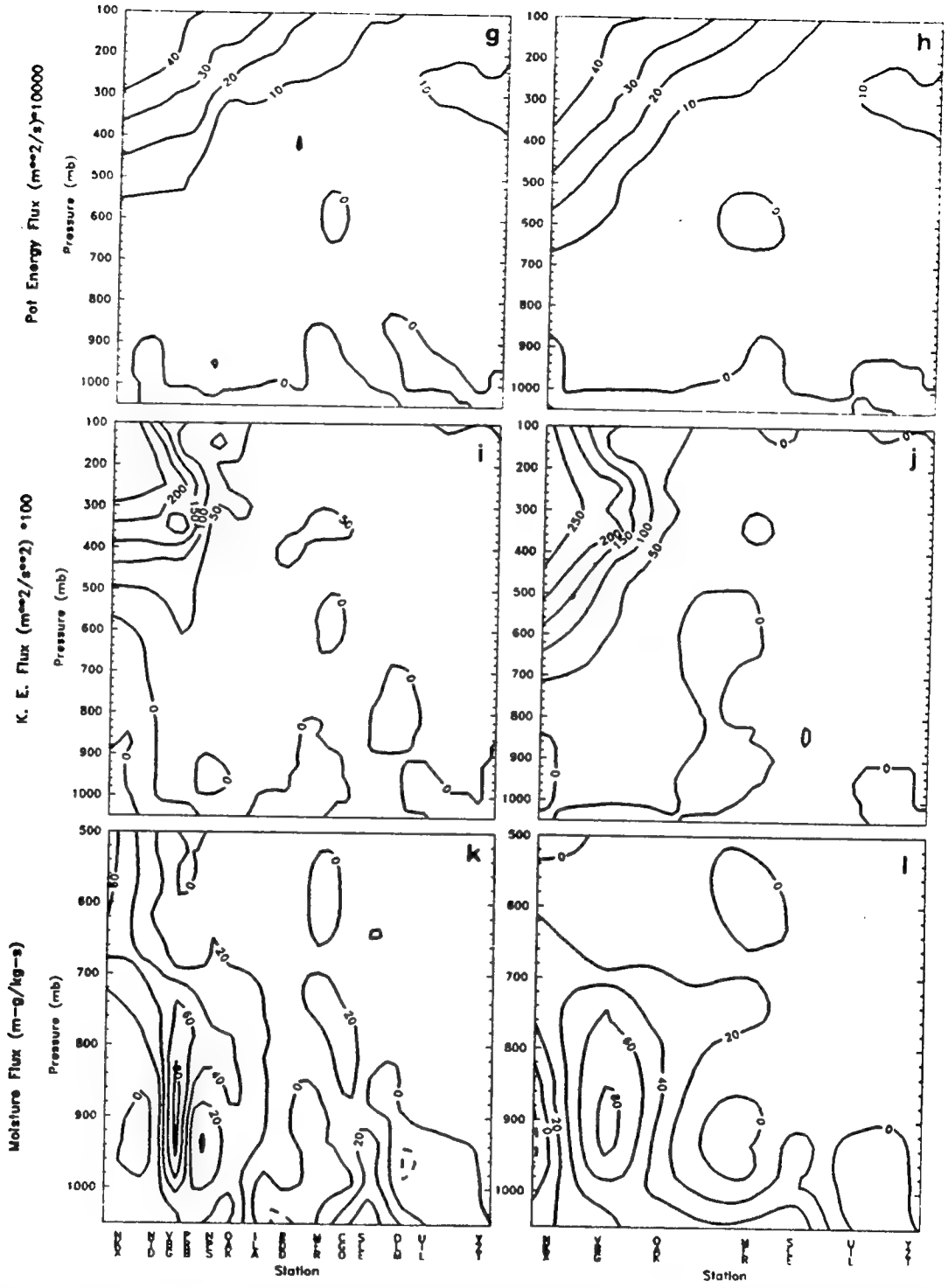


0300 UTC 6 Mar vertical cross sections for (g) ALL potential energy flux, (h) NWS potential energy flux, (i) ALL kinetic energy flux, (j) NWS kinetic energy flux, (k) ALL moisture flux, and (l) NWS moisture.

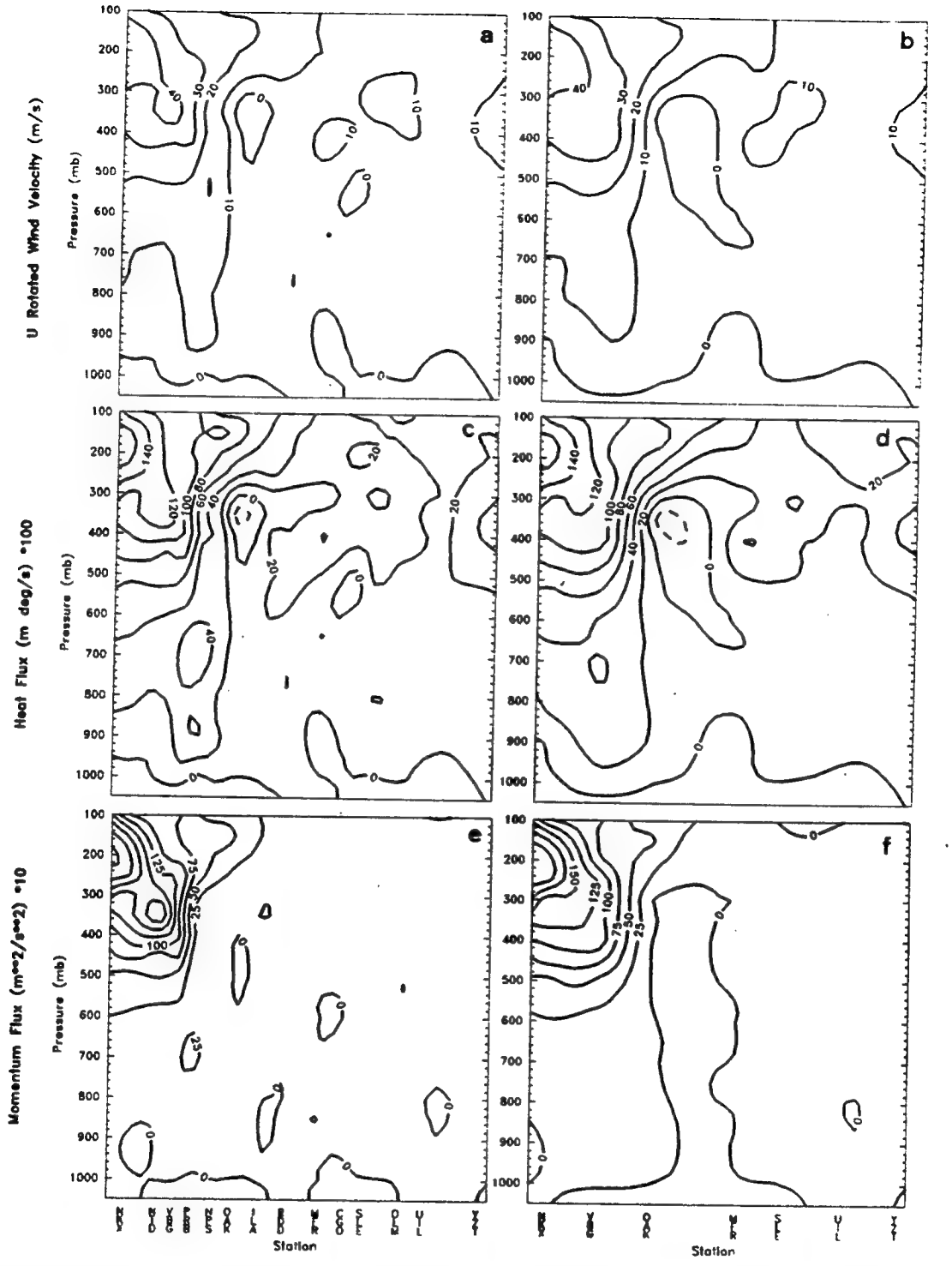


0600 UTC 6 Mar Vertical cross sections for (a) ALL $U_r$ flux, (b) NWS $U_r$ flux, (c) ALL heat flux, (d) NWS heat flux, (e) ALL momentum flux, and (f) NWS momentum flux.

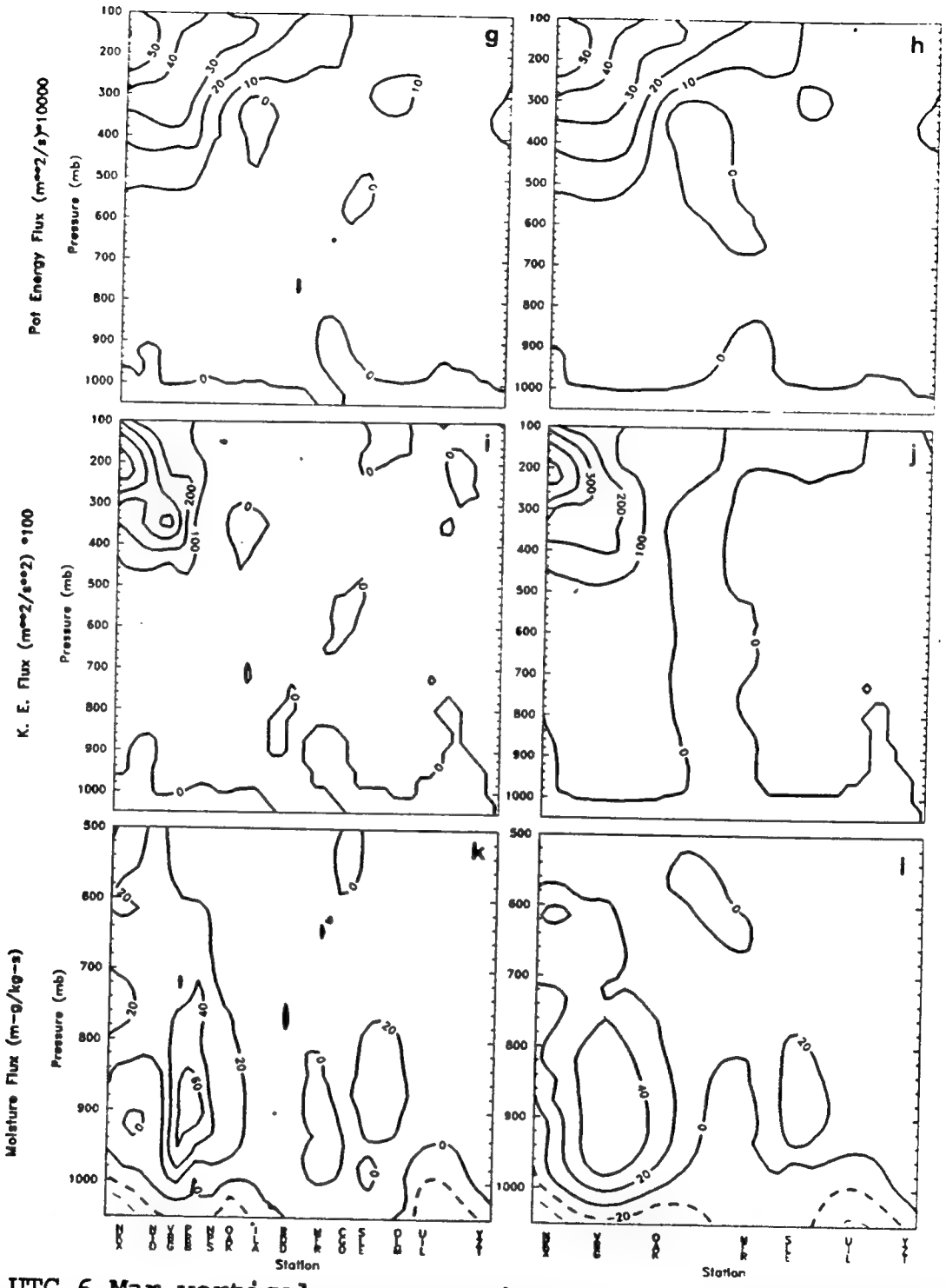


0600 UTC 6 Mar vertical cross sections for (g) ALL potential energy flux, (h) NWS potential energy flux, (i) ALL kinetic energy flux, (j) NWS kinetic energy flux, (k) ALL moisture flux, and (l) NWS moisture.

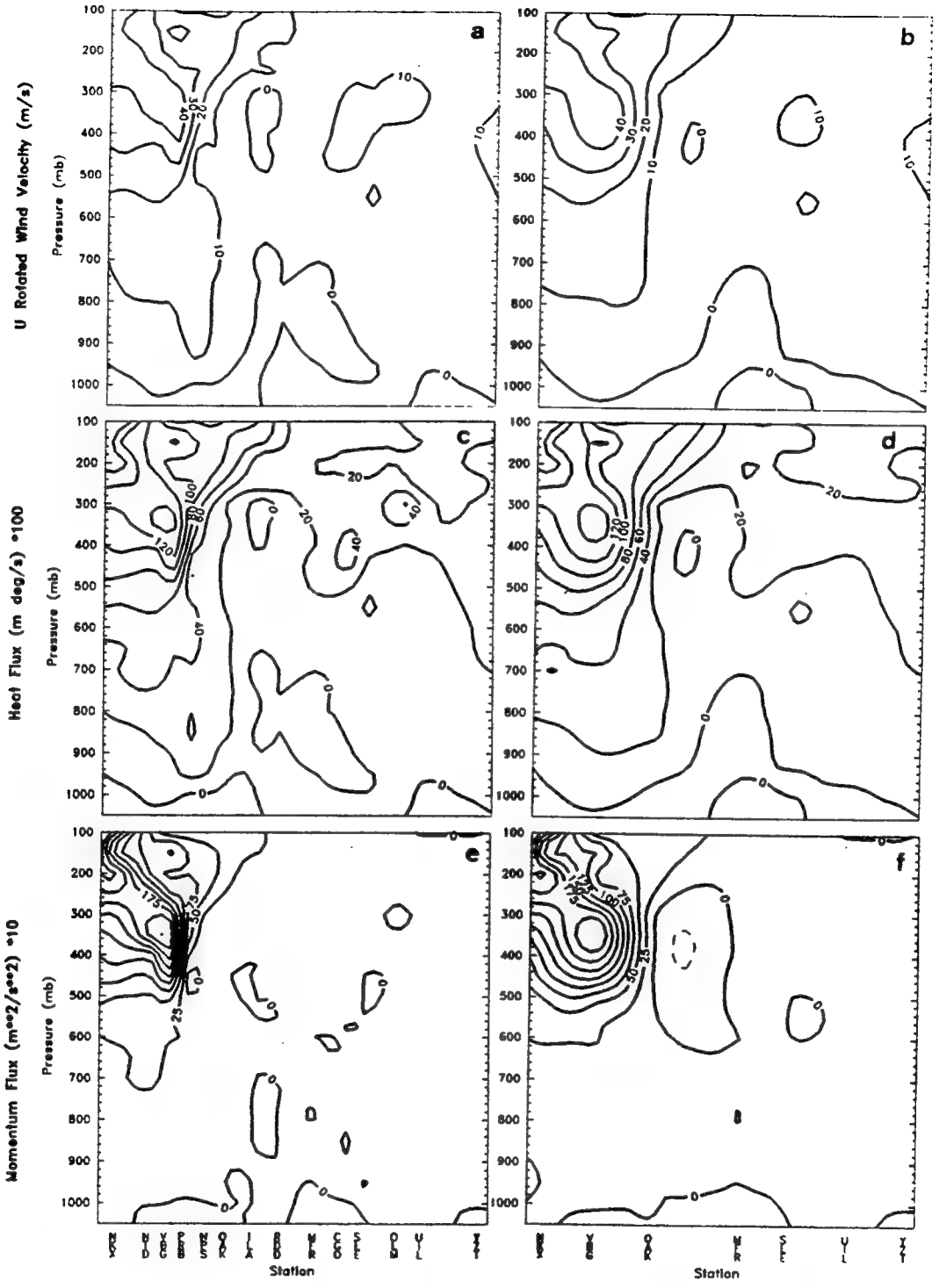


0900 UTC 6 Mar Vertical cross sections for (a) ALL $U_r$ flux, (b) NWS $U_r$ flux, (c) ALL heat flux, (d) NWS heat flux, (e) ALL momentum flux, and (f) NWS momentum flux.

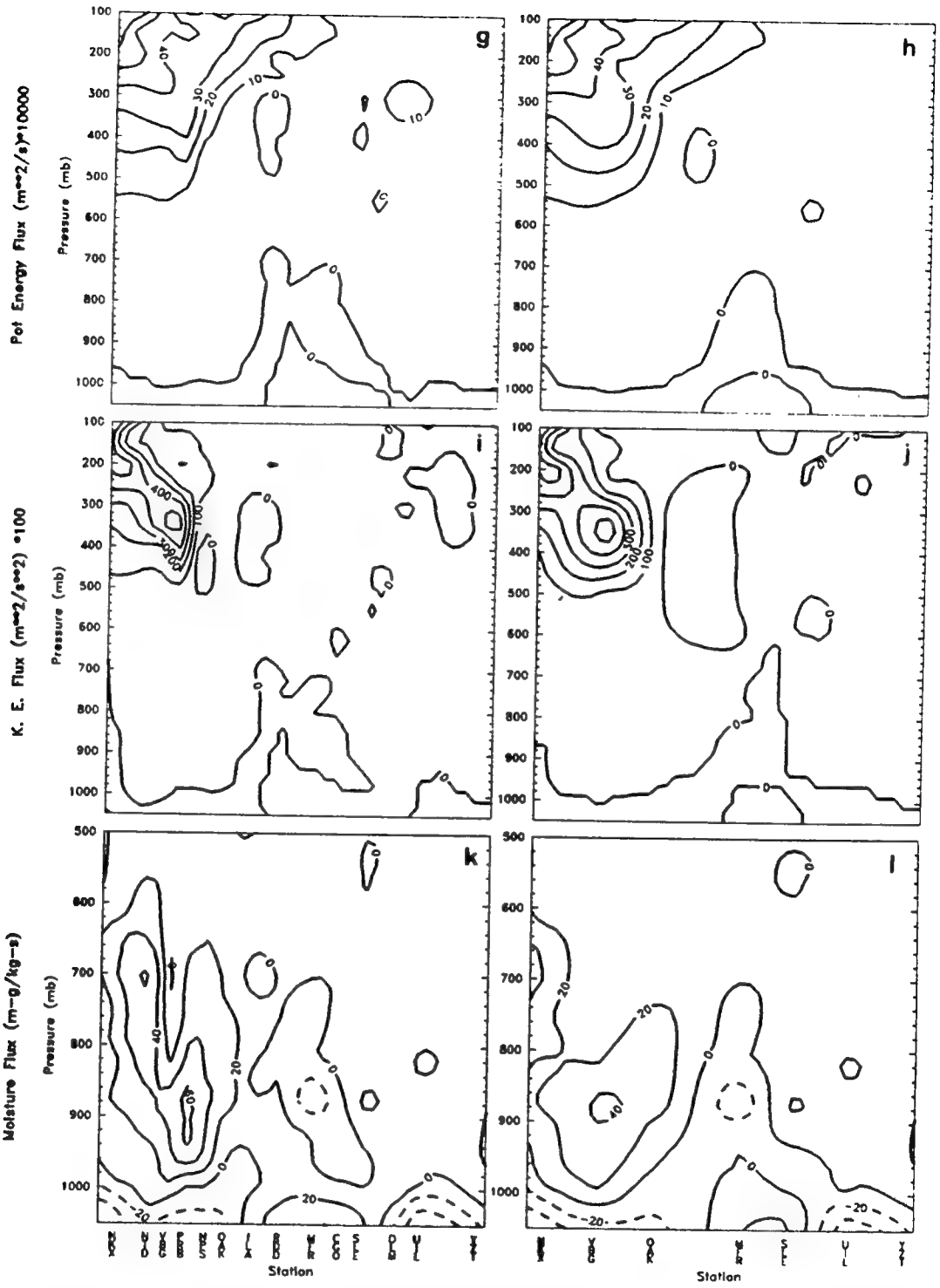


0900 UTC 6 Mar vertical cross sections for (g) ALL potential energy flux, (h) NWS potential energy flux, (i) ALL kinetic energy flux, (j) NWS kinetic energy flux, (k) ALL moisture flux, and (l) NWS moisture.

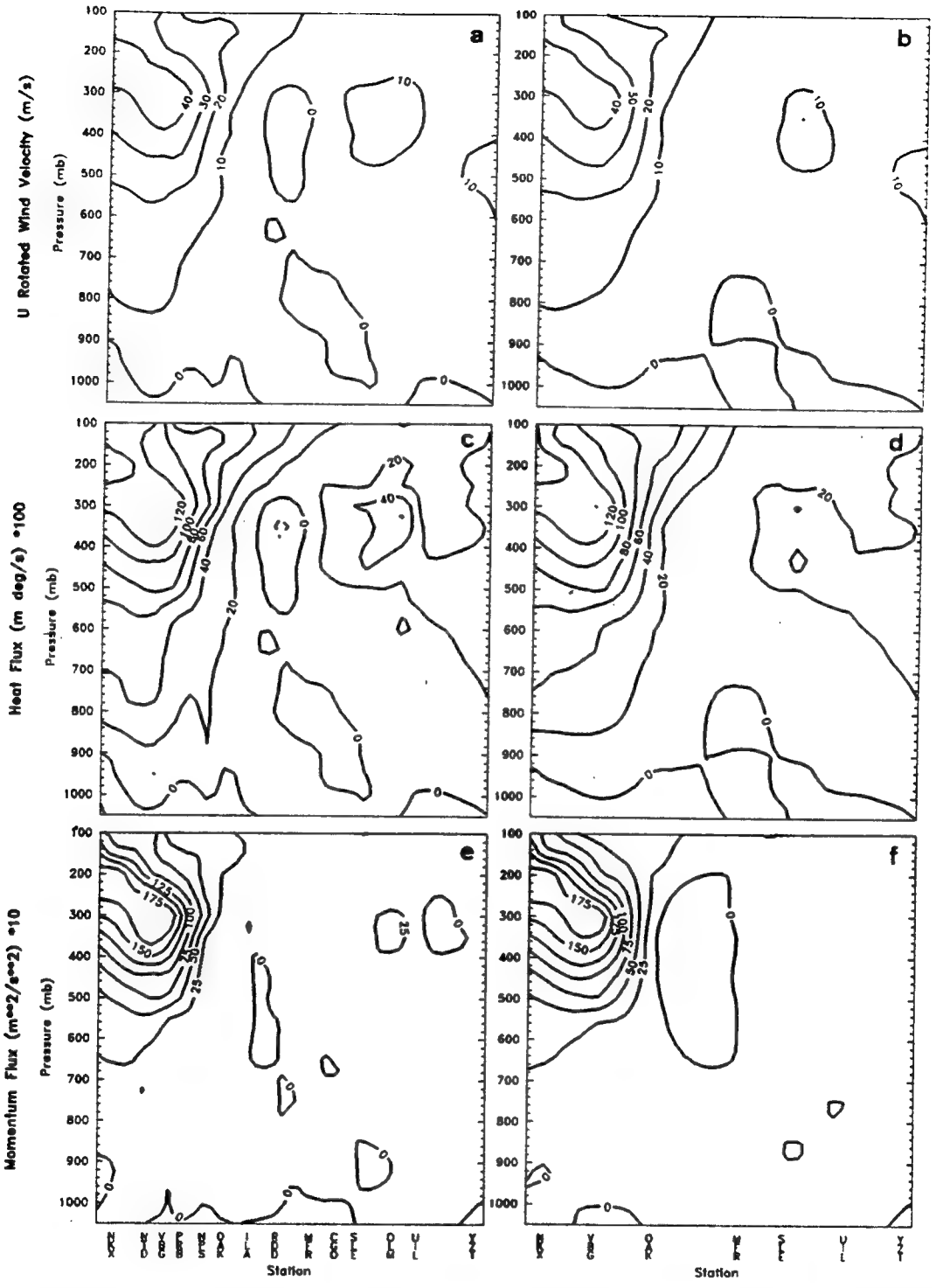


1200 UTC 6 Mar Vertical cross sections for (a) ALL $U_r$ flux, (b) NWS $U_r$ flux, (c) ALL heat flux, (d) NWS heat flux, (e) ALL momentum flux, and (f) NWS momentum flux.

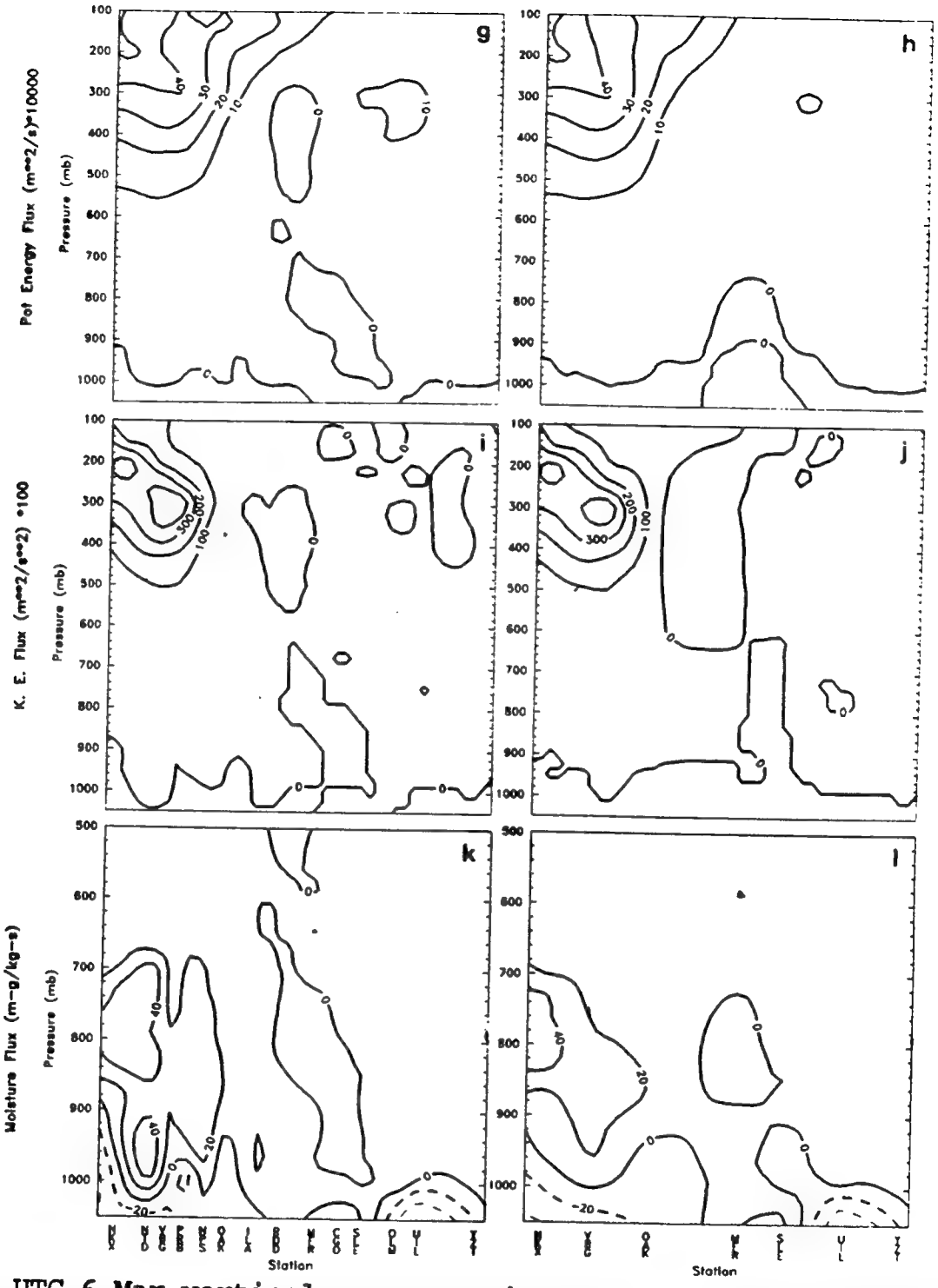


1200 UTC 6 Mar vertical cross sections for (g) ALL potential energy flux, (h) NWS potential energy flux, (i) ALL kinetic energy flux, (j) NWS kinetic energy flux, (k) ALL moisture flux, and (l) NWS moisture.

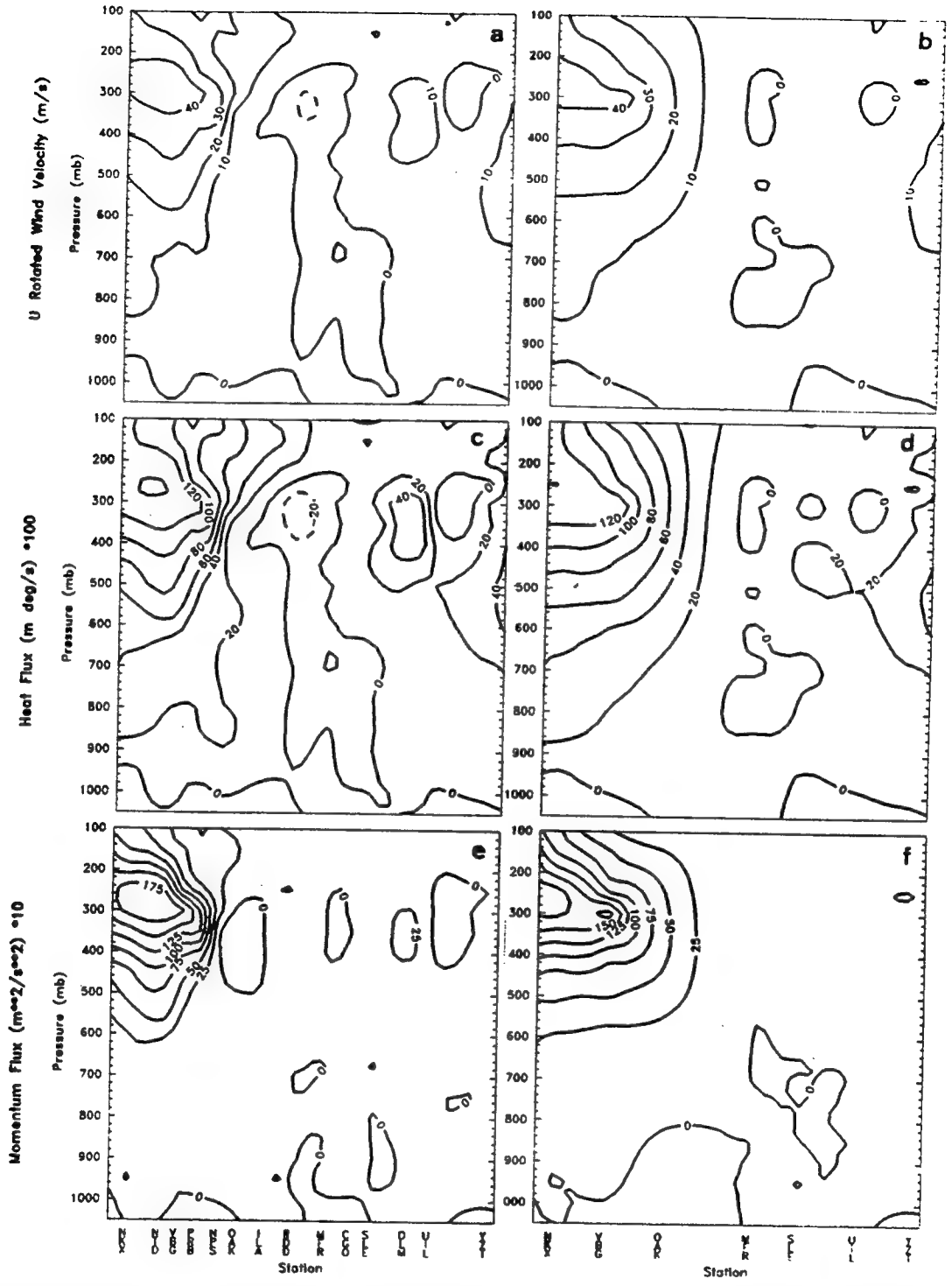


1500 UTC 6 Mar Vertical cross sections for (a) ALL $U_r$ flux, (b) NWS $U_r$ flux, (c) ALL heat flux, (d) NWS heat flux, (e) ALL momentum flux, and (f) NWS momentum flux.

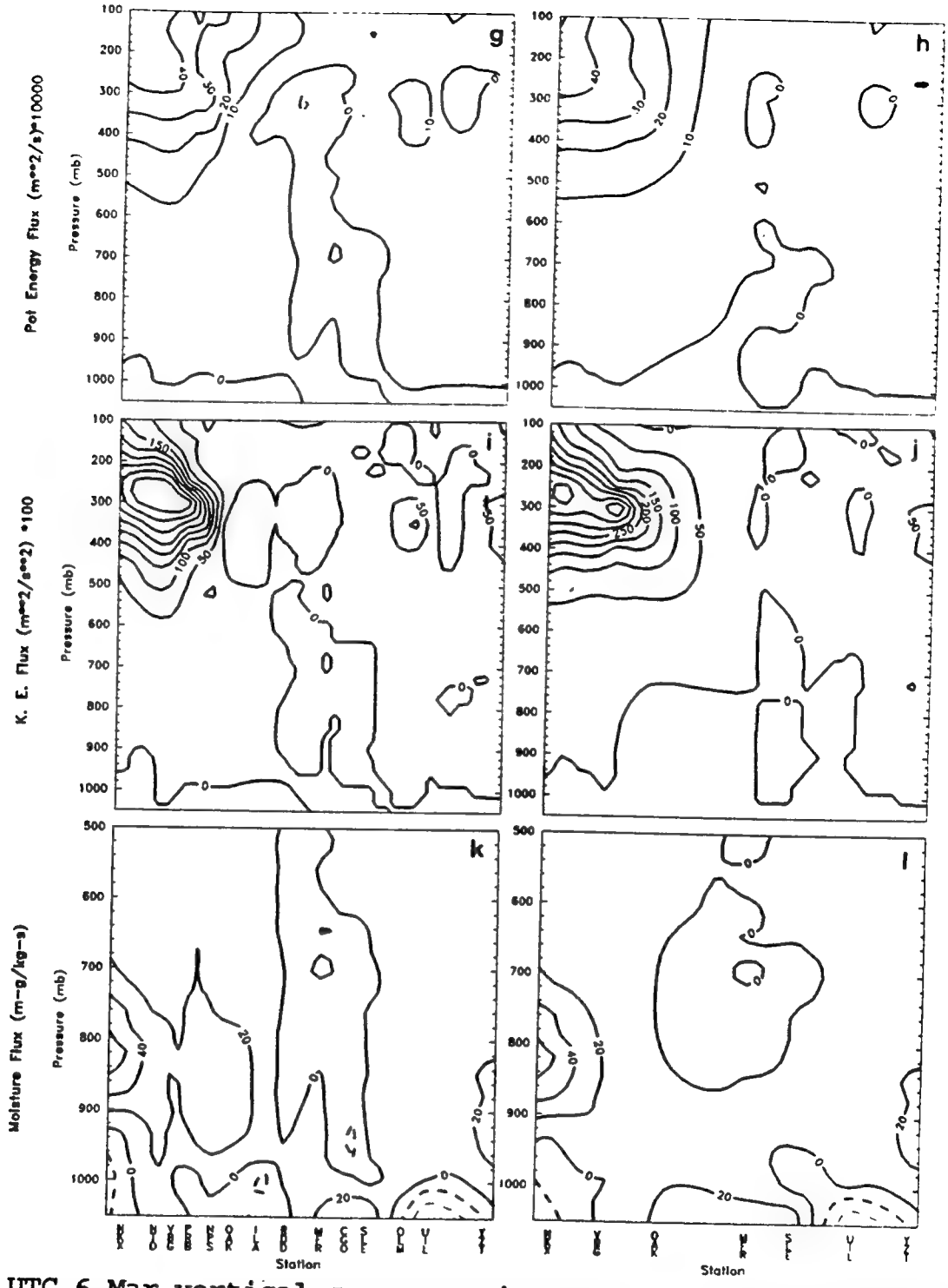


1500 UTC 6 Mar vertical cross sections for (g) ALL potential energy flux, (h) NWS potential energy flux, (i) ALL kinetic energy flux, (j) NWS kinetic energy flux, (k) ALL moisture flux, and (l) NWS moisture.

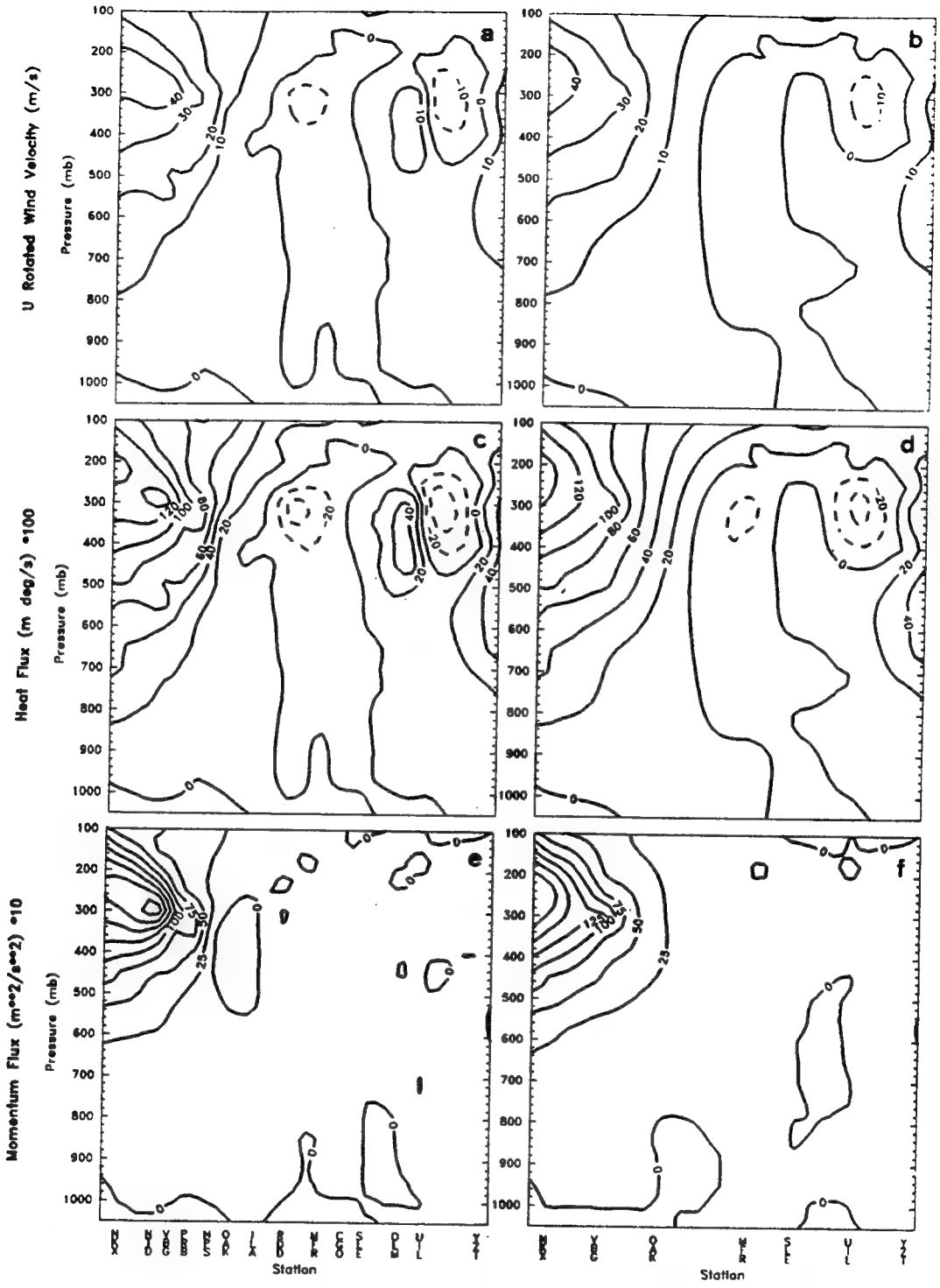


1800 UTC 6 Mar Vertical cross sections for (a) ALL $U_r$ flux, (b) NWS $U_r$ flux, (c) ALL heat flux, (d) NWS heat flux, (e) ALL momentum flux, and (f) NWS momentum flux.

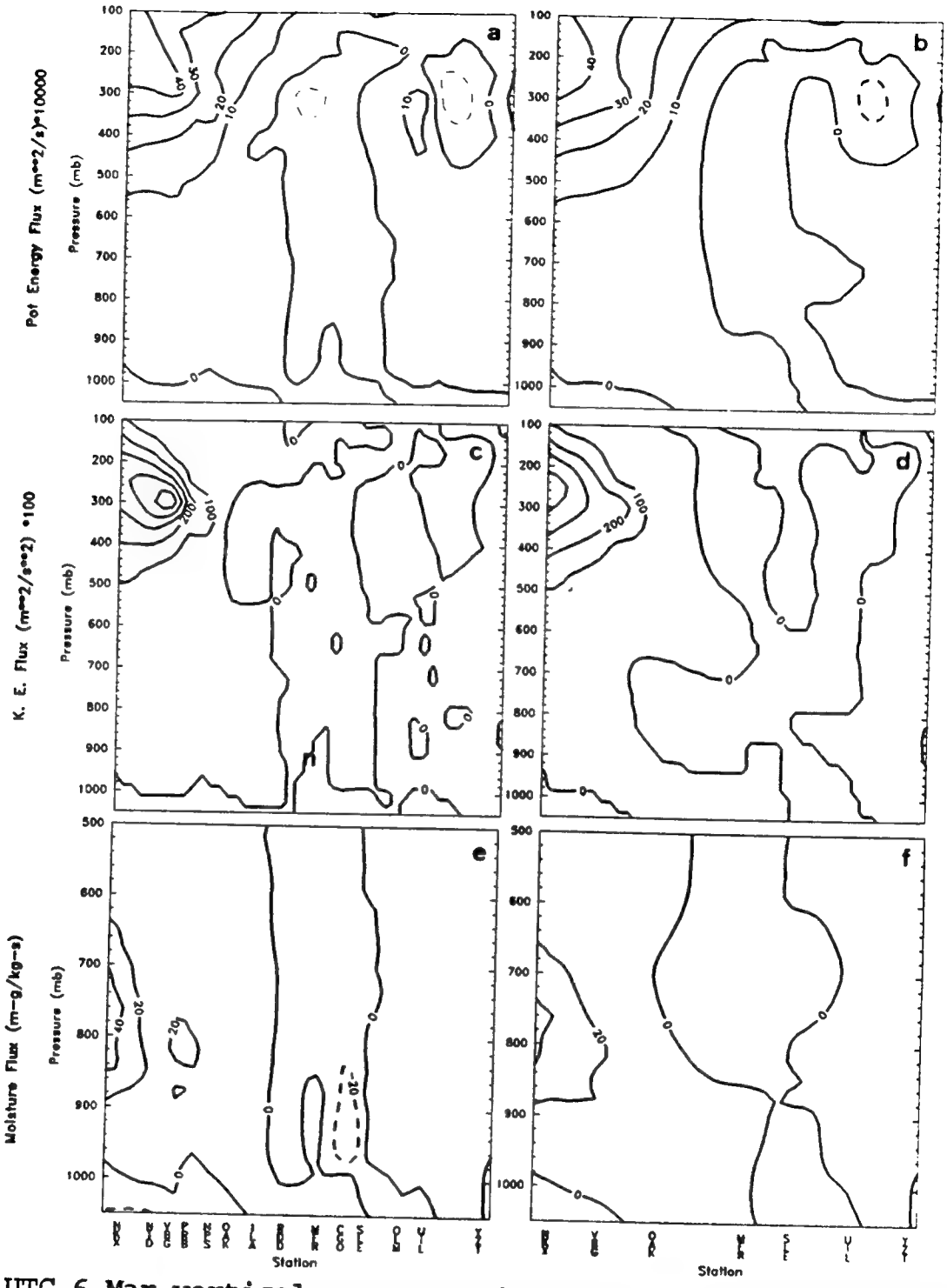


1800 UTC 6 Mar vertical cross sections for (g) ALL potential energy flux, (h) NWS potential energy flux, (i) ALL kinetic energy flux, (j) NWS kinetic energy flux, (k) ALL moisture flux, and (l) NWS moisture.

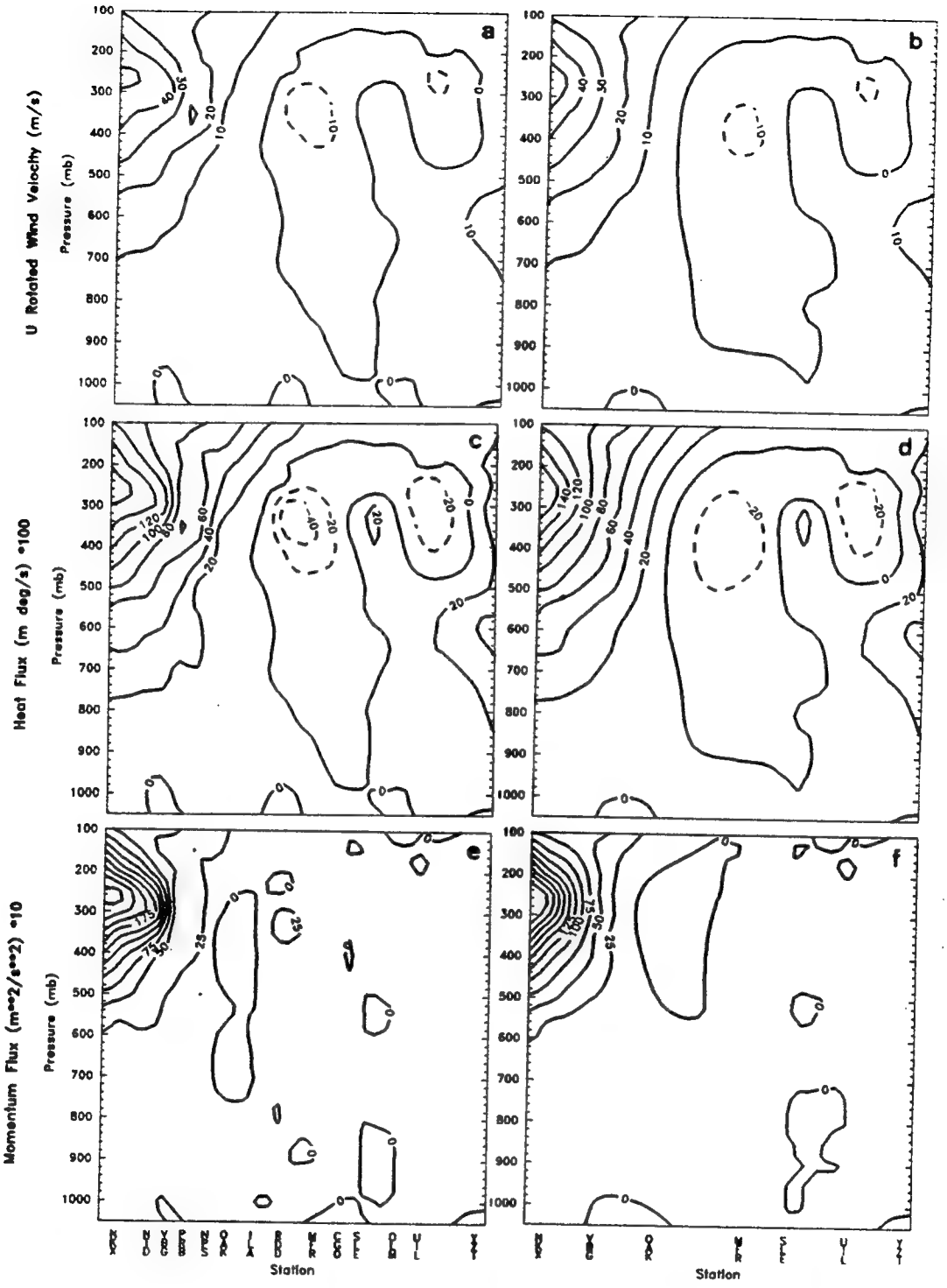


2100 UTC 6 Mar Vertical cross sections for (a) ALL $U_r$ flux, (b) NWS $U_r$ flux, (c) ALL heat flux, (d) NWS heat flux, (e) ALL momentum flux, and (f) NWS momentum flux.

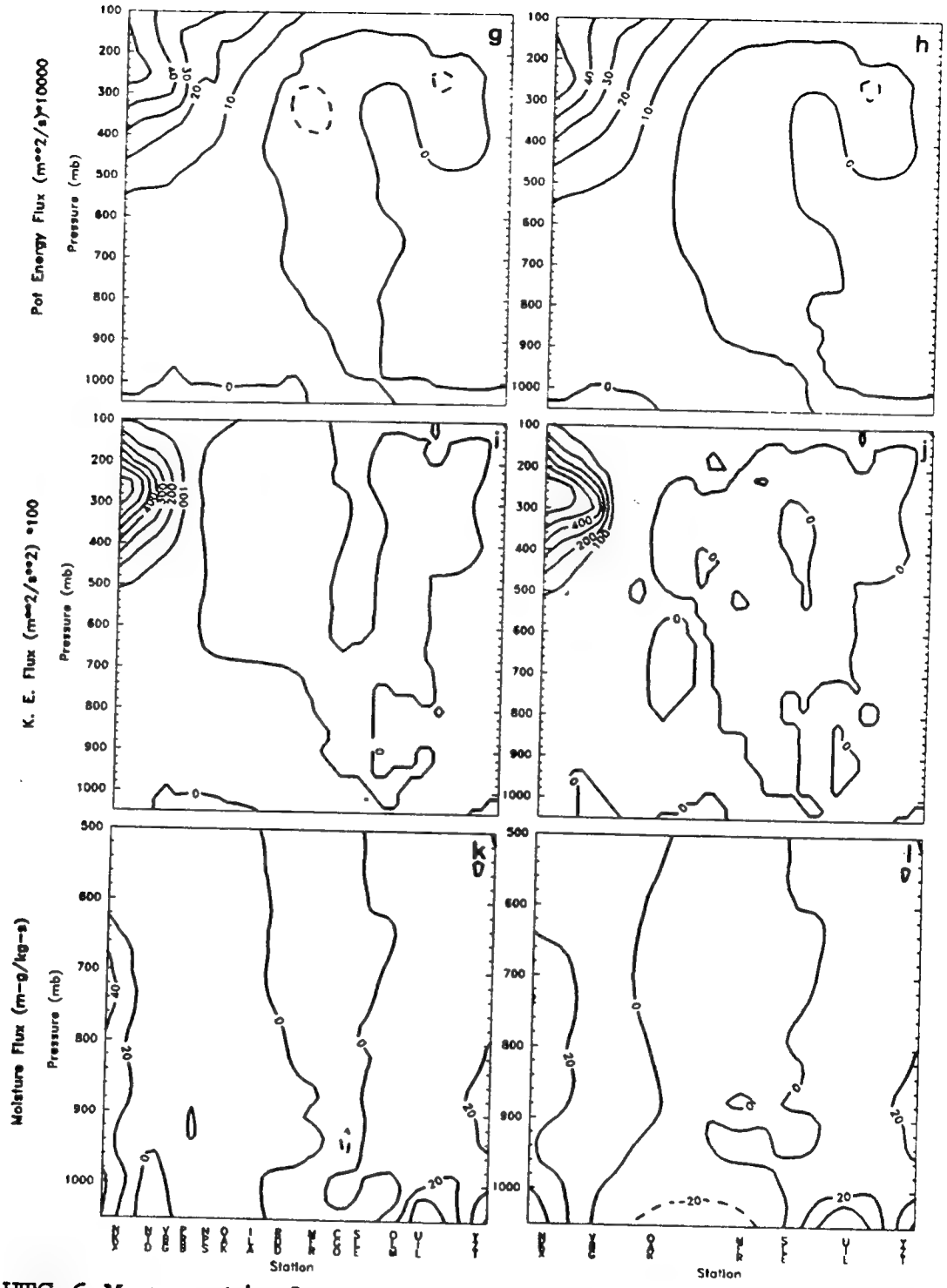


2100 UTC 6 Mar vertical cross sections for (g) ALL potential energy flux, (h) NWS potential energy flux, (i) ALL kinetic energy flux, (j) NWS kinetic energy flux, (k) ALL moisture flux, and (l) NWS moisture.

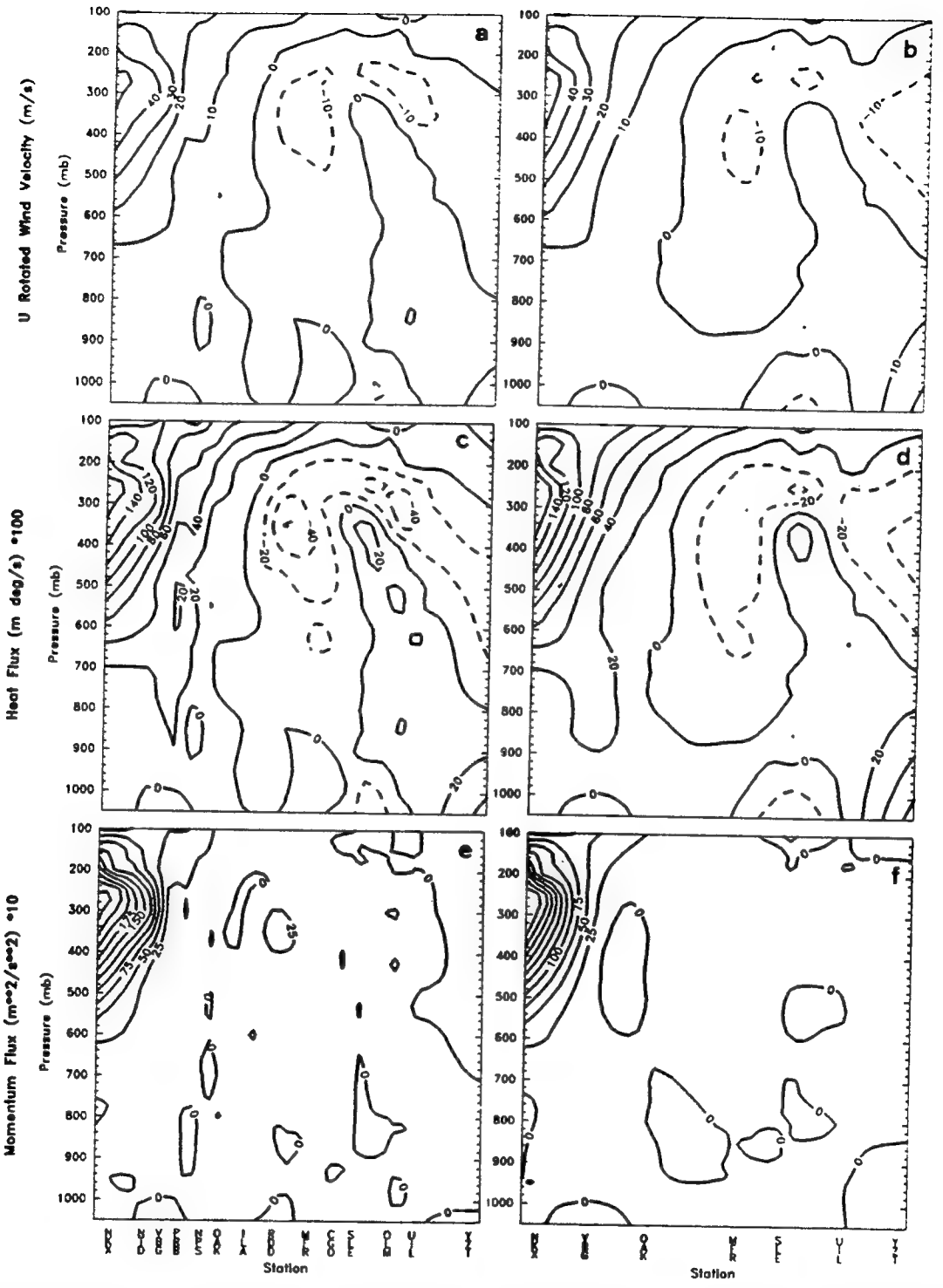


0000 UTC 7 Mar Vertical cross sections for (a) ALL $U_r$ flux, (b) NWS $U_r$ flux, (c) ALL heat flux, (d) NWS heat flux, (e) ALL momentum flux, and (f) NWS momentum flux.

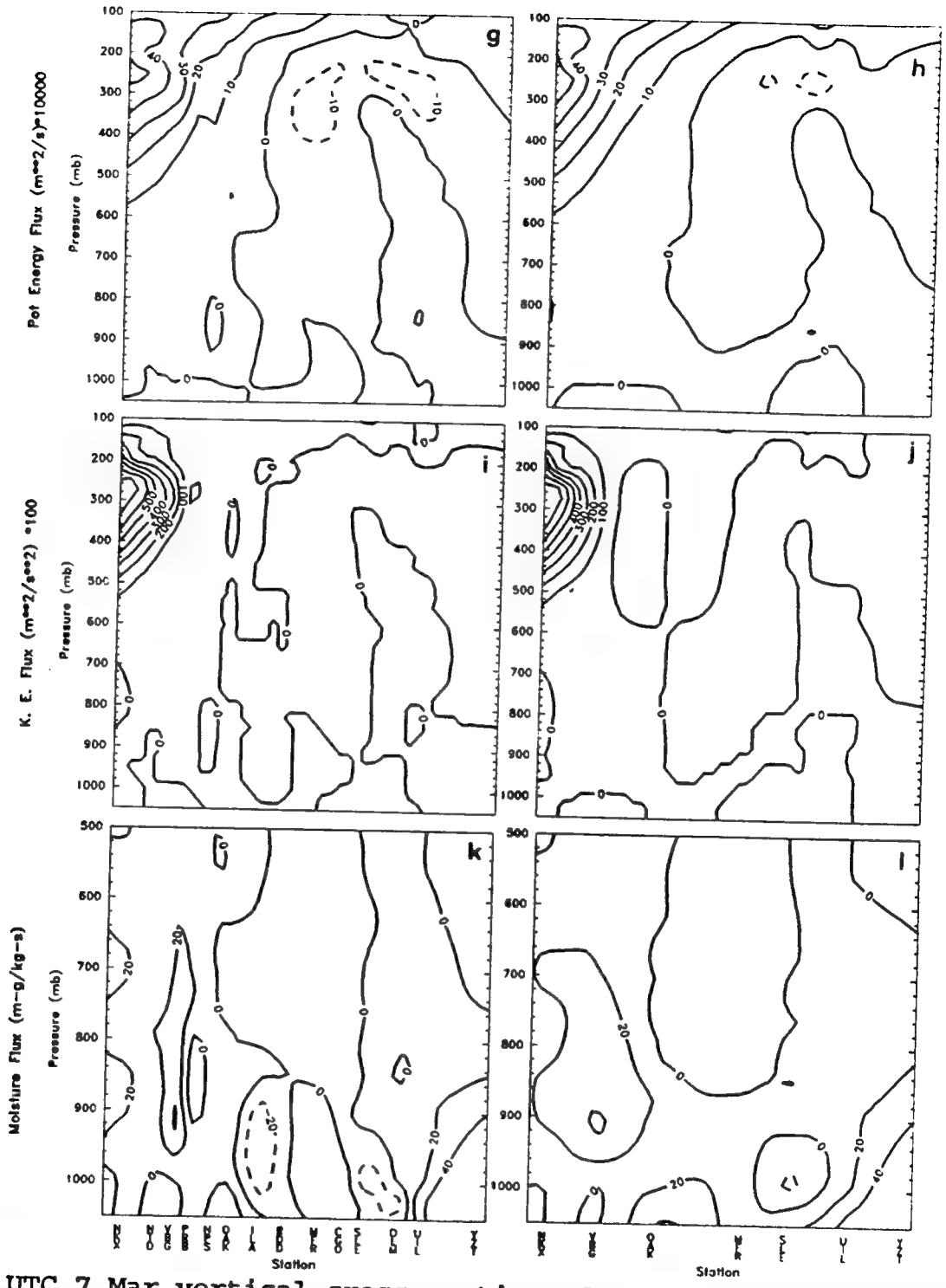


0000 UTC 7 Mar vertical cross sections for (g) ALL potential energy flux, (h) NWS potential energy flux, (i) ALL kinetic energy flux, (j) NWS kinetic energy flux, (k) ALL moisture flux, and (l) NWS moisture.

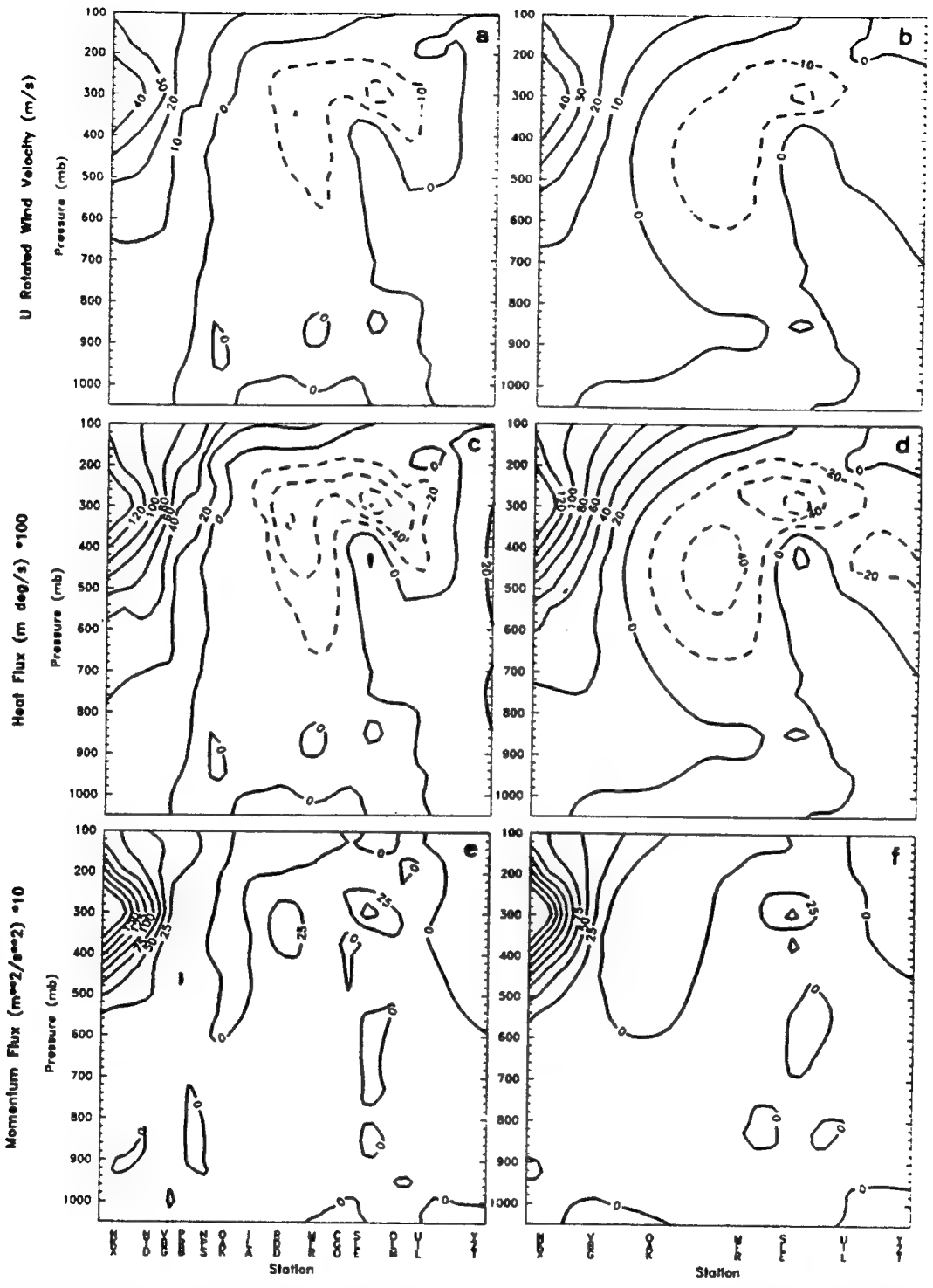


0300 UTC 7 Mar Vertical cross sections for (a) ALL $U_r$ flux, (b) NWS $U_r$ flux, (c) ALL heat flux, (d) NWS heat flux, (e) ALL momentum flux, and (f) NWS momentum flux.

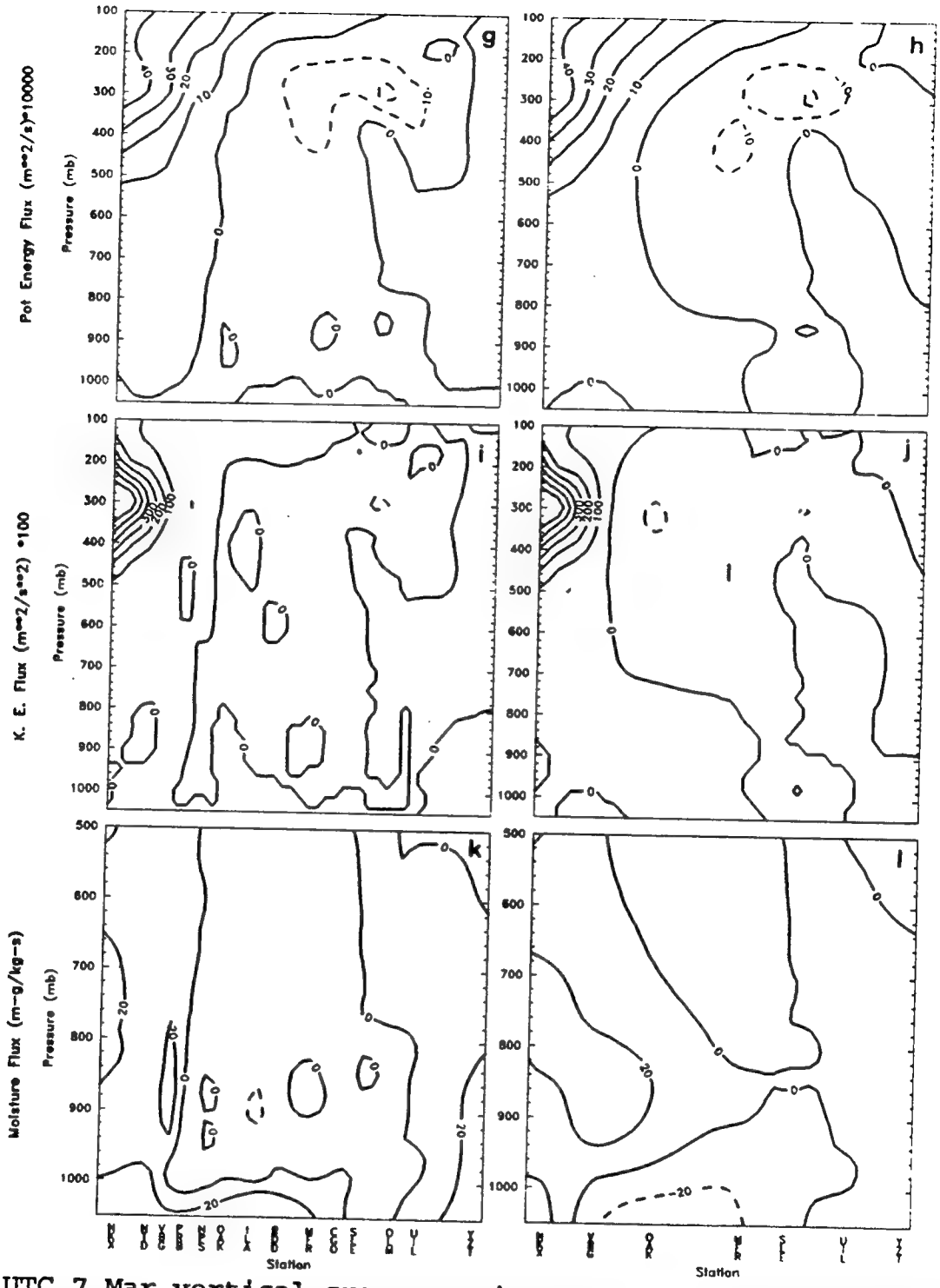


0300 UTC 7 Mar vertical cross sections for (g) ALL potential energy flux, (h) NWS potential energy flux, (i) ALL kinetic energy flux, (j) NWS kinetic energy flux, (k) ALL moisture flux, and (l) NWS moisture.

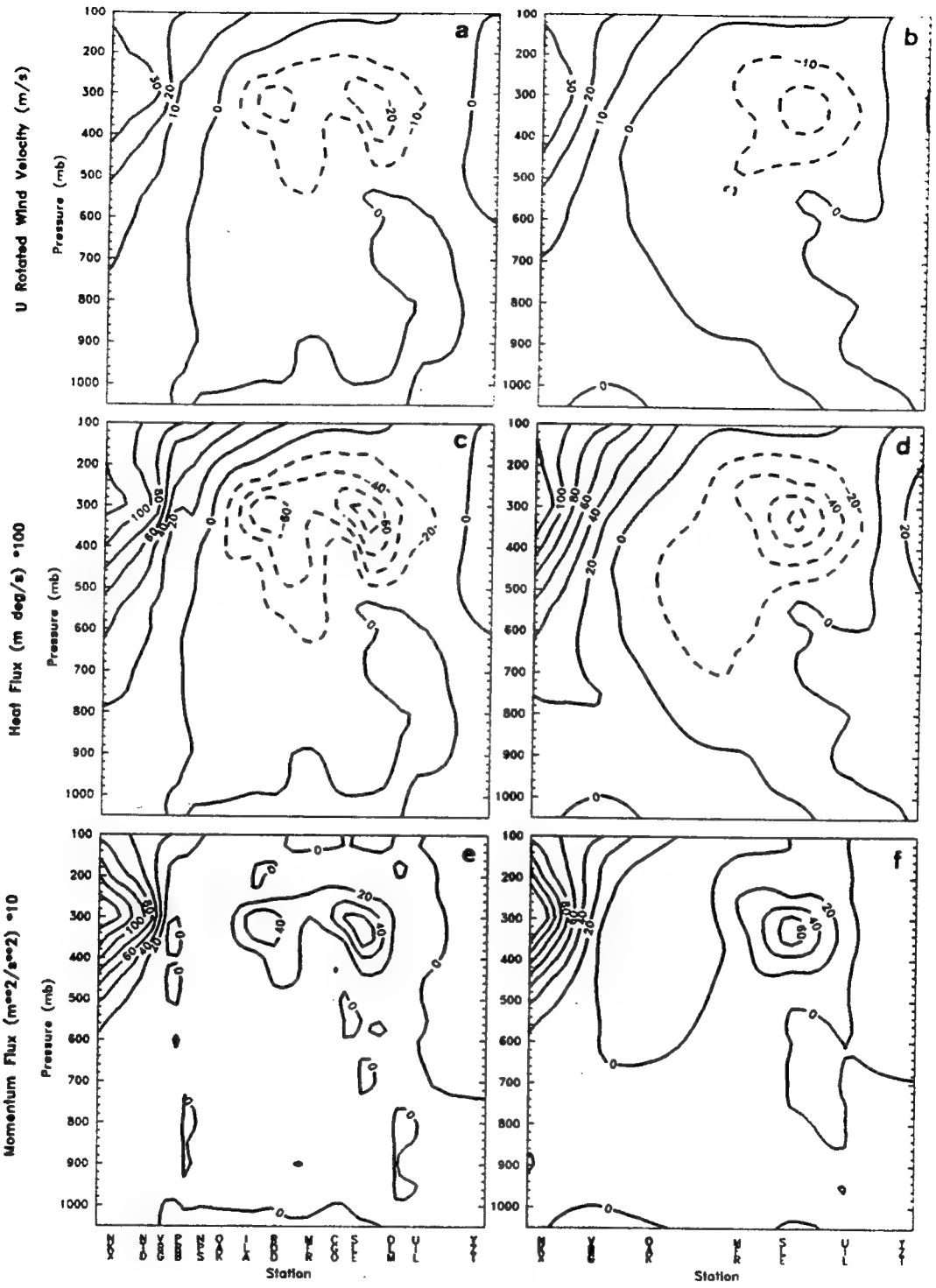


0600 UTC 7 Mar Vertical cross sections for (a) ALL $U_r$ flux, (b) NWS $U_r$ flux, (c) ALL heat flux, (d) NWS heat flux, (e) ALL momentum flux, and (f) NWS momentum flux.

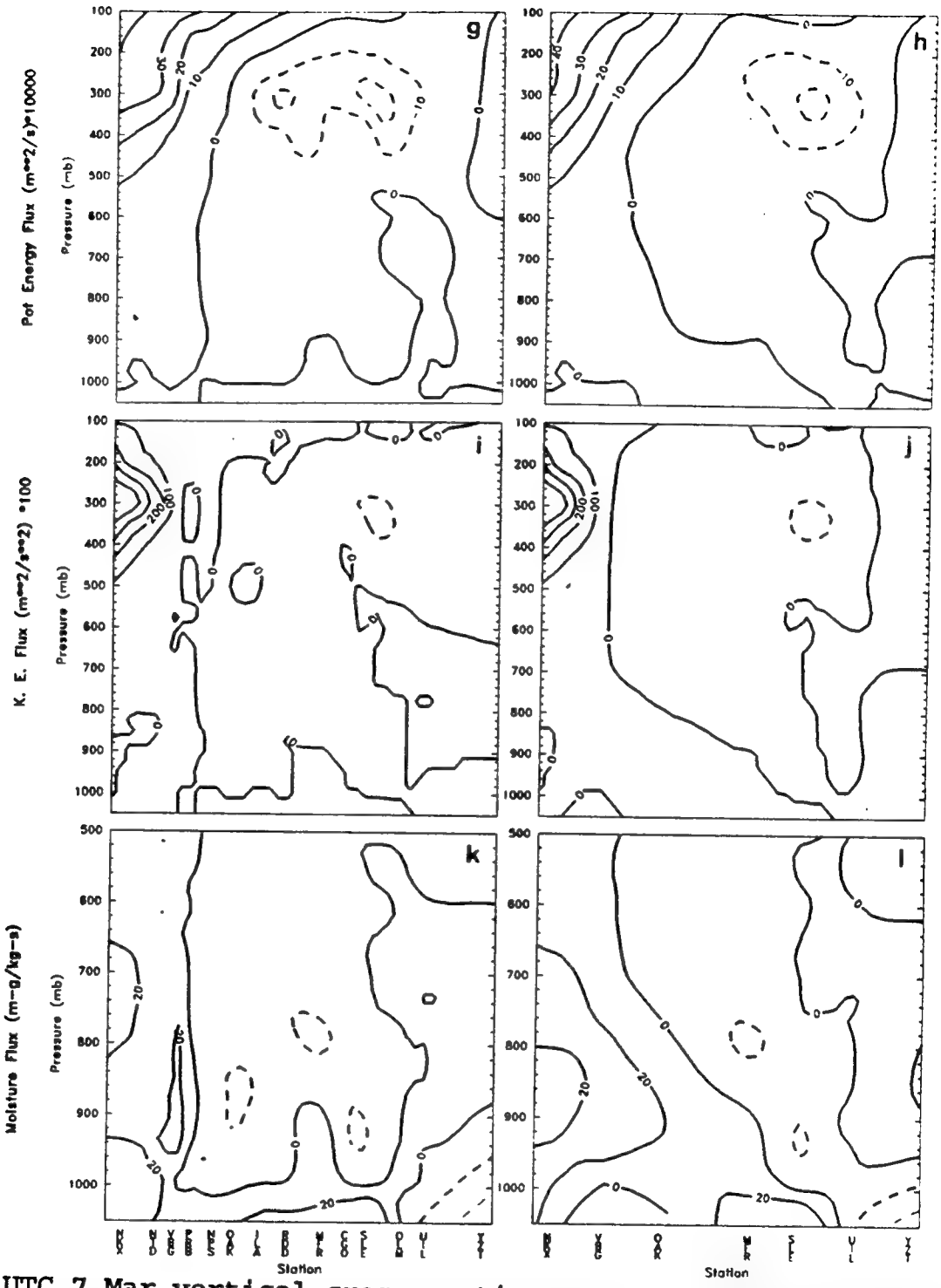


0600 UTC 7 Mar vertical cross sections for (g) ALL potential energy flux, (h) NWS potential energy flux, (i) ALL kinetic energy flux, (j) NWS kinetic energy flux, (k) ALL moisture flux, and (l) NWS moisture.

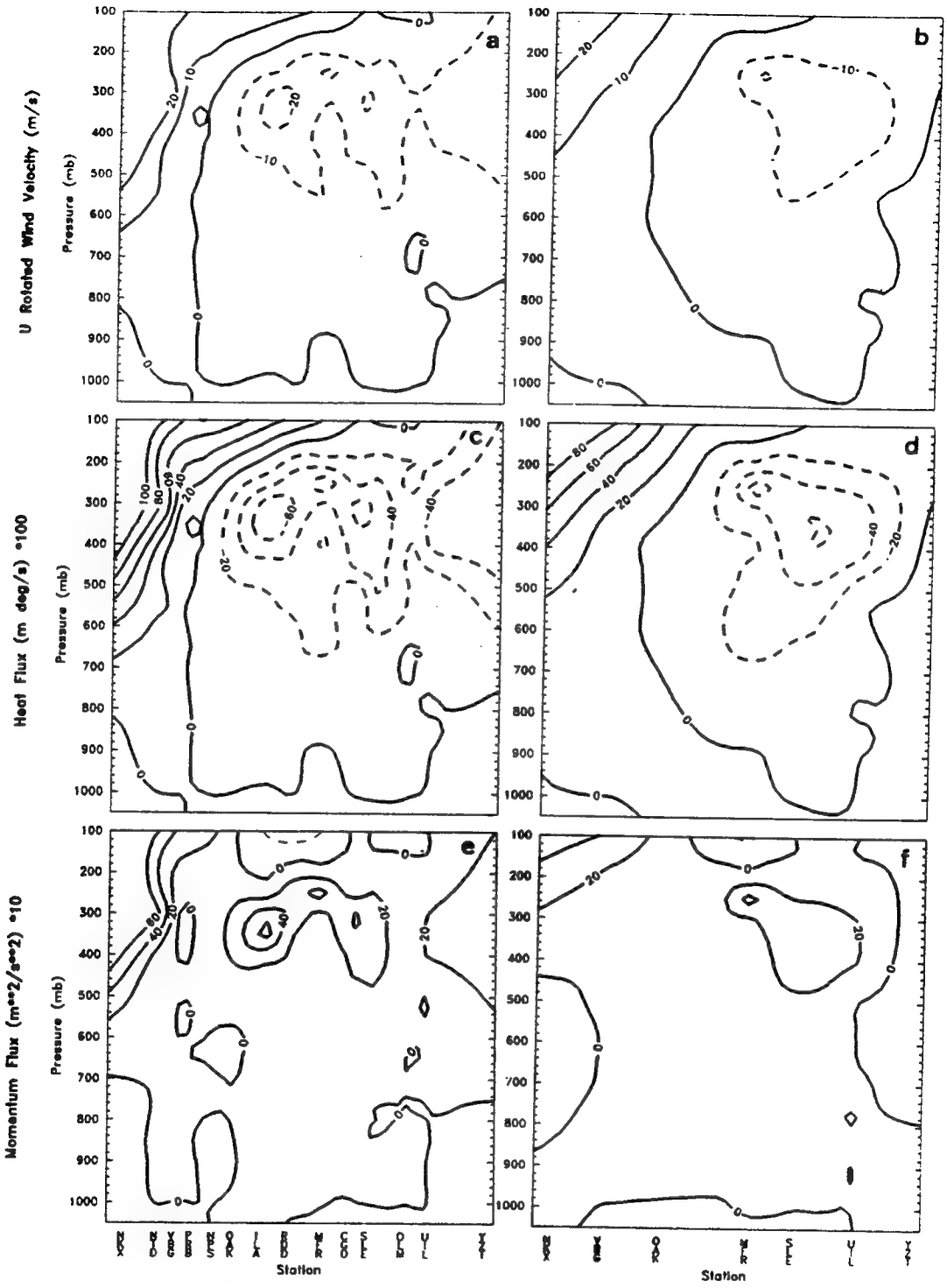


0900 UTC 7 Mar Vertical cross sections for (a) ALL $U_r$ flux, (b) NWS $U_r$ flux, (c) ALL heat flux, (d) NWS heat flux, (e) ALL momentum flux, and (f) NWS momentum flux.

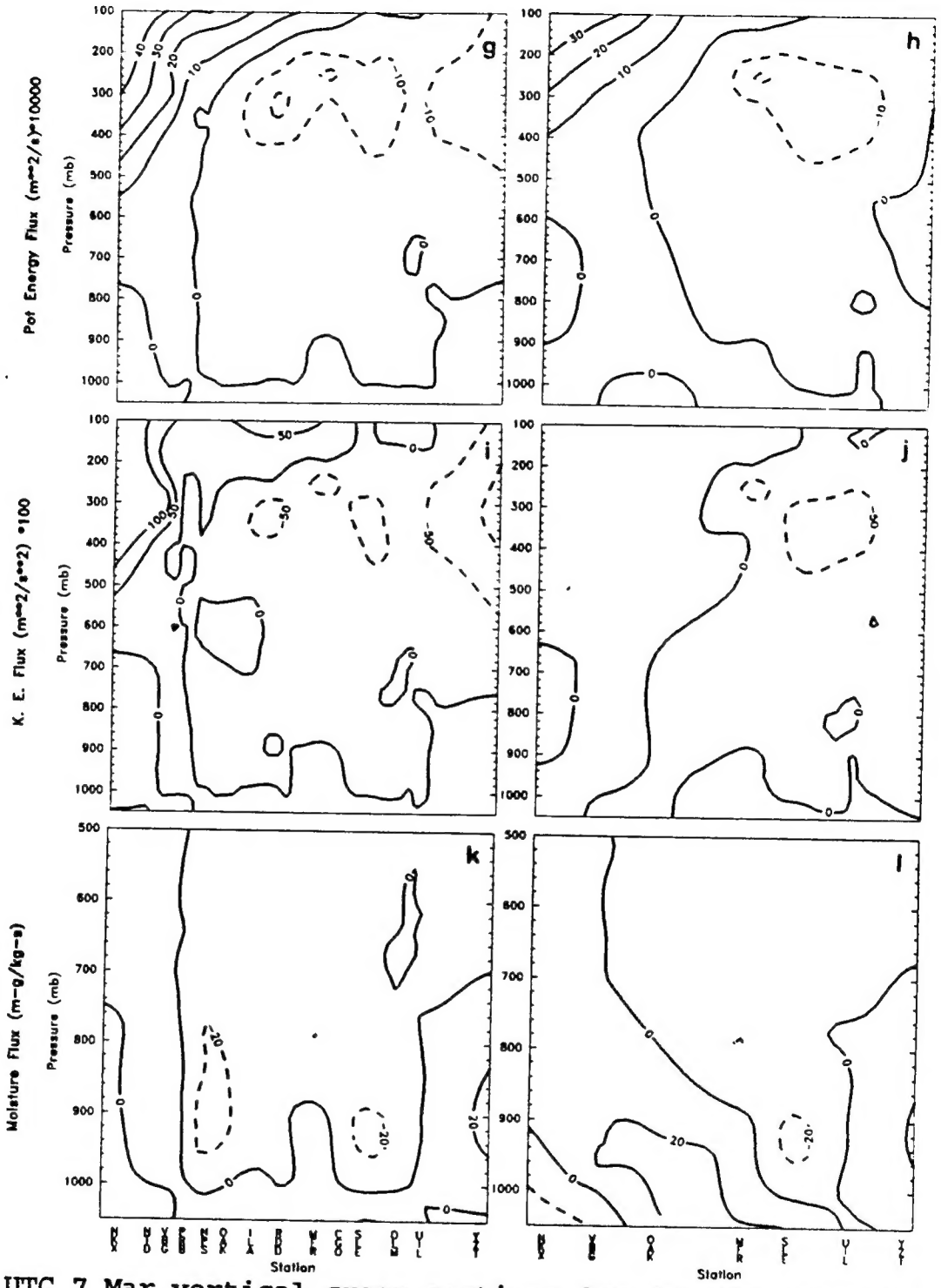


0900 UTC 7 Mar vertical cross sections for (g) ALL potential energy flux, (h) NWS potential energy flux, (i) ALL kinetic energy flux, (j) NWS kinetic energy flux, (k) ALL moisture flux, and (l) NWS moisture.

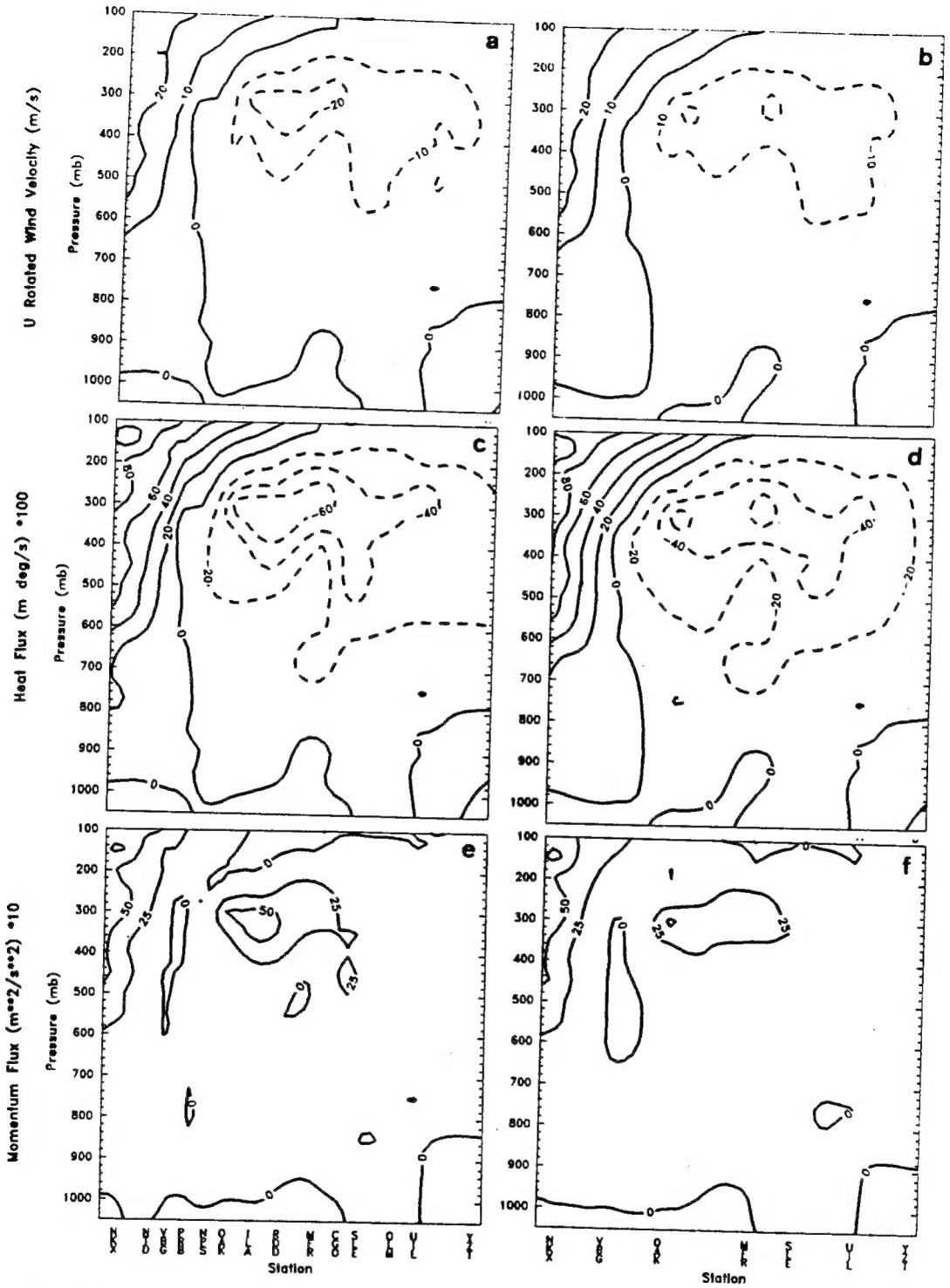


1200 UTC 7 Mar Vertical cross sections for (a) ALL $U_r$ flux, (b) NWS $U_r$ flux, (c) ALL heat flux, (d) NWS heat flux, (e) ALL momentum flux, and (f) NWS momentum flux.

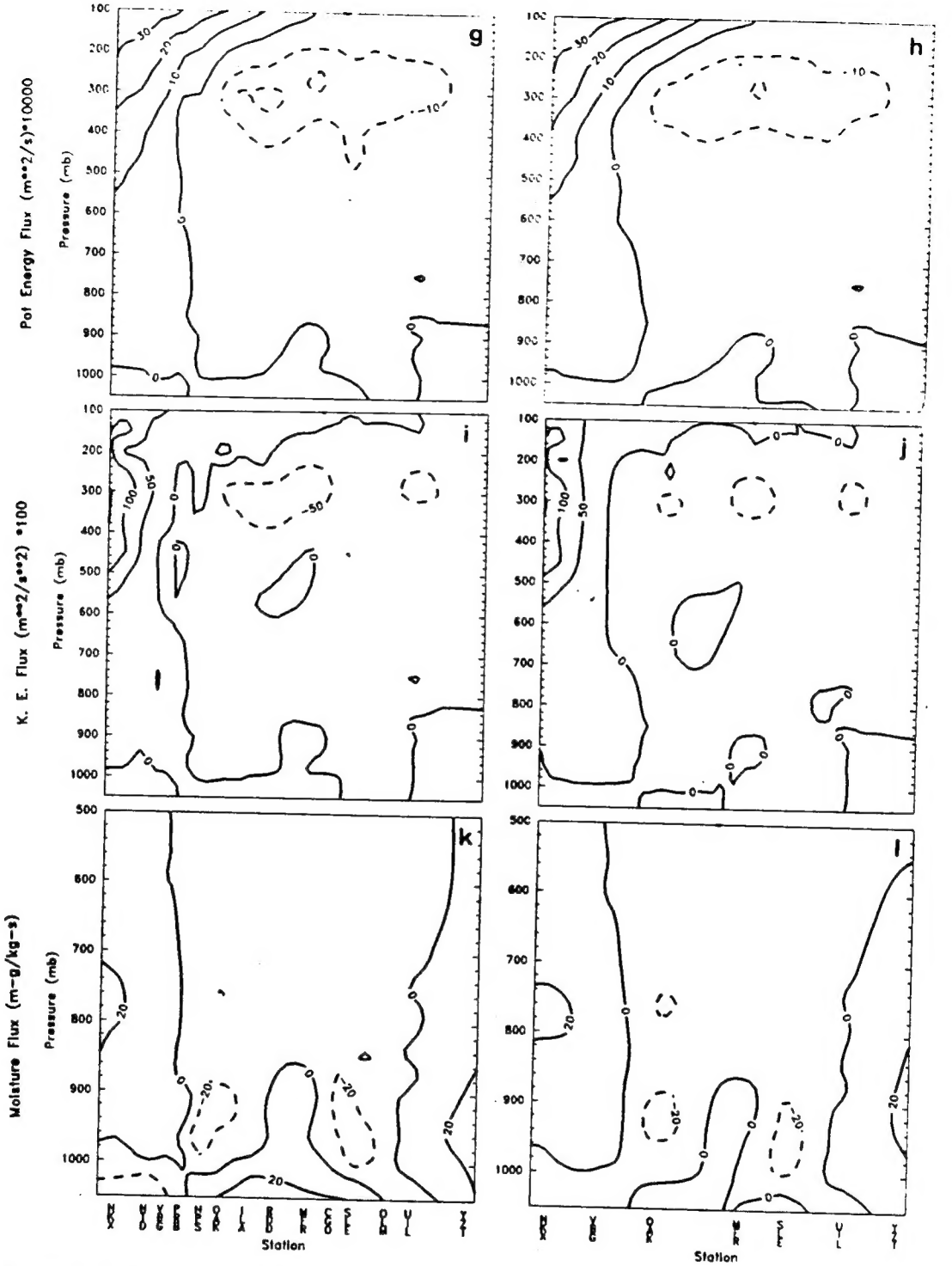


1200 UTC 7 Mar vertical cross sections for (g) ALL potential energy flux, (h) NWS potential energy flux, (i) ALL kinetic energy flux, (j) NWS kinetic energy flux, (k) ALL moisture flux, and (l) NWS moisture.

**INITIAL DISTRIBUTION LIST**

| | | No. Copies |
|---|---|---|
| 1. | Defense Technical Information Center<br>Cameron Station<br>Alexandria, Virginia 22304-6145 | 2 |
| 2. | Library, Code 52<br>Naval Postgraduate School<br>Monterey, California 93943-5101 | 2 |
| 3. | Meteorology Department<br>Naval Postgraduate School<br>Code MR/HY<br>589 Dyer Rd Rm 254<br>Monterey, California 93943-5114 | 1 |
| 4. | Dr. Paul Hirschberg<br>Naval Postgraduate School<br>Code MR/HS<br>589 Dyer Rd Rm 254<br>Monterey, California 93943-5114 | 1 |
| 5. | Dr. Russell Elsberry<br>Naval Postgraduate School<br>Code MR/ES<br>589 Dyer Rd Rm 254<br>Monterey, California 93943-5114 | 1 |
| 6. | Steven J. Bolduc<br>928 Roundtable Ct<br>Virginia Beach, Virginia 23464 | 1 |
| 7. | STORM Project Office<br>NCAR, P.O. Box 3000<br>Boulder, Colorado 80307 | 1 |
| 8. | Commanding Officer<br>FNMOC<br>7 Grace Hooper Ave. Stop 4<br>Monterey, California 93943-0001-0120 | 1 |
| 9. | Library<br>Department of Meteorology<br>University of Washington<br>Seattle, Washington 98105 | 1 |